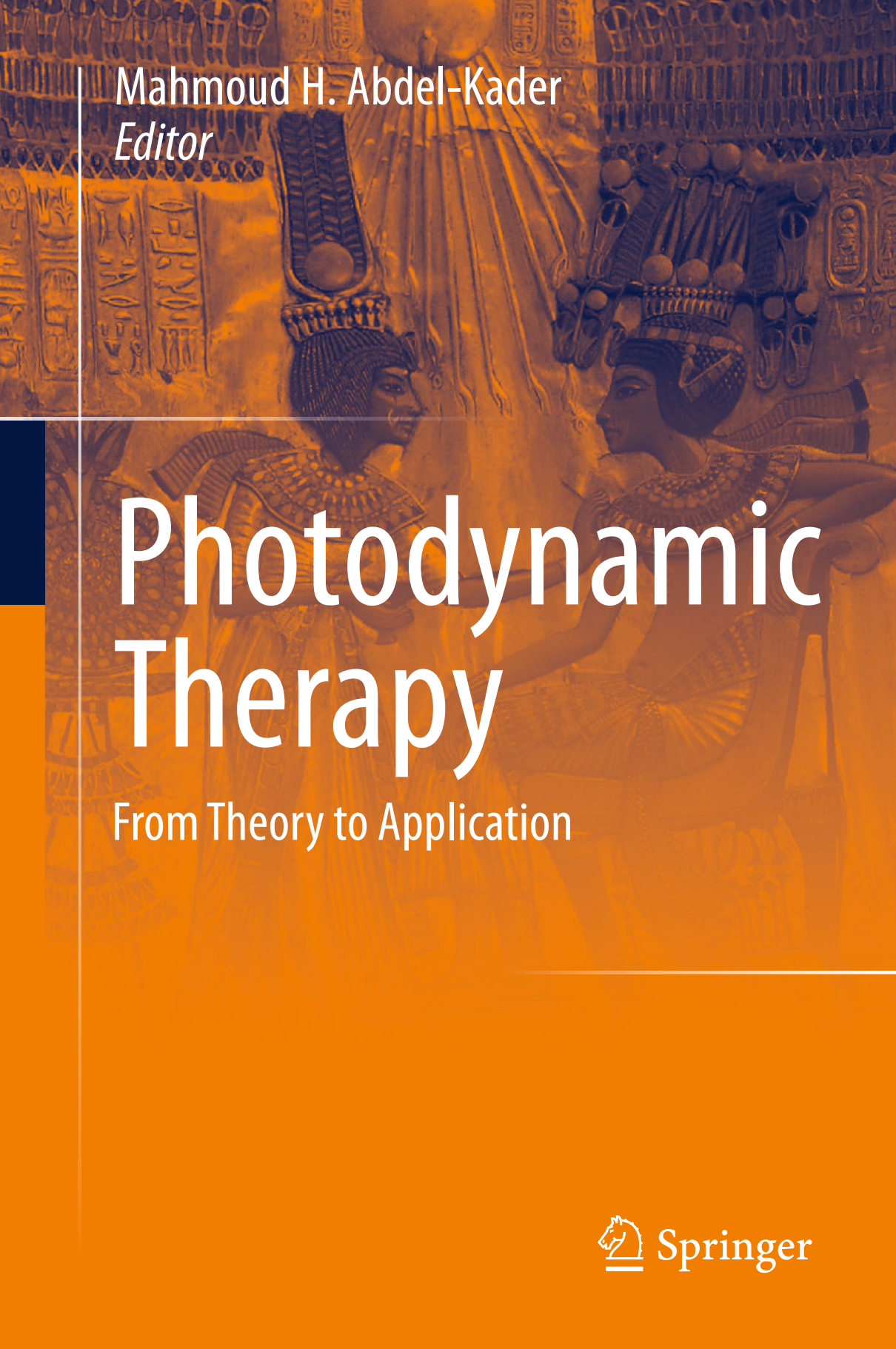
Mahmoud H. Abdel-Kader
Editor
Photodynamic Therapy
From Theory to Application
Springer

Photodynamic Therapy

Mahmoud H. Abdel-Kader
Editor

Photodynamic Therapy

From Theory to Application

Springer

Editor
Mahmoud H. Abdel-Kader
German University of Cairo
New Cairo
Egypt

ISBN 978-3-642-39628-1 ISBN 978-3-642-39629-8 (eBook)
DOI 10.1007/978-3-642-39629-8
Springer Heidelberg New York Dordrecht London

Library of Congress Control Number: 2013953248

Cover Image: Tutankhamun. Photo by Jerzy Strzelecki
Source: http://commons.wikimedia.org/wiki/File:Tutanchamon_%28js%29_3.jpg

Printed on acid-free paper

Springer is part of Springer Science+Business Media (www.springer.com)

This book is gratefully dedicated to Egypt and its great people, the birthplace and founders of Photodynamic Therapy,

To my late wife Nagwa El-Kady for her lifelong stand behind me during all my scientific achievements,

To my wonderful son and daughters (Wael, Reham, and Sara) who taught me to be free,

And to the young generation of researchers and scientists who will hopefully use this book to help them on the path towards improving mankind's health

Mahmoud H. Abdel-Kader

Foreword

Photodynamic therapy (PDT) is a photochemistry-based approach that uses light to activate specific chemicals that, in the activated state, impart cytotoxicity. Historically, the concept of combining light with a chemical agent dates back over 5000 years when ancient civilizations in Egypt and India applied this combination to treat several disorders. It is therefore most appropriate that this book, entitled *Photodynamic Therapy: From Theory to Application*, is the result of a workshop and conference organized by Prof. Mahmoud H. Abdel-kader in Cairo, Egypt, a birthplace of early PDT, under the sponsorship of the German University in Cairo.

Although PDT has received regulatory approval worldwide for several indications, it has by no means achieved the recognition and the breadth of applications that it deserves. There have been major milestones in both the basic understanding of the process of PDT and expanded vision of its applications. Perhaps a clearer integrated document that brings these together will help show the full potential of PDT where the best is yet to come.

With this purpose in mind, Prof. Abdel-kader has strived to present key aspects of the application of PDT in medicine and society, while providing a strong basic science component to the book. The authors are experts in the field and have made major contributions to its evolution to bring it to its current state. Each chapter provides a comprehensive understanding of the specific aspect of PDT that it is dedicated to. The book starts with a chapter on the *History of Photodynamic Therapy*, followed by chapters on fundamentals of photochemistry/photophysics, basic molecular biological mechanisms, and emerging variants such as photochemical internalization. There are sections on the applications of PDT to pathogen destruction, new antibiotic susceptibility diagnostics, and specific clinical applications written by experts practicing PDT.

I anticipate that, with the breadth of basic and applied aspects of PDT, this book could serve as a standard reference for researchers and students at all levels, as well as clinical specialists interested in the topic, and those in industry exploring new areas for development.

Boston, MA, USA — Tayyaba Hasan, Ph.D.

Preface

I think you might dispense with half your doctors if you would only consult Dr. Sun more

—Henry Ward Beecher

Light was used thousands of years ago by the Egyptians, Chinese, and Indians for the treatment of certain skin diseases; however, the actual birth of photodynamic therapy (PDT) was established roughly 100 years ago by the work of Scientists, namely Raab, von Tappeiner, and Finsen. Current interest in PDT only resurfaced in the early 1970s with the emergence of the water-soluble photosensitizer Hematoporphyrin Derivatives (HPD).

Photodynamic therapy is a promising new modality for cancer treatment, which involves the combination of a photosensitizing agent, which is selectively taken up and retained by Tumor cells, and light of an appropriate wavelength. Separately, each of these factors is harmless; however, when they are combined in the presence of oxygen, cytotoxic reactive oxygen species are produced, which leads to irreversible cellular damage and causes cell death and tumor destruction. It is a treatment modality for the management of cancer that can be added to surgery, radiotherapy, chemotherapy, immunotherapy, and targeted molecular therapies.

The idea of writing a book on PDT came to me over 20 years ago. I was encouraged to pursue this vision after I obtained impressive results in the control of noxious insects and parasites that represent one of the biggest health problems in Egypt, especially the Schistosoma, which Egyptians have been suffering from since ancient Egyptian times. The successful field application using PDT for the control of Malaria in African swamps was the real challenge and has shown to be a promising implementation of PDT. However, as one can realize from the extensive work published every day, that there is rapid progress in the clinical application. It is worth mentioning, that the greatest progress in PDT has been in the diagnosis and treatment of malignant tumors.

The driving force to initiate the book process was when an international conference on Photodynamic Therapy was held in the German University in Cairo (GUC) on February 2, 2012. I was honored to be the chairperson of this conference and most of the Authors that contributed to the book participated as keynote speakers. I shared my vision with my colleagues, and they all willingly welcomed the idea and agreed to contribute to the book.

This book will acquaint readers with the history and basic principles of PDT, as well as the fundamentals of the theory, methods, and instrumentation of clinical diagnosis and treatment of cancer. It will also discuss nononcological applications such as functional targeting of bacteria, treatment of microbial infection and vector control of Malaria, Filaria, and Dengue Fever, and the control of other parasites and noxious insects. The Authors, all experts and pioneers in their field, discuss the reasons behind the treatment with PDT along with its advantages and pitfalls. This comprehensive book is unique in its structure as it combines both the theory and application of PDT.

It is also worth mentioning that this book will tackle state-of-the art research and fill in the holes left by other literatures. Since both Scientists and Physicians have contributed to this book, this cooperation will hopefully assist in bridging the gap between the bench and the clinic. *Photodynamic Therapy: From Theory to Application* will be considered a standard reference for researchers of different levels whether they are postgraduate students or active researchers in chemistry, biochemistry, biology, and biophysics. It will also be in high demand for physicians and specialists working on medical diagnosis and treatment in the field of cancer, antimicrobial PDT, as well as the photodynamic control of parasites and noxious insects.

Mahmoud H. Abdel-Kader Ph.D.
Department of Pharmaceutical Technology,
German University in Cairo,
New Cairo, Egypt

and

Department of Laser Application in Photochemistry and Photobiology,
The National Institute of Laser Enhanced Science (NILES), Cairo University,
Giza, Egypt
e-mail: mahmoud.abdelkader@guc.edu.eg

Acknowledgments

The thankful receiver bears a plentiful harvest

—William Blake

I would like to express my gratitude to the many people who saw me through this book; to all those who provided.

It would have never been possible without the support of the Authors of the various chapters of this book, whom I am very grateful to, the distinguished researchers and leading experts in their field of study.

The scientific and family atmosphere provided at the German University in Cairo, that I really appreciate. The best environment for research and fostering academic achievements that facilitates to complete this book. Here my gratefulness and special thanks to Prof. Dr. Ashraf Mansour, the Prime Founder and Chairman of the Board of Trustees of the GUC; a person who stands up for what he believes in, a special thanks for his inspiration and faith in science.

My gratefulness to the co-workers at the National Institute of Laser Enhanced Sciences (NILES), Cairo University, my thanks for their dedication and commitment.

Special thanks goes to my youngest and smart co-workers for working hard and helped me to finalize my contribution in this book Dr. Nabila Hamdi and Dr. Reham Abdel-Kader; the pleasant buds Pakinam Farouk, Noha Warraky, Nada Abdel-Bassier, Aya Sebak, Mai Magdy, Nada El-Hakim, Haidy El-Borombaly, and Ingy Maher.

My sincere gratitude for the great efforts exerted by Zeinab Baghdady, for her continuous support and assistance in every task related to this book. To my office Samira Kandil and Hanan El-Sayed; the administrative support is also highly appreciated.

I would also like to acknowledge the support and advice of Elizabeth Hawkins at Springer-Verlag.

Finally, I hope that this book can be seen as a "thanks" to the countless people, who have helped make my life what it is today.

About the Editor

Mahmoud H. Abdel-Kader
Professor of Photochemistry, Cairo University
President of the German University in Cairo
Email: mahmoud.abdelkader@guc.edu.eg

Prof. Mahmoud H. Abdel-Kader is a Professor of Photochemistry and currently, the President of the German University in Cairo, since 2002. Prof. Abdel-Kader received his Ph.D. (Dr. rer. nat.) in Spectroscopy and Photochemistry at Stuttgart University, Germany in 1979, under the supervision of Prof. Dr. Theodor Foerster and Prof. Dr. H.E.A. Kramer. He got a post doctoral position at the Institute of Physical Chemistry, University of Karlsruhe, from 1982 to 1983. From 1983 to 1984, he was a Senior Researcher at the Federal Institute of Technology, EPFL, Lausanne, Switzerland. He was a Visiting Professor at both Georgia Institute of Technology, Atlanta, USA and the Institute for Laser Technology in Medicine and Metrology, Ulm University. He then served the position of Vice Dean of the National Institute of Laser-Enhanced Sciences (NILES), in Cairo University.

Prof. Abdel-Kader has supervised over 80 master's theses and doctoral dissertations. He has published over 100 publications in peer reviewed journals and in conference proceedings. Also, he is an inventor of 8 patents. He has given more than 80 invited talks and plenary lectures at both national and international meetings. Prof. Abdel-Kader's research interests include: Laser Spectroscopy to study the Kinetics and mechanism of Ultrafast Chemical Reaction (Photochemical Isomerization, Protolytic Reactions and Electron Transfer Processes), Utilization of Solar Energy in Photochemical Conversions for Malaria, Filaria and Dengue Fever Vector control, Parasites such as Schistosomiasis and Agricultural pests using environmentally friendly (natural extract) Photosensitizers and Application of

Nanoparticles in Photodynamic Diagnosis and Therapy of Cancer.

Prof. Abdel-Kader was elected as Officer, then Chair of the European Society for Photobiology (ESP) outside Europe (1997–2001). He was awarded the distinguished State Prize in Chemistry, in Egypt, 1996 as well as the State Medal in Chemistry, 1998. Recently, Prof. Abdel-Kader was awarded the 2012 Excellence Award of Science from Cairo University.

About the Foreword Author

Prof. Tayyaba Hasan, Ph.D.

E-mail: thasan@mgh,harvard.edu

Tayyaba Hasan, Ph.D., is a Professor of Dermatology at Harvard Medical School (HMS) and a Professor of Health Sciences and Technology (Harvard-MIT). She is based at the Wellman Center for Photomedicine. Dr. Hasan received her Ph.D. in Organic Chemistry from the University of Arkansas followed by postdoctoral training in Biochemistry at the University of Pennsylvania after which she joined the Harvard Medical School, Massachusetts General Hospital in 1982 as a Research Scientist. Dr. Hasan's research is directed to basic and translational studies in photochemistry, photobiology, and photodynamic therapy. The major research theme of the group is Mechanisms and Image Guided Optimization of Photodynamic Therapy. More broadly, the research program includes investigations in cancer, microbiology, infectious diseases, arthritis, and cardiovascular pathologies.

Contents

Contributors

Mahmoud H. Abdel-Kader Department of Pharmaceutical Technology, German University in Cairo, New Cairo, Egypt

Ron Allison 20th Century Oncology, Greenville, NC, USA

Kristian Berg Department of Radiation Biology, Norwegian Radium Hospital, Oslo University Hospital, Montebello, Oslo, Norway

Hubert van den Bergh Department of Chemistry, Ecole Polytechnique Fédérale De, Lausanne, Switzerland

Hans-Peter Berlien Department of Laser Medicine, Ev. Elisabeth Klinik, Berlin, Germany

Monica Camerin Department of Biology, University of Padova, Padova, Italy

Fabrizio Cardin Faculty of Medicine and Surgery, Department of the Elderly, Unity of Geriatric Surgical Clinic, University of Padova, Padova, Italy

Ilaria Cattin Veterinary Clinic "Prato della Valle", Padova, Italy

Olimpia Coppellotti Department of Biology, University of Padova, Padova, Italy

Furio Corsi Veterinary Clinic "Prato della Valle", Padova, Italy

Tarek Eltayeb Departement of Laser application in Photochemistry and Photobiology, National Institute of Laser Enhanced Sciences, Cairo University, Cairo, Egypt

Clara Fabris Department of Biology, University of Padova, Padova, Italy

Laura Guidolin Department of Biology, University of Padova, Padova, Italy

Tayyaba Hasan Harvard Medical School, Massachusetts General Hospital, Boston, Massachusetts, USA

Guilio Jori Department of Biology, University of Padova, Padova, Italy

Shazia Khan Harvard Medical School, Massachusetts General Hospital, Boston, Massachusetts, USA

Herwig Kostron Department of Neurosurgery, University Innsbruck, Innsbruck, Austria

Barbara Krammer Department of Molecular Biology, University of Salzburg, Salzburg, Austria

Keyvan Moghissi Goole and District Hospital, Goole, East Yorkshire, UK

Ole-Jacob Norum Department of Orthopedical Oncology, Oslo University Hospital, Norwegian Radium Hospital, Oslo, Norway

Patrycja Nowak-Sliwinska Department of Chemistry, Ecole Polytechnique Fédérale De, Lausanne, Switzerland

Carsten Phillipp Department of Laser Medicine, Ev. Elisabeth Klinik Berlin, Berlin, Germany

Pål K. Selbo PCI Biotech AS and Department of Radiation Biology, Oslo University Hospital, Radium Hospital, Oslo, Norway

Michel Sickenberg Departement of Chemistry, Ecole Polytechnique Fédérale De, Lausanne, Switzerland

Marina Soncin Department of Biology, University of Padova, Padova, Italy

Ulrich Steiner Department of Chemistry, University of Konstanz, Konstanz, Germany

Rudolf Steiner Institute of Laser Technologies in Medicine and Metrology, University of Ulm, Ulm, Germany

Thomas Verwanger Department of Molecular Biology, University of Salzburg, Salzburg, Austria

Marie Vikdal Department of Radiation Biology, Oslo University Hospital, Norwegian Radium Hospital, Oslo, Norway

Anette Weyergang Department of Radiation Biology, Oslo University Hospital, Norwegian Radium Hospital, Oslo, Norway

Part I
History

Photodynamic Therapy (PDT) Tree

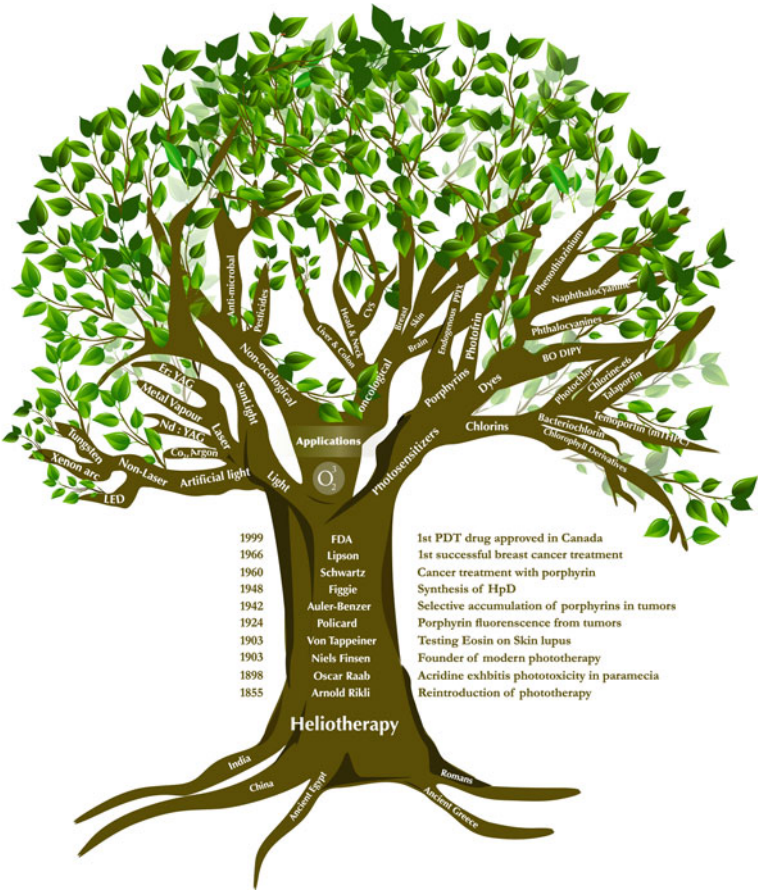

The history of Photodynamic Therapy (PDT) and its development is illustrated as a tree. Unlike other living organisms, trees are constantly growing. This is especially true in the case of our PDT tree, which is continually growing and never ceases to develop.

The roots of the PDT tree represent the origins of PDT, which started out as heliotherapy (light therapy) and dates back to Ancient Egypt, India, and China.

The development of PDT, symbolized by the trunk, started out when PDT was reintroduced by Arnold Rikli and ends with the approval of the first PDT drug in 1999.

PDT involves three key components: a photosensitizer (PS), a light source, and tissue oxygen. The branches of the PDT tree portray this definition of PDT, the different photosensitizers, light sources, and oxygen, along with the products of this combination, which are the various oncological and non-oncological applications.

Chapter 1
History of Photodynamic Therapy

Mahmoud H. Abdel-Kader

From Ancient Egyptians to Present Day

1.1 Introduction

Photodynamic therapy (PDT) is a form of phototherapy that involves three key components: a photosensitizer, a light source, and tissue oxygen. When these components are combined together, they become toxic to the targeted cells [1]. The wavelength of the light source needs to be appropriate for exciting the photosensitizer (ps) to produce reactive oxygen species "ROS". These ROS are generated during PDT through two types of reactions. Type I reaction involves electron/hydrogen transfer directly from the ps, producing ions, or electron/hydrogen abstraction from a substrate molecule to form free radicals. Type II reaction produces the electronically excited and highly reactive state of oxygen known as singlet oxygen [2]. PDT is used clinically to treat a wide range of oncological and nononcological medical conditions [3] and is recognized as a treatment strategy that is both minimally invasive and minimally toxic [4].

PDT has been used for many years, but is only now becoming widely accepted and utilized, even though it has many advantages over other types of treatments. First, PDT avoids systemic treatment since treatment occurs only where light is delivered. Therefore, it is not necessary for the patient to undergo systemic treatment when treating localized disease and side effects are also avoided. Another advantage is that PDT is selective. The photosensitizing agent will selectively accumulate in cancer cells and the surrounding normal tissues are spared. PDT can also be used when surgery is not possible. If a patient has cancer in an organ or part of an organ that cannot be removed surgically (e.g., the upper bronchi of the lung), PDT can still treat the site. Moreover, it is a procedure that is

M. H. Abdel-Kader (✉)
Department of Pharmaceutical Technology, German university of Cairo, New Cairo, Egypt
e-mail: mahmoud.abdelkader@guc.edu.eg

M. H. Abdel-Kader
Department of Laser application in Photochemistry and Photobiology, The National Institute of Laser Enhanced Sciences (NILES), Cairo University, Giza, Egypt

M. H. Abdel-Kader (ed.), *Photodynamic Therapy*,
DOI: 10.1007/978-3-642-39629-8_1, © Springer-Verlag Berlin Heidelberg 2014

Fig. 1.1 Ancient Egyptians worshipped the sun, which eventually led them discover the connection between sunlight and health [7]. *Sources* http://en.wikipedia.org/wiki/File:Akhenaten_as_a_Sphinx_%28Kestner_Museum%29.jpg

low in cost. Finally, PDT is a repeatable therapy. Unlike radiation therapy, PDT can be used again and again. Hence, it offers a means of long-term management of cancer even if complete cure is not possible [4].

1.2 Phototherapy (Origin of PDT)

The origin of light as a therapy in medicine and surgery can be traced from ancient times to modern days. Phototherapy began in Ancient Egypt, Greece, and India but disappeared for many centuries and was rediscovered by western civilization at the beginning of the twentieth century [5] (Fig. 1.1).

Long ago, it was thought that sunlight was the only aspect in the cure of disorders such as vitiligo, psoriasis, rickets, skin cancer and even psychosis, i.e., sunlight was given all the credit. This treatment process (using sunlight) is known as phototherapy or, as it was previously called, heliotherapy. As science advanced, however, it was found that there were usually endogenous substances involved when curing these disorders and that the photodynamic process was a more accurate mechanism for explaining the healing powers of light [6, 7].

The practice of phototherapy, or heliotherapy as it was once called, dates back to ancient times. Early reports on the use of heliotherapy were found to date back to about 3000 BC in Ancient Egypt and India [6, 7]. In Ebers Papyrus, 1550 BC, ancient Egyptians utilized phototherapy using plants like the *Ammi majus*, parsnip, parsley, and Saint-John's-wort to make a powder that was applied on depigmented lesions [6]. When the patient was exposed to sunlight, it led to skin pigmentation, an effect that is similar to sunburn [6, 7]. Also, in one of India's sacred books, *Atharava-Veda* 1400 BC, patients suffering from vitiligo were given certain plant extracts of the Bavachee plant, the *Psoralea corylifolai*, and asked to stand in the sunlight for some time [6].

Phototherapy was introduced in China by Lingyan Tzu-Ming in the first century BC during the Han dynasty [7]. Four centuries later, during the Tang dynasty, it became a ritual practice where people used to expose a piece of green paper with

red dye to sunlight, soak it in water, and consume it to benefit from some of the healing powers of the sun [7, 8].

It was during the second century BC that phototherapy first got the name "heliotherapy" by the Greek doctor Hippocrates, who was called the "Father" of medical science [4]. He was the first Greek to practice medicine as an empirical science at a time when it was practiced only by priests. Hippocrates recommended sunlight for restoration of health. He had first known about the healing powers of sunlight from his travels to Egypt, where sunlight treatment was well-known [6, 7, 9].

The Romans who followed continued to utilize sunlight as a treatment, especially for skin diseases. They invented the "Therms" which are historically famous Roman public baths set in sunlight. With the decline of the Roman Empire and the spread of Christianity, Roman baths and the concept of heliotherapy disappeared [6, 7, 9].

Later on, in the thirteenth Century, Ibn El-bitar described in his book, Mofradat Al Adwiya "Terminologies of Pharmaceuticals" the treatment of vitiligo with a tincture of honey and powdered Aatrillal seeds (that was later classified as *Ammi majus*). Administration of this tincture was both topical and oral followed by exposure to direct sunlight for 1–2 h [10].

It was not until the late 1800s and early 1900s that phototherapy began to flourish again. Arnold Rikli, the Swiss natural healer and physician, reintroduced the healing powers of sunlight that had been forgotten for many centuries [9]. In this regard, this is why he is often considered the pioneer of modern phototherapy. Although he was the first to draw the world's attention toward the value of light, air and sunbaths, he was not well-known since most of his writings were not translated into English [11]. One of his first great accomplishments was the establishment of a National Medicine Institute in the year 1855, in Bled, Slovenia [12]. For as long as 50 years, Arnold Rikli worked on developing natural therapies that are still valid today. His famous quote: "Water is good, Air is better and Light is best of all", is regarded as the core of heliotherapy [6].

Phototherapy, found useful in the treatment of lupus vulgaris, was used for the treatment of two other diseases: pulmonary tuberculosis and rickets. Following the same evolution processes, treatment attempts started with the utilization of sunlight which was then replaced by artificial ultraviolet (UV) radiation sources. By the end of the first quarter of the twentieth century, phototherapy became famous and widely applied in northern Europe and northern cities of North America [6, 7, 13].

A great contributor to the foundation of modern phototherapy was the Danish doctor Niels Ryberg Finsen (1860–1904) [6]. He owned a medical institute in Copenhagen to which he attached a sun garden, where he allowed his patients to sunbathe in the sunlight in an attempt to cure lupus vulgaris (skin tuberculosis) and prevent scarring in patients with smallpox [6, 14]. In his first attempts he used natural sunlight, but he soon changed to artificial light sources or filtered sunlight. In 1893, he realized that the skin of smallpox patients showed best results with red light. Later in 1903, he demonstrated the beneficial effect of UV rays on the human body; this led to his attempt at the artificial generation of UV rays. First, he separated UV from infrared and visible radiation using devices containing quartz

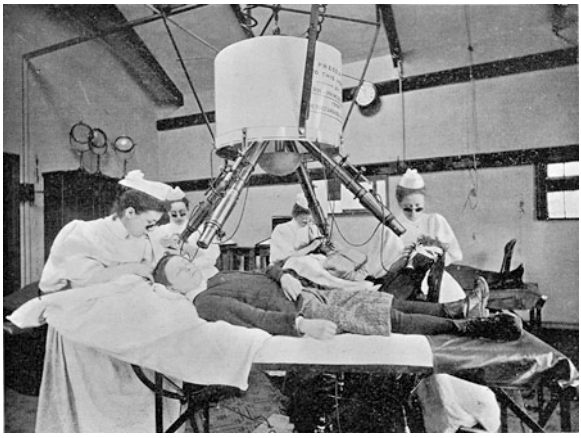

Fig. 1.2 Set of apparatus devised by Finsen for treating lupus. Credit: Wellcome library, London. *Sources* ©Wellcome images, Wellcome library ©Bridgeman art library/ private collection/The Stapleton collection

lenses and filters. Then, he used UV radiation from the carbon arc lamp for the treatment of skin tuberculosis. The outcome of this invention was a Nobel Prize in medicine [6] (Fig. 1.2).

These lamps were replaced afterward by much more convenient sealed quartz mercury—vapor lamps in 1904 that were cooled by water or air and were designed by Kromayer, a German dermatologist [7]. Such lamps were more efficient sources of UV radiation than carbon arc ones [7].

Nowadays, a wide range of coherent and noncoherent sources can be used. Laser sources include; dye lasers pumped by argon, or metal vapor lasers and frequency-doubled neodymium-doped yttrium aluminum garnet lasers (Nd: YAG). The nonlaser sources include tungsten filament, xenon arc, metal halide, and fluorescent lamps. New exciting developments such as light emitting diodes (LEDs) and femtosecond lasers are also being used [15].

1.3 Photosensitizers

The idea of using a dye as a ps came from an observation by Oscar Raab, a student of Professor H. Tappeiner at the Pharmacological Institute of the Ludwig Maximilian University of Munich, in the winter of 1897–1898. He noted that the toxic effect of acridine dye on paramecia was minimal on a day where there was a thunderstorm in comparison to its efficacy on a normal day. From this observation, he concluded that light, in some way, activates the acridine dye to kill paramecia. In other words, he hypothesized that acridine dye converts light into an active chemical energy, a finding that formed the basis of PDT [6] (Fig. 1.3).

Professor H. Tappeiner was considered one of the pioneers of photobiology. He introduced the term "Photodynamic Action" (*Photodynamische Wirkung*) in 1904. In 1903–1905, the von Tappeiner group started to investigate the efficacy of PDT on tumors and other skin diseases such as lupus of the skin and condylomata of the

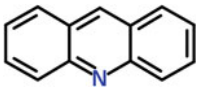

Fig. 1.3 Acridine general structure

female genitalia using different dyes such as eosin, fluorescein, sodium dichloroanthracene disulfonate and Grubler's Magdalene red. These dyes were mostly applied topically; however, in some cases, intratumoral injections were also attempted. Results of these studies were favorable [6]. In 1905, H. Tappeiner and H. Jesionek investigated the effect of the ps, eosin (Fig. 1.4), on facial basal cell carcinoma after long-term exposure either to sunlight or arc-lamp light (Fig. 1.5). This treatment caused total tumor resolution and a 12-month relapse-free period in two-thirds of the patients. Tappeiner's group later performed several studies on PDT and found out that the underlying mechanism of PDT involved ROS which implied that oxygen was required for this kind of therapy [16].

The most important event in the advance of PDT is the discovery and development of hematoporphyrin (hp) (Fig. 1.6). It was produced by Scherer as an impure form when he separated iron from dried blood by the addition of sulfuric acid in 1841. The spectrum and florescence of this compound were then described by Thudichun in 1867 and in 1871 Hoppe-Seyler gave it its name. The photodynamic properties of hp were studied on paramecia, erythrocytes, mice, guinea pigs and humans after exposure to sunlight in the period of 1908–1913 [6]. In 1908, Hausmann started performing experiments on hp toxicity [13]. Soon after, he performed experiments on white mice and realized that the phototoxic effects were dependent on the ps and light doses. He hypothesized that these phototoxic effects led primarily to peripheral tissue damage [17]. Studying the phototoxic effect of hp on humans was first attempted by the German doctor Friedrich Meyer Betz in 1912. He self-administered 200 mg intravenously and then exposed himself to sunlight. Due to the phototoxic effect of hp, he suffered from edema and hyperpigmentation for more than 2 months following the injection [6] (Fig. 1.7).

The next important phase in the discovery of hp was the observation of its tumor-localizing properties. In 1924 Policard first observed that UV radiation produced red fluorescence in experimental rat sarcomas and hypothesized that the fluorescence was associated with endogenous hp accumulation. He associated this accumulation with the secondary infection of hemolytic bacteria [6]. However, years later, when Kordler observed similar fluorescence in other tumors not involving bacteria (breast carcinoma), it was realized that the fluorescence was due

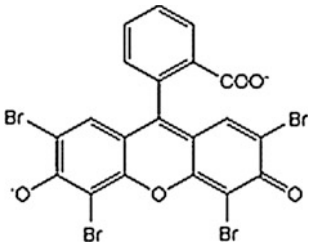

Fig. 1.4 Eosin **Y** structure

Fig. 1.5 Eosin on facial basal cell carcinoma after long-term exposure either to sunlight or arc-lamp light

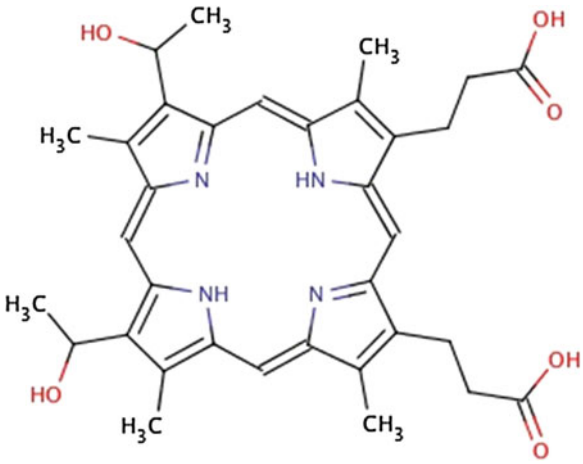

Fig. 1.6 Hematoporphyrin structure

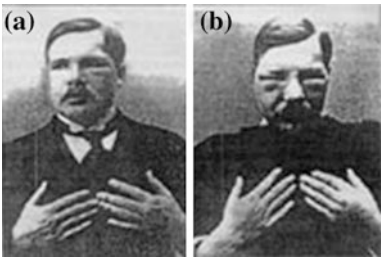

Fig. 1.7 Meyer Betz self administration of hematoporphyrin, 1912. *Sources* Tappeiner, Jesionek. Therapeutische versuche mit fluoreszierenden Stoffen// Munch. Med. Wschr.—1903.—Vol. 50.—P. 2042–2044

to the presence of endogenous porphyrins. In 1942, Auler and Banzer were most likely the first to study the accumulation of injected porphyrins in tumors. They injected tumor-bearing rats with hp and found out that it accumulated in primary and metastatic tumors as well as in lymph nodes. When the rats were exposed to light, promising results were observed [6]. In 1948, Figge and coworkers proposed the use of porphyrins as a treatment for cancer when they observed the high affinity of porphyrins toward not only malignant cells, but also all rapidly dividing cells including embryonic and regenerating cells [18]. This implied that sensitive organs

were protected from being damaged by radiation. In the 1950s, Richard Cremer introduced the treatment of jaundice in newborn babies using phototherapy [6].

The following phase was the discovery of hematoporphyrin derivatives "HpD". It was a giant step forward in the evolution of PDT. This was done by S. Schwartz who was the first to observe that hp itself was impure and consisted of a mixture of porphyrins and other impurities. S. Schwartz managed to separate them by treatment with a mixture of concentrated sulfuric and acetic acid. He found out that hp itself had poor tumor-localizing properties and was a weak phototoxic agent compared to other components in the mixtures "which were later called, HpD". These derivatives were two times more phototoxic than hp itself [6]. HpD was used to diagnose tumors by S. Schwartz, in the year 1960 [19]. In the same year, Lipson and Baldes carried out a study where they concluded that systemic HpD followed by endoscopic control should be used for diagnosis of tumors [6]. A few years later, in 1966, Lipson and coworkers investigated the potential selective and destructive effect of HpD on an extended recurrent ulcerated cancer of the mammary gland in a female patient after exposure to filtered light from a xenon lamp [20]. In 1976, J. F. Kelly and M. E. Snell examined the efficacy of HpD against human bladder tumors implanted in immunocompromised mice and pronounced selective tumor destruction was observed [6, 21].

The modern era of PDT began with the pioneering work of Dougherty and coworkers at the Roswell Park Memorial Cancer Institute in Buffalo in the 1970s. They started purification of HpD by removing the monomers and called the product Photofrin. Later, in 1978, they used HpD for cutaneous or subcutaneous cancer treatment using lasers as an alternative to arc lamps since lasers have the advantage of using flexible fibers [5, 6, 16] to avoid damage of normal skin since large HpD doses were required for extended tumors [22].

The *Ammi majus* plant, another natural ps, which was used by the Ancient Egyptians, was analyzed by Fahmy et al. an Egyptian pharmacologist, for its constituents and found that it contained the natural anaerobic photosensitizers psoralens (furocumarins), namely 8-methoxypsoralen "8-MOP" and 5-methoxypsoralen (5-MOP) [10]. El Mofty started to treat vitiligo patients with 8-MOP and sun exposure. The mechanism was found to be based on the photo-activation of psoralens, which, when active, induce vesiculation in the skin and cause re-epithelialization and repigmentation of depigmented skin [23] (Fig. 1.8).

After Fahmy et al. separated 8-MOP, PUVA (Psoralens + UVA treatment) appeared by the year 1974 [24]. PUVA was a combined treatment of 8-MOP and Ultraviolet-A phototherapy [25]. 8-MOP was the most important compound from the psoralen plant extract, since it was discovered that it inhibits the DNA S-phase "synthesis phase" of the cell cycle. Therefore, it began to be used for the treatment of psoriasis [26]. There are three forms of this treatment (oral, topical, and bath PUVA) [25, 26]. As this issue gained more interest, Honigsmann used 5-MOP as an alternative to 8-MOP to reduce the incidence of side effects [27]. However, side effects due to UV-A compared to those of UV-B were still apparent, namely the increased risk of melanoma and nonmelanoma skin cancer [28]. After that the use of PUVA started to decline with the development of narrowband UV-B, which is

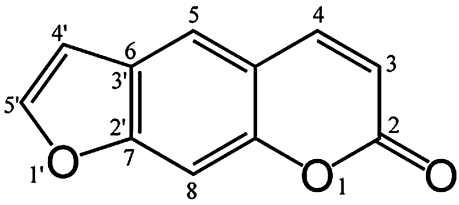

Fig. 1.8 Psoralens structure

much more effective and safer than UV-A and broadband UV-B. Moreover, it is well tolerated by patients when taken at sub-erythemogenic doses. Therefore, it represents an important modality for treatment of psoriasis [29].

Recently, ps were categorized according to direct chemical structure into three broad families: Porphyrin, Chlorines and Dyes. The first family consists of hp and its derivatives e.g., Photofrin, Photosan and Photocan [30]. They differ in the fractions of their monomers, dimers and oligomers [15]. From the photosynthesis process (the primary natural process that involves light), the second family, chlorophyll-like substances named chlorines, was discovered. The degradation products of chlorophyll, the purines and chlorophyll-like substances in bacteria and algae, e.g., bacteriochlorins were also found to possess excellent photosensitizing properties. The third family, which was discovered earlier but is still of great potential, are the dyes discovered by Raab in 1897 e.g., Phthalocyanine and Naphthalocyanine [30].

These families can be further categorized into three generations. Examples of first-generation ps from the porphyrin family are hp (and its derivatives) which are comprised of endogenous ps originating from cells that produce their own ps [31]. Examples of second-generation ps are Chlorin e6 "Ce6" (Chlorines), Phthalocyanine and Naphthalocyanine (Dyes), among others. The third generation includes monoclonal antibodies that bind selectively to an antigen on cancer cells, which is still in progress [30, 31].

Many ps' have been synthesized or discovered. These ps' have different characteristics and different benefits. Therefore throughout the years, various studies have taken place in order to explore new clinical applications, as well as to investigate each ps. Each ps has its own history of studies that explains its uses and development and will be represented throughout the rest of the chapter.

1.4 Hematoporphyrins and its Derivatives

Hp is one of the most important and widely used ps known. Therefore, many studies have been performed to investigate the effect of this Ps for different applications. Studies using HpD go back as early as 1980 when Perria et al. who was the first to use PDT in the treatment of human gliomas, concluded that high dose photoradiation of HpD could be used as an adjuvant to radiotherapy and surgery and have no further complications [32]. Further studies throughout the

years have been done by different scientists to compare HpD efficacy in PDT. The results of one of these studies concluded that porphyrins achieve selective tumor killing and sparing of normal brain with a maximal depth of tumor, as mentioned by Karagianis et al. in 1996 [33]. In 2003, Szurko et al. found out that the photodynamic action of different types of porphyrins was able to inhibit growth of melanoma at nontoxic concentrations when cell death was caused by necrosis [34]. Studies made by Daicoviciu et al. in 2010, where they evaluated rats subcutaneously administered with Walker 256 carcinoma. They demonstrated that porphyrins could be used efficiently in in vivo PDT treatment [35]. More studies are being examined daily. One of the latest is a study by Li et al. in 2013 examining the effect of hematoporphyrin monomethyl ether "HMME"-mediated PDT, which is a promising porphyrin-related ps, on the mitochondria of canine breast cancer cells. Results attributed damages of mitochondrial structure and mitochondrial dysfunction [36].

1.4.1 Photofrin

Although hp is an important photosensitizer, we cannot neglect the importance of other photosensitizers. One of the widely used derivatives of hp is photofrin. Attention has been drawn to it in a number of studies, from the 1980s until modern day. A study performed by Muller and Wilson in 1995 showed that photofrin-PDT prolonged the survival of patients suffering from malignant gliomas [37]. In 2000, Marks et al. performed phase I/II trial on patients with recurrent pituitary adenomas and outcomes were very satisfying with improvement of visual acuity or field defects in majority of the patients, along with a decrease of hormone levels in functional adenoma patients, and a reduction of tumor volume [38]. Saczko et al. conducted an in vitro study in 2005 that showed that the percentage of apoptotic cells in human Beidegröm Melanoma "BM" cell lines increased when the period of irradiation or the concentration of photofrin increased [39]. Moreover, an interesting preclinical study in 2006, performed by Gomer et al. showed that Photofrin-mediated PDT strongly activated angiogenic growth factors, proteinases and Cyclooxygenase-2 "COX 2" derived prostaglandins within the tumor microenvironment. Therefore, it has been reported that, to enhance the effectiveness of PDT, inhibitors of such angiogenic and proinflammatory pathways should be used [40].

1.4.2 Endogenous Photosensitizers

Endogenous photosensitizers are an interesting type of photosensitizers that are found in the body. Examples of these Ps are Ribofalvin (vitamin B_{12}) [41] and Protoporphyrin IX (Pp IX). PpIX is an intermediate of heme synthesis; its

physiological concentration is low due to the controlled expression of its precursor 5-Aminolevulinic acid ALA whose expression is controlled through feedback via Heme concentration. ALA is a prodrug that is enzymatically converted to the active ps PPIX. Exogenous administration of ALA breaks the feedback control, causing the accumulation of PpIX [31] (Fig. 1.9).

Many studies have been performed regarding the use of endogenous ps in treating different tumors such as brain tumors. In 1998 Lilge et al. found that ALA-induced PpIX is useful for treating most adult intracranial neoplasms photodynamically [42]. In 2003, Stummer et al. examined new methods for the complete removal of malignant gliomas, which cannot be easily achieved by normal radical resections. One of the methods was removal of the glioma, then administration of the metabolic precursor 5-ALA, which appeared to be advantageous [43]. A few years later, Stummer et al. performed another study; results indicated that complete resection of gliomas was enhanced by aid of the fluorescence mediated by ALA, which, in turn, enhanced progression-free survival [44]. In 2006, Nowis et al. performed a study using a DNA-microarray analysis, heme oxygenase-1 "HO-1" induction was observed in colon adenocarcinoma cells that showed an increased resistance to PDT. When an inhibitor of heme oxygenase -1, zinc (II) propoporphyrin IX was used, the effect of PDT treatment was enhanced [45]. Further studies were done in 2007 on the ps ALA by Karmakar et al. They utilized ALA to induce apoptosis of human malignant glioblastoma photodynamically and study the underlying mechanism of apoptosis. The results of their experiment indicated activation of proteolytic pathways, and investigated the mechanism of action [46].

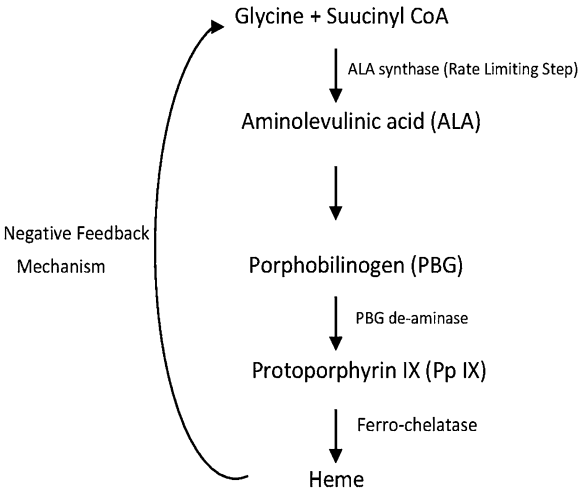

Fig. 1.9 Synthesis of protoporphyrin IX. *Sources* Meyer-Betz Untersuchungen über die biologische (photodynamische) Wirkung des Hämatoporphyrins und andere Derivate des Blut- und Gallenfarbstoffes. Dtsch Arch Klin Med 1913; 112: 476–503

1.4.3 Second-Generation Porphyrins

Since porphyrin-based ps have dominated the PDT field, there has been further progress regarding PDT as a treatment method in various studies. Thereby, the development of new ps has been essential. These newly discovered ps include second-generation porphyrins and porphyrin derivatives as well as third-generation ps which have arisen with the aim of alleviating the problems encountered with first-generation porphyrins and improving the efficacy of PDT. In 1999, Schmidt et al. investigated the possible use of a second-generation ps called benzoporphyrin derivative "BPD" in PDT using the LED technology. Their results illustrated that BPD and LED light sources minimize toxicity of normal brain tissue at doses that can cause glioma cell apoptosis in vitro when used at proper concentrations and light doses. Results suggested that BPD is a possible new-generation ps that could be used for the treatment of different malignant brain disorders [47].

Verteporfin

Verteporfin (Fig. 1.10) is a second-generation benzoporphyrin derivative that is indicated for the treatment of patients with predominantly classic subfoveal choroidal neovascularization due to age-related macular degeneration, pathologic myopia, or presumed ocular histoplasmosis [48].

Studies were performed on the use of verteporfin to treat lesions that don't respond to conventional therapy such as choroidal melanoma. Hu et al. in 2002 used a liposomal preparation of verteporfin against pigmented choroidal melanoma and evaluated tumor destruction suggesting that PDT can be used for the management of the tumors [49]. Then, in 2003, Barbazetto et al. performed an experiment on patients who did not respond to previous conventional therapy such as brachytherapy and transpupillary thermotherapy. Their results indicated that PDT may have the potential to manage choroidal melanoma; however, additional studies are required to prove this [50]. By the year 2005, a study applied PDT using verteporfin to animals with choroidal melanoma, and the animals responded to the treatment [51]. These studies conclude that PDT along with the use of Verteporfin can be used for the management of choroidal melanoma.

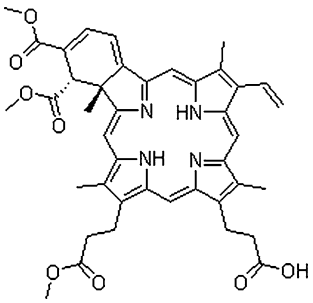

Fig. 1.10 Verteporfin structure

1.5 Chlorines

Throughout the years, different chlorophyll analogues have been discovered or developed such as the first-generation bacteriochlorins or second and third-generation ps, e.g., chlorin e6.

1.5.1 Bacteriochlorin

Some studies using these chlorophyll analogues focused on melanoma. In 2010, it was shown by Baldea et al. that PDT may be used as a method of treatment against melanoma, however, high melanin levels in melanomas can adversely affect PDT effectiveness and since the absorption of melanin is on the blue region of light, the photodynamic efficacy significantly decreases with photosensitizers in this absorption region. Another reason is the known antioxidant ability of melanin and its inhibition of ROS [52]. In the same year, Mroz et al. performed a study which demonstrated that three newly introduced bacteriochlorins overcame melanoma resistance successfully. They also proved that bacteriochlorins are superior to other ps such as Photofrin. [53]. Dabrowski et al. in 2012, studied the effect of sulfonamide bacteriochlorin on melanoma on mice injected with the ps intraperitoneally and observed improvement in the median tumor growth delay, as well as better selectivity of the sulfonamide bacteriochlorin [54].

1.5.2 Chlorin e6 (Ce6)

Figure. 1.11 has been widely used as a second- and third-generation photosensitizer [55]. It is a reduced porphyrin, which is why they are structurally similar. Ce6 is a promising representative of the chlorines platform [56] since it has many advantages including low toxicity, easy synthesis and production, fast and sufficiently selective accumulation in target tissue, and higher photosensitizing efficacy over porphyrins or photofrin [55]. For these reasons, many researchers have made efforts to prepare and utilize Ce6 alone and with different carriers.

In 1991, Bachor et al. investigated the difference in effect between free Ce6 and microsphere-bound Ce6 “Ce6-MS” on human bladder carcinoma. It was found that Ce6-MS was more efficient than free Ce6 in causing photodynamic destruction of human bladder carcinoma cells due to both the higher uptake and different mechanism of action of Ce6-MS. Furthermore, Ce6-MS are retained for a longer period of time intracellularly than are free Ce6 [57]. A study was carried out in 1997 by Schmidt et al. where low-density lipoprotein “LDL” was used as a carrier molecule. Results of this study showed that LDL-Ce6 conjugate increased the efficiency and selectivity of PDT [58]. Another study was performed in 2000, by

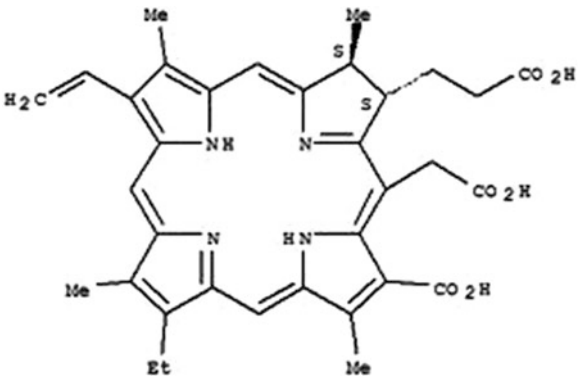

Fig. 1.11 Chlorin-e6 structure

Gijsens et al. on breast adenocarcinoma using the conjugate Sn-Ce6 in order to achieve selective targeting to the breast adenocarcinoma cells which are known to over express epidermal growth factor "EGF" receptors. This led to the hypothesis that these receptors could be used as a carrier for SnCe6. It was concluded that the conjugates caused specific and potent photodynamic activity on the cells [59]. In a study performed in 2001, Hamblin et al. found that Ce6 has increased phototoxicity in ovarian cancer cells when attached to polyethylene glycol "PEG" [60]. In 2004, results of a study performed by Sheleg et al. that evaluated the effect of Ce6 on skin metastases showed that there was complete regression and no recurrence during the study period after single or multiple PDT courses [61]. Jeong et al. 2011, performed a study that showed that the Ce6 conjugated to human serum albumin "HSA" has a more specific biodistribution toward tumor tissues and enhanced therapeutic results compared to the free form [62].

1.5.3 Chlorophyll Derivatives (CpD)

Abdel-Kader and his coworkers have recently focused their research on the newly discovered photosensitizer consisting of chlorophyll derivatives "CpD" for both oncological and nononcological uses. These ps are appealing because they can be easily obtained from natural resources. CpD have many advantages over other ps. It was found that the wavelength applicable (670 nm) to CpD was longer than that of HpD (630 nm) which meant that tissue penetration of CpD would be better than that of HpD. Also, superior cytotoxicity and higher cellular concentration were noted when CpD were used [63]. In 2012, Gomaa et al. examined the efficacy of PDT using CpD on a breast cancer cell line. Results proved that chlorophyll derivatives are a better candidate for breast cancer cell toxicity, because of its higher efficacy at tumor cell killing as well as its safety to normal cells. As illustrated from the results of the karyotyping and FISH technique, CpD is non-mutagenic and nontoxic to living cells [64].

1.5.4 Photochlor (HPPH)

Photochlor, or 2-[1-hexyloxyethyl]-2-devinyl pyropheophorbide-alpha "HPPH" (Fig. 1.12) is a lipophilic, second-generation, chlorin-based ps. In 2001, Lobel et al. used HPPH or Photochlor in an in vivo study for treating rat malignant gliomas using PDT. They concluded that HPPH localized in tumor cells more than in normal brain cells and could be used as adjuvant therapy in treating gliomas [65].

1.5.5 Temoporfin (mTHPC)

Temoporfin, m-tetrahydroxyphenylchlorin "mTHPC" (Fig. 1.13) is a second-generation ps (based on chlorin) used in PDT mainly to treat squamous cell carcinoma of the head and neck. It is promoted by its brand name Foscan in the European Union. Temoporfin is photoactivated at 652 nm by red light. Patients can remain photosensitive for several weeks after treatment. In many regards mTHPC fits many of the requirements of an ideal ps, and thus may be regarded as ''better'' than Photofrin. It can be prepared as a chemically pure compound and shows enrichment in tumor versus normal tissue. In addition, mTHPC requires smaller quantities for administration, shorter treatment times, and a lower light dose to achieve the desired PDT response [66]. Biel et al. in 2002 evaluated tumor response using Foscan-PDT in patients with recurrent head and neck cancer. Results were found to be a therapeutic option of significant benefit to patients with advanced head and neck cancer [67]. Campbell et al. in 2004 carried out a study demonstrating that mTHPC-PDT is a useful initial treatment for vulval intraepithelial neoplasia type III "VIN III" and has a very significant benefit over surgery. Patients were injected with mTHPC intravenously and the area of VIN was irradiated with a diode laser. They were evaluated at different time intervals after treatment and results showed no recurrence of VIN at the original site in all patients reviewed. [68]. In 2012, Sayed et al. investigated foscan, its derivatives and their photocytotoxicity in human hepatocellular carcinoma "HCC". Results showed that Foscan and its derivatives can effectively induce early apoptotic

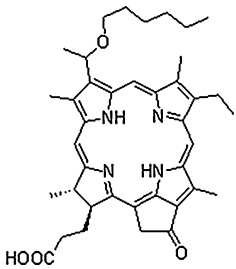

Fig. 1.12 Photochlor structure

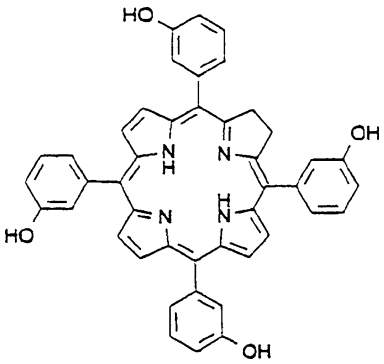

Fig. 1.13 Temoporfin structure

responses in HCC cells [69]. In 2013, Sherifa et al. performed another study on the novel ps, Fospeg®, which is a liposomal formulation of the photosensitizer Foscan® (commercial name of mTHPC). The results indicate that fospeg-mediated PDT is a promising strategy for treatment of HCC and needs to be further explored in vivo [70].

1.5.6 Talaporfin

More ps were investigated in 2008 for their potential use of PDT in brain tumors. One of these was talaporfrin (Fig. 1.14), a second-generation ps derived from chlorophyll.

Namatame et al. investigated a combination of talaporfin sodium "TS" and they came to the conclusion that talapofrin-PDT caused apoptosis as well as coagulation necrosis in rat C6 glioma [71]. Also, in 2013, Tsutsumi et al. demonstrated that TS-induced glioma cell line apoptosis in a dose-dependent manner [72].

1.6 Dyes

As previously mentioned, Oscar Raab was the first to propose the use of dyes as photosensitizers. Later, von Tappeiner performed studies using different types of dyes to examine the efficacy of PDT. The most common dyes used now are phthalocyanines, which belong to the second-generation ps, phthalocyanine demonstrates higher absorption in the 650–800 nm range and short tissue accumulation [73]. They are relevant for clinical use due to their strong absorption in the far-red spectral band [6]. In 2007, Kolarova et al. preformed a study using- Chloro-Aluminium phthalocyanines "ClAlPcS" along with a semiconductor laser (as the light dose). This procedure was shown to have a lethal effect on melanoma cells [74]. In 2010, Robertson et al. concluded that the new ps metallophthalocyanine "MPc",

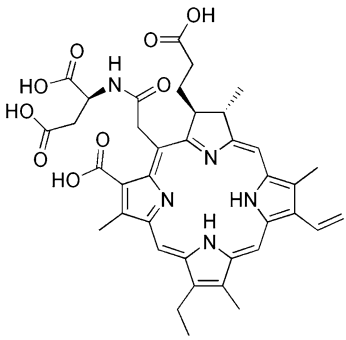

Fig. 1.14 Talaporfin structure

in combination with laser, produced a better outcome in malignant melanoma destruction and had ideal ps characteristics [75]. In 2011, Maduray et al. performed an in vitro study on different cells with the aim of investigating the possible cytotoxic effects of the water-soluble photosensitizer zinc tetrasulfophthalocyanines "ZnTSPc". It was concluded that when ZnTSPc is used in low concentrations and activated by the proper light dose it results in the death of the melanoma cells while sparing the healthy tissues from such damage [76].

1.7 Conclusion

Phototherapy is a treatment modality that dates back to ancient times. The different investigations and studies that have been performed throughout the years have led to its development and given us the PDT we know today. It is now considered a promising, less invasive treatment method of malignant and premalignant diseases and has been approved for the treatment of certain types of neoplasms. The field of PDT is now so large and the growing scientific understanding of the underlying photochemistry, biology, and physiology of PDT should be taken advantage of for the development of new and better clinical treatments. If more research studies were performed to help identify new indications as well as to expand those already existing, this may help propagate the awareness of PDT and its usefulness among the general public. PDT will have a great future if we are successful in making it better known. Since we are in the era of proof based science, it is expected that much effort will be put into studies and research on PDT, so that one day we can live in a world with accepted consensus on PDT. Each successful research and treatment will be an addition to patients and to the world of science and human-beings.

References

1. Wang SS, Chen J, Keltner L, Christophersen J, Zheng F, Krouse M, Singhal A (2002) New technology for deep light distribution in tissue for phototherapy. Cancer J 8:154–163
2. Dougherty TJ, Gomer CJ, Henderson BW, Jori G, Kessel D, Korbelik M, Moan J, Peng Q (1998) Photodynamic therapy. J Natl Cancer Inst 90:889–905
3. Huang Z (2005) A review of progress in clinical photodynamic therapy. Technol Cancer Res Treat 4(3):283–293
4. Agostinis P, Berg K, Cengel KA, Foster TH, Girotti AW, Gollnick SO, Hahn SM, Hamblin MR, Juzeniene A, Kessel D, Korbelik M, Moan J, Mroz P, Nowis D, Piette J, Wilson BC, Golab J (2011) Photodynamic therapy of cancer: an update. CA Cancer J Clin 61:250–281
5. Daniell MD, Hill JS (1991) A history of photodynamic therapy. Aust N Z J Surg 61:340–348
6. Moan J, Peng Q (2003) European society photobiology. Photodynamic therapy (comprehensive series in photochemical and photobiological sciences). Chapter 1: an outline of the history of PDT. The royal society of chemistry, pp 1–9
7. McDonagh AF (2001) Phototherapy: from ancient Egypt to the new millennium. J Perinatol 21:7–12
8. Needham J, Gwei-Djen L (1983) Science and civilisation in China, vol 5, part 5. Cambridge University Press, Cambridge, 12, p 181–184
9. Hobday R (1999) The healing sun: sunlight and health in the 21st century. Findhorn press, Scotland, p 90
10. Fahmy IR, Abu-Shady H (1948) Ammi majus Linn: The isolation and properties of ammoidin, ammidin and majudin, and their effect in the treatment of leukoderma. Q J Pharmacol 21:499–503
11. Koeing C (2005) Specilized Hydro-, Balneo- and medicinal bath therapy. iUniverse Inc., Bloomington, p 49
12. Milhench H (2007) Flavors of Slovenia: food and wine from central Europe's hidden gem. Hippocrene books, Inc., New York, p 121
13. Hausmann WH (1910) Die sensibilisierende Wirkung des Hamatoporphyrins. Biochem Z 30:276–316
14. Finsen NR (1903) Remarks on the red-light treatment of small-pox. Br Med J 1:1297
15. Brancaleon L, Moseley H (2002) Laser and non-laser light sources for photodynamic therapy. Lasers Med Sci 17:173–186
16. Jesionek H, Tappeiner H (1905) Zur Behandlung der Hautcarcinome mit fluoreszierenden Stoffen. Dtsch Arch Klin Med 82:223–226
17. Hausmann WH (1908) Die sensibilisierende Wirkung tierischer Farbstoffe und ihre physiologische Bedeutung. Wien Klin Wochenschr 21:1527–1529
18. Figge FHJ, Weiland GS, Manganiello OJ (1948) Cancer detection and therapy. Affinity of neoplastic, embryonic, and traumatized tissues for porphyrins and metalloporphyrins. Proc Soc Exp Biol Med 68:640–641
19. Lipson RL, Baldes EJ, Olsen AM (1961) The use of a derivative of hematoporphyrin in tumor detection. J Nat Cancer Inst 26:1–8
20. Lipson RL, Gray MJ, Baldes EJ (1966) Hematoporphyrin derivative for detection and management of cancer. In: Proceedings of the 9th international cancer congress. Tokyo, Japan, p 393
21. Dougherty TJ (1987) Studies on the structure of porphyrins contained in Photofrin II. Photochem Photobiol 46:569–573
22. Dougherty TJ (1989) Photodynamic therapy—new approaches. Semin Surg Oncol 5(1):6–16
23. El-Mofty AM (1968) Vitiligo and Psoralens. Pergamon Press, Oxford, p 147
24. Hönigsmann H (2013) History of phototherapy in dermatology. Photochem Photobiol Sci 12:16–21

25. Dawe RS, Cameron H, Yule S, Man I, Wainwright NJ, Ibbotson SH, Ferguson J (2003) A randomized controlled trial of Narrowband ultraviolet B vs. bath-psoralen plus ultraviolet a photochemotherapy for psoriasis. Br J Dermatol 148:1194–1204
26. Roelandts R (1991) The history of photochemotherapy. Photodermatol Photoimmunol Photomed 8:184–189
27. Hönigsmann H, Jaschke E, Gschnait F, Brenner W, Fritsch P, Wolff K (1979) 5-Methoxypsoralen (Bergapten) in photochemotherapy of psoriasis. Br J Dermatol 101:369–378
28. Stern RS, Nichols KT, Väkevä LH (1997) Malignant melanoma in patients treated for psoriasis with methoxsalen (psoralen) and ultraviolet A radiation (PUVA). The PUVA follow-up study. N Engl J Med 336:1041–1045
29. Barbagallo J, Spann CT, Tutrone WD, Weinberg JM (2001) Narrowband UVB phototherapy for the treatment of psoriasis: a review and update. Cutis J 68:345–347
30. Allison RR, Downie GH, Cuenca R, Hu X, Childs CJH, Sibata CH (2004) Photosensitizers in clinical PDT. Photodiagn Photodyn Ther 1(1):27–42
31. Nyokong T, Ahsen V (2012) Photosensitizers in medicine, environment, and security. In: Heuck G, Lange N (eds) Chapter 8: exogenously induced endogenous photosensitizers. Springer, New York, p 391
32. Perria C, Capuzzo T, Cavagnaro G, Datti R, Francaviglia N, Rivano C, Tercero VE (1980) Fast attempts at the photodynamic treatment of human gliomas. J Neurosurg Sci 24:119–129
33. Karagianis G, Hill JS, Stylli SS, Kaye AH, Varadaxis NJ, Reiss JA, Phillips DR (1996) Evaluation of porphyrin C analogues for photodynamic therapy of cerebral glioma. Br J Cancer 73:514–521
34. Szurko A, Kramer-Marek G, Widel M, Ratuszna A, Habdas J, Kus P (2003) Photodynamic effects of two water soluble porphyrins evaluated on human malignant melanoma cells in vitro. Acta Biochim Pol 50:1165–1174
35. Daicoviciu D, Filip A, Ion RM, Clichici S, Decea N, Muresan A (2010) Oxidative photodamage induced by photodynamic therapy with methoxyphenyl porphyrin derivatives in tumour-bearing rats. Folia Biol (Praha) 57:12–19
36. Li HT, Song XY, Yang C, Li Q, Tang D, Tian WR, Liu Y (2013) Effect of hematoporphyrin monomethyl ether-mediated PDT on the mitochondria of canine breast cancer cells. Photodiagn Photodyn Ther
37. Muller PJ, Wilson BC (1995) Photodynamic therapy for recurrent supratentorial gliomas. Semin Surg Oncol 11:346–354
38. Marks PV, Belchetz PE, Saxena A, Igbaseimokumo U, Thomson S, Nelson M, Stringer MR, Holroyd JA, Brown SB (2000) Effect of photodynamic therapy on recurrent pituitary adenomas: clinical phase I/II trial–an early report. Br J Neurosurg 14:317–325
39. Saczko J, Kulbacka J, Chwilkowska A et al (2005) The influence of photodynamic therapy on apoptosis in human melanoma cell line. Folia Histochem Cytobiol 43:129–132
40. Gomer CJ, Ferrario A, Luna M, Rucker N, Wong S (2006) Photodynamic therapy: combined modality approaches targeting the tumor microenvironment. Lasers Surg Med 38:516–521
41. Cardoso DR, Libardi SH, Skibsted LH (2012) Riboflavin as a photosensitizer. Effects on human health and food quality. J Food Funct 3(5):487–502
42. Lilge L, Wilson BC (1998) Photodynamic therapy of intracranial tissues: a preclinical comparative study of four different photosensitizers. J Clin Laser Med Surg 16:81–91
43. Stummer W, Reulen HJ, Novotny A, Stepp H, Tonn JC (2003) Fluorescence-guided resections of malignant gliomas–an overview. Acta Neurochir Suppl 88:9–12
44. Stummer W, Pichlmeier U, Meinel T, Wiestler OD, Zanella F, Reulen HJ (2006) ALA-Glioma study group. Fluorescence-guided surgery with 5-aminolevulinic acid for resection of malignant glioma: a randomised controlled multicentre phase III trial. Lancet Oncol 7:392–401
45. Nowis D, Legat M, Grzela T et al (2006) Heme oxygenase-1 protects tumor cells against photodynamic therapy-mediated cytotoxicity. Oncogene 25:3365–3374

46. Karmakar S, Banik NL, Patel SJ, Ray SK (2007) 5-Aminolevulinic acid-based photodynamic therapy suppressed survival factors and activated proteases for apoptosis in human glioblastoma U87MG cells. Neurosci Lett 415:242–247
47. Schmidt MH, Reichert KW 2nd, Ozker K, Meyer GA, Donohoe DL, Bajic DM, Whelan NT, Whelan HT (1999) Preclinical evaluation of benzoporphyrin derivative combined with a light-emitting diode array for photodynamic therapy of brain tumors. Pediatr Neurosurg 30:225–231
48. Dhalla MS, Blinder KJ, Wickens J (2006) Photodynamic Therapy with Verteporfin in Age-related Macular Degeneration. US Sens Disord Rev 7–12
49. Hu L, Wu X, Song Y, Young LH, Gragoudas ES (2002) Photodynamic therapy of pigmented choroidal melanomas in rabbits. Zhonghua Yan Ke Za Zhi 38:491–494
50. Barbazetto IA, Lee TC, Rollins IS, Chang S, Abramson DH (2003) Treatment of choroidal melanoma using photodynamic therapy. Am J Ophthalmol 135:898–899
51. Donaldson MJ, Lim L, Harper CA, Mackenzie JG, Campbell W (2005) Primary treatment of choroidal amelanotic melanoma with photodynamic therapy. Clin Exp Ophthalmol 33:548–549
52. Baldea I, Filip AAG (2010) Photodynamic therapy in melanoma-an update. J Physiol Pharmacol 63:109–118
53. Mroz P, Huang YY, Szokalska A et al (2010) Stable synthetic bacteriochlorins overcome the resistance of melanoma to photodynamic therapy. FASEB J 24:3160–3170
54. Dabrowski JM, Arnaut LG, Pereira MM, Urbanska K, Stochel G (2012) Improved biodistribution, pharmacokinetics and photodynamic efficacy using a new photostable sulfonamide bacteriochlorin. Med Chem Commun 3:502–505
55. Huang L, Zhiyentayev T, Xuan Y, Azhibek D, Kharkwal GB, Hamblin MR (2011) Photodynamic Inactivation of bacteria using polyethylenimine–chlorin(e6) conjugates: effect of polymer molecular weight, substitution ratio of chlorin(e6) and pH. Lasers Surg Med 43:313–323
56. Spikes J (1990) New trends in photobiology: chlorins as photosensitizers in biology and medicine. J Photochem Photobiol, B 6:259–274
57. Bachor R, Scholz M, Shea CR, Hasan T (1991) Mechanism of photosensitization by microsphere-bound chlorin e6 in human bladder carcinoma cells. Cancer Res 51:4410–4414
58. Schmidt-Erfurth U, Diddens H, Birngruber R, Hasan T (1997) Photodynamic targeting of human retinoblastoma cells using covalent low-density lipoprotein conjugates. Br J Cancer 75:54–61
59. Gijsens A, Missiaen L, Merlevede W, de Witte P (2000) Epidermal growth factor-mediated targeting of chlorin e6 selectively potentiates its photodynamic activity. Cancer Res 60:2197–2202
60. Hamblin MR, Miller JL, Rizvi I, Ortel B, Maytin EV, Hasan T (2001) Pegylation of a chlorin(e6) polymer conjugate increases tumor targeting of photosensitizer. Cancer Res 61:7155–7162
61. Sheleg SV, Zhavrid EA, Khodina TV et al (2004) Photodynamic therapy with chlorin e(6) for skin metastases of melanoma. Photodermatol Photoimmunol Photomed 20:21–26
62. Jeong H, Huh M, Lee SJ, Koo H, Kwon IC, Jeong SY, Kim K (2011) Photosensitizer-conjugated human serum albumin nanoparticles for effective photodynamic therapy. Theranostics 1:230–239
63. Park YJ, Lee WY, Hahn BS, Han MJ, Yang WI, Kim BS (1989) Chlorophyll derivatives–a new photosensitizer for photodynamic therapy of cancer in mice. Yonsei Med J 30:212–218
64. Gomaa I, Ali SE, El-Tayeb TA, Abdel-kader MH (2012) Chlorophyll derivative mediated PDT versus methotrexate: an in vitro study using MCF-7 cells. Photodiagn Photodyn Ther 9:362–368
65. Lobel J, MacDonald IJ, Ciesielski MJ, Barone T, Potter WR, Pollina J, Plunkett RJ, Fenstermaker RA, Dougherty TJ (2001) 2-[1-hexyloxyethyl]-2-devinyl pyropheophorbide-a (HPPH) in a nude rat glioma model: implications for photodynamic therapy. Lasers Surg Med 29:397–405

66. Senge MO, Johan C (2011) Brandt, Temoporfin (Foscan_,5,10,15,20Tetra(mhydroxyphenyl)chlorin) a second-generation photosensitizer. Photochem Photobiol 87:1240–1296
67. Biel M, D'Cruz A, McCaffrey T (2002) Foscan-mediated photodynamic therapy (PDT) in the palliative treatment of patients with advanced head and neck cancer incurable with surgery or radiotherapy. Proc Am Soc Clin Oncol, p 21
68. Campbell SM, Gould DJ, Salter L, Clifford T, Curnow A (2004) Photodynamic therapy using meta-tetrahydroxyphenylchlorin (Foscan) for the treatment of vulval intraepithelial neoplasia. Br J Dermatol 151:1076–1080
69. Sayed O, Zekri AN, Bahnasawy A, Ghaffar R, Khaled H, Abdel-Kader RM, Abdel Aziz AI, Abdel-Kader MH (2012) Foscan derivatives induce intrinsic appoptosis of human hepatocellular Carcinoma. 4th international meeting of the European platform for photodynamic medicine (EPPM) Brixen/Bressanone. South Tyrol, Italy, 2012
70. Sherifa G, Saad Zaghloul MA, Elsayed OF, Rueck A, Steiner R, Abdelaziz AI, Abdel-Kader MH (2013) Functional characterization of Fospeg, and its impact on cell cycle upon PDT of Huh7 hepatocellular carcinoma cell model. Photodiagn Photodyn Ther 10:87–94
71. Namatame H, Akimoto J, Matsumura H, Haraoka J, Aizawa K (2008) Photodynamic therapy of C6-implanted glioma cells in the rat brain employing second-generation photosensitizer talaporfin sodium. Photodiagn Photodyn Ther 5:198–209
72. Tsutsumi M, Miki Y, Akimoto J, Haraoka J, Aizawa K, Hirano K, Beppu M (2013) Photodynamic therapy with talaporfin sodium induces dose-dependent apoptotic cell death in human glioma cell lines. Biol Pharm Bull 36:215–2
73. Jia X, Jia L (2012) Nanoparticles improve biological functions of phthalocyanine photosensitizers used for photodynamic therapy. Curr Drug Metab 13:1119–1122
74. Kolarova H, Nevrelova P, Bajgar R, Jirova D, Kejlova K, Strnad M (2007) In vitro photodynamic therapy on melanoma cell lines with phthalocyanine. Toxicol In Vitro 21:249–253
75. Robertson CA, Abrahamse H (2010) The in vitro PDT efficacy of a novel metallophthalocyanine (MPc) derivative and established 5-ALA photosensitizing dyes against human metastatic melanoma cells. Lasers Surg Med 42:766–776
76. Maduray K, Karsten A, Odhav B, Nyokong T (2011) In vitro toxicity testing of zinc tetrasulfophthalocyanines in fibroblast and keratinocyte cells for the treatment of melanoma cancer by photodynamic therapy. J Photochem Photobiol, B 103:98–104

Part II
Theory and Mechanism

Chapter 2
Fundamentals of Photophysics, Photochemistry, and Photobiology

Ulrich E. Steiner

Abstract This chapter provides an introduction to the photophysical and photochemical fundamentals that should represent a useful scientific background for applicants of photodynamic therapy (The references given in the abstract provide some access to generally recommended textbooks or reviews of the various areas.). First, the absorption of light and the basics of spectrophotometry (Parson in Modern Optical Spectroscopy. With exercises and examples from biophysics and biochemistry. Springer-Verlag, Berlin Heidelberg, 2007; Burgess and Frost in Standards and best practice in absorption spectrometry. Blackwell Science, London, 1999; Gore in Spectrophotometry and Spectrofluorimetry. Oxford University Press, Oxford, 2000) are dealt with, including a theoretical background to understand absorption spectra. Then follows a survey of photophysical processes with the characteristic pathways of radiationless and radiative decay of electronically excited states (Lakowicz in Principles of fluorescence spectroscopy. Springer Science+Business Media, New York, 2006), electronic energy transfer and a brief introduction into singlet oxygen (Schweitzer and Schmidt, Chem Rev 103:1685–1757, 2003). The photochemistry part (Turro et al. in Principles of molecular photochemistry: an introduction. University Science Books, Sausalito, 2009; Klán and Wirz in Photochemistry of organic compounds. From concept to practice. Wiley, Chichester, 2009; Stochel et al. in Bioinorganic Photochemistry, Wiley, Chichester, 2009) explains the concept of photoreactions as excited state chemistry and changes of chemical properties and chemical reactivity as a consequence of the modified electronic structure in the excited state. Elementary processes dealt with comprise photoinduced electron transfer (Kavarnos in Fundamentals of photoinduced electron transfer. VCH Publishers, New York, 1993), excited state proton transfer and *cis/trans*-photoisomerization. Photobiological aspects, such as photosynthesis and vision (Kohen et al. in Photobiology.

U. E. Steiner (✉)
Department of Chemistry, University of Konstanz, D-78457 Konstanz, Germany
e-mail: ulrich.steiner@uni-konstanz.de

M. H. Abdel-Kader (ed.), *Photodynamic Therapy*,
DOI: 10.1007/978-3-642-39629-8_2,

Academic Press, San Diego, 1995; Batschauer in Photoreceptors and Light Signaling. Comprehensive Series in Photochemical and Photobiological Sciences. The Royal Society of Chemistry, Cambridge, 2003), are briefly outlined.

2.1 Photophysics

2.1.1 Light and Color

Their specific colors are one of the important sensory properties of chemical compounds. In nature, the green of leaves, the yellow, red and blue of flowers, and the red of blood are prominent indicators of chlorophyll, flavonoids, anthocyanins, and hemoglobin, respectively. What our vision senses as uniform, single colors, is usually the impression of light that can still be decomposed into a spectral continuum of colors by the optical effect of dispersion exhibited by a prism or a grating. Spectrally pure light is characterized as electromagnetic radiation of a definite wavelength λ. The range of wavelengths from about 400 nm to about 750 nm represents the visible part of the electromagnetic spectrum (Fig. 2.1), that extends from the region of γ-rays at the short wavelength end to the region of radio waves at the long wavelength end.

The characteristic color of a chemical compound is due to its characteristic absorption of parts of the visible spectrum from the ambient white light. The remaining transmitted or remitted spectral mixture of light determines the color

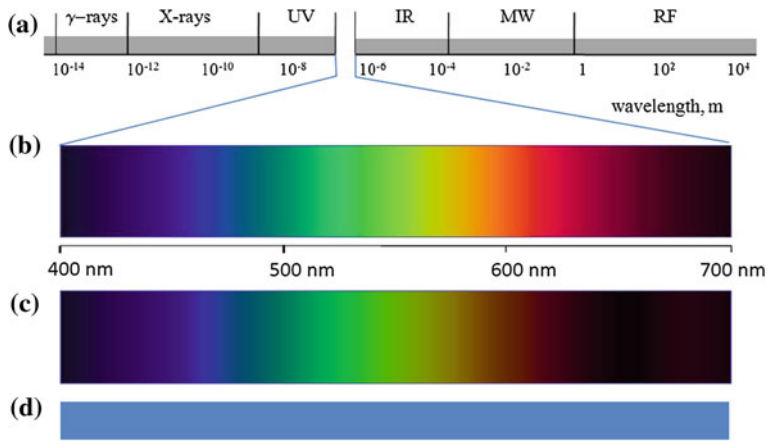

Fig. 2.1 **a** Regions of the electromagnetic spectrum and localization of the UV/vis range, **b** colors of the visible spectrum of a white light source, **c** colors of the visible spectrum after transmission through a solution of methylene *blue*, **d** perceived color of the methylene *blue* solution

that we see. However, it is the spectral characteristics of the *absorbed* light that carries the essential information on the electronic structure of the molecules and their concentration if we are dealing with dilute systems such as solutions. Quantitative measurements of the absorption characteristics in the UV to near infrared define the realm of UV/vis spectrophotometry or, in another term relating to the underlying physical process: electronic absorption spectroscopy.

2.1.2 Spectrophotometry

The most convenient way to measure the absorption characteristics of a chemical compound is by employing a homogenous transparent solution in some solvent [1–3]. If the solution is dilute, it is usually justified to assume that the absorption characteristics are determined by the individual solute molecules. In a spectrophotometer, the transmission of light through a sample cuvette is measured as a continuous function of the wavelength. For relating the observed transmission to the absorption of the solute molecules it is important to eliminate any light attenuation effect due to the cuvette windows and the solvent. Such effects are due to reflection of some part of the incident light intensity at the outer and inner surfaces of the cuvette windows and to light scattering inside the solution (cf. Fig. 2.2). Therefore, it is convenient to compare the transmitted light of the sample cuvette to that of a similar reference cuvette containing only the solvent, thereby eliminating the role of all factors except for the absorption by the solute. If we denote the intensities transmitted behind the sample cuvette and the reference cuvette by I_S and I_R, respectively, when they are both hit by the same light intensity I_0, the transparence T as related to pure absorption is defined as

$$T = \frac{I_S}{I_R} \tag{2.1}$$

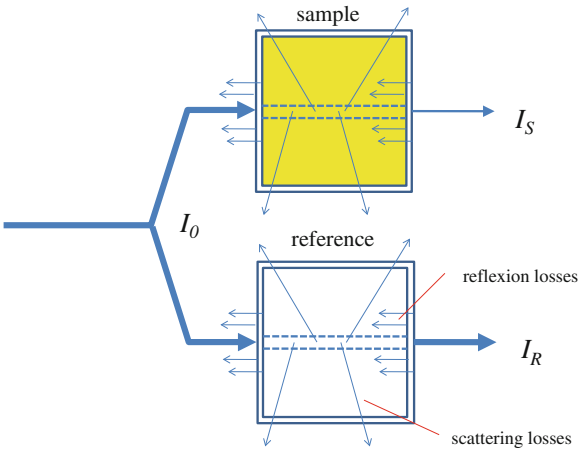

Fig. 2.2 Effects diminishing the transparency of a solution and separation of the absorption effect of the solute by comparing sample and reference

According to Lambert's law, T decreases exponentially with the optical path length d of the light (cf. Fig. 2.3):

$$T = 10^{-k \cdot d} \tag{2.2}$$

The attenuation factor k is specific for the given solute, its concentration and the wavelength of the light. According to Beer's law it is proportional to the concentration c of the absorbing compound:

$$k = \varepsilon(\lambda) \cdot c \tag{2.3}$$

Here $\varepsilon(\lambda)$ is the molar decadic absorption coefficient. Although the penetration of light into an absorbing medium does not come to an end sharply, as shown in Fig. 2.3, the typical "penetration depth" is conventionally characterized by a finite length, given by

$$d_p \equiv \frac{1}{k \cdot \ln 10} \tag{2.4}$$

After a path length d_p, the light intensity has dropped to about 37 % of its initial value.

Equation (2.3) is the basis for quantitative analytical determinations by photometry. Here it is customary to introduce the absorbance A as a new quantity which is directly proportional to the concentration c:

$$A \equiv k \cdot d = \varepsilon \cdot c \cdot d \tag{2.5}$$

Introducing this expression into Eq. (2.2) we arrive at Lambert–Beer's law

$$T = 10^{-A} \tag{2.6}$$

$$A = -\lg T \tag{2.7}$$

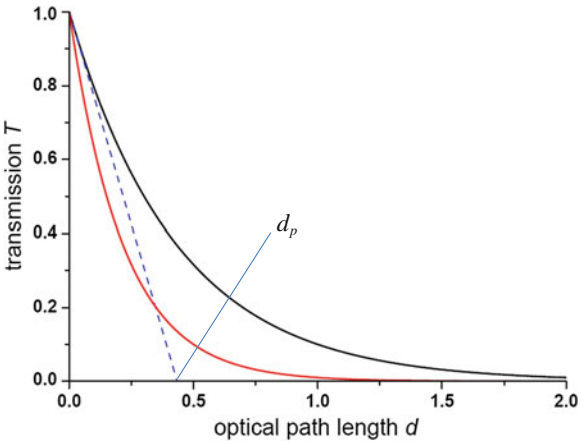

Fig. 2.3 Lambert's law for transmission T as a function of optical path length d for two attenuation factors $k = 1$ (*black curve*) and $k = 2$ (*red curve*). The *dashed line* indicates the definition of the "penetration depth" d_p

Customary spectrophotometers automatically record the wavelength dependence of the absorbance. Such records are called absorption spectra. Other than transmission spectra, they exhibit strict proportionality to the concentration of the sample at any wavelength (cf. Fig. 2.4). However, one should take care of spectral changes that may occur upon associations of molecules at higher concentrations.

2.1.3 Theoretical Basis of Absorption Spectra

The simplest appearance of absorption spectra is found for isolated atoms in the gas phase. These spectra exhibit isolated sharp absorption lines, i.e., very narrow ranges of wavelength where light absorption does occur. As was first shown by Bohr, these lines (more easily detected as emitted light after excitation of the atoms) reflect the pattern of energy quantization in the atoms. A key to his theory was Einstein's suggestion that the energy of light is quantized, whereby the energy E_{ph} of the light quanta (photons) is determined by the frequency v of the light:

$$E_{ph} = hv \tag{2.8}$$

Since, for a wave with frequency v and wavelength λ the following equation holds

$$v \cdot \lambda = c \tag{2.9}$$

where c is the speed of light, the photon energy can be also expressed by the wavelength

$$E_{ph} = \frac{h \cdot c}{\lambda} \tag{2.10}$$

According to Bohr's postulate, light can be only absorbed if the photon energy exactly matches the energy difference between two possible energy states n and m of the atom.

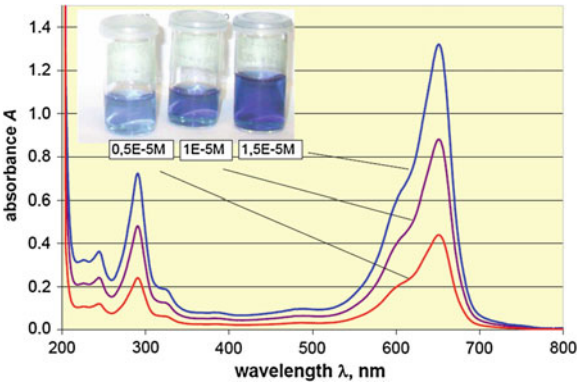

Fig. 2.4 Absorption spectra of methylene *blue* in methanol at three different concentrations. According to which the absorbance can be calculated from the measured transmission T by

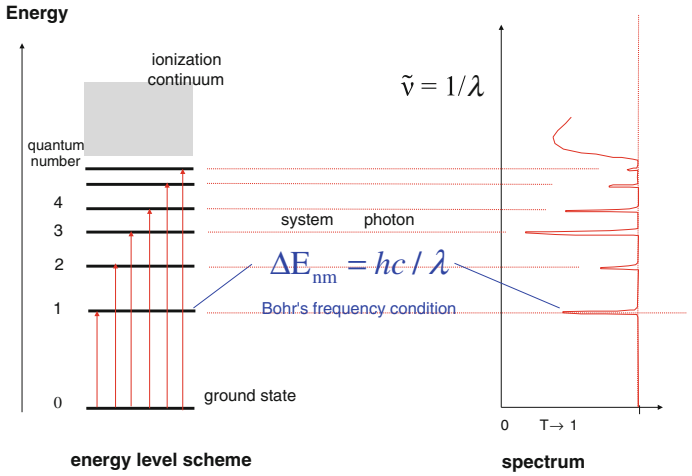

Fig. 2.5 Relation between absorption spectrum (*right*) and energy level scheme (*left*) in isolated atoms. The absorption spectrum, when plotted on a frequency scale, represents an image of the energy level scheme of the atom

$$\Delta E_{nm} = \frac{hc}{\lambda} \tag{2.11}$$

In case of an absorption spectrum, it is usually the energy spacing between the ground state, the *normal* state of the atom, and any of its higher (i.e., *excited*) states. These ideas are illustrated in Fig. 2.5.

In case of molecular compounds in condensed media, the typical appearance of the absorption spectrum is as shown for the example of methylene blue in Fig. 2.4. It is characterized by an almost continuous absorption across the full wavelength range, however structured by broad absorption peaks and broad minima. The absorption peaks exhibit spectral widths of some 50–100 nm and they differ in their absolute heights (intensities). The spectral regions of the peaks are termed absorption bands. In the following we will clarify three questions:

1. What determines the positions of the bands?
2. What determines the widths of the bands?
3. What determines the intensities of the bands?

The explanations are illustrated by Fig. 2.6. Here, a schematic absorption spectrum of chlorophyll a is plotted over a vertical axis. We realize that, with reference to Eq. (2.10), the scales of photon energy and wavelength run in opposite directions. As in the atomic case, in the molecular case, too, the energy scale of the absorbed light has to be seen against the energy scale of the molecular energy levels.

A molecular energy level scheme comprises much more levels than an atomic one, where energy can be only deposited in the form of electronic excitations. In molecules, the atoms can vibrate against each other. They can do so in N-6 modes

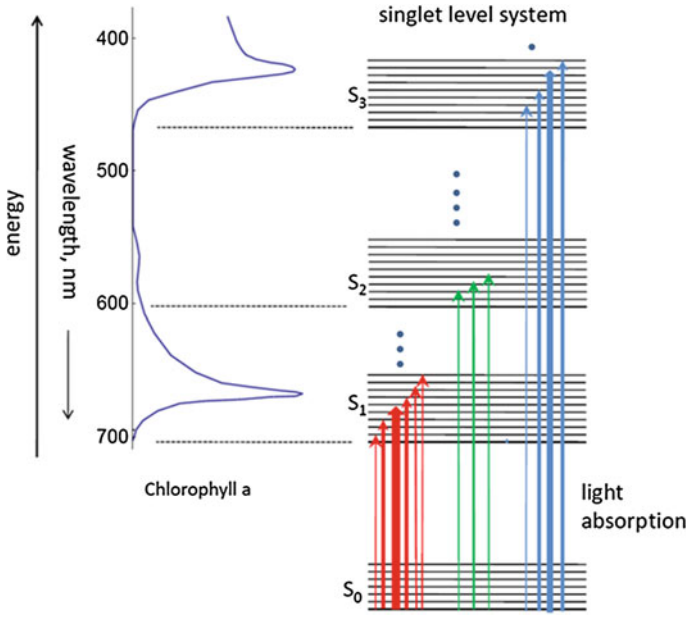

Fig. 2.6 Molecular energy level scheme and its relation to the molecular absorption spectrum. For details cf. text. Adapted with permission from Ref. [12], Schmidt W, Optische Spektroskopie, p. 58, Copyright © 2000 Wiley–VCH Verlag GmbH & Co KGaA

(*N*-5 in linear molecules). The vibrational energy of each of these modes is quantized in multiples of $h\nu_{vib}$, where ν_{vib} is the vibrational frequency of the mode. Thus, their energy level schemes represent uniformly spaced ladders with step widths much smaller than typical electronic excitation energies, but extending (as indicated by the dots in Fig. 2.6) up to typical bond breakage energies which are normally larger than the spacing between the electronic levels. In Fig. 2.6, the vibrational level structure is represented in a very schematic way, displaying just the vibrational progression of one representative mode. In reality *N*-6 (or *N*-5 if it is a linear molecule) such vibration energy ladders have to be superimposed. Since different vibrational modes can be excited to various degrees at the same time, the number of possible combinations of vibrational states increases drastically with increasing total vibrational energy.

Apart from electronic excitation and vibration of the nuclei, a molecule can also rotate, which adds another, still finer level substructure to the one depicted in Fig. 2.6. In solution, these rotational levels are broadened, because free rotations are hindered. Therefore, the total level scheme of a molecule in solution essentially corresponds to a continuum which accounts for the apparent continuous nature of the absorption spectrum. Nevertheless, the band structure of molecular absorption spectra shows, that on absorption of a photon, the transitions to any of the electronic-vibrational-rotational (*rovibronic*) states are not equally probable. In the first place, it is still the interaction of the electromagnetic light wave with the

electrons that is responsible for photon absorption. The excitation of an electron occurs on a much shorter time scale than the period of a molecular vibration, such that, on the time scale of a vibration, the electronic excitation is practically instantaneous. Since the valence electrons excitable by light are responsible for the chemical bonds and for the forces on the atoms, when they vibrate out of their equilibrium positions, a rearrangement of the electron distribution on excitation may result in a change of forces between the atoms and thereby, after excitation, the molecule will start to vibrate stronger or weaker than before it was excited. The particular values of the shifts of vibrational potential curves between electronic ground and excited states will determine which electronic-vibrational (*vibronic*) level combination will have the highest probability of excitation. In a qualitative way, this relation is expressed in the Franck–Condon principle, in a quantitative way the intensity distribution over an absorption band is determined by the Franck–Condon factors of the vibrational levels that are connected by the transition. In general, the position of a band maximum, i.e., the vibronic transition of highest probability, is not too far from the pure electronic transition. Therefore, the pattern of the band maxima positions is rather close to the purely electronic energy level scheme of a molecule. The widths of the bands are determined by the extent to which vibrations are excited together with the electron, and are therefore governed by the Franck–Condon principle.

The electronic excitation energies can be qualitatively estimated from the molecular orbital picture of the electronic structure. In molecules it is customary to classify the orbitals according to their nodal properties with respect to the chemical bonds (cf. Fig. 2.7). If an orbital wave function does not change its sign when orbiting around a chemical bond, it is classified as a σ-orbital. If there are two sign changes on a full circle around a bond, it is classified as a π-orbital. If there is no node along the chemical bond, the orbital is bonding, i.e., it causes attraction of the adjacent atoms. Orbitals with a node along the bond are antibonding, i.e., they cause repulsion between the adjacent atoms if populated by an electron. Antibonding orbitals are denoted by an asterisk in combination with the Greek symbol.

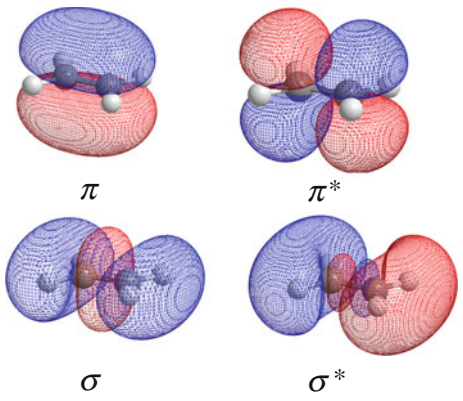

Fig. 2.7 Representation of σ, σ^*, π, and π^* molecular orbitals in ethylene

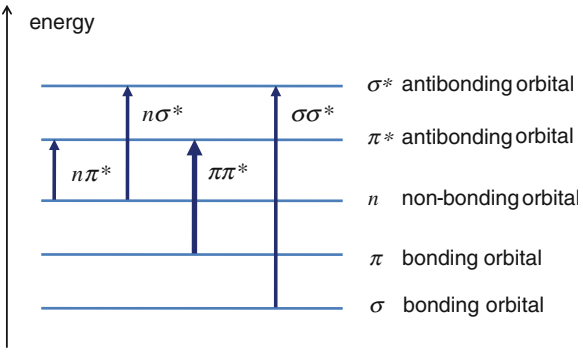

Fig. 2.8 Schematic overview of characteristic types and energy ordering of electronic transitions in molecules

In organic compounds containing atoms other than hydrogen and carbon, so-called hetero atoms such as nitrogen and oxygen, some of the electron pairs of the heteroatom do not participate in bonding or antibonding. These are called *n*-electrons (nonbonding electrons).

Roughly, the energetic order of the various types of molecular orbitals is: σ, π, n, π^*, σ^*. Electronic transitions between these orbitals are assigned the labels of the orbitals involved. Hence, we may distinguish $n\pi^*$, $n\sigma^*$, $\pi\pi^*$, and $\sigma\sigma^*$ transitions which are typically ordered in energy as shown in Fig. 2.8. The bands in the visible are usually of $n\pi^*$ or $\pi\pi^*$ nature.

Finally, we are left with the third of the questions posed above, regarding the intensity of the electronic absorption bands. This intensity can be interpreted as the probability per time unit of a molecule to undergo a certain transition in an electromagnetic field of a given wavelength and strength, or else as the probability of absorption of a photon of a given energy on passing a certain number of uniformly distributed molecules. This process requires electric interaction between the electrons and the light field. Classically, it can be described in analogy to the absorption of energy by an oscillating dipole antenna in a radio wave field. We should note, however, that the energy eigenstates of the molecule are stationary, i.e., there is no oscillation of the electrons that could represent the dipole antenna. Such a situation, i.e., real oscillation of charge, occurs only when different energy eigenstates are coherently superimposed or mixed. Then the electron cloud oscillates with a frequency given by Bohr's condition, Eq. (2.11). The rate at which this oscillator takes up energy from the radiation field is proportional to the square of the electric dipole moment of the oscillating charge. The charge distribution of the oscillator can be obtained by multiplying the wavefunctions of the two states involved in the transition. We will demonstrate this procedure for the transition between the highest occupied molecular orbital (HOMO) and the lowest unoccupied molecular orbital (LUMO) in naphthalene. Since these orbitals are π-orbitals, we are dealing with a $\pi\pi^*$ transition. In Fig. 2.9, the representations of the orbitals and of the transition charge density distribution are shown. The charge distribution can be assigned to four partial dipoles, two weak ones pointing downward, two strong ones pointing upward. Thus, there is a resultant transition

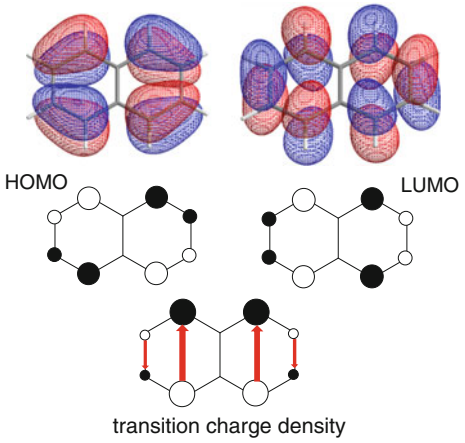

Fig. 2.9 HOMO and LUMO of naphthalene. *Upper row*: isocontour plot from an extended Hückel calculation. Middle row: Hückel MO coefficient representation, *Lower row*: HOMO → LUMO transition charge density with partial dipoles. *Black* and *white circles* represent positive and negative values, respectively, of molecular orbitals and the charge density

dipole moment along the short axis of the naphthalene molecule, meaning that this transition can absorb energy from a radiation field where the electrical vector oscillates (is polarized) parallel to the direction of the short axis.

The HOMO–LUMO transition in naphthalene gives rise to a moderately strong absorption band with a maximum absorption coefficient of about 6,000 M^{-1} cm^{-1}. It corresponds to the second band in the spectrum shown in Fig. 2.10. Note that a log-scale is used for the absorption coefficient in order to accommodate bands of very different intensity in one diagram. It is also worth of note that, in general, excited electronic states cannot be precisely described by a single electron configuration as we have assumed for the HOMO → LUMO excitation in naphthalene, where it is rather well justified. In general, one has to mix different electron configurations to arrive at a realistic description of a specific excited state. For example, in naphthalene the first and third excited states are approximately obtained from combining two configurations, one involving excitation of an electron from the HOMO to the LUMO + 1 orbital and the other from the HOMO-1 orbital to the LUMO orbital. Their combinations result in a lowest excited state with a very small transition dipole moment (band ① in Fig. 2.10) and in the third excited state with a very large transition dipole moment (band ③ in Fig. 2.10) in the transition from the ground state to these states. For different types of transitions, the absorption coefficients can vary over a very wide range. An overview of typical cases and orders of magnitude is presented in Table 2.1.

2.1.4 Photophysical Processes in the Excited State

The general "map" for the processes taking place after electronic excitation of molecules is the so-called Jablonski scheme shown in Fig. 2.11 [4]. It shows two energy ladders, termed the singlet and the triplet system. Singlet and triplet refers to the spin multiplicity of an electronic state. In a singlet state, the spins of all

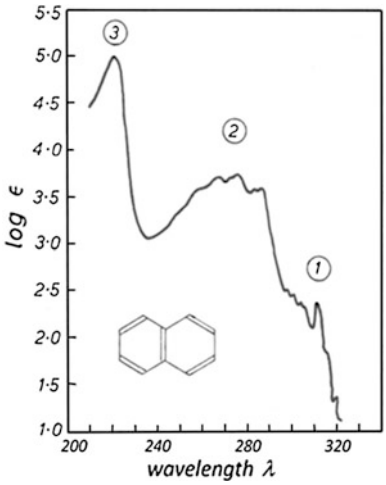

Fig. 2.10 UV absorption spectrum of naphthalene in ethanol. Reprinted from Ref [13], Murrell JN (1963) The theory of the electronic spectra of organic molecules. Methuen & Co, London, reproduced with permission by J. N. Murrell

Table 2.1 Typical ε_{max}-values of light-absorbing compounds

Category	ε_{max}	Class of compounds and orbitals involved
Strong absorption	5,000–100,000 M^{-1} cm^{-1}	Organic dyes, acid/base indicator dyes, π-orbitals
Medium strong absorption	500–5000 M^{-1} cm^{-1}	Complexes of subgroup elements with π-electron ligands (e.g., MnO_4^-, $Fe(SCN)_3$) charge transfer transitions between metal *d*-orbitals and ligand π-orbitals (LMCT, MLCT-transitions)
Weak absorption	<100 $M^{-1}cm^{-1}$	E.g. aquo-, ammin-, chloro- fluoro- complexes of subgroup elements d-electrons of the metal ions
Very weak absorption	<1 $M^{-1}cm^{-1}$	Ions of rare earths f-orbitals of the metal ions

electrons are paired and the total spin is zero. For normal molecules with an even number of electrons, this is generally the case for the ground state which is therefore given the term symbol S_0 (for the exception of molecular oxygen cf. below). In a triplet state, the spin angular momentum of two unpaired electrons adds up to a spin quantum number of 1. Since three different spatial orientations of such a spin can be distinguished, the multiplicity of the state is 3, hence the term triplet state. On excitation, at least two electrons will reside in singly occupied molecular orbitals. Hence the Pauli principle does no longer restrict their mutual spin alignment and singlet states as well as triplet states are possible. For states that can be described by a single electron configuration, the triplet state is usually at lower energy than the singlet state because in triplet states the unpaired electrons still do avoid close encounters due to the Pauli principle, and therefore their average repulsion energy is less than for the corresponding singlet configuration.

Radiationless transitions. Let us follow the fate of a molecule after its excitation to a higher vibronic (i.e., electronically and vibrationally excited) state.

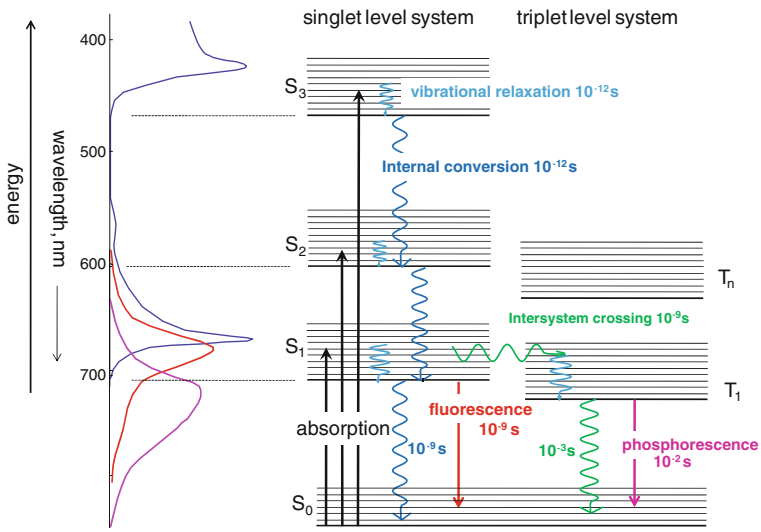

Fig. 2.11 Jablonski scheme representing the typical photophysical processes in molecules. For details cf. text. The time constants given are to be understood as typical orders of magnitude. Deviations from these typical values by one or two orders of magnitude may be found in specific systems. Adapted with permission from Ref. [12] Schmidt W, Optische Spektroskopie, p. 58, Copyright © 2000 Wiley–VCH Verlag GmbH & Co KGaA

Vibrational excitation means that the molecule is in a "hot" state. In a condensed medium, there are many collisions between the molecule and its surroundings, and the excess vibrational energy is easily transferred to the "cold" molecules of the medium. Thus, within typically an order of magnitude of 10^{-12} s, the molecule has undergone a *vibrational relaxation* to the more or less vibrationless excited electronic state. Further relaxation requires the intramolecular transformation of electronic energy into vibrational energy which is termed *internal conversion*. Since the steps of the electronic energy ladder are usually much larger than the vibrational energy quanta, such a transformation goes along with a strong change in the motional state of the nuclei and it is the harder to realize the larger the electronic energy gap (so-called energy gap law). Typical times for internal conversion steps between the higher excited states are on the order of 10^{-12} s. Since the energy gap between S_1 and S_0 is usually larger than between the higher states, the $S_1 \rightarrow S_0$ internal conversion is much slower, typically on the order of 10^{-9} s. A famous exception to this behavior is the case of azulene, where the $S_2 \rightarrow S_1$ internal conversion is much slower than the $S_1 \rightarrow S_0$ one, which however also reflects the rule of the energy gap law, because the $S_2 - S_1$ energy gap is exceptionally high in that case.

Intersystem Crossing. Changing an electronic state from singlet to triplet requires a spin flip of one of the unpaired electrons. Such processes can be only achieved by the action of an effective magnetic field. The magnetic component of

the light field is too weak to compete with the effects of the electric field component while it induces an electronic transition between different orbitals. However, there is an intramolecular perturbation, spin–orbit coupling, which can cause spin flips during radiationless and radiative transitions.

Spin–orbit coupling is a relativistic effect that may be visualized as the action of an effective magnetic field seen by the electrons while orbiting around the charged nuclei. Seen from the electron, the relative motion of the nucleus in an atom corresponds to a ring current that produces a magnetic field along which the electron spin tends to align. The effect increases linearly with the orbital momentum of the electron, but much more strongly (to the fourth power) with the nuclear charge. In nonlinear organic molecules, the molecular orbitals have little directed orbital momentum. Thus, spin–orbit coupling effects in such molecules are usually weak and hence there is little mixing between singlet and triplet states. However, spin–orbit coupling effects can be enhanced by the presence of heavy atoms (i.e., with nuclei of high electric charge) and/or during transitions between orbitals that involve a rotation of a p-orbital at some hetero atomic center, such as occurring e.g., in transitions between $n\pi^*$ and $\pi\pi^*$ excited states. Therefore, radiationless (and radiative, c.f. below) intersystem crossing processes are particularly effective between singlet and triplet states differing in their electronic orbital nature.

Apart from the strength of spin–orbit coupling between two electronic states, the electronic energy gap between them is the second important factor for the rate of a radiationless transition between a singlet and a triplet state or vice versa. The energy gap law holds in this case, too, just as for internal conversion processes between states of the same multiplicity. Therefore, the radiationless transition from T_1 to S_0 is much slower than from excited singlets to the triplet system. Typical orders of magnitude are 10^{-9} s for the latter and 10^{-2} s for the former. However, such numbers should be taken with care, because deviations by one or more orders of magnitude are possible, depending on the specific case.

Photoluminescence. When looking at dye solutions, one often can observe some extra "glow" in the sample, adding to the spectrally filtered transmitted light (cf. the photo of methylene blue bottles in Fig. 2.4). This phenomenon is due to a spontaneous, undirected emission of light and its spectral characteristics are specific for the emitting molecules, but rather independent of the wavelength of the light absorbed. Spectrally, this photoluminescence appears in a band positioned on the long wavelength side of the first absorption band and with a band shape resembling a mirror image of that absorption band. (cf. Fig. 2.11). If excited by a very short light pulse of less than a nanosecond, it is possible to observe the decay of the photoluminescence in time and to distinguish two components of very different life time: a short one, *fluorescence*, with a life time characteristic of the S_1 state and a long-lived one, *phosphorescence*, with a life time characteristic of the T_1 state. While the fluorescence intensity may come close to the intensity of the absorbed light (i.e., may reach a quantum yield of 1), at room temperature, the phosphorescence is usually very weak because the emission is spin-forbidden and its rate is much smaller than the rate of radiationless deactivation of T_1. Thus, the

quantum yield of phosphorescence is small under such conditions. At low temperatures, in rigid matrices, however, the radiationless transitions may be slowed down to an extent that the phosphorescence quantum yield can become appreciable, too.

The independence of photoluminescence spectra of the wavelength of absorption, known as Kasha's rule, is a consequence of the energy gap law making electronic energy relaxation by internal conversion fast until the S_1 or T_1 state is reached. Only here, further radiationless deactivation is slow enough for an emission process to compete. In principle, emission can also occur from a higher excited state, but the quantum yields of such processes are very low because of the dominance of radiationless deactivation processes. The exception of azulene has been mentioned above. The mirror image rule for the relation between first absorption band and photoluminescence band is rationalized by the Franck–Condon principle. It predicts similar intensities for transitions between vibronic states with the same combination of vibrational quantum numbers, irrespective of whether the higher vibrational quantum number is associated with the ground state or the excited state (Fig. 2.12).

Electronic energy transfer. For many situations in nature and technology, it is important that electronically excited states cannot only be produced by direct absorption of light, but also by accepting the electronic energy through a radiationless pathway from some other electronically excited species that has absorbed the light in the first place. Examples of such processes can be found in photosynthesis and in bioanalytical applications (vide infra). The production of molecular singlet oxygen, a reactive key species in photodynamic therapy, is another case of particular interest for this book. Like the probability of the absorption of photons, the rates of electronic energy transfer processes are subject to specific rules. In the latter case, these are mainly concerned with the conservation of spin and the

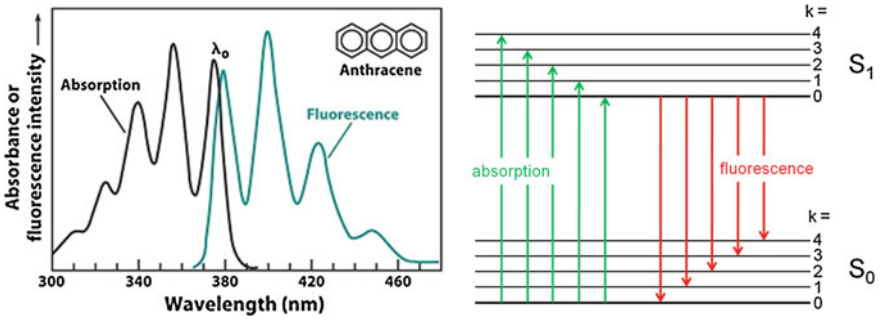

Fig. 2.12 Mirror-image relationship between absorption and emission exemplified for the case of fluorescence of anthracene. *Left*: fluorescence and absorption spectrum (the latter recorded by the intensity change of fluorescence at a fixed wavelength as the excitation wavelength is scanned). Adapted with permission from ref [14]., Byron CM, Werner TC, J Chem Educ 1991, 68:433–436. Copyright © 1991 American Chemical Society. *Right*: correspondence scheme for vibronic transitions. For details cf. text

distance dependence of the energy transfer rate between the energy donor and the energy acceptor. It is in compliance with the spin conservation criterion that a donor in an excited singlet can transfer its energy to an acceptor in a singlet ground state, when the donor undergoes a transition to its singlet ground state and the acceptor ends up in an excited singlet state, usually in the S_1 state. This type of energy transfer is termed singlet–singlet energy transfer, or—according to its most prominent mechanism—Förster *resonance energy transfer*. In practical applications it also goes by the name of *fluorescence resonance energy transfer*. The acronym FRET allows for both readings. In case of triplet excited donors, the spin conservation principle allows only for the creation of triplet excited acceptor molecules, if their ground state is singlet. However, in the case of acceptors with a triplet ground state, spin-allowed energy transfer from triplet excited donors leads to excited singlet states. The case of molecular oxygen (cf. below) is a prominent example. Let us consider the FRET case first (cf. Fig. 2.13). As described above, shortly after its photoexcitation, a donor is usually in its vibrationless first excited singlet state, which has a typical lifetime of about 1 ns. A close-by acceptor molecule can directly "sense" the electric field of the transition dipole related to the electronic excitation of the donor and it can take up its energy if there is a resonance, i.e., an exact energy matching with an electronic transition in the acceptor. This process does not require the spontaneous emission of a photon by the donor but takes place in a radiationless fashion. The mechanism of the energy transfer is based on the dipole–dipole interaction between the transition dipole moments of donor and acceptor. The energy of the interaction between the two transition dipoles is proportional to the strength of the transition dipoles and to the inverse of the third power of the distance R between donor and acceptor. Since the rate of the energy transfer process is proportional to the square of the interaction energy, it depends on

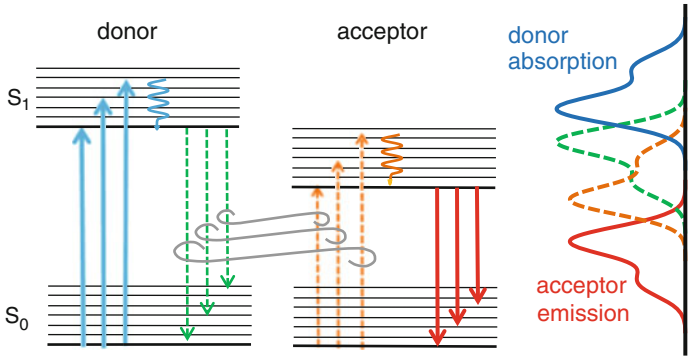

Fig. 2.13 Principle of the FRET process. The concerted transitions of donor and acceptor require energy matching of fluorescence of the donor (*dashed green arrows* and spectrum) and absorption of the acceptor (*dashed orange arrows* and spectrum). However, they occur without emission of the donor. After the energy transfer to the acceptor, its specific fluorescence spectrum can be observed (*red arrows*, spectrum)

the distance R as the inverse of the sixth power of R. This leads to the famous Förster relation for the rate constant k_{FRET} of this type of energy transfer:

$$k_{\mathrm{FRET}} = k_0 \left(\frac{R_0}{R}\right)^6 \tag{2.12}$$

Here k_0 stands for the rate constant of spontaneous deactivation of the excited donor and R_0 is the so-called Förster radius. At this separation of donor and acceptor, the rate constant of energy transfer and spontaneous decay of the excited donor are equal, i.e., under such conditions the overall decay rate of the donor is two times as fast as in the absence of an acceptor and the efficiency of energy transfer amounts to 50 %. The value of the Förster radius R_0 is determined by the strength of the two interacting transition dipoles. As Förster has shown, the resonance condition and the role of the strengths of the two transition dipoles can be exactly described by the overlap of the fluorescence spectrum of the donor and the absorption spectrum of the acceptor. Nevertheless, the process does not involve spontaneous emission of a photon by the donor and its reabsorption by the acceptor. Donor and acceptor pairs with good interaction are characterized by high values of R_0 which in favorable cases may reach values as high as 50–80 Å. In bioanalytical applications, FRET experiments, even with single molecule resolution, have become a convenient tool to probe distances and conformational changes within complexes of biomacromolecules.

If suitable donor and acceptor molecules are fixed on conformationally mobile parts of a biomacromolecular complex their separation will undergo a dynamic change. Preferentially, the range of distances should comprise the Förster radius R_0. In such a case, the efficiency of energy transfer will undergo appreciable changes which can be read from the ratio of fluorescence intensities of donor and acceptor. Figure 2.14 shows a prominent recent example [15], where single molecule emission is used to probe the dynamics of the donor–acceptor distance and thereby the systematic motion of the rotating part of F_0F_1-ATPase of *Escherichia coli*. Using this technique, it can be demonstrated how the sense of the rotation changes with the environmental conditions under which ATP is synthesized or hydrolyzed, respectively.

Triplet–triplet energy transfer. Since excited triplet states live much longer than excited singlets, the chance that they can transfer energy before they decay is higher, or can be effected with the same efficiency at lower concentrations of the acceptor species. As with singlet–singlet energy transfer, there is also conservation of the overall spin in triplet–triplet energy transfer processes. Whereas, however, there is spin conservation in each of the partners of a singlet–singlet energy transfer, there is spin conversion from triplet to singlet in the donor and singlet to triplet in the acceptor. Therefore, this process is not induced by the coupling of two transition dipole moments, which are very weak for spin-forbidden transitions, and it does not have a long-range character as in the Förster mechanism. Efficient triplet–triplet energy transfer is made possible by the synchronous exchange of two electrons related to the two singly occupied orbitals in each of the two species

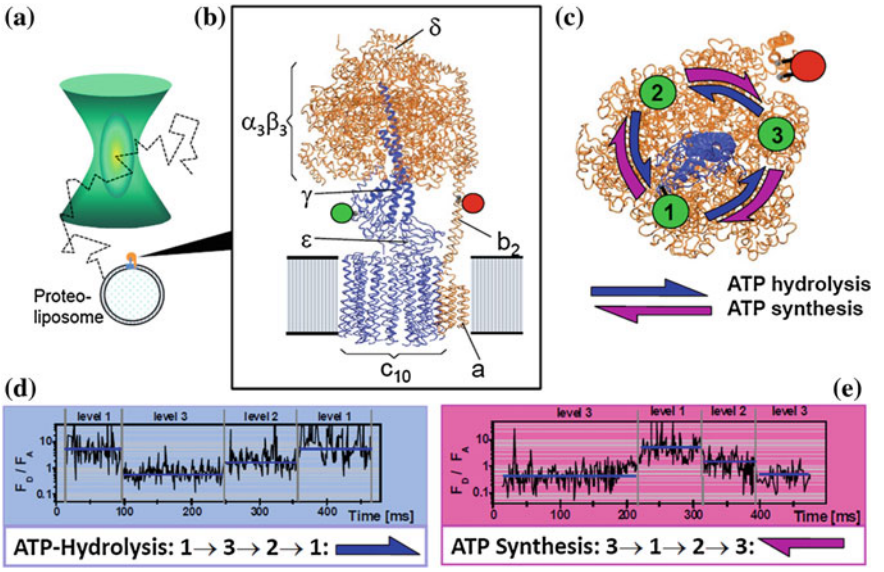

Fig. 2.14 Application of single molecule FRET to detect the three stages of ATPase operation in ATP synthesis and hydrolysis [15]. **a** Fluorescence from a fluorescence labeled ATPase molecule on a proteoliposome is detected while the latter diffuses through the focus of a laser beam. **b** Side view of model of F_0F_1-ATPase from *E. coli.* The FRET donor (*green circle*) is bound to the γ subunit, the FRET acceptor (*red circle*) to the b subunits. 'Rotor' subunits are *blue*, 'stator' subunits are *orange*. **c** Cross-section at the fluorophore level. During enzyme action the FRET donor on the rotor part adopts the sequence of positions 1, 2, and 3, differing in distance to the static FRET acceptor, such that energy transfer is most efficient in position 3 and least efficient in position 1. **d** Time-dependent record of acceptor/donor fluorescence ratio under ATP hydrolysis conditions. **e** Under ATP synthesis conditions. Note that the time sequence of positions 1–3 is reversed between situations **d** and **e**. Adapted from Nature Structural and Molecular Biology 11:135–141, Copyright © 2004 Macmillan Publishers Ltd. Adaptation by courtesy of Prof. C.A.M Seidel

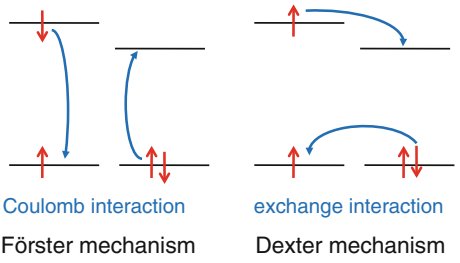

Fig. 2.15 Illustration of concerted, spin-conserving two-electron motion in the Förster and the Dexter mechanism of electronic energy transfer in singlet–singlet and triplet–triplet energy transfer, respectively

involved in the process. This principle is depicted in Fig. 2.15. The so-called exchange mechanism was first suggested by Dexter. It requires some spatial overlap of the electronic wavefunctions of the two species which can be only achieved if the two molecules get into close contact.

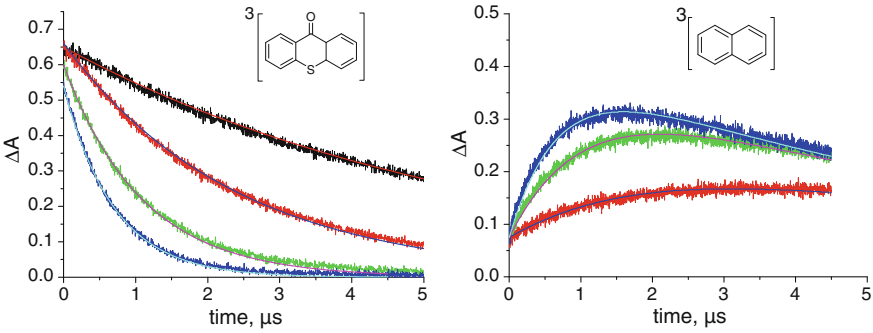

Fig. 2.16 Experimental example of triplet–triplet energy transfer between thioxanthone triplet (donor) and naphthalene (acceptor). Transient absorption signals are shown for two wavelengths, where characteristic absorptions of the two triplets are found. *Left*: transient absorption of thioxanthone triplet for (from *above*) concentrations 0, 0.1, 0.3, 0.5 mM of naphthalene. *Right*: transient absorption of naphthalene triplet for (from *below*) concentrations of 0.1, 0.3, and 0.5 mM of naphthalene

In Fig. 2.16, an example of the observation of triplet–triplet energy transfer is shown. Here, thioxanthone is the triplet energy donor and naphthalene the acceptor. Since, at room temperature, phosphorescence is usually too weak, an observation by transient absorption is the standard method of detection for triplets at ambient temperatures. As with singlet–singlet energy transfer, a matching of energies of donor and acceptor triplets is a condition for an efficient process in the case of triplet–triplet energy transfer, too. As in the former case, electronic energy transfer also comprises the excitation of vibrations (cf. Fig. 2.13) the probability of which is controlled by the Franck–Condon principle (cf. the special example of singlet oxygen formation below). Since the donor usually ends up in some vibrationally excited ground state and the acceptor in a vibrational excited triplet state, the best conditions for energy matching are given if the purely electronic energy of the donor is higher than that of the acceptor, i.e., $E_T(D) > E_T(A)$.

Singlet oxygen formation by electronic energy transfer [5]. In photodynamic therapy, singlet excited molecular oxygen plays a central role. Figure 2.17 shows the electron configurations related to the lowest electronic states of molecular oxygen. They differ in the populations of the lowest π^* orbitals. These orbitals represent the antibonding combinations of the atomic p-orbitals having their axis perpendicular to the molecular axis. In Fig. 2.17, the representations of two real-valued orbitals termed LUMO a and LUMO b are shown. The orbitals LUMO a and LUMO b represent wave functions with an orbital angular momentum of quantum number 1. But the sense of the electron rotation around the molecular axis, i.e., whether it is a right-hand or left-hand turn, is not defined for these orbitals. Instead, they represent situations where right and left sense rotation are equally mixed. The π orbitals $\pi_{\pm 1}^*$ are obtained from them as symmetric and antisymmetric linear combinations but with the imaginary number $\pm i$ as a phase factor. The complex orbitals π_{+1}^* and π_{-1}^* represent states with sharply defined

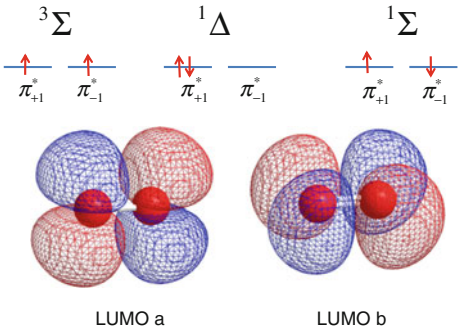

Fig. 2.17 Orbital configurations of the lowest electronic states of molecular oxygen. The states differ in the two-electron configuration of the degenerate two π^* orbitals. For details cf. text

right or left sense rotations, respectively. In an isolated O_2 molecule, these states are exactly degenerate for symmetry reasons.

In the lowest electronic state of O_2, i.e., in its ground state, each of the two π^* orbitals is singly occupied and the spins of the two unpaired electrons are parallel, according to Hund's rule. Hence the ground state of O_2 is a triplet state and therefore paramagnetic. Since the orbital angular momenta of π^*_{+1} and π^*_{-1} are equal, but opposite in sign, they cancel each other, so that the total orbital angular momentum is zero. This fact is expressed by the term symbol Σ. If both electrons share the same π^*orbital, their spins must be opposite, such that the total spin is zero. On the other hand, their orbital angular momenta add up to a quantum number of 2 for the total orbital angular momentum. These properties are denoted by the term symbol $^1\Delta$. Finally, if the two electrons are in different π^* orbitals, but with opposite spins we generate a singlet state with total orbital angular momentum quantum number 0, i.e., a $^1\Sigma$ state. One should note that the single configurations shown in Fig. 2.17 for $^1\Sigma$ and $^1\Delta$ do not give the full representation of the wave functions of the two states. The full wave functions include the complementary configurations, too, where the populations of the two π^* orbitals are just exchanged. The energies of the two lowest excited states of O_2 are 94 kJ/mol ($^1\Delta$) and 157 kJ/mol ($^1\Sigma$) above the $^3\Sigma$ ground state. The energy differences are due to the differences in electron–electron repulsion reflecting the different average distances between the two electrons for the different configurations.

Singlet-excited oxygen can be produced by energy transfer from donors in excited singlet or triplet states. In case of excited singlet state donors, spin conservation requires that these undergo a transition from the excited singlet to the lowest excited triplet state. For energy reasons, the singlet/triplet gap must be greater than about 90 kJ/mol in order to populate the lowest excited singlet of oxygen. Furthermore, a diffusive encounter between molecular oxygen and the donor has to occur within a few nanoseconds, due to the short lifetime of the excited donor singlet. These conditions are not easy to fulfill in an effective way. Therefore, excited triplets as energy donors are the usual method to generate singlet excited molecular oxygen.

In Fig. 2.18, a scheme for the population and depopulation of excited states of molecular oxygen is shown. On encounter of the triplet donor and the triplet ground state oxygen molecule, the total spin of the pair can be 0, 1, or 2,

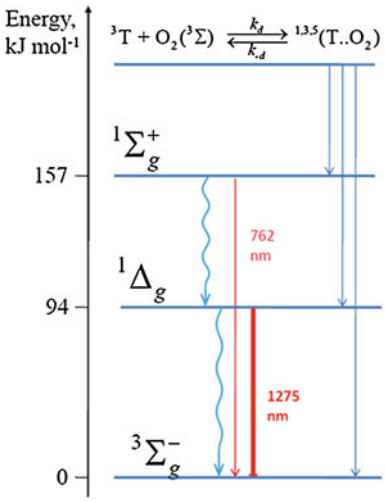

Fig. 2.18 Level scheme of lowest electronic states of molecular oxygen. Radiationless deactivation processes require interaction with surrounding molecules taking up the vibrational energy

corresponding to an overall singlet, triplet or quintet state, respectively. The statistical weights of these states are 1/9, 1/3, and 5/9, respectively. A deactivation of the encounter complex to a state comprising the singlet ground state of the donor and a singlet-excited oxygen species is only possible from the encounter complex with singlet multiplicity. However, there is rapid equilibrium between the encounter complexes in their different multiplicities [16], so that eventually all excited donor triplets may lead to the formation of singlet-excited oxygen, if the triplet lifetime is long enough. The ratio at which the two different singlet states of oxygen are formed is governed by the energy gap law (vide supra) [5]. In the encounter complex, the radiationless transition rate from the energy level of the excited donor to that of a specific excited state of oxygen is at a maximum for energy gaps between 0 and about 80 kJ/mol. For larger energy gaps, the rate quickly decreases. Thus, e.g., for 9-bromoanthracene, a triplet sensitizer with a triplet energy of 168 kJ/mol, the energy gap to both, the $^1\Sigma$ and the $^1\Delta$ state of oxygen is within the range of maximum rate and they are both populated with about 50 % probability [17]. On the other hand, for 2-acetonaphtone with a triplet energy of 248 kJ/mol, the energy gap to $^1\Sigma$ is 154 kJ/mol, i.e., in the region where the rate is strongly decreasing, but for the population of $^1\Delta$ with an energy gap of 91 kJ/mol the rate is still close to the maximum. This situation explains why, with this triplet energy donor, the $^1\Sigma$ and the $^1\Delta$ state of oxygen are formed at a ratio of 17:83 [17]. For most practical purposes, however, it is important to note that in condensed phases the radiationless deactivation of $O_2(^1\Sigma)$ to $O_2(^1\Delta)$ takes place on the nanosecond time scale and it is unimportant whether $O_2(^1\Delta)$ is formed directly in the encounter of triplet excited donor and ground state oxygen or through the $^1\Sigma$ state. It must be added, though, that in cases of donors with low oxidation potential, the encounter complexes of triplet donor and singlet ground state molecular oxygen may be deactivated through the intermediacy of a charge

transfer state, wherefrom the population efficiency of the two excited singlet states of oxygen is lower than in the previous mechanism [18].

In condensed media, the lifetimes of the two singlet-excited oxygen species differ by about six orders of magnitude [5]. They are determined by radiationless transfer of electronic energy to vibrational energy of the surrounding medium which can occur directly or, with higher rate, in the presence of charge transfer interaction. Particularly long lifetimes are observed in perhalogenated solvents such as CCl_4 with lifetimes of 130 ns for $O_2(^1\Sigma)$ and 31 ms for $O_2(^1\Delta)$. Particularly short lifetimes are observed in solvents with OH-vibrations, such as H_2O with a lifetime of 3.8 μs for $O_2(^1\Delta)$. That this behavior is due to the specific frequency of OH-vibrations, can be concluded from a much longer lifetime of 62 μs in D_2O.

In photodynamic therapy, the lifetime of singlet oxygen determines the average length d the excited oxygen molecule can diffuse away from the point where it was created. According to Einstein's square law

$$d^2 = 6D\tau \tag{2.13}$$

where D is the diffusion coefficient and τ the lifetime of the diffusing species. In living cells, the value of D for molecular oxygen is about 1.4×10^{-5} cm^2s^{-1} and the lifetime of $O_2(^1\Delta)$ 0.04 μs. Hence the diffusion length under such conditions amounts to about 20 nm [5].

2.2 Photochemistry and Photobiology

Photochemistry, in a modern sense, is the area dealing with chemical processes in electronically excited states [6–11]. Since such states are normally generated by the absorption of light, it is clear that only absorbed but not transmitted light can cause photoinduced chemical change. This principle was first stated as the Grotthus-Draper law. Because light is absorbed in units of photons, each molecule undergoing a photoreaction has to absorb a photon.[1] However, since electronically excited states may relax to the ground state by dissipating their excess energy either in radiative or radiationless processes, the probability that a molecule undergoes a chemical transformation after absorption of a photon is generally not unity. This probability is called the photochemical quantum yield of the photochemical process under consideration. The inverse of this quantity is the number of photons a molecule has to absorb on the average before it will undergo a photoreaction.

Just as normal thermal reactions, photoreactions, too, are characterized by certain changes of nuclear coordinates. The electronic energy as a function of the nuclear coordinates may be viewed as spanning a hypersurface of potential energy on which the nuclear system undergoes periodic vibrational motion and, in some

[1] This does not apply to radical chain reactions, where one absorbed photon may result in many product molecules.

cases, nonperiodic translocations, the latter representing chemical change and the path of lowest energy between the minima the reaction coordinate. Whereas, however, in a normal thermal reaction, the system never leaves the potential surface of the ground state, in a photoreaction, there is necessarily a cross-over from a higher potential surface to that of the ground state (*diabatic* change) where every reaction eventually must end. According to Förster [19], photoreactions may be classified according to the three cases depicted in Fig. 2.19. They are distinguished from each other by the way the system undergoes its transition to the ground state potential surface. In case (a), the chemical change is completely achieved in the excited state. Only after vibrational relaxation in the excited photoproduct the system undergoes a radiationless decay to the ground state. Such photoreactions are called *adiabatic*, because the potential energy hypersurfaces, representing the change of the total energy of the system under *adiabatically* slow motions of the nuclei, are also called *adiabatic* energy surfaces. Proton transfer reactions in the excited state represent the most prominent type of such adiabatic reactions. In case (b), a radiationless cross-over from the higher to the lower potential surface takes place before the configuration of a stable product is reached in the excited state. Such situations may occur, if potential minima on the excited energy hypersurface are situated between minima of the ground state hypersurface. Photochemical *cis/trans*-isomerizations provide examples of such reactions. Finally, in case (c), the chemical change occurs in the electronic ground state after radiationless deactivation of the excited state and with the aid of the vibrational excess energy, i.e., from a "hot" ground state, before this vibrational energy is dissipated to the environment.

Another important classification of photoreactions refers to their molecularity, i.e., whether they are intramolecular (monomolecular) of intermolecular (bimolecular). In the second case, the reaction partner of an excited molecule is usually a ground-state molecule. For such bimolecular reactions, the probability of a photoreaction, i.e., its photochemical quantum yield, depends on the concentration of the unexcited reaction partner.

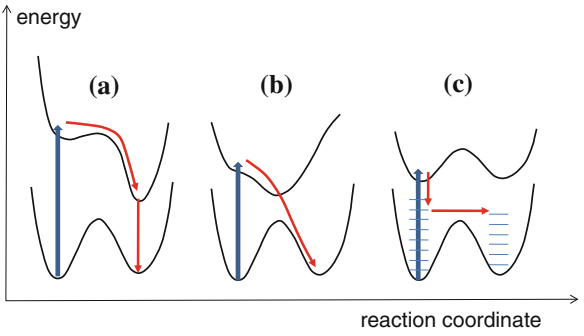

Fig. 2.19 Three cases of photochemical reactions according to Förster's classification [19]: **a** adiabatic photoreaction, **b** diabatic photoreaction, **c** hot ground state reaction. For details cf. text

Scheme 2.1 General reaction scheme of a bimolecular photoreaction competing with monomolecular deactivation

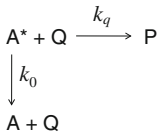

Accounting for the rates of the various processes in Scheme 2.1 we can derive the following expression for the photochemical quantum yield of product P from A*:

$$\Phi_P = \frac{k_q[Q]}{k_0 + k_q[Q]} \tag{2.14}$$

If there are no other deactivation channels, the quantum yield achieves a limiting value of 1 only for infinitely high concentration $[Q]$ of the ground state reaction partner. The concentration $[Q]_{1/2}$ at which half of the limiting quantum yield is attained, is determined by the rate constants k_q and k_0:

$$[Q]_{1/2} = \frac{k_0}{k_q} \tag{2.15}$$

After these general introductory remarks we will now regard some representative examples of elementary photochemical reactions.

2.2.1 Photoelectron Transfer Reactions

Photoexcitation caused by the absorption of light may be viewed as the separation of electron pairs, whereby one of the previously paired electrons is lifted up in energy into an empty orbital and a positive hole is left in the orbital where the electron came from. In this sense, the excitation is tantamount to an intramolecular charge separation. This is a rather formal view, however, since the involved orbitals normally penetrate each other strongly, such that the centers of gravity of the two orbitals may even coincide and no dipole moment results. Electron and hole can quickly recombine, a process denoted above as radiationless deactivation, and release the absorbed energy as heat to the environment. However, further spatial separation of (excited) electron and hole, as occurring by an electron transfer or hole transfer to a neighboring molecule and still further on, may occur with little loss of energy, but prevents rapid recombination of hole and electron. Thus, photo electron transfer reactions represent an ideal means of conserving light energy as chemical energy on longer time scales. This principle lies at the heart of natural processes such as photosynthesis and technical processes as used in photovoltaics (cf. Fig. 2.20).

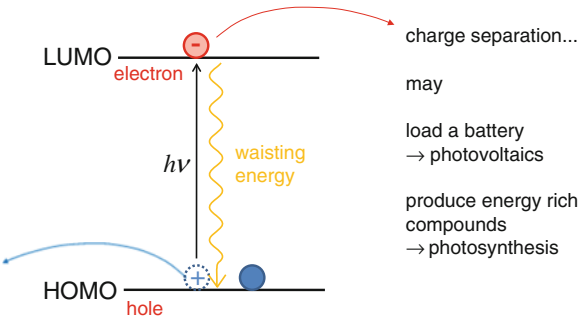

Fig. 2.20 Photoelectron transfer as a means of long-term storage of the photoexcitation energy

A general electron transfer reaction between an electron donor D and an electron acceptor *A* may be represented as[2]

$$A + D \rightarrow A^- + D^+ \tag{2.16}$$

The standard thermodynamic driving force of this reaction is given by the negative value of its standard Gibbs energy $\Delta G^{\ominus}_{et}$

$$\Delta G^{\ominus}_{et} = -F(E^{\ominus}(A^-/A) - E^{\ominus}(D/D^+)) \tag{2.17}$$

As expressed in this equation, $\Delta G^{\ominus}_{et}$ is determined by the difference of the standard electrode potentials for the reduction of *A*, $E^{\ominus}$ (A^-/A), and for the oxidation of *D*, $E^{\ominus}$ (D/D^+). The symbol *F* represents Faraday's constant. The more positive the value of $E^{\ominus}$ (A^-/A), the stronger *A* acts as an oxidant. Likewise, the more negative the value of $E^{\ominus}$ (D/D^+), the stronger *D* acts as a reductant. For organic molecules, these potentials are usually not strong enough to oxidize or reduce some other organic species. As shown in Fig. 2.21, the situation is, however, drastically changed, if *A* or *D* are electronically excited.

If the donor reacts from an excited state, the Gibbs free energy becomes more negative by the amount of the excitation energy of the donor:

$$\Delta G^{\ominus}_{et} = F \cdot (E^o(D/D^+) - E^o(A^-/A)) - E^*_D \tag{2.18}$$

Thus in an excited state a molecule is a stronger electron donor, i.e., a better reductant than in its ground state. Likewise, if the acceptor reacts from an excited state, the Gibbs free energy becomes more negative by the excitation energy of the acceptor:

$$\Delta G^{\ominus}_{et} = F \cdot (E^o(D/D^+) - E^o(A^-/A)) - E^*_A \tag{2.19}$$

Thus, in an excited state a molecule is also a stronger electron acceptor, i.e., a better oxidant than in its ground state.

[2] Here the charges should be considered as formal, because *A* and *D* themselves might be charged species, i. e. ions.

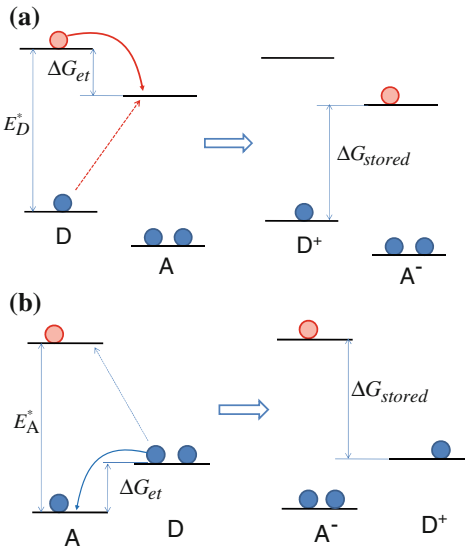

Fig. 2.21 Energetics of photoelectron transfer reactions. **a** Photoexcited donor. **b** Photoexcited acceptor. Photoexcitation makes a donor a stronger reductant and an acceptor a stronger oxidant. Excited state processes are marked with *solid curved arrows*. For comparison ground state processes are shown by *straight dashed arrows*

Due to these relations, photoinduced electron transfer reactions are quite frequent phenomena and, in many cases, these reactions are quite fast. This brings us to the question of how the rate of an electron transfer reaction and its thermodynamic driving force are related. It has been shown, both theoretically and experimentally that, other factors, such as the overlap of the electronic wavefunctions, determined by the separation between donor and acceptor, being equal, there is a strong correlation between the rate of electron transfer and the Gibbs free energy change of the process [4]. In Fig. 2.22, essential results are illustrated. In theoretical respect, the Marcus theory represented a great breakthrough [21–23]. Its main idea focuses on the change of the nuclear coordinates induced by the electron transfer and introduces the parameter λ, the so-called *reorganization energy*, corresponding to the change of electronic energy that would ensue if the system would adopt the nuclear configuration of the product but would remain in the initial electronic state present before the electron transfer. If $-\Delta G_{\mathrm{et}}$ is smaller than λ the electron transfer needs activation energy and the reaction gets faster the more negative ΔG_{et}. This is called the *normal* Marcus regime. If $-\Delta G_{\mathrm{et}}$ exceeds the value of λ the reaction is activationless and exergonic. The excess energy has to be converted to vibrational energy which is the same situation that led to the energy gap law of radiationless transitions, i.e., the rate decreases as ΔG_{et} tends to more and more negative values. This regime is called the *inverted* Marcus regime. In a brilliant series of experiments by Closs and coworkers this prediction of the Marcus theory was demonstrated to be correct [20].

The most important case of a photoinduced electron transfer reaction in nature is represented by the primary process of photosynthesis. The so-called photosynthetic reactions centers represent protein complexes containing a sophisticated

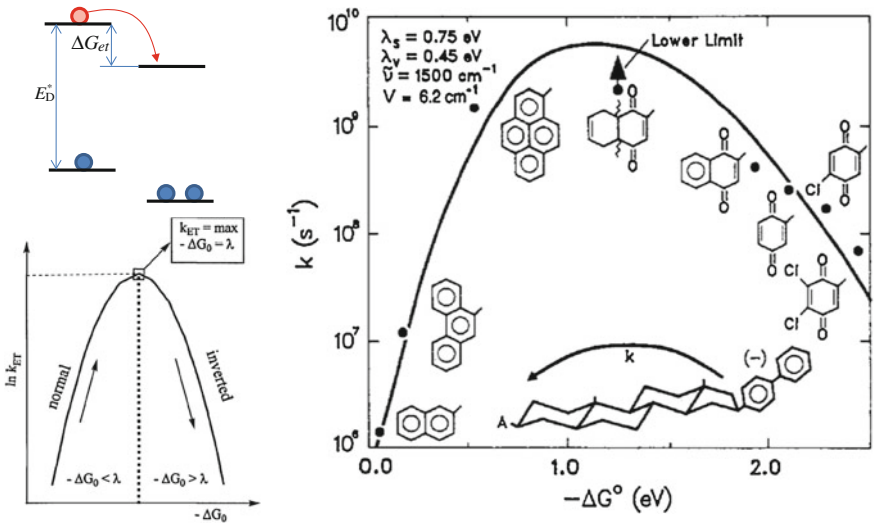

Fig. 2.22 *Left*: Schematic dependence of electron transfer rate constant on the free Gibbs energy (The ΔGet value determining the electron transfer rate in the encounter pair of donor and acceptor differs from the expressions given in Eqs. (2.18) and (2.19) by a term accounting for the different Coulomb energies of the donor/acceptor pair before and after the electron transfer. In polar environments, however, this term is usually small.) according to R. Marcus. In the "normal" region the electron transfer reaction needs to be activated, in the "inverted" region, the transformation of electronic excess energy into vibrational degrees of freedom is rate determining. The reorganization energy parameter λ determines the transition region. *Right*: Experimental verification of the Marcus prediction (Reprinted with permission from ref [20]., Miller JR, Calcaterra LT, Closs GL J. Am. Chem. Soc. 106:3047–3049. Copyright © 1984, American Chemical Society). The rate constant of electron transfer between the biphenyl anion rigidly connected to various electron acceptors is log-plotted versus the negative GIBBS free energy of the reactions. It should be noted that the symmetrical classical Marcus parabola is distorted with a gentler slope in the inverted Marcus region, if the quantum nature of nuclear vibrations is taken into account

arrangement of prosthetic groups controlling the primary electron transfer processes. Today, the structure of such reaction centers in photosynthetic bacteria as well as in plants is known to a high atomic resolution [25]. Figure 2.23 shows the active molecules and processes involved in a bacterial reaction center.

After excitation of the special pair, occurring mainly through singlet–singlet energy transfer from accessory antenna pigments, a photoelectron transfer to the first electron acceptor, a close-by bacteriochlorophyll molecule occurs within about 3 ps which is followed by an even faster hop-on process of the transferred electron to a pheophytin molecule. From here, the electron is transferred to an ubiquinone molecule, a process occurring in about 200 ps. Finally, with the intermediacy of a ferredoxin molecule, the ubiquinone in the second branch accepts the photoelectron, a process occurring on the time scale of about 10 μs. In purple bacteria, the electron returns from the final quinone acceptor to the oxidized special pair within about 1 s, thus completing an electron transfer cycle. The

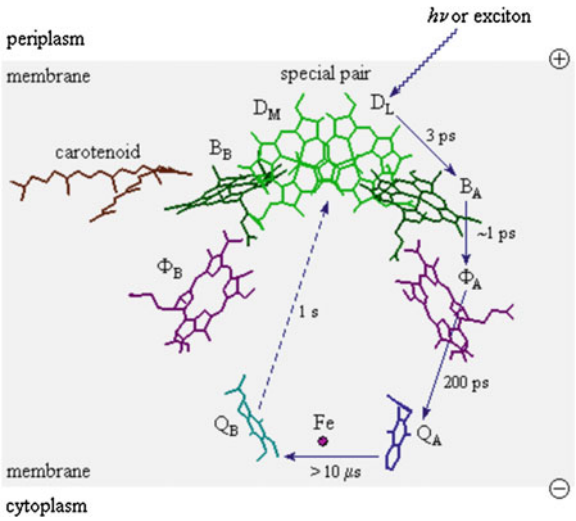

Fig. 2.23 Structure and primary photoelectron transfer pathways in bacterial reaction centers. Like in plants, these reaction centers consist of two almost symmetric branches comprising two bacteriochlorophyll molecules D_M and D_L, interacting directly with each other and representing the "special pair" D, two bacteriochlorophylls B_A and B_B, two bacteriopheophytins Φ_A and Φ_B and two quinones Q_A and Q_B. Only the *right*-hand side branch is active in the electron transfer process. Reprinted from http://metallo.scripps.edu/promise/PRCPB.html (cf. Ref. [24]) with permission by K. N. Degtyarenko

energetic benefit of the bacteria results from a proton and electric potential gradient that is generated between the two sides of the photosynthetic membrane, because the electron transport is accompanied by a proton transport from the periplasm to the cytoplasm. Protons flowing back along the gradient through the channel of membrane spanning ATPase can drive chemical energy storage through phosphorylation of ADP to ATP (cf. Fig. 2.14). In plants, there are two types of photosynthetic reaction centers. The photoelectron transfer chain from reaction center I leads to the reduction of the $NADP^+$. The oxidized special pair in reaction center I is reduced at the end of the photoelectron transfer chain from reaction center II, which in turn recovers its electron by the oxidation of water, mediated by a close-by manganese complex and leading to the generation of molecular oxygen.

2.2.2 Excited State Proton Transfer Reactions

Electronically excited states behave differently from the ground state because the distribution of electron density over the atoms in a molecule is changed. As was shown in the last section, this goes along with a change in the effective redox-potential, leading to stronger oxidation and reduction power. Likewise, the ability

to accept or donate protons is changed upon electronic excitation. This effect can be measured by the change of the acid dissociation constant K_a, usually expressed by the pK_a value:

$$pK_a = -\log K_a \tag{2.20}$$

For excited states, the pK_a is usually denoted with an asterisk, i.e., as pK_a*. As an example, the case of 2-naphthol is shown in Fig. 2.24. In a diagram representing the fractions of undissociated (acid) and dissociated (basic) form as a function of *pH*, the pK_a value can be read from the point where both forms are present in equal amounts. In the ground state, 2-naphthol exhibits a pK_a of 9.2, i.e., it is a rather weak acid. In the first excited singlet state the pK_a* jumps up to a value of 2, i.e., the compound turns to a fairly strong acid. The reason for this, is a shift of electron density away from the oxygen atom to the aromatic ring system when an electron is excited from the LUMO to the HOMO.

Proteolytic processes in the excited singlet state can be easily monitored by fluorescence spectroscopy. If a molecule is excited, for example at a pH where the acidic form prevails in the ground state, but the fluorescence observed is specific to the basic form, this means that a deprotonation of the excited acidic form must have taken place during its excited state lifetime. Furthermore, this is evidence of the fact that the system remains on the excited state potential surface during the reaction and thus represents an example of an adiabatic photoreaction. In Fig. 2.25, the situation is illustrated for 2-naphthol. The position of the equilibrium between the acidic (neutral, protonated) and the basic (anionic, deprotonated) form at a particular *pH* can be judged from the absorption spectra. At *pH* values greater than 8, changes toward the shape of the final spectrum associated with the basic form become clearly visible. (cf. left-hand side of Fig. 2.25). The fluorescence spectra on the right-hand side of Fig. 2.25 were taken at delay times of several

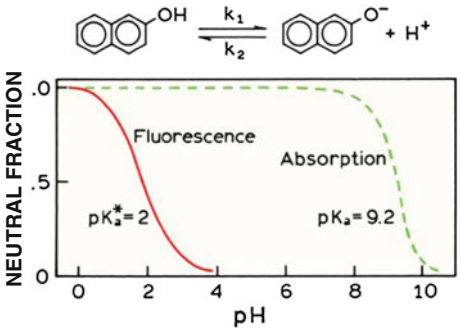

Fig. 2.24 pH-dependence of proteolytic dissociation equilibrium of 2-naphthol in the ground and in the excited singlet state. Reprinted with permission from Fig. 7.43 in Ref. [4], Lakowicz JR, Principles of fluorescence spectroscopy. Third Edition. Springer Science+Business Media, Copyright © 2006, 1999, 1983 Springer Science+Business Media, LLC, with kind permission from Springer Science+Business Media B.V

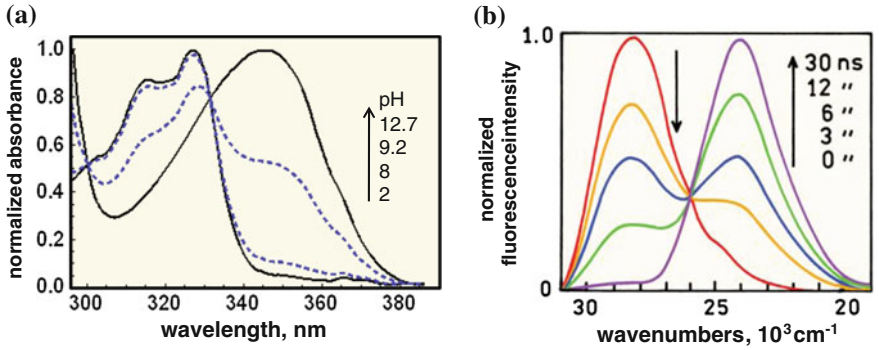

Fig. 2.25 *Left*: absorption spectra of 2-naphthol at various *pH* values *Right*: fluorescence spectra recorded in solutions of *pH* 6.6 at various delay times after a short laser pulse. The spectra are corrected for the intensity decrease due to the decay of the excited state population. *Left*: adapted from Fig. 7.42, *right*: reproduced from Fig. 7.47 in Ref. [4], Lakowicz JR, Principles of fluorescence spectroscopy. Third Edtion. Springer Science+Business Media, Copyright © 2006, 1999, 1983 Springer Science+Business Media, LLC, with kind permission from Springer Science+Business Media B.V

nanoseconds after a short excitation pulse at a *pH* of 6.6. At this *pH*, the molecule in its ground state equilibrium is still completely undissociated. Immediately after excitation, the fluorescence spectrum corresponds to the mirror image of the absorption band of the acidic form, but then it is gradually converted to a band at longer wavelength, characteristic of the 2-naphtholate anion. This observation reflects the time scale of the deprotonation process.

The fluorescence observations accompanying proteolytic equilibria in the excited state were first explained by Förster, who suggested the spectroscopic/thermodynamic cycle, the so-called Förster cycle, represented in Fig. 2.26. From the cycle and the principle of conservation of energy, spectroscopic and thermodynamic energies can be combined and lead to the following relation:

$$pK_a^* - pK_a = \frac{E_{A^-} - E_{HA}}{2.3\,RT} \tag{2.21}$$

It allows to estimate the pK_a* value from the spectroscopic energies E_{A^-} and E_{AH} of the basic and the acidic form, respectively. These energies can be taken either from the absorption spectra or from the fluorescence spectra. As follows qualitatively from Eq. (2.21), the excited state is more acidic (has a lower pK_a* value) than the ground state, if the absorption (or the emission) of the basic form is at lower energy (longer wavelength) than of the acidic form. This is usually the case for neutral acids (cf. the naphthol case shown in Fig. 2.25). The opposite is generally true if the basic from is neutral, e.g., in aromatic amines.

Excited state proton transfer reactions can be also found in natural systems. A prominent example is the emission of the green fluorescent protein [27] that has acquired great significance because it can be genetically engineered and

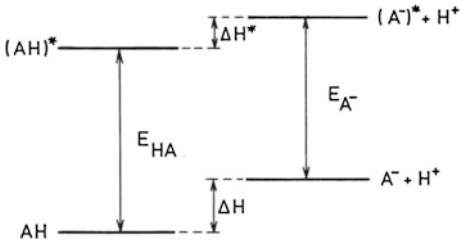

Fig. 2.26 Scheme of the Förster cycle relating spectral and thermodynamic quantities for proton transfer in ground and excited states. Reprinted with permission from Ref. [26], Marciniak B, Kozubek H, Paszyc S (1992) *Journal of Chemical Education*, Vol. 69, No. 3, 1992, pp. 247–249. Copyright © 1992, Division of Chemical Education Inc

implemented as a fluorescence marker to study cell biological problems in many organisms. The fluorescent chromophore is shown in Fig. 2.27. In the ground state, the phenolic OH group is undissociated, although part of a hydrogen bonded network of various amino acids. On excitation, a proton transfer takes place along this network and the emission arising is characteristic of the anionic, i.e., deprotonated chromophore.

2.2.3 Photochemical Cis/Trans-Isomerizations

Whereas, internal molecular rotations around single bonds between carbon and heteroatoms are fairly and easily achieved, internal rotations around double bonds are hindered by high activation barriers. Such barriers arise from the decreasing overlap of the vicinal p_π-orbitals as the π-plane of the neighboring centers adopts a perpendicular configuration. In Fig. 2.27, the energetic effect of such a rotation on the energy of the π-molecular orbitals is schematically shown for the case of ethylene. During the rotation, the energies of HOMO and LUMO approach each other. At 90°, i.e., in the perpendicular configuration, both orbitals become

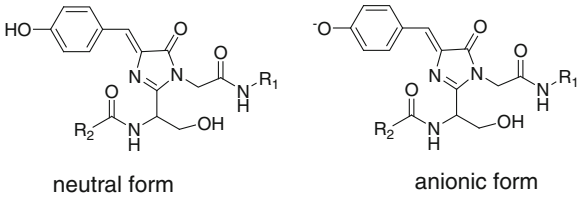

Fig. 2.27 Fluorescent chromophore of the green fluorescent protein. R_1 and R_2 represent the continuation of the protein chain, wherein the chromophore was formed from a serine/tyrosine/glycine motif. On excitation to the S_1 state, the neutral form is rapidly deprotonated and emits the fluorescence specific of the anionic form

degenerate and are nonbonding. Continuing the rotation to 180° HOMO and LUMO are interchanged as compared to the situation at the beginning. Thus, considering the state energy of the electronic configurations with both π-electrons in the HOMO, the ground state, would be raised up to the energy of S_2 (in that simple picture) after rotation by 180°. The first excited singlet, corresponding to an electron configuration with one electron in the HOMO and one in the LUMO, would keep its energy unchanged on such a rotation, and the S_2 state, with both electrons in the LUMO in the beginning, would end up as S_0 after a 180° rotation. Although this description is rather simplified, it conveys the essential concept and demonstrates the electronic origin of the potential curves in the ground and excited states.

A representation of the S_1 and S_2 potential surfaces of stilbene versus two relevant coordinates as calculated by a full ab initio quantum chemical calculation is also shown in Fig. 2.28. From it, the dynamics of a molecule after excitation to the excited state may be anticipated. After exciting the molecule in its *trans*-conformation ($\phi = 180°$) it finds itself on a very flat surface and will eventually proceed toward the perpendicular ($\phi = 90°$) conformation where the potential surface exhibits a minimum. Upon radiationless deactivation to the lower potential surface of the ground state, the molecule will end up on a potential hill and may proceed further to the right or to the left, i.e., toward the *cis*-conformation or back

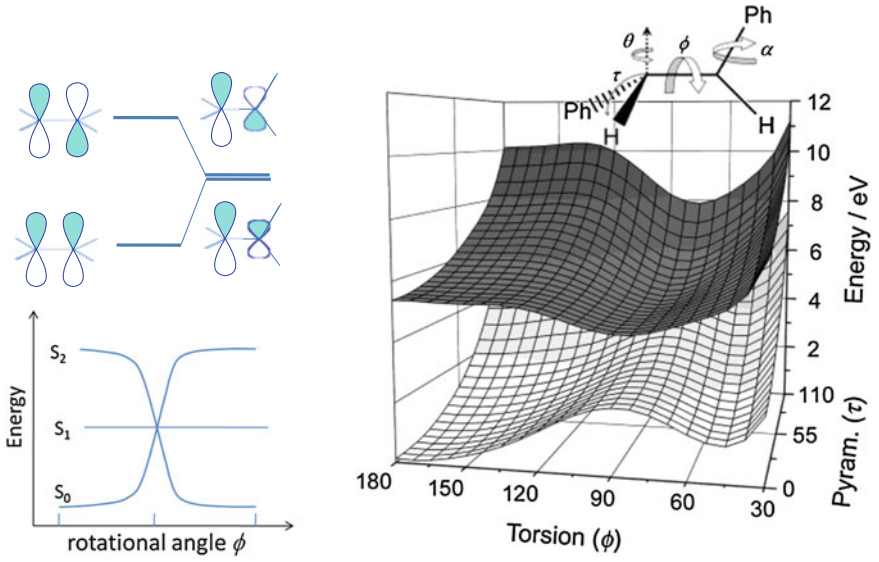

Fig. 2.28 *Left*, *top*: effect of of C–C bond rotation angle ϕ on π orbitals and energy scheme of ethylene. *Left*, *bottom*: schematic energy dependence for different configurations of two electrons in the MO scheme above. *Right*: quantum chemical potential surfaces for S_o and S_1 of stilbene along the coordinates ϕ of C–C bond rotation and τ of pyramidal distortion as defined in the figure. *Right*-hand side reprinted with permission from Ref [28]., Quenneville J, Martínez TJ J Phys Chem A 107:829–837, Copyright © 2003, American Chemical Society

to the *trans*-conformation. Experimentally, it is indeed found that the quantum yields from *trans* to *cis* or from *cis* to *trans* are both on the order of 50 % [29]. It must be mentioned, though, that the real mechanism of this photoreaction may be much more complex and may involve the potential surface of the excited triplet state, too, as well as distortions of additional motional degrees of freedom such as the pyramidal distortion indicated in Fig. 2.28 as points of transition between different potential surfaces.

Whereas, for C=C double bonds, rotation around the bond is the only way to achieve the *cis/trans*-isomerization, there are other options in the case of double bonds involving heteroatoms. A much studied system is azobenzene which is used as a chemical actinometer and is a very prominent candidate in modern research about molecular devices. Here the photoisomerization process implies a rehybridization at one of the nitrogen atoms with an intermediate linearization of the N=N–C angle [30, 31] (Fig. 2.29).

In nature, *cis/trans*-photoisomerization provides the mechanism of two important biological functions. The first is the process of vision where the key chromophore is the polyene retinal, chemically bound through a azomethine function (Schiff base) to the protein opsin to form the rhodopsin unit, which is to be found in the light sensitive cells of the retina [32]. In the dark, the retinylidene group is in an 11-*cis* configuration (cf. Fig. 2.30). It isomerizes to the all-*trans* form upon light excitation. This process triggers a sequence of events during which the retinal is released and new rhodopsin is generated by the binding of fresh 11-*cis* retinal to the opsin.

The *cis/trans*-photoisomerization of rhodopsin serves another important function in photosynthetic archaea as *halobacterium halobium,* a single-celled microorganism that stands extreme habitats such as hot springs and salt lakes. Here the dark state of the retinylidene moiety is all-*trans* (cf. Fig. 2.30) and undergoes a *trans* to *cis* photoisomerization of the double bond at position 13 upon which a proton at the azomethine nitrogen atom is released. Again, this process is part of a cycle, which, in this case, however, does not elicit a nerve signal but serves to pump protons across the cell membrane, so that a proton gradient between inner and outer space of the membrane is created [33]. Thus, the light energy is transformed to osmotic energy and later to chemical energy via the transformation of ADP to ATP.

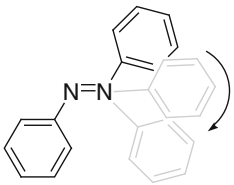

Fig. 2.29 Photoisomerization pathway of azobenzene

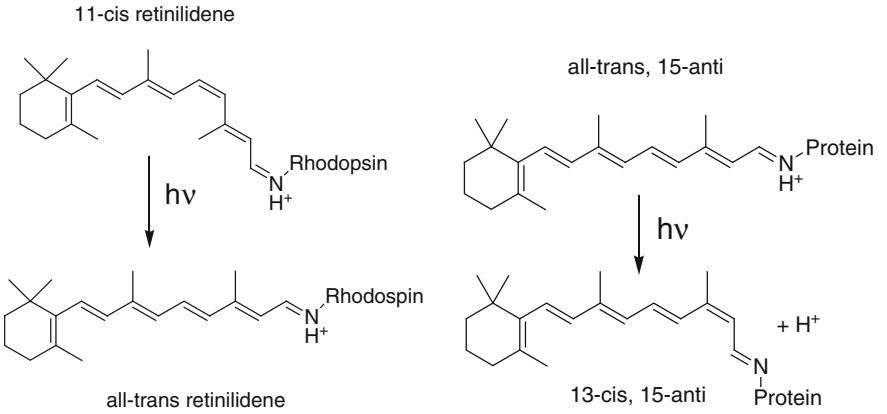

Fig. 2.30 *Left*: Primary photochemical process in vision. *Right*: Primary photochemical process of light-driven proton pump involving bacteriorhodopsin in halobacteria

References

1. Parson WW (2007) Modern optical spectroscopy. With exercises and examples from biophysics and biochemistry. Springer, Berlin Heidelberg
2. Burgess C, Frost T (eds) (1999) Standards and best practice in absorption spectrometry. Blackwell Science, London
3. Gore MG (ed) (2000) Spectrophotometry & Spectrofluorimetry. Oxford University Press, Oxford
4. Lakowicz JR (2006) Principles of fluorescence spectroscopy. Springer Science+Business Media, New York
5. Schweitzer C, Schmidt R (2003) Physical mechanisms of generation and deactivation of singlet oxygen. Chem Rev 103(5):1685–1757
6. Turro NJ, Scaiano JC, Ramamurthy V (2009) Principles of molecular photochemistry: an introduction. University Science Books, Sausalito
7. Klán P, Wirz J (2009) Photochemistry of organic compounds. From concept to practice. Wiley, Chichester
8. Stochel G, Brindell M, Macyk W, Stasicka Z, Szacilowski K (2009) Bioinorganic photochemistry. Wiley, Chichester
9. Kavarnos GJ (1993) Fundamentals of photoinduced electron transfer. VCH Publishers, New York
10. Kohen E, Hirschberg J, Santus R (1995) Photobiology. Academic Press, San Diego
11. Batschauer A (ed) (2003) Photoreceptors and light signalling. Comprehensive series in photochemical and photobiological sciences. The Royal Society of Chemistry, Cambridge
12. Schmidt W (2000) Optische spektroskopie. Wiley-VCH, Weinheim
13. Murrell JN (1963) The theory of the electronic spectra of organic molecules. Methuen&Co, London
14. Byron CM, Werner TC (1991) Experiments in synchronous fluorescence spectroscopy for the undergraduate instrumental chemistry course. J Chem Educ 68:433–436
15. Diez M, Zimmermann B, Börsch M, König M, Schweinberger E, Steigmüller S, Reuter R, Felekyan S, Kudryavtsev V, Seidel CAM, Gräber P (2004) Proton-powered subunit rotation in single membrane-bound F_0F_1-ATP synthase. Nat Struct Mol Biol 11:135–141

16. Schmidt R (2006) Quantitative determination of $^1S_g^+$ and ^1D_g singlet oxygen in solvents of very different polarity. General energy gap law for rate constants of electronic energy transfer to and from O_2 in the absence of charge transfer interactions. J Phys Chem A 110:2622–2628
17. Bodesheim M, Schütz M, Schmidt R (1994) Triplet state energy dependence of the competitive formation of O_2 ($^1S_g^+$), O_2 (^1D_g) and O_2 ($^3S_g^-$) in the sensitization of O_2 by triplet states. Chem Phys Lett 221:7–14
18. Schmidt R (2006) The effect of solvent polarity on the balance between charge transfer and non-charge transfer pathways in the sensitization of singlet oxygen by pp* triplet states. J Phys Chem A 110(18):5990–5997
19. Förster T (1970) Diabatic and adiabatic processes in photochemistry. Pure Appl Chem 24:443–449
20. Miller JR, Calcaterra LT, Closs GL (1984) Intramolecular long-distance electron transfer in radical anions. The effect of free energy and solvent on reaction rates. J Am Chem Soc 106:3047–3049
21. Marcus RA (1956) On the theory of oxidation-reduction reactions involving electron transfer. I. J Chem Phys 24:966–978
22. Marcus RA (1956) Electrostatic free energy and other properties of states having nonequilibrium polarization. I J Chem Phys 24:979–989
23. Marcus RA (1957) On the theory of oxidation-reduction reactions involving electron transfer. III. Applications to data on the rates of organic redox reactions. J Chem Phys 26:872–877
24. Degtyarenko KN, North ACT, Findlay JBC (1999) PROMISE: a database of bioinorganic motifs. Nucleic Acids Res 27:233–236
25. Deisenhofer J, Michel H (1992) High-resolution crystal structures of bacterial photosynthesis reaction centers. In: Ernster L (ed) Molecular mechanisms in bioenergetics. Elsevier, Amsterdam, pp 103–120
26. Marciniak B, Kozubek H, Paszyc S (1992) Estimation of pK_a* in the first excited singlet state. J Chem Educ 69:247–249
27. Tsien RY (1998) The green fluorescent protein. Annu Rev Biochem 67:509–544
28. Quenneville J, Martínez TJ (2003) Ab initio study of cis-trans photoisomerization in stilbene and ethylene. J Phys Chem A 107:829–837
29. Gegiou D, Muszkat KA, Fischer E (1968) Temperature dependence of photoisomerization. V. The effect of substituents on the photoisomerization of stilbenes and azobenzenes. J Am Chem Soc 90:3907–3918
30. Rau H, Lüddecke E (1982) On the rotation-inversion controversy on photoisomerization of azobenzenes. Experimental proof of inversion. J Am Chem Soc 104:1616–1620
31. Rau H (1984) Further evidence for rotation in the pp* and inversion in the np* photoisomerization of azobenzenes. J Photochem 26:221–225
32. Stuart JA, Brige RR (1996) Characterization of the primary photochemical events in bacteriorhodopsin and rhodopsin. In: Lee AG (ed) Rhodopsin and G-protein linked receptors, part A, vol 2. JAI Press, Greenwhich, Conn, pp 33–140
33. Haupts U, Haupts C, Oesterhelt D (1995) The photoreceptor sensory rhodopsin I as a two-photon-driven proton pump. Proc Natl Acad Sci 92:3834–3838

Chapter 3
Molecular Biological Mechanisms in Photodynamic Therapy

Barbara Krammer and Thomas Verwanger

Abstract Cellular and molecular photodamage mechanisms are initiated by light-activation of a photosensitizer following its accumulation in cellular targets. While lethal doses of photodynamic therapy (PDT) eliminate vessels and cells, sublethal effects occur, e.g., during fluorescence diagnosis (FD). Accordingly, the events subsequent photoactivation lead to different cellular endpoints being primarily growth stimulation, damage repair, autophagy, apoptosis, and necrosis. Activation of survival pathways seems to be not only involved in growth stimulation, but also in PDT damage transmission. Sublethal PDT results from activation of cellular damage protection and adaptive mechanisms, and can modulate signaling pathways and immune reactions. Autophagy may serve to rescue cells or lead to cell death under special conditions. Lethal PDT activates stress response, e.g., via mitochondria or ER, inducing apoptosis. If the damage is too severe, the cellular energy level low or the plasma membrane leaky, cells will die by necrosis.

Abbreviations

AIF	Apoptosis-inducing factor
AKT	Protein kinase B
ALA	Aminolevulinic acid
ANT	Adenine nucleotide translocator
AP-1	Activator protein 1
APAF-1	Apoptotic protease activating factor-1
Bak	Bcl-2 homologous antagonist/killer
Bax	Bcl-2–associated X protein
BCL-2	B-cell lymphoma 2
BID	BH3 interacting-domain death agonist

B. Krammer (✉) · T. Verwanger
Department of Molecular Biology, University of Salzburg, Salzburg, Austria
e-mail: barbara.krammer@sbg.ac.at

T. Verwanger
e-mail: thomas.verwanger@sbg.ac.at

M. H. Abdel-Kader (ed.), *Photodynamic Therapy*,
DOI: 10.1007/978-3-642-39629-8_3,

COX-2	Cyclooxygenase-2
DUSP-1	Dual specificity phosphatase 1
ECM	Extracellular matrix
ERK2	Extracellular signal-regulated kinase 2
FAS	TNF receptor superfamily, member 6
c-fos	FBJ murine osteosarcoma viral oncogene homolog
FD	Fluorescence diagnosis
HO-1	Heme oxygenase 1
c-jun	Jun proto-oncogene
JNK	c-Jun N-terminal kinase
MAPK	Mitogen-activated protein kinase
mHK	Mitochondria-bound hexokinase
mTOR	Mammalian target of rapamycin
NF-kappa B	Nuclear factor 'kappa-light-chain-enhancer' of activated B-cells
PDD	Photodynamic diagnosis
PDT	Photodynamic therapy
PI3 K	Phosphatidylinositol-3-kinase
PpIX	Protoporphyrin IX
RNS	Reactive nitrogen species
ROS	Reactive oxygen species
SERCA2	Sarco/endoplasmic Ca^{2+} -ATPase-2
UPR	Unfolded protein response
VEGF	Vascular endothelial growth factor

3.1 Introduction

Fluorescence diagnosis (FD) or photodynamic diagnosis (PDD) and photodynamic therapy (PDT) are methods for the selective detection and treatment of premalignant or malignant lesions [1], of several other diseases like microbial infections or of abnormal vessel growth by minimally invasive procedures lacking of major side effects and relevant mutagenicity. This is achieved via a so-called photosensitizer which is activated by visible light with a wavelength matching its absorption maxima: The subsequent photosensitizer deactivation occurs either via fluorescence, which is used for target detection, or via chemical reactions in its triplet state. In the presence of oxygen, the chemical reactions are induced by electron or energy transfer, by which reactive oxygen (ROS) or nitrogen species (RNS) are formed. Since photosensitizers generally selectively accumulate in (pre)malignant tissues, in contrast to normal tissues, and in some other targets like bacteria, FD, and PDT can be used for tumor treatment or, e.g., disinfection. Most of the photosensitizers for PDT are porphyrin-based or naturally occurring such as

hypericin, a constituent of the St. John's wort; many of them are currently tested and several of those are already approved and clinically used [2].

The present review shall give an overview on some molecular biological effects of PDT in tumor tissues and cells.

The efficiency of PDT depends on the type of photosensitizer, drug concentration, and intracellular localization, incubation time, irradiation parameters (fluence, power density, and wavelength), oxygen availability, and the susceptibility of the target including antioxidant defense mechanisms. The sequence of steps leading to tissue damage will be described in the following.

3.2 Development of Intracellular Damage

After application of a photosensitizer or a prodrug to the patient by several routes such as intravenous or topical, the substance reaches the target tissue directly or via blood transportation, accumulating in vessels and/or tumor cells and/or extracellular matrix (ECM). In cases where the prodrug aminolevulinic acid (ALA)—a natural precursor of the protoporphyrin IX (PpIX) in the heme synthesis—is applied in excess, PpIX is accumulated in mitochondria and serves as an endogenous photosensitizer. Uptake to cells occurs by various active or passive mechanisms depending on the type of the used photosensitizer. In the time interval between photosensitizer accumulation and irradiation a relocalization of the photosensitizer to other subcellular targets or even efflux from the cell may occur. Positioned irradiation of the photosensitizer by lasers, lamps, or LEDs activates the substance. In the presence of molecular oxygen, especially singlet oxygen, other ROS and additionally RNS are locally formed; the latter mainly in the vascular response [3, 4]. Depending not only on the localization of the photosensitizer and on the amount of generated reactive species, but also on general and immediate antioxidant defense mechanisms of the cell, the extent of the primary cell damage originates from oxidation of the molecules located at or very close to the damage site within the diffusion range of the reactive species. Proteins and lipids are oxidized; DNA only, if it is located next to the nuclear membrane, since most clinically applied photosensitizers enter the nucleus, if at all, to a minor degree [5]. This may account for the absence of major mutagenic effects of PDT.

Induction of minimal damage is obviously tolerated by the cells or may even lead to growth stimulation by some photosensitizers.

Once protein oxidation and lipid peroxidation and their consequences cannot be prevented or repaired by, e.g., vitamin E supply, upregulation of protective genes [6], or hypoxia-induced resistance to PDT in the case of vessels [7], damage development continues until an irreversible endpoint is reached. Amount and kind of damage development again are influenced by cell physiological parameters, be it the amount of $[Ca^{2+}]i$ [8], genetic/molecular response, and onset of signaling pathways [6] or the interaction with the cell environment such as the ECM. At the level of organelle photodamage, the cells could still survive by the rescue

mechanism of autophagy by which the damaged targets are engulfed intracellularly in autophagosomes, which fuse with lysosomes in order to eliminate the "garbage". This seems to occur after PDT with ER- and mitochondria-localizing photosensitizers such as hypericin in apoptosis-competent cells. In contrast, photodamage to lysosomes may lead to the abortion of an autophagic response [9].

If cells and vessels are not rescued by autophagy, the target tissue is eliminated. Damage to vessels may lead to a vascular shut-down, blood flow stasis, and hypoxia [10]; often accompanied by nitric oxide production [3] or hypoxia-induced gene expression [6] like that of vascular endothelial growth factor (VEGF) [11]. Damage to the ECM has an impact on, e.g., collagens and matrix metalloproteases [12]. Lethal damage to tumor cells can be classified into several "deadly" endpoints ranging from autophagy to necrosis.

The endpoints of cellular damage development will be described subsequently under molecular aspects.

3.3 Molecular Mechanisms in Sublethal Damage Processing

Sublethal PDT is the result of low-dose conditions, which are, e.g., present during FD, used for stimulation of anticancer immune responses [13, 14] or which are inevitable in deeper tissue layers, which receive less irradiation and/or lower photosensitizer concentrations than the surface. At the transition between "no effect" and damage, harmless or even stimulating PDT may be applied, which indeed counteracts tumor eradication, but would be advantageous for, e.g. wound healing.

A stimulatory effect on cell growth found after hypericin-PDT on human tumor cells [15] or after aluminum phthalocyanine-mediated-PDT on osteoblastic cells [16] has been observed in a few cases only. In the case of hypericin-PDT, it can be suggested that the known stimulation of the survival pathways of $p38^{MAPK}$ and JNK is responsible for the growth promotion [17]. Also the activated transcription factor NF-kappa B mediates therapy resistance and growth stimulation. After PDT of glioblastoma cells, inhibition of NF-kappa B could improve the therapeutic effect [18].

By increasing the PDT dose, the cells activate rescue mechanisms ranging from immediate response to scavenge ROS and RNS by, e.g., reduced glutathione or superoxide dismutase to long-lasting strategies to neutralize oxidized products and eliminate their consequences. The mechanisms include, e.g., the use of vitamins or the induction or upregulation of gene and protein expression, which assist in cell-specific [6] or more general repair and adaptive strategies. This includes, e.g., induction/upregulation of VEGF [19], HO-1 [20], JNK1, $p38^{MAPK}$, and PI3K, while irreversibly inhibiting ERK2 [20, 21], $p38^{MAPK}$-mediated COX-2 [22] and Bcl-2 phosphorylation [23].

Autophagy of damaged organelles is the final rescue mechanism to protect the cells from death. The process can be initiated by those light-activated photosensitizers, which are localizing in ER, mitochondria, and partly in lysosomes. Autophagy may occur independently of apoptosis; in the case of defective apoptotic pathways it may lead to cell death, as it will be described below. The current state of knowledge is reviewed in detail by Reiners et al. [9].

3.4 Molecular Mechanisms in Lethal Damage Processing

Whether photodamage is lethal will be determined not only by the PDT protocol and the above-described protection mechanisms, but also by the cellular physiology and the influence of cellular environment as the ECM in tissue. It can be hypothesized that signaling pathways for induction of cell death and survival are active in parallel in the same cell, until the cell has to make a decision on the basis of the summary of all information available. In the case of hypericin-PDT on A431 cells, e.g., the strongly upregulated MAPK phosphatase 1 (DUSP1) could have the function of the switch between survival and apoptosis [6]. Autophagic cell death is "switched on", when the apoptotic pathway is blocked, as found in Bax/Bak knock-out mice with mTOR and PI3K/AKT playing a role in the autophagic pathway [9, 24]. A decision between apoptosis and necrosis is based *inter alia* on intracellular energy supply, since apoptosis as an energy-consuming process is dependent on ATP or alternative energy sources [25]. Necrosis induction is also promoted by leakiness of the cellular membrane, which is likely to be caused by photosensitizer localization in this target.

If photosensitizer localization (e.g., in mitochondria), the extent of damage and some special events like loss of BCL-2 favor apoptosis induction, the latter may be executed by mainly two ways. The mitochondrial pathway is triggered at the mitochondria either directly [25] or via the ER stress pathway. In the case of direct induction, it is likely that the adenine nucleotide translocator ANT is oxidized by ROS, the mitochondrial membrane potential is decreased and the mitochondrial permeability transition pores are opened. Subsequently, cytochrome c is released from the mitochondrial intermembrane space, forming an apoptosome with apoptotic protease activating factor-1 (APAF-1) and procaspase 9. By this, active procaspase 9 is provided, which subsequently activates the executing caspases 3 and 6, as shown with squamous cell carcinoma cells [25, 26]. Also loss of BCL-2 and lysosomal damage can lead to apoptosis induction.

While in most cases, when apoptosis is executed via the mitochondrial pathway, cytochrome c release and caspase 9, 3, 6, and 7 activation lead to cell decomposition, also the apoptosis inducing factor (AIF) may generate DNA and cell fragmentation in a caspase-independent manner [27]. In addition, the receptor-mediated pathway may be induced via an external signal or by an internal feedback loop, occasionally by ROS-dependent FAS- aggregation, activating FAS receptor, adaptor protein, and caspase 8. The latter may lead to activation of the

caspases 3, 6, and 7 directly or via the mitochondrial pathway, mediated by the proapoptotic Bcl-2 member Bid.

Also some particular events are described such as a release of the mitochondria-bound hexokinase mHK, mediated by a pH drop following hypericin-PDT [28].

The expression of many genes and proteins was found to be altered following apoptosis-inducing PDT, depending on the cell line, treatment protocol, and time after treatment. Upregulation of c-jun and c-fos, both together forming the transcription factor AP-1, was detected in several studies. In addition, treatment of human squamous cell carcinoma cells with hypericin-PDT resulted 1.5–8 h later in up- and down-regulation of genes concerning apoptosis, cytoskeleton, and cell attachment, oxidative stress, proliferation and cell cycle, mitogen-activated protein kinase signaling, protein transport, energy metabolism, and some more [6]. The molecular mechanisms of PDT-induced apoptosis using hypericin are furthermore presented in detail in a review of Buytaert et al. [29]. The authors describe the induction of apoptosis via the ER stress pathway, which leads to apoptosis or may alternatively result in autophagy, when cells are apoptosis-incompetent, as mentioned above.

The ER stress pathway is favored, if the photosensitizer is located in the ER, as it applies to hypericin. In this case, irradiation leads to an immediate sarco/endoplasmic Ca^{2+} -ATPase-2 (SERCA2) pump photodamage, to ER Ca^{2+} depletion and to disruption of Ca^{2+} homeostasis, which induces apoptosis via Bax and Bak or autophagy, when Bax and Bak are not available [30]. In addition, the accumulation of unfolded proteins in the ER triggers the unfolded protein response (UPR). Expression profiling 7 h after hypericin-PDT of bladder cancer cells confirmed differential changes in ER stress response and UPR, autophagy, proliferation, inflammation, and antioxidant defense [29].

Autophagy is stimulated by various stress signals such as oxidative stress and may be induced or prevented by destruction of lysosomes. As mentioned above, autophagic processes lead to cell death, when apoptosis is induced, but cannot be executed if the proapoptotic Bax and Bak proteins are absent [9]. mTOR and PI3 K/AKT seem to play a role in the autophagic pathway [9, 24].

Also mitotic cell death was observed following hypericin-PDT, which is suggested to be generated by hypericin-enhanced ubiquitinylation of the heat-shock protein 90 [31].

If the damage is too severe, the cellular energy level low or the cytoplasmic membrane leaky, cells will die by necrosis.

References

1. Dolmans DE, Fukumura D, Jain RK (2003) Photodynamic therapy for cancer. Nat Rev Cancer 3(5):380–387
2. Agostinis P, Berg K, Cengel KA, Foster TH, Girotti AW, Gollnick SO, Hahn SM, Hamblin MR, Juzeniene A, Kessel D, Korbelik M, Moan J, Mroz P, Nowis D, Piette J, Wilson BC, Golab J (2011) Photodynamic therapy of cancer: an update. CA Cancer J Clin 61(4):250–281

3. Korbelik M, Parkins CS, Shibuya H, Cecic I, Stratford MR, Chaplin DJ (2000) Nitric oxide production by tumour tissue: impact on the response to photodynamic therapy. Br J Cancer 82(11):1835–1843
4. Price M, Kessel D (2010) On the use of fluorescence probes for detecting reactive oxygen and nitrogen species associated with photodynamic therapy. J Biomed Opt 15(5):051605
5. Krammer B, Hubmer A, Hermann A (1993) Photodynamic effects on the nuclear envelope of human skin fibroblasts. J Photochem Photobiol, B 17(2):109–114
6. Sanovic R, Krammer B, Grumboeck S, Verwanger T (2009) Time-resolved gene expression profiling of human squamous cell carcinoma cells during the apoptosis process induced by photodynamic treatment with hypericin. Int J Oncol 35(4):921–939
7. Casas A, Di Venosa G, Hasan T, Al B (2011) Mechanisms of resistance to photodynamic therapy. Curr Med Chem 18(16):2486–2515
8. Hubmer A, Hermann A, Uberriegler K, Krammer B (1996) Role of calcium in photodynamically induced cell damage of human fibroblasts. Photochem Photobiol 64(1):211–215
9. Reiners JJJ, Agostinis P, Berg K, Oleinick NL, Kessel D (2010) Assessing autophagy in the context of photodynamic therapy. Autophagy 6(1):7–18
10. Krammer B (2001) Vascular effects of photodynamic therapy. Anticancer Res 21(6B):4271–4277
11. Bhuvaneswari R, Gan YY, Lucky SS, Chin WW, Ali SM, Soo KC, Olivo M (2008) Molecular profiling of angiogenesis in hypericin mediated photodynamic therapy. Mol Cancer 7:56
12. Pazos MC, Nader HB (2007) Effect of photodynamic therapy on the extracellular matrix and associated components. Braz J Med Biol Res 40(8):1025–1035
13. Korbelik M (2011) Cancer vaccines generated by photodynamic therapy. Photochem Photobiol Sci 10(5):664–669
14. Sanovic R, Verwanger T, Hartl A, Krammer B (2011) Low dose hypericin-PDT induces complete tumor regression in BALB/c mice bearing CT26 colon carcinoma. Photodiagnosis Photodyn Ther 8(4):291–296
15. Berlanda J, Kiesslich T, Engelhardt V, Krammer B, Plaetzer K (2010) Comparative in vitro study on the characteristics of different photosensitizers employed in PDT. J Photochem Photobiol, B 100(3):173–180
16. Zancanela DC, Primo FL, Rosa AL, Ciancaglini P, Tedesco AC (2011) The effect of photosensitizer drugs and light stimulation on osteoblast growth. Photomed Laser Surg 29(10):699–705
17. Agostinis P, Vantieghem A, Merlevede W, de Witte PA (2002) Hypericin in cancer treatment: more light on the way. Int J Biochem Cell Biol 34(3):221–241
18. Coupienne I, Bontems S, Dewaele M, Rubio N, Habraken Y, Fulda S, Agostinis P, Piette J (2011) NF-kappaB inhibition improves the sensitivity of human glioblastoma cells to 5-aminolevulinic acid-based photodynamic therapy. Biochem Pharmacol 81(5):606–616
19. Schmidt-Erfurth U, Schlotzer-Schrehard U, Cursiefen C, Michels S, Beckendorf A, Naumann GO (2003) Influence of photodynamic therapy on expression of vascular endothelial growth factor (VEGF), VEGF receptor 3, and pigment epithelium-derived factor. Invest Ophthalmol Vis Sci 44(10):4473–4480
20. Kocanova S, Buytaert E, Matroule JY, Piette J, Golab J, de Witte P, Agostinis P (2007) Induction of heme-oxygenase 1 requires the p38MAPK and PI3 K pathways and suppresses apoptotic cell death following hypericin-mediated photodynamic therapy. Apoptosis 12(4):731–741
21. Assefa Z, Vantieghem A, Declercq W, Vandenabeele P, Vandenheede JR, Merlevede W, de Witte P, Agostinis P (1999) The activation of the c-Jun N-terminal kinase and p38 mitogen-activated protein kinase signaling pathways protects HeLa cells from apoptosis following photodynamic therapy with hypericin. J Biol Chem 274(13):8788–8796
22. Hendrickx N, Volanti C, Moens U, Seternes OM, de Witte P, Vandenheede JR, Piette J, Agostinis P (2003) Up-regulation of cyclooxygenase-2 and apoptosis resistance by p38

MAPK in hypericin-mediated photodynamic therapy of human cancer cells. J Biol Chem 278(52):52231–52239
23. Vantieghem A, Xu Y, Assefa Z, Piette J, Vandenheede JR, Merlevede W, De Witte PA, Agostinis P (2002) Phosphorylation of Bcl-2 in G2/M phase-arrested cells following photodynamic therapy with hypericin involves a CDK1-mediated signal and delays the onset of apoptosis. J Biol Chem 277(40):37718–37731
24. Buytaert E, Dewaele M, Agostinis P (2007) Molecular effectors of multiple cell death pathways initiated by photodynamic therapy. Biochim Biophys Acta 1776(1):86–107
25. Berlanda J, Kiesslich T, Oberdanner CB, Obermair FJ, Krammer B, Plaetzer K (2006) Characterization of apoptosis induced by photodynamic treatment with hypericin in A431 human epidermoid carcinoma cells. J Environ Pathol Toxicol Oncol 25(1–2):173–188
26. Skulachev VP (2001) The programmed death phenomena, aging, and the Samurai law of biology. Exp Gerontol 36(7):995–1024
27. Furre IE, Shahzidi S, Luksiene Z, Moller MT, Borgen E, Morgan J, Tkacz-Stachowska K, Nesland JM, Peng Q (2005) Targeting PBR by hexaminolevulinate-mediated photodynamic therapy induces apoptosis through translocation of apoptosis-inducing factor in human leukemia cells. Cancer Res 65(23):11051–11060
28. Miccoli L, Beurdeley-Thomas A, De Pinieux G, Sureau F, Oudard S, Dutrillaux B, Poupon MF (1998) Light-induced photoactivation of hypericin affects the energy metabolism of human glioma cells by inhibiting hexokinase bound to mitochondria. Cancer Res 58(24):5777–5786
29. Buytaert E, Matroule JY, Durinck S, Close P, Kocanova S, Vandenheede JR, de Witte PA, Piette J, Agostinis P (2008) Molecular effectors and modulators of hypericin-mediated cell death in bladder cancer cells. Oncogene 27(13):1916–1929
30. Buytaert E, Callewaert G, Hendrickx N, Scorrano L, Hartmann D, Missiaen L, Vandenheede JR, Heirman I, Grooten J, Agostinis P (2006) Role of endoplasmic reticulum depletion and multidomain proapoptotic BAX and BAK proteins in shaping cell death after hypericin-mediated photodynamic therapy. Faseb J 20(6):756–758
31. Blank M, Mandel M, Keisari Y, Meruelo D, Lavie G (2003) Enhanced ubiquitinylation of heat shock protein 90 as a potential mechanism for mitotic cell death in cancer cells induced with hypericin. Cancer Res 63(23):8241–8247

Part III
Methods and Instrumentation

Chapter 4
Diagnostic and Laser Measurements in PDT

Rudolf Steiner

Abstract The diagnosis of tissue alterations by fluorescence spectroscopy or different modalities of fluorescence imaging is widely used to detect precancerous or cancerous lesions. Demarcation of such lesions supports the efficient treatment either by photodynamic therapy (PDT) or conventional surgical intervention. Autofluorescence of tissue intrinsic chromophores like flavines, Nicotinamide-Adenine-Dinucleotide-Hydrogen (NADH), collagens or porphyrins excited by UV or blue light and change of the concentrations of the fluorescent compounds is an indication of tissue alterations. More specific is the use of fluorescent sensitizers enriched in target cells after local or systemic application. Meanwhile, sensitizers of the third generation are developed or coupled to nanoparticles as carriers. For application of the optimum light dose in PDT, dosimetry measurements must be performed with devices adapted to the geometry of the specific organ to be treated. The use of fluorescent sensitizers as diagnostic and therapeutic agents in dermatology goes back to Hermann von Tappeiner (1847–1927), director of the pharmacological institute at the university in Munich, in the late 19th century [1]. According to the findings of his student Raab (Z Biol 39:524–546, 1900) who discovered a light dependent phototoxicity in his cellular experiments [2], von Tappeiner introduced and published the term "photodynamic" in von Tappeiner and Jodlbauer (Dtsch Arch Klein Med 80:427–487, 1904). Since then, phototherapy continuously developed and Finsen Ackroyd et al. (Photochem Photobiol 74:656–669, 2001) were awarded the Nobel Prize 1903 after he had treated 800 patients suffering from Lupus vulgaris.

R. Steiner (✉)
Institute for Laser Technologies in Medicine and Metrology,
University of Ulm, Ulm, Germany
e-mail: rudolf.steiner@ilm.uni-ulm.de

M. H. Abdel-Kader (ed.), *Photodynamic Therapy*,
DOI: 10.1007/978-3-642-39629-8_4, © Springer-Verlag Berlin Heidelberg 2014

4.1 Fundamentals of Fluorescence

Molecules may have different electronic states. The lowest energy state is called ground state S_0. When additional energy is absorbed, this may happen by absorption of a photon with Energy, $E = hv$ [3], then the molecule is excited and an energy transfer from S_0 to higher orbitals (singlet states) occurs, generally to S_1 as is illustrated in Fig. 4.1. From the excited state, the atom or molecule in about 10^{-7} s returns to the ground state by heat conversion of the energy or by emission of a photon (fluorescence).

The absorption of the photon energy depends on the wavelength and can be described by the formula:

$$I_{(\lambda)} = I_0 10^{-\varepsilon(\lambda)\, c\, d} = I_0 e^{-\mu a\, d}$$

where $\varepsilon(\lambda) =$ extinction coefficient, $c =$ concentration of absorbing molecules, and $d =$ path length of the light through the medium. In an equal expression, normally used by physicists, μ_a (cm^{-1}) is the absorption coefficient.

The fluorescence intensity per solid angle, $I_{F(\lambda)}$, is proportional to the excitation intensity I_0 multiplied by the quantum efficiency η of the molecule:

$$I_{F(\lambda)} = I_0[1 - 10{-}^{\varepsilon(\lambda)\, c\, d}]\, \eta\, \Omega/4\pi, \text{ with}$$

η: quantum yield and Ω: solid angle of isotropic fluorescence radiation.

From Fig. 4.1, it can be derived that the emission wavelength of the fluorescence is less in energy and therefore red-shifted (Fig. 4.2). This was first discovered by Stokes in 1852.

The energy levels of an atom or a molecule are often presented as a Jablonski diagram. In Fig. 4.3 the arrow A means the absorption of a photon and an electron transfer from the ground state to a higher singlet state from which by internal

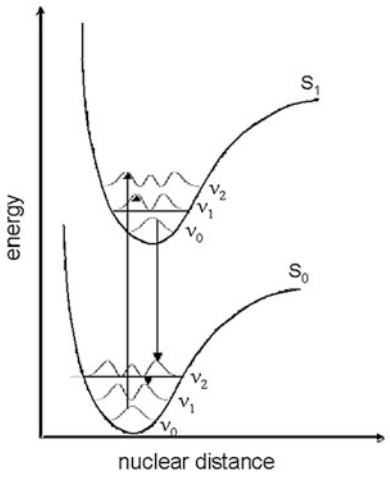

Fig. 4.1 Potential diagram of electronic states of a molecule in ground state S_0 and excited state S_1 with vibration levels v_i

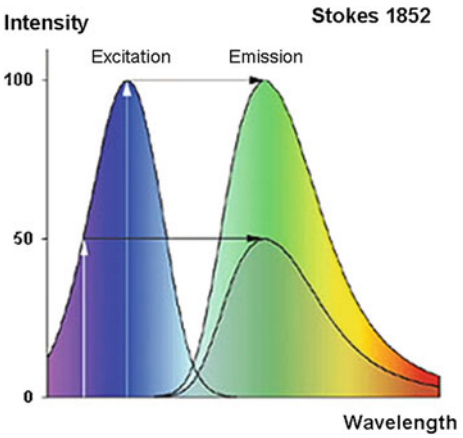

Fig. 4.2 Stokes red-shift of fluorescence emission. Excitation and emission are mirror-inverted in form

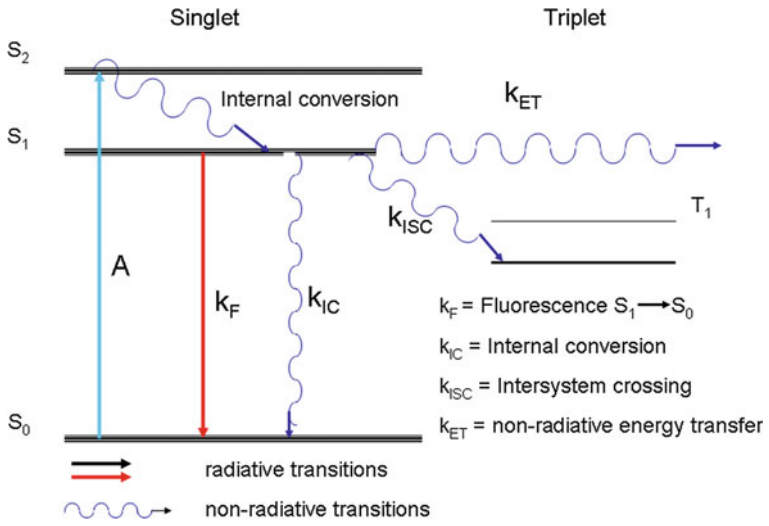

Fig. 4.3 Jablonski diagram of energy levels of an excited molecule. The sum of the kinetic rate constants is related to the lifetime of the excited state

conversion the energy of the electron drops down to the lowest singlet S_1 state. The energy is dissipated as heat. Now energy transfer from singlet state S_1 may happen in case of fluorescence by emission of a photon to the ground state with rate constant k_F or by non radiative energy transfer also to another molecule with rate constant k_{ET}. In sensitizer molecules, the efficiency of the sensitizer is also determined by the probability of intersystem crossing from the S_1 state to the long lasting triplet state T with rate constant k_{ISC}.

The overall rate constant k of the excited singlet state is the sum of all rate constants and correlated with the lifetime τ:

$$k = k_F + k_{\mathrm{IC}} + k_{\mathrm{ISC}} + k_{\mathrm{ET}} = 1/\tau.$$

Fluorescence intensity is normally emitted isotropic, equal in all directions, and is not polarized. But when excited with polarized laser light, fluorescence emission may have a certain degree of polarization P.

Degree of polarization: $P = (I_{\parallel} - I_{\perp})/(I_{\parallel} + I_{\perp})$ where $I_{\parallel}$ is part of the fluorescence intensity parallel to the exciting beam and $I_{\perp}$ vertical.

The fluorescence anisotropy is defined as r.

$$r = \left(I_{\parallel} - I_{\perp}\right)/\left(I_{\parallel} + 2I_{\perp}\right).$$

Molecules may rotate during fluorescence lifetime or change orientation. Therefore, from fluorescence anisotropy a time constant τ_{r} for rotation diffusion can be calculated.

$\tau_r = \eta V/k_B\mathrm{T}$, where k_B = Boltzmann constant = 1.38×10^{-23} J/°K,T and °K = temperature, η = viscosity.

For spherical molecules and molecular weight M in kilo Dalton (kDa) the rotation diffusion constant in ns is approximately: τ_r [ns] = M(kDa)/2 which is $\approx$ 10 ns per 20 kDa.

Fluorescence anisotropy for rod-shaped molecules with optical transmission dipole moment parallel to the molecular axis is

$$r(t) = (r_0 - r_\infty)e^{-t/\tau r} + r_\infty$$

and the rotation diffusion $\tau_r \sim \eta$ corresponds to the viscosity.

Fluorescence anisotropy is measured with a simple experimental scheme like in Fig. 4.4. It is important for measuring cellular membrane phenomena. One example is Laurdan, when integrated into the membrane bi-layer, the generalized fluorescence anisotropy is a measure of membrane fluidity or membrane transport phenomena. The inset in Fig. 4.4 shows the polarization dependent fluorescence kinetics of glioblastoma cells incubated with Laurdan.

The intrinsic fluorescence of tissue covers a wide spectral range from 300 to 700 nm (Fig. 4.5). Amino acids, Collagen, and Elastin contribute in the UV and deep blue region, Nicotinamide-Adenine-Dinucleotide-Hydrogen (NADH) in the blue, Flavines in the green-yellow, and Porphyrins in the red part of the spectrum. According to the composition of the layered skin and the concentrations of the different fluorophores in different layers and depths, depth-resolved fluorescence of the tissue when excited with different wavelengths, 349 and 457 nm, will be possible [4].

NADH fluorescence is sensitive to ischemia, neoplasia, oxygen concentration, and metabolic functions of the tissue. Detection of lung cancer, precancerous, and malignant lesions, by autofluorescence bronchoscopy (AFB) of mucosal tissue is already in clinical practice [5, 6]. The aim is to detect early stages of dysplasia

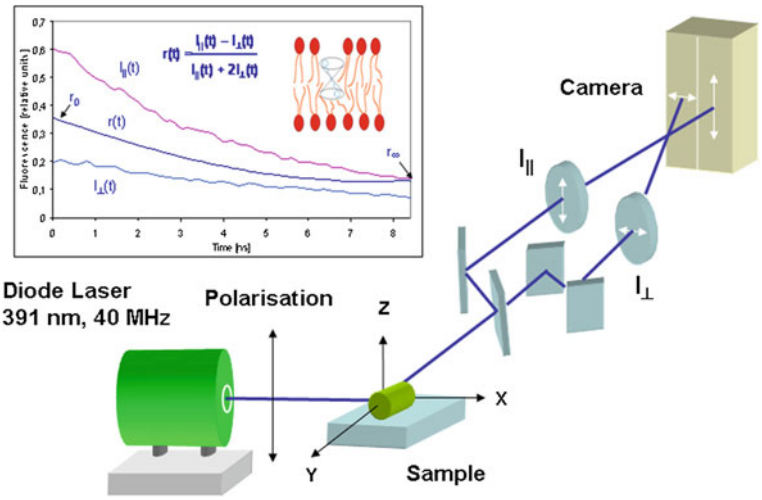

Fig. 4.4 Scheme of fluorescence polarization measurements. The inset is an example for glioblastoma cell incubated with Laurdan. (Courtesy of H. Schneckenburger, University of Applied Sciences, Aalen)

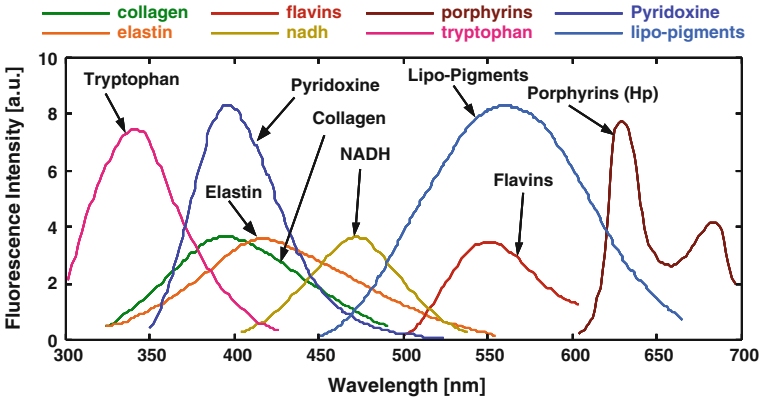

Fig. 4.5 Fluorescence spectra of different molecules in the tissue covering the whole spectral range from 300 to 700 nm

which cannot be imaged by spiral computer tomography (SCT) or standard CT [7]. Sputum cytology exhibits only 33 % of sensitivity and 64 % specificity [8]. In several studies, the advantages of AFB compared to white light bronchoscopy (WLB) are reported [9–12]. In a study with 4,983 patients [12], 1,148 male subjects had a pathologically confirmed lung cancer and AFB exhibited a 3.41 times higher possibility of lung cancer in male subjects.

Combining AFB and WLB increase the specificity and make AFB an efficient method in the detection of preinvasive and invasive bronchial cancer lesions. The sensitivities of AFB and WLB were 94.7 and 65.8 %, respectively, whereas the specificities were 57.0 and 83.6 %, respectively [11]. The lower value for the specificity of AFB is because of higher false-positive values due to fluorescence of some nonmalignant lesions as well. Figure 4.6 gives an example of how to specify the characteristic fluorescence of lung cancer in the upper airways. Three wavelengths are used, blue (442 nm), green (520 nm), and red (630 nm). With blue light the tissue is excited and most of the fluorescent molecules are located in the submucosa layer. In normal healthy mucosa (Fig. 4.6a), green fluorescence is dominant (see also spectrum in Fig. 4.6d). When a malignant lesion in the mucosa layer is present, then, due to increased vascularisation, the intensity of the blue excitation is lowered by the blood absorption. The same happens with the green emitted fluorescence. The intensity relation between green and red is inverted and the amount is strongly reduced. The spectral changes are evaluated, calibrated and displayed in false colors as overlay in the white light image (Fig. 4.6c). Several companies have devices for AFB on the market).

Excitation of tissue with infrared ultra-short laser pulses and two-photon absorption or second harmonic microscopy are advanced technologies to get diagnostic information [13] which became more important during the last years.

Another possibility to detect cancer of different organs, skin, bladder, lung or mouth, is photodynamic diagnosis (PDD) using a tumour-selective photosensitizer.

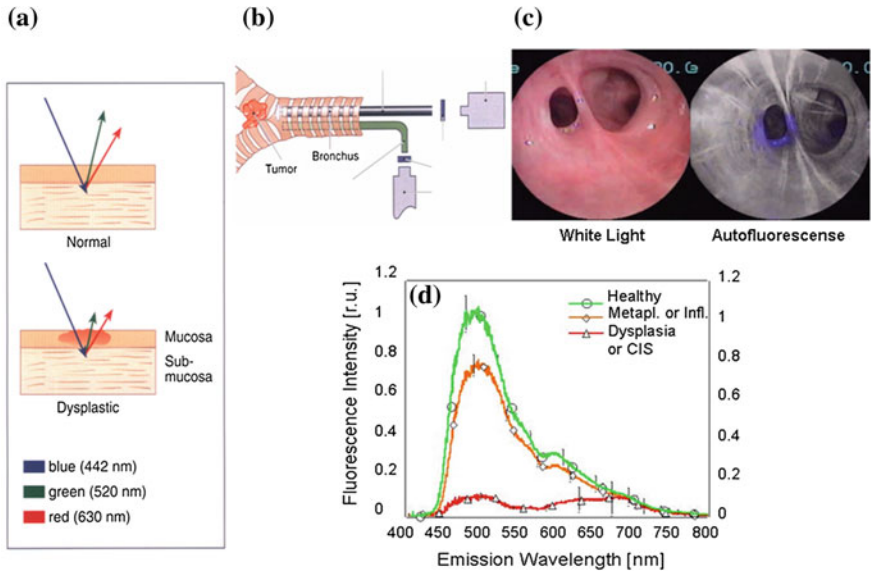

Fig. 4.6 Method of autofluorescence bronchoscopy, **a** absorption and fluorescence conditions of the three wavelengths, **b** bronchoscope, **c** example of an imaged lung cancer and **d** spectral conditions for healthy and cancerous tissue (Courtesy of Richard Wolf GmbH)

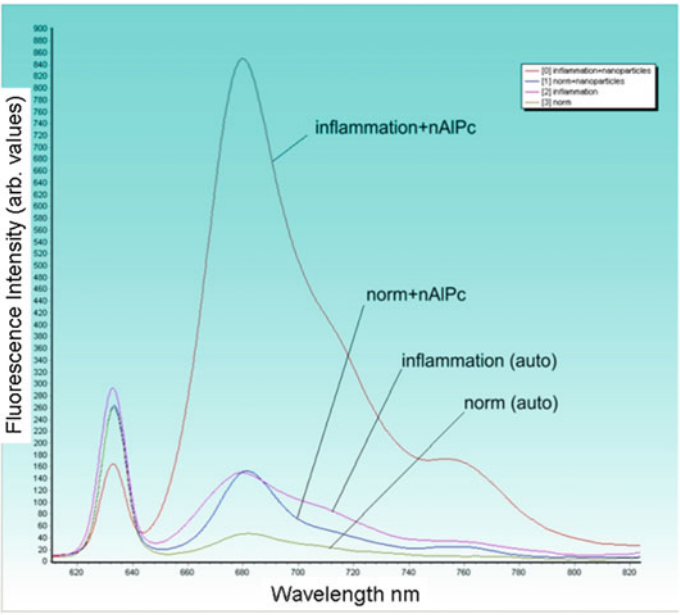

Fig. 4.7 Example of the bio-transformation of AlPc-nanoparticles to the fluorescent active monomeric form in skin inflammation (*large peak*) compared to normal skin and inflammatory tissue alone

First trials were undertaken by Baumgartner [14] using inhalation of a 5-amino-levulinic acid (5-ALA) spray for fluorescence detection of early stage lung cancer. Conventional clinical inhalation technique was a suitable method for topical 5-ALA application. With the uptake of 5-ALA, by the lung tissue and subsequent synthesis of fluorescent Protoporphyrin IX (PPIX), bronchial cancer could be detected.

4.1.1 Sensitizers

The PDT is now more than hundred years old and the sensitizers exist in first, second, and even third generation. The structures of most sensitizers are porphyrins, chlorophylls, and dyes. The first sensitizers were hematoporphyrin derivatives (DHE, "Photofrin") synthesized from heme [15]. Other examples are 5-ALA, Phthalocyanines, m-tetrahydroxyphenylchlorin (mTHPC), or mono-L-aspartyl chlorine e6 (Talaporfin, NPe6).

Several photosensitizers are commercially available for clinical use, with trademarks such as Photofrin, Photosens, Allumera, Visudyne (Verteporfin), Foscan, Metvix, Hexvix, Cysview, and Laserphyrin. New sensitizers are in

development, e.g., PVP-Hypericin, Antrin, Photochlor, Photrex, Cevira, Lumacan, Visonac, Amphinex, and Azadipyrromethene (ADPM).

Parallel to the development of molecular photosensitzers, nanoparticles and functionalized nanoparticles with high photostability and high quantum yield will become more important in future for PDD and also for PDT. Emission maximum of such nanoparticles depend on the particle size and can be shifted to the demand of specific applications. Nanoparticles are normally prepared from gold or compositions of semiconductors. Other possibilities are nanoparticles prepared from insoluble organic photosensitzers like Phthalocyanines, nAlPc, or Chlorophylls [16]. They have interesting characteristics and are only fluorescent by uptake in inflammatory tissues or tumors (Fig. 4.7). There, a biotransformation of nAlPc occurs to the active monomer form, especially interesting for skin diseases.

Depending on the physico-chemical characteristics of the molecules the sensitizers enter differently into cells and are located in the cells and accumulated in different cellular organs. Therefore, the fluorescence behavior and cellular reaction mechanisms are different. That is why cancer specific sensitizers are approved for PDD and PDT. Despite the differences, the sensitizers aim to achieve certain characteristics:

- efficient light absorption at longer wavelengths, because the spectral range between 700 and 850 nm has the deepest penetration into the tissue,
- high singlet oxygen quantum yield,
- high photostability (low photobleaching),
- high quantum yield of natural fluorescence for PDD by fluorescence spectroscopy and for optical dosimetry measurements,
- low dark toxicity not to be harmful for patients exposed to sunlight,
- fast metabolism to be eliminated from the body,
- preferential uptake in cancer tissue with high contrast to the neighboring normal tissue.

The absorption conditions of several sensitizers are summarized in Fig. 4.8 and the physico-chemical characteristics with uptake conditions and intracellular localization in Fig. 4.9.

Fig. 4.8 Maximum absorption of different sensitizers

Sensitizer	Absorption wavelength (nm)
Photofrin	**630**
5-ALA induced PPIX	**635**
Chlorin (Foscan)	**652**
Purpurin (Purlytin)	**665**
Phthalocyanin	**675**
Benzoporphyrin derivate	**695**
Texaphyrin (Antrin)	**730**
Indocyanin green	**805**

drug	uptake	localization
hydrophilic, neg. AlPcS4, 5-ALA Chlorine e6, TPPS4 Hypericin derivative	endocytosis	endosomes lysosomes ER
hydrophilic, pos. Methylene Blue Phthalocyanine der.	endocytosis	lysosomes mitochondria
Lipophilic Photophrin mTHPC, Hypericin	diffusion LDL-endocytosis	membranes organelles

Fig. 4.9 Physico-chemical characteristics of sensitizers with corresponding cellular uptake and localization

An interesting new development of near-infrared fluorescent proteins for whole-body imaging techniques for tumor localization, cell migration, and other studies involving deep-tissue imaging are the dimeric fluorescent proteins, Katushka, eqFP650, and eqFP670 [17]. The first one is claimed the brightest fluorescent protein with emission maximum above 635 nm, and the second displays the most red-shifted emission maximum and high photostability. The authors demonstrated that the dye Katushka, prepared from stable lines of transgenic *Xenopus laevis* is not cytotoxic. Some sensitizers have the potential to find its way from a second to third generation photosensitizer [18]. This may be the case for mTHPC which exists in solution form (Foscan®) and also in nanoformulations (Fospeg®, Foslip®).

4.2 Clinical Applications

4.2.1 Bladder Cancer

The use of PDT for treatment of bladder cancer, first licensed in Canada 1993 with Photofrin, was not quite satisfactory because 70–80 % of patients relapsed within a year [15]. PDD, however, gained more importance for the detection of inconspicuous early stage urothelial carcinoma of the bladder. Meanwhile, fluorescence diagnosis has been approved in Europe for the detection of bladder cancer after instillation of 5-ALA, ALA (Hexvix®), solution, and PDD is also recommended by the European Association of Urology as well as the Austrian Association of Urology for the diagnosis of carcinoma in situ of the bladder [19].

Drawback of PDD with ALA and its derivatives is the lower specificity because of false positive results. In several clinical studies [19], the sensitivity of PDD is compared to white light cystoscopy (WLC). The values for PDD varied from 92 to 97 % and for WLC from 67 to 84 %. The specificity, however, had a spread from 40 to 67 % for PDD and from 66 to 78 % for WLC. A combination and digital

overlay of both imaging technologies intermittently may further improve diagnostic accuracy, especially for systems used in an outpatient environment.

More promising results reveal studies with Hypericin [20] where the specificity is increased from 95 to 98 %. Also exact dosimetry and quantification of ALA-induced fluorescence improves the specificity of bladder cancer detection [21]. The enhanced diagnosis of hardly visible carcinoma in situ, CIS, by PDD is one of the most remarkable benefits of this method and improves management of patients suffering from this disease. The probably shorted incubation time after instillation of PVP-Hypericin into the bladder for the fluorescence detection will be an additional benefit for the management of patients.

5-aminolelulinic acid is a natural substance and plays a role in the intracellular biochemical pathways as a heme precursor. Administration of ALA in excess enhances the Protoporphyrin IX (PPIX) synthesis which is the fluorescent compound. The higher metabolism in cancer cells give rise to higher content of PPIX and in consequence to enhanced fluorescence compared to the surrounding healthy tissue. Figure 4.10 shows an example of bladder cancer diagnosis in comparison to WLC where the two satellite cancerous lesions are hardly to see. ALA can be applied as solution or cream for topical applications in dermatology. A comprehensive overview of the basic principles and clinical applications of ALA is reported in the book by Pottier et al. [22].

New studies with Polyvinylpyrrolidone-Hypericin (PVP-Hypericin) demonstrate the potential of this sensitizer for PDD of early stages of bladder cancer. The incubation time can be shortened to about 30 min with sensitizer uptake of the cancer tissue to get sufficient fluorescence intensity for high-contrast images (Fig. 4.11).

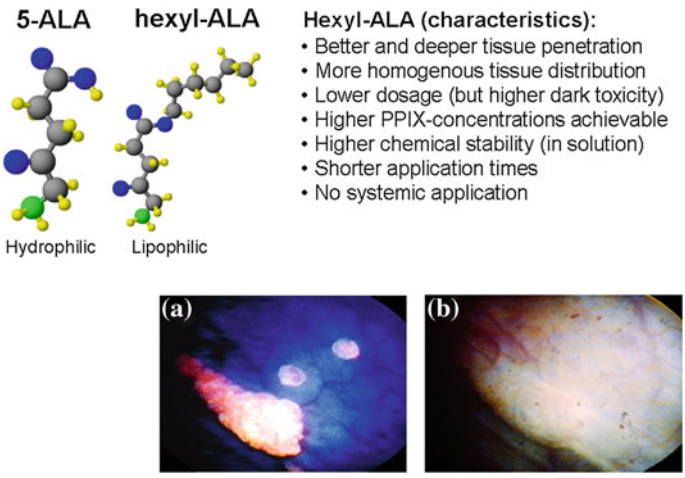

Fig. 4.10 Comparison of 5-ALA and hexyl-ALA. **a** PDD of bladder cancer with 5-ALA, **b** white light picture of the same bladder region (courtesy of Laser-Forschungslabor Grosshadern)

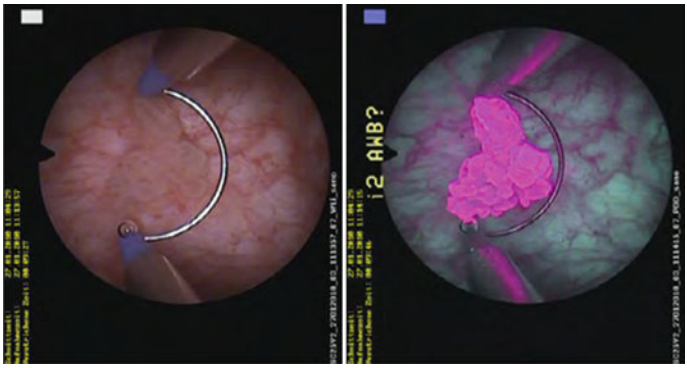

Fig. 4.11 PDD of early cancer stage in the bladder with PVP-Hypericin (courtesy of Sanochemia Pharmazeutika AG)

Hypericin, a component of St. Johns Wort, is one of the most powerful photosensitizer in nature. Because of its hydrophobicity, the substance must be dissolved in a mixture of DMSO, PEG, and water for systemic application. Hypericin seems to be quite an effective fluorescence marker for the detection of glioma in vivo. Taking into account tissue autofluorescence, the fluorescence ratios between tumor and normal tissue as well as infiltration zone and normal tissue were about 19.8:1 and 2.5:1, respectively [23]. Another possibility is the polymeric nanoencapsulation of hypericin (NPs) to overcome the delivery and stability problems and enable intravenous administration [24]. Comparing hypericin-loaded nanoparticles to free drug for the fluorescence photodetection of ovarian micrometastases it turned out that hypericin-loaded NPs showed improved selective accumulation of hypericin and higher fluorescence intensities in ovarian micrometastases.

The first system for PDD has been developed in 1995 by company KARL STORZ with matched optical components, the D-Light C light source, the optics, and the sensitive endocamera. Such systems are available for PDD in ENT, neurosurgery, and laparoscopy. A flexible PDD video-cystoscope is available from Richard Wolf GmbH with the Combilight light source.

4.2.2 Skin Cancer

PDD/PDT is routinely used for superficial skin cancers and precancerous lesions (actinic keratosis) in dermatology. 5-ALA-assisted fluorescence examination is a useful tool to visualize the malignant or premalignant lesion and determine its margin. The fluorescent skin area is normally larger than the visible tumor size. Besides demarcation of the tumor, the fluorescence intensity can also be used to monitor the PDT effect during and after irradiation of the sensitized malignant

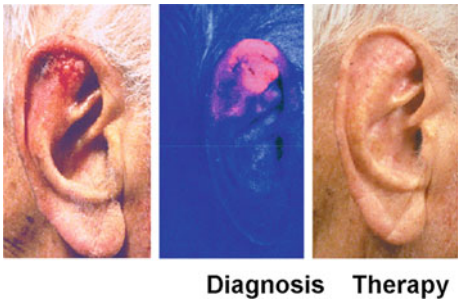

Fig. 4.12 Squamous cell carcinoma. Fluorescence diagnosis with Metvix® and photodynamic treatment (PDT) (courtesy of C. Fritsch, Düsseldorf)

tissue. For diagnostic purpose of superficial skin lesions 5-ALA or Metvix® (methyl-5-aminolaevulinate) are used. Diagnosis and therapy of superficial squamous cell carcinoma using 5-ALA with topical application are very promising [25]. For thicker and deeper lesions, however, systemic administration of the photosensitizer is indispensable. After fluorescence imaging of the tumor size the photodynamic effect of the sensitizer together with light irradiation treats the tumor with excellent cosmetic results as demonstrated in Fig. 4.12.

Not only fluorescence imaging technologies are used to detect and monitor tumor lesions but also local spectroscopic examination of the tissue gives good results to judge tissue modifications [26, 27].

Multiple actinic keratosis can be visualized by application of Metvix® cream and treated with lamps (Waldmann) or LEDs selected for red light emission. An example is given in Fig. 4.13.

Basal cell carcinoma (BCC) exists in different forms: sclerodermiform (10 %), nodular (33 %), and superficial (57 %). Normally, BCC do not metastasize but can aggressively destroy the tissue. PDD helps to demarcate the BCC lesion (Fig. 4.14) for surgical intervention. Only superficial BCC lesions can be treated by PDT successfully. A comparison of fluorescence diagnostics of basal cell carcinomas (BCCs) with Metvix® and 5-ALA to visual clinical examination is reported in [28]. The authors found that the fluorescence contrast using Metvix® is significantly higher than the contrast after application of 5-ALA.

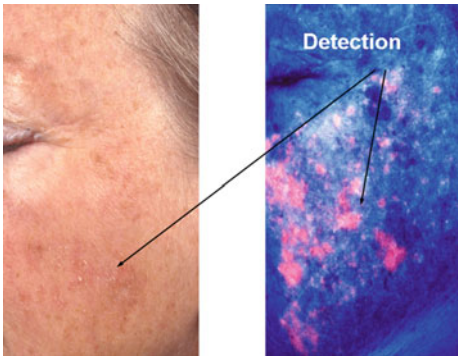

Fig. 4.13 Diagnostic imaging of actinic keratosis with Metvix® (courtesy of C. Fritsch, Düsseldorf)

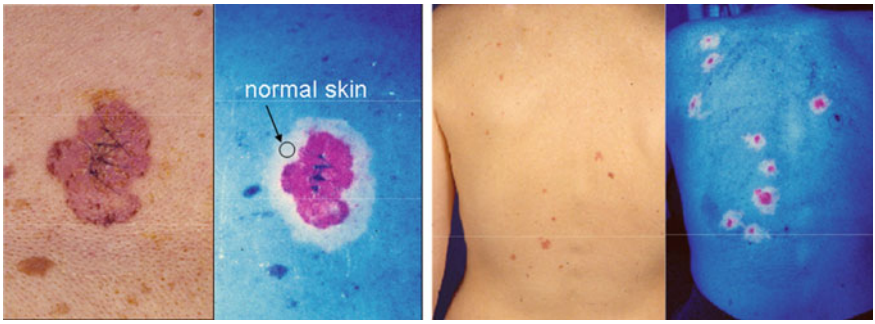

Fig. 4.14 BCC with Metvix® (courtesy of C. Fritsch, Düsseldorf)

Also Bowen's disease can be visualized with Metvix® and treated in multiple PDT sessions until the patient is cured. Negative results, no fluorescence with Metvix® can be detected with malignant melanoma, viral warts, benign melanocytic lesions, seborrhoic keratosis, and condylomata.

First approaches are published for visualization and PDT treatment of malignant melanoma with aluminium tetrasulfophthalocyanines, AlPcS4 [29] at a concentration of 40 μg/ml and a laser light dose of 4.5 J/cm^2 at 672 nm wavelength.

4.3 Diagnostics of Other Tumor Types

The percentage of adenocarcinoma within esophageal carcinomas was more than 2 decades ago only 5 %. But meanwhile, due to the dramatic increase of Barrett-carcinoma, it is the most frequent malignant esophageal tumor in the western countries. The risk that an adenocarcinoma develops from a Barrett-esophagus is 30- to 125-times higher than in normal population [30]. Also the fast development of endoscopic technologies and new diagnostic methods lead to a more frequent diagnosis of early stage neoplasias. In case of intraepithelial neoplasias or carcinomas limited to the mucosa, endoscopic mucosal resection and PDT have been performed more and more often as an alternative to radical surgical resection. High resolution video endoscopy is the standard diagnostic of Barrett-esophagus together with PPIX-enhanced fluorescence after 5-ALA oral application. For PDT also Dihematoporphyrin (DHE, sensitizer of the first generation) and mTHPC are effectively used, but which create more side effects. Problematic are still the dosimetry and the homogeneous irradiation of the Barrett-esophagus. Also autofluorescence endoscopy on the basis of the natural fluorescence of endogenous fluorophores calculating the red to green ratio (R/G) of the autofluorescence images is a powerful tool to detect tissue alterations. An increased R/G ratio in cancerous tissue changes in 96 % of the cases is reported in [31].

PDD of prostate cancer with 5-ALA is validated in clinical trials [32, 33]. Fluorescence markers for PDD of tumor margins during surgery would enhance the surgical radicality. PDD with 5-ALA- induced PPIX fluorescence imaging during radical prostatectomy might be an effective method for reducing the rate of positive surgical margin (PSM) which is associated with biochemical recurrence in 11–38 % of patients undergoing radical prostatectomy.

Optical and especially fluorescence diagnosis of in head and neck oncology is rapidly developing and can be translated to enhance patient treatment and overall quality of life [34].

PDD is successfully applied also in brain tumors, malignant glioma, using 5-ALA [35] or the new sensitizer hypericin [23] for fluorescence image-guided resection of the tumors. Further and new applications of PDD serve as detection method for metastasis of ovarian cancer [36] or lung cancer.

4.4 Methodological and Technical Aspects

It was mentioned that dosimetry in PDT and PDD is a crucial factor for diagnostic decisions and therapy control. Spectroscopic fluorescence measurements are usually the way to collect data on photosensitizer concentration, photobleaching, or accumulation in tumors compared to healthy tissue. With a flexible optical fiber bundle, containing a central fiber for fluorescence excitation surrounded by several detection fibers, the distal tip is in contact or in short distance to the tissue for the measurements. The fluorescence spectral intensity, monitoring the sensitizer amount in the tissue, is digitally calibrated and displayed. There are devices on the market [37] and very frequently used is the system LESA-01-BIOSPEC of the company BioSpec, Moscow [38]. It measures with high sensitivity tissue auto-fluorescence and all popular photosensitizers for quantitative determination of the photosensitizer concentration in vivo. Dosimetry results of PpIX in human non-melanoma skin cancers and precancers show that PpIX accumulation correlates with the degree of malignancy [39].

Besides molecular sensitizers different functionalized nanoparticles, mostly gold nanoparticles [40], are in experimental stage for tumor diagnosis. Their advantages are high fluorescence quantum yield and photostability. A new approach is the use of nanoparticles produced of aluminium phthalocyanine (nAlPc). Such nAlPc, produced in different size, are not fluorescent in water suspension. In the body, however, they start to be fluorescent but only in inflamed tissue [41]. Experiments reveal that stimulated macrophages after internalization of nAlPc begin to fluoresce due to single molecules being dissolved from the nanoparticles. An example is demonstrated in Fig. 4.15.

Accurate surgical removal of tumors depends on the quality of tumor imaging. New techniques for imaging aggressive brain tumors (glioblastoma) involve triple-modality nanoparticles [42]. After being injected into the blood, the nanoparticles are able to penetrate brain tumor cells and tag them with a label that the cells can

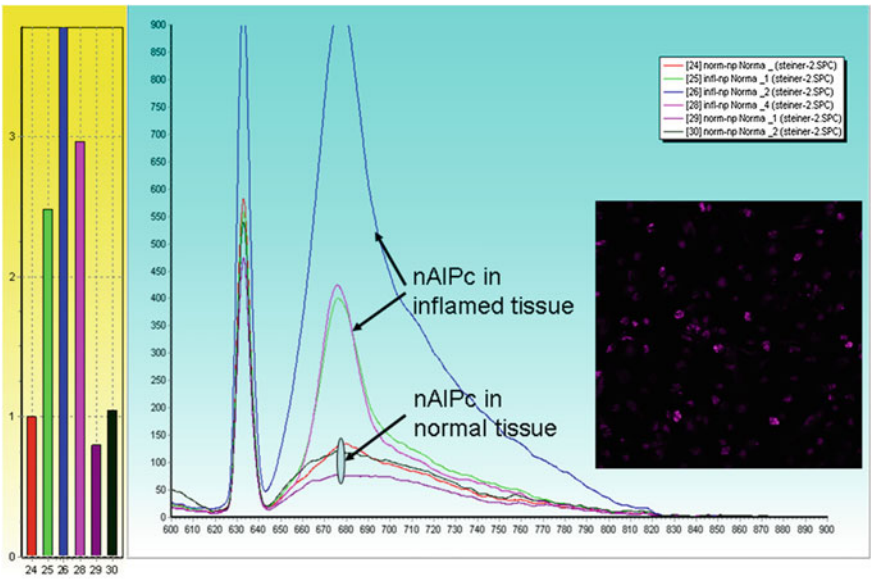

Fig. 4.15 Spectra of nAlPc fluorescence in mouse normal and inflamed tissue, excited with 633 nm wavelength. Inset shows the nAlPc fluorescence of stimulated macrophages. Graph on the left side displays the calibrated fluorescence intensities of the normal tissue (24, 29, 30) and inflamed tissue (25, 26, 28). Spectra are measured with LESA-01 BIOSPEC

be more easily detected by three complementary imaging technologies: MRI, which images the entire brain and the tumor, photoacoustic imaging, which can visualize the tumor in three dimensions and surface-enhanced Raman spectroscopy (SERS) imaging, which has ultra-high sensitivity and resolution and therefore can visualize microscopic residual tumor.

4.4.1 Fluorescence Lifetime Imaging

Fluorescence of a fluorophor has a specific lifetime depending on the chemical environment of the molecule. Therefore, the fluorescence decay time of molecules helps to identify molecules and intracellular pathways even if the fluorescence spectra would be identical. Fluorescence-guided tumor resection is very well accepted in the case of bladder cancer and some types of brain tumor, respectively. However, false positive results are one of the major problems of fluorescence diagnosis, which will make the discrimination between tumor tissue and inflammation difficult. But fluorescence lifetime imaging (FLIM) and especially spectral-resolved FLIM (SLIM) [43] can significantly improve the diagnostic value.

The fluorescence decay of a fluorophor, in many cases, does not follow a simple exponential profile. A very complex situation may arise, when more than one

compound has to be analyzed. This could be the case when endogenous fluorophores of living cells or in tissues have to be discriminated to identify oxidative metabolic changes or during PDT, when different photosensitizer metabolites are observed simultaneously. In those cases, a considerable improvement could be achieved when time-resolved and spectral-resolved techniques are simultaneously available.

Time-resolved imaging considers the fluorescence lifetime τ of a fluorophor which for most organic molecules is in the sub-nanosecond to nanosecond time range. Although fluorescence lifetimes can be in principal obtained in the frequency or time domain, the technique described considers only the time domain version. In this case, the sample is excited by picosecond pulses at high repetition rate (kHz–MHz). For the detection of time-resolved fluorescence, time-correlated single-photon-counting (TCSPC) or time-gating techniques are used. The TCSPC technique is based on the measurement of the arrival time of the first emitted photon relative to the excitation pulse. Single photons are detected by fast photomultipliers (PMTs). This technique enables highest accuracy [44].

Applications presented here focus on the detection of NADH and 5-ALA (5-ALA) induced porphyrins. With respect to NADH, the discrimination between protein bound and free coenzyme was investigated in squamous carcinoma cells from different origin. These measurements allow a deeper understanding of the metabolic state of the cells. The redox ratio, which means the ratio between the fluorescence intensity of FAD versus NADH is known to depend on the metabolic state [45]. This ratio is correlated with the fluorescence lifetimes of NADH and FAD. For low grade and high grade precancerous tissue, a shortening of the lifetime of NADH was recently reported, whereas FAD exhibited an elongation [46].

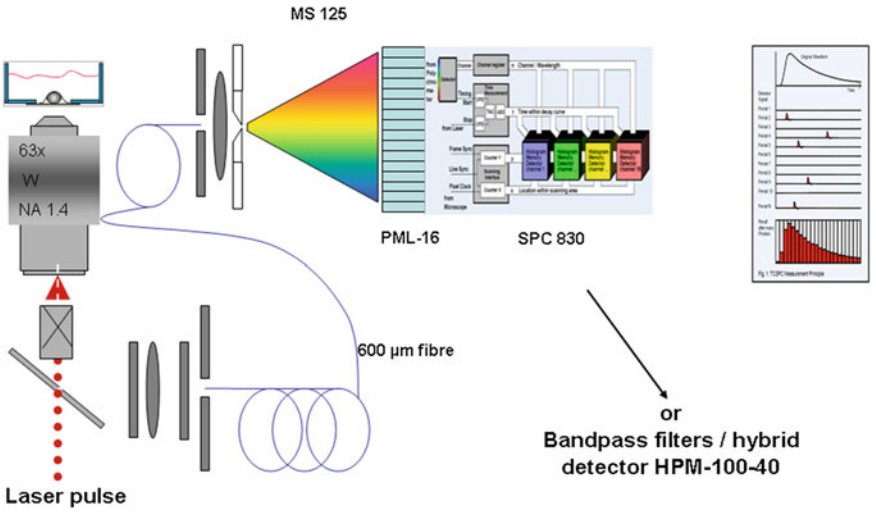

Fig. 4.16 Schematic diagram of the setup for SLIM. For explanation see text

A schematic scheme of the measurement setup is given in Fig. 4.16. In order to investigate multispectral FLIM of NADH and FAD, a tunable Ti: Sapphire laser (Mai Tai AX HPDS, Spectra Physics) is coupled to a laser scanning microscope (LSM710, Carl Zeiss, Germany). The Mai Tai laser is a mode-locked 80 MHz "high performance" DeepSee laser with a tuning range of 690–1,040 nm, a maximum optical output power of about 2.8 W at 800 nm and a pulse width below 100 fs. For cellular studies of the autofluorescence, cells were excited with two photons at 720 nm, the power at the input of the microscope was reduced to 60 mW. Spectral detection of FLIM was done using narrow band pass filters at 436 nm (BP 436 ± 10 nm) and 470 nm (BP 470 ± 10 nm) and a two channel TCSPC system (Becker&Hickl GmbH, Berlin, Germany) consisting on a Simple-Tau-152-DX, SPC-Image, and the hybrid detector HPM-100-40. This system was coupled to the LSM 710.

For each photon, the TCSPC module determines the location within the scanning area and the time of the photon within the laser pulse period. These parameters are used to build up a two-dimensional photon distribution over the scan area, and the time of the fluorescence decay. The results are presented at an image size of 256 × 256 pixels and 256 time channels. A scan time of 782 ms was used and a collection time of 60 s to record the data. The microscope objective lens was a 20 × magnification NA 0.8 water immersion lens ("Plan-Apochromat" 20x/0.8, Carl Zeiss, Germany). With the used zoom factor of two, an area of 212 × 212 μm^2 was evaluated.

In order to measure the fluorescence lifetime of 5-ALA-induced porphyrins, a PML-16 multichannel PMT module with the TCSPC 830 (Becker&Hickl GmbH, Berlin, Germany) was attached to the output of a MS 125 spectrograph (LOT-Oriel) described in [43]. The PML 16 contains a 16 channel Hamamatsu R5900-01-L16 multi-anode PMT and the TCSPC routing electronics [44]. The spectrograph with a grating of 600 lines/mm has a 200 nm spectral range spread over the 16 channels of the detector. Fluorescence light from the sample is coupled into a 1000 μm silica/silica fiber with the end of the fiber coupled to the input focal plane of the spectrograph. For fluorescence excitation, a 405 nm ps pulsed diode laser (BDL-405-SMC, Becker&Hickl GmbH, Berlin, Germany) is coupled to a 600 μm silica/silica fiber. Pulse repetition rate of the diode laser is 40 MHz. With this system, the spectral-resolved fluorescence lifetime data of 5-ALA-induced porphyrins is measured within the illuminated area.

The time-resolved fluorescence of NADH was studied in the human oral keratinocyte line OKF6/TERT-2 and two human oral squamous cell carcinoma SCC-4 and SCC-25 cells. Protein bound NADH was studied within 436 ± 10 nm and free NADH within 470 ± 10 nm. Excitation wavelength was in both cases 720 nm. A two exponential fitting procedure was used to calculate the fluorescence lifetimes of bound and unbound NADH. The distribution of the short component for both spectral regions (BP 436 and BP 470) is shown in Fig. 4.17, the distribution for the long component in Fig. 4.18.

Interestingly, two lifetimes were found for the short component being attributed to the unbound NADH. The unbound coenzyme should be found in a higher

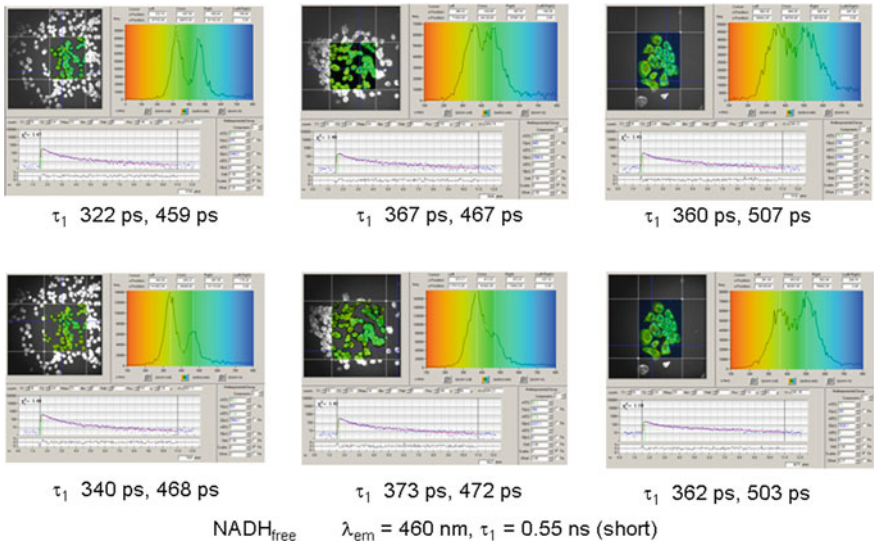

Fig. 4.17 FLIM and distribution histogram of the short lifetime component of bound (BP 436) and free (BP 470) NADH

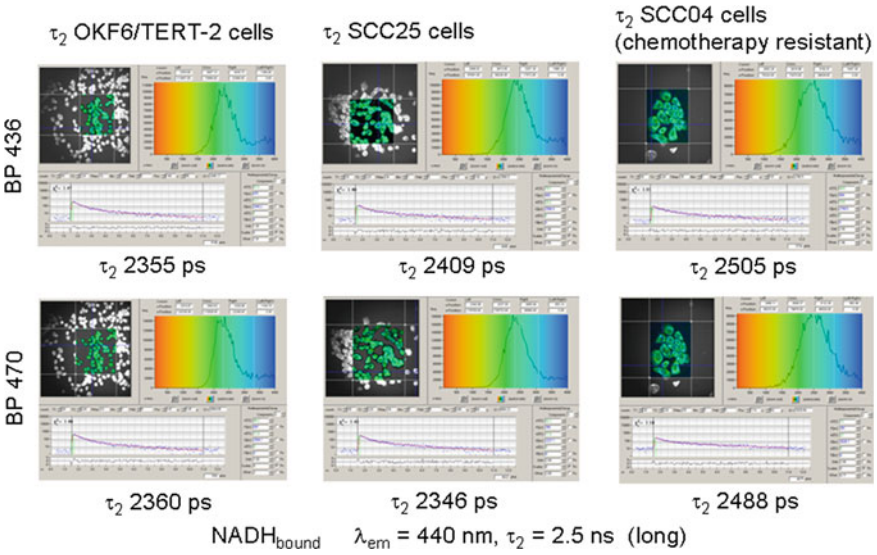

Fig. 4.18 FLIM and distribution histogram of the long lifetime component of NADH bound (BP 436) and unbound (BP 470)

amount within the range BP 470. In fact, the intensity of the short component is higher in the channel BP 470. The difference in the short lifetimes is marginal for the three types of cells; it seems that SCC-4 cells exhibit the longest lifetime τ_1.

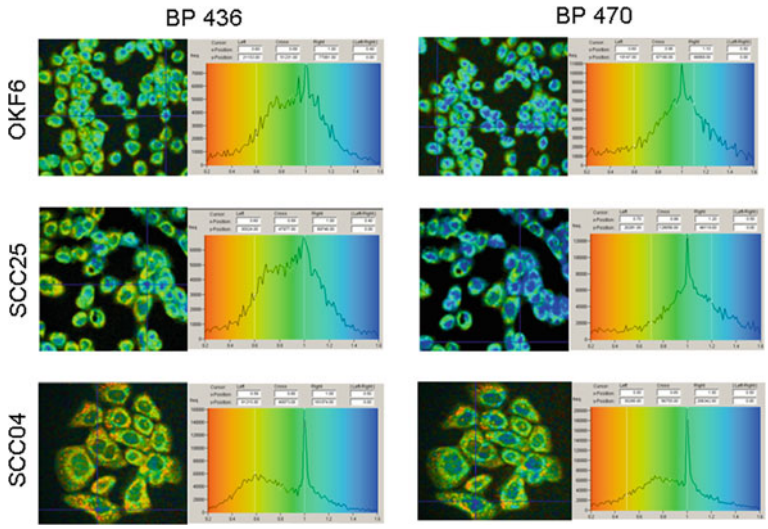

Fig. 4.19 Distribution of $a_1\tau_1/a_2\tau_2$ in false colors and histogram for the three cell lines in the two spectral regions BP 436 and BP 470

For the long lifetime component τ_2, the difference is more significant (see Fig. 4.18). Again, SCC-4 cells possess the longest value, which may reflect a different protein binding state.

The lifetime is the crucial parameter to describe the different binding environments for NADH. However, for characterization of different cell types, the distribution of the intensity of the short compound versus the intensity of the long compound gives a more detailed image of the intracellular variation. Therefore, the intensity ratio $I\tau_1/I\tau_2$, will be calculated which is equal to $a_1\tau_1/a_2\tau_2$, where a_1 and a_2 are the amplitudes of the short and long lifetime component, respectively. The image of $a_1\tau_1/a_2\tau_2$ in false colors and the histogram for the three cell lines within the two different spectral regions is demonstrated in Fig. 4.19. For SCC-4 the long lifetime component is prominent and the concentration is high in the cytoplasm and seems to be correlated with mitochondria (see orange color in channel BP 436). The two other cells (OKF6/TERT-2 and SCC-25) demonstrate a similar histogram with a higher concentration of the short compound, localized significantly in the cell nucleus. This fact is interesting because free NADH in the cell nucleus is known to play a role in gene expression [47]. Cell metabolism of OKF6 and SCC-25 on the one hand and SCC-4 on the other hand seems to be different.

The evaluation of the spectral and time-resolved fluorescence characteristics of 5-ALA-induced porphyrins in OKF6, SCC-4, and SCC-25 cells has been performed on the chorioallantois membrane (CAM) of advanced brooded hen eggs. The cells were incubated for 3 h with 5-ALA and analyzed with the 16-channel detector. The mean lifetime values calculated with a single exponential fitting

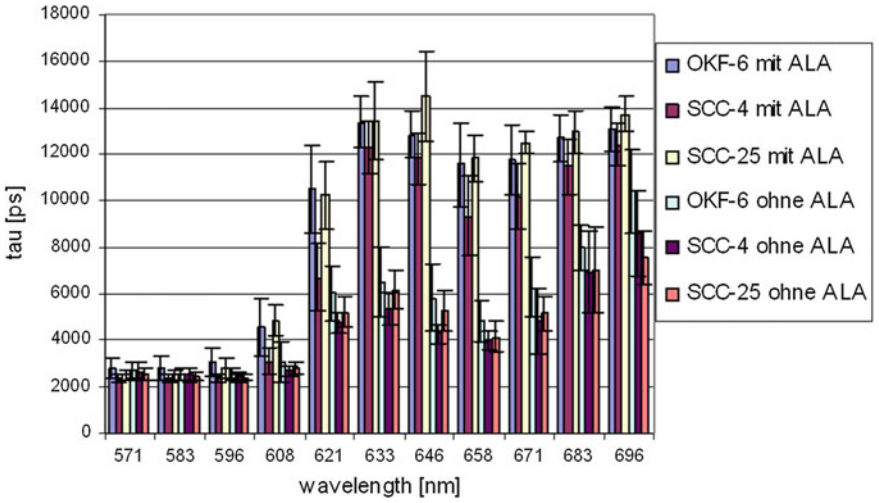

Fig. 4.20 Mean fluorescence lifetimes of 5-ALA induced porphyrins, autofluorescence and standard deviations in OKF6, SCC-4 and SCC-25 cells. Mean value from seven single measurements

procedure and standard deviations within the different spectral channels for the three cells is demonstrated in Fig. 4.20.

Administration of 5-ALA stimulates porphyrin synthesis like protopophyrin IX (PpIX), uroporphyrin I and III (UroI and III), and coproporphyrin (Copro) in cells (Fig. 4.21). PpIX is assumed to be the most important component.

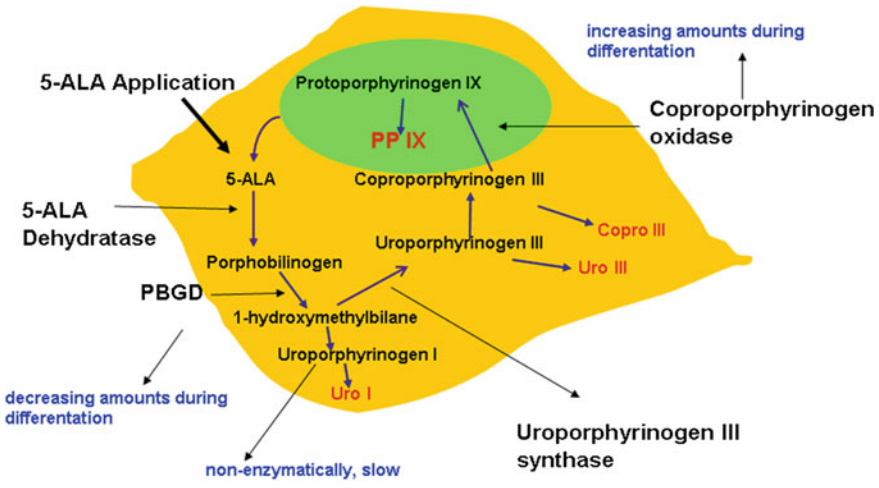

Fig. 4.21 Protein synthesis pathways after administration of 5-ALA and PDT

The main fluorescence band of PpIX is found in the channel around 633 nm, a second band is found at 696 nm. As can be seen in Fig. 4.20, the fluorescence lifetime which correlates with PpIX is between 12 and 14 ns for all cell types and seems to be shorter for SCC-4, the difference is, however, statistically not significant. However, the fluorescence at 621 nm, which correlates with Uro and/or Copro exhibits a lifetime which is statistically significant shorter in the case of SCC-4.

From the literature, it is known that the lifetime of Uro is around 6 ns, which coincides well with the SCC-4 cells [48]. The first three channels correlate with the autofluorescence, channel 658 and 671 nm with aggregates and photoproducts. From these measurements 5-ALA metabolism seems to be different for OKF6 and SCC-25 on the one hand and SCC-4 on the other hand.

As demonstrated, FLIM and SLIM can be the right method to measure cell metabolism and to discriminate different cell types. Cell metabolism, especially the redox-state of the cells is reflected by the fluorescence behavior of enzymes which are responsible for the autofluorescence. As an example, studies of the fluorescence lifetime of the most important coenzyme of the respiratory chain, the protein bound and unbound NADH in cells of different origin have been performed.

Measurements of the lifetimes of 5-ALA-induced porphyrins in the same types of cells indicated that the normal keratinocyte line OKF6 and the squamous carcinoma cell SCC-25 behave similar, both with respect to autofluorescence and 5-ALA-induced fluorescence. The more aggressive squamous carcinoma cell SCC-4 behaved differently. Also cell growth and morphology were similar in the case of OKF6 and SCC-25. It seems that the fluorescence lifetime reflects cell metabolism in a very sensitive way. Improvement of fluorescence diagnosis by FLIM and SLIM could therefore be a method to overcome problems like false positive results or discrimination between different tumor states, tumor, and inflammation.

References

1. von Tappeiner H, Jodlbauer A (1904) Ueber die Wirkung der photodynamischen (fluorescierenden) Stoffe auf Protozoen und Enzyme. Dtsch Arch Klein Med 80:427–487
2. Raab O (1900) Ueber die Wirkung fluorescierender Stoffe auf Infusorien. Z Biol 39:524–546
3. Steiner R (2011) Basic laser physics. In: Raulin C, Karsai S (eds) Laser and IPL technology in dermatology and aesthetic medicine. Springer, Berlin Heidelberg, pp 3–22
4. Wu Y, Xi P, Qu JY, Cheung T-H, Yu M-Y (2004) Depth-resolved fluorescence spectroscopy reveals layered structure of tissue. Opt Express 12(14):3218–3223
5. Hirsch FR et al (2001) Early detection of lung cancer: clinical perspectives of recent advances in biology and radiology. Clin Cancer Res 7:5–22
6. Escargel B et al (2009) Early diagnosis of lung cancer: impact of autofluorescence bronchoscopy. Rev Pneumol Clin 65:287–291
7. Sutedja TG et al (2001) Autofluorescence bronchoscoy improves staging of radiographically occult lung cancer and has an impact on therapeutic strategy. Chest 120(4):1327–1332
8. Loewen G et al (2007) Autofluorescence bronchoscopy for lung cancer surveillance based on risk assessment. Thorax 62:335–340

9. Divisi D, di Tommaso S, de Vico A, Crisci R (2010) Early diagnosis of lung cancer using a SAFE-3000 autofluorescence bronchoscopy. Interact CardioVasc Thorac Surg 11:740–744. doi:10.1510/icvts.2010.242123
10. Lam B et al (2006) The clinical value of autofluorescence bronchoscopy for the diagnosis of lung cancer. Eur Respir J 28:915–919
11. Xiao YL et al (2010) Comparison of the autofluorescence bronchoscope and the white light bronchoscope in airway examination. Chin J Cancer 29:1018–1022
12. Thakur A, Gao L, Ren H, Yang T, Chen T, Chen M (2012) Descriptive data on cancerous lung lesions detected by auto-fluorescence bronchoscope: a five-year study. Ann Thorac Med 7(1):21–25
13. Perry SW, Burke RM, Brown EB (2012) Two-photon and second harmonic microscopy in clinical and translational cancer research. Ann Biomed Eng 40(2):277–291
14. Baumgartner R et al (1996) Inhalation of 5-aminolevulinic acid: a new technique for fluorescence detection of early stage lung cancer. J Photochem Photobiol B 36:169–174
15. Ackroyd R, Kelty C, Brown N, Reed M (2001) The history of photodetection and photodynamic therapy. Photochem Photobiol 74:656–669
16. Vasilchenko SY et al (2010) Application of aluminium phthalocyanine nanoparticles for fluorescent diagnosis in dentistry and skin autotransplantology. J Biophoton 3(5–6):336–346
17. Shcherbo D et al (2010) Near-Infrared fluorescent proteins. Nat Methods 7:827–829
18. Senge MO (2012) mTHPC—a drug on its way from second to third generation photosensitizer? Photodiagn Photodyn Ther 9:170–179
19. Jocham D, Stepp H, Waidelich R (2008) Photodynamic diagnosis in urology: state-of-the-art. Eur Urol 53:1138–1150
20. D'Hallewin M-A, Bezdetnaya L, Guillemin F (2002) Fluorescence detection of bladder cancer: a review. Eur Urol 42:417–425
21. Zaak D, Frimberger D, Stepp H et al (2001) Quantification of 5-aminolevulinic acid induced fluorescence improves the specificity of bladder cancer detection. J Urol 166:1665–1668
22. Pottier R, Krammer B, Stepp H, Baumgartner R (eds) (2006) Photodynamic therapy with ALA, a clinical handbook. RSC Publishing, Cambridge UK
23. Noell S, Mayer D, Strauss WSL, Tatagiba MS, Ritz R (2011) Selective enrichment of hypericin in malignant glioma: pioneering in vivo results. Int J Oncol 38:1343–1348
24. Zeisser-Labouèbe M, Delie F, Gurny R, Lange N (2009) Benefits of nanoencapsulation for the hypericin-mediated photodetection of ovarian micrometastases. Eur J Pharm Biopharm 71:207–213
25. Zang X et al (2012) Fluorescence examination and photodynamic therapy of facial squamous cell carcinoma—a case report. Photodiagn Photodyn Ther 9:87–90
26. Andersson-Engels S, af Klinteberg C, Svanberg K, Svanberg S (1997) In vivo fluorescence imaging for tissue diagnostics. Phys Med Biol 42:815–824
27. Loschenov VB, Konov VI, Prokhorov AM (2000) Photodynamic therapy and fluorescence diagnostics. Laser Phys 10:1188–1207
28. Sandberg C, Paoli J, Gillstedt M et al (2011) Fluorescence diagnostics of basal cell carcinomas comparing methyl-aminolaevulinate and aminolaevulinic acid and correlation with visual clinical tumour size. Acta Derm Venerol 91:398–403
29. Maduray K, Odhav B, Nyokong T (2012) *In vitro* photodynamic effect of aluminium tetrasulfophthalocyanines on melanoma skin cancer and healthy normal skin cells. Photodiagn Photodyn Ther 9:32–39
30. Pech O, Ell C (2004) Ösophaguskarzinome—Diagnostik und Therapie. Chir Gastroenterol 20:7–12
31. Sieron-Stoltny K, Kwiatek S, Latos W et al (2012) Autofluorescence endoscopy with "real-time" digital image processing in differential diagnostics of selected benign and malignant lesions in the oesophagus. Photodiagn Photodyn Ther 9:5–10
32. zaak D, Sroka R, Khoder W et al (2008) Phootdynamic diagnosis of prostate cancer using 5-aminolevulinic acid—first clinical experiences. Urology 72:345–348

33. Adam C, Salomon G, Walther S et al (2009) Photodynamic diagnosis using 5-aminolevulinic acid for the detection of positive surgical margins during radical prostatectomy in patients with carcinoma of the prostate: a multicentre, prospective, phase 2 trial of a diagnostic procedure. Eur Urol 55:1281–1288
34. Jerjes WK, Upile T, Wong BJ et al (2011) The future of medical diagnostics: review paper. Head Neck Oncol 3:38.1–38.8
35. Stepp H, Beck T, Pongartz T et al (2007) ALA and malignant glioma: fluorescence-guided resection and photodynamic treatment. J Environ Pathol Toxicol Oncol 26:157–164
36. Guyon L, Ascencio M, Collinet P, Mordon S (2012) Photodiagnosis and photodynamic therapy of peritoneal metastasis of ovarian cancer. Photodiagn Photodyn Ther 9:16–31
37. Pogue BW, Samkoe KS, Gibbs-Strauss SL, Davis SC (2010) Fluorescent molecular imaging and dosimetry tools in photodynamic therapy. Methods Mol Biol 635:207–222
38. http://www.biospec.ru
39. Warren CB, Lohser S, Chang S, Bailin PA, Maytin EV (2009) In-vivo fluorescence dosimetry of aminolevulinate-based protoporphyrin IX (PpIX) accumulation in human nonmelanoma skin cancers and precancers. Proc SPIE 7380:73801M-1–73801M-8
40. Huang X, El-Sayed MA (2010) Gold nanoparticles: optical properties and implementations in cancer diagnosis and photothermal therapy. J Adv Res 1:13–38
41. Vasilchenko SY et al (2010) Application of aluminum phthalocyanine nanoparticles for fluorescent diagnostics in dentistry and skin autotransplantology. J Biophoton 3:336–346
42. Kircher MF, de la Zerda A, Jokerst JV et al (2012) A brain tumor molecular imaging strategy using a new triple-modality MRI-photoacoustic-Raman nanoparticle. Nat Med 18:829–834
43. Rück A, Hülshoff CH, Kinzler I, Becker W, Steiner R (2007) SLIM: a new method for molecular imaging. Micr Res Techn 70:485–492
44. Becker W (2005) Advanced time-correlated single photon counting techniques. Springer, Berlin Heidelberg (Springer Series in Chemical Physics)
45. Chance B, Schoener B, Oshino R, Itshak F, Nakase Y (1979) Oxidation-Reduction ratio studies of mitochondria in freeze-trapped samples. J Biol Chem 254:4764–4771
46. Skala MC, Riching KM, Gendron-Fitzpatrick A et al (2007) In vivo multiphoton microscopy of NADH and FAD redox states, fluorescence lifetimes, and cellular morphology in precancerous epithelia. PNAS 104(49):19494–19499
47. Li D, Zheng W, Qu JY (2008) Time-resolved spectroscopic imaging reveals the fundamentals of cellular NADH fluorescence. Opt Lett 33:2365–2367
48. Kinzler I, Haseroth E, Hauser C, Rück A (2007) Role of mitochondria in cell death induced by Photophrin-PDT and ursodeoxycholic acid by means of SLIM. Photochem Photobiol Sci 6:1332–1340

Chapter 5
Implementation of Laser Technologies in Clinical PDT

Hans-Peter Berlien

Abstract "Photodynamic therapy" (PDT) is a term encompassing a collection of both curative and palliative modalities, traditionally described as treating precancerous lesions and superficial tumors using light. The list of medical fields in which PDT has managed to find a place as an accepted option for specific problems includes gastroenterology, dermatology, gynaecology, ophthalmology, and ENT. It is increasing importance underlined by a comparison with both traditional chemotherapy and radiotherapy, which can often significantly compromise patient's health. The therapeutic use of these well-established therapies is accordingly limited by their toxicity. In contrast, PDT cannot only show a distinct degree of tumor specificity, but can be repeatedly applied without apparently damaging the health of the patient.

5.1 Introduction

5.1.1 The Basis of PDT

"Photodynamic therapy" (PDT) is a term encompassing a collection of both curative and palliative modalities, traditionally described as treating precancerous lesions and superficial tumors using light. The list of medical fields in which PDT has managed to find a place as an accepted option for specific problems includes gastroenterology, dermatology, gynaecology, ophthalmology, and ENT. It is increasing importance underlined by a comparison with both traditional chemotherapy and radiotherapy, which can often significantly compromise patient's health. The therapeutic use of these well-established therapies is accordingly

H.-P. Berlien (✉)
Department of Laser Medicine, Elizabeth-Klinik, Berlin, Germany
e-mail: lasermed.elisabeth@pgdiakonie.de

M. H. Abdel-Kader (ed.), *Photodynamic Therapy*,
DOI: 10.1007/978-3-642-39629-8_5, © Springer-Verlag Berlin Heidelberg 2014

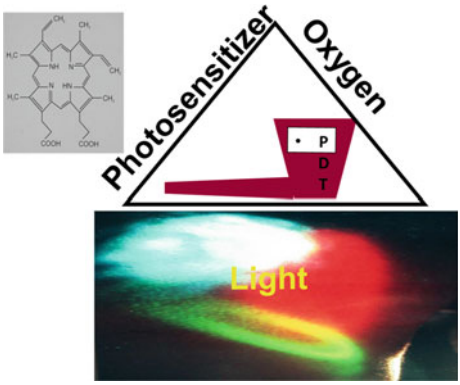

Fig. 5.1 Basics of PDT. The Trias of PDT

limited by their toxicity. In contrast, PDT cannot only show a distinct degree of tumor specificity, but can be repeatedly applied without apparently damaging the health of the patient.

Historically, PDT looks back on a long empirical evolution. Its beginnings are to be found in antiquity in Egypt. However, a satisfactory theory as to how it actually works could be developed only during the last few decades. In principle, substances, called *photosensitizers,* absorb optical energy and transmit this to oxygen molecules, thereby forming highly aggressive forms of oxygen-based molecules. The latter is often denoted by the term "reactive oxygen species" ("ROS"). PDT's ancient roots are explicable because of the natural occurrence of photosensitizers with a significant capacity for forming ROS. These include, for example, bilirubine and the flavines. Following, the uptake of photosensitizer by individual cells or cell groups, the absorption of light with consequent generation of ROS results in their death. Essentially, the therapeutic value arises from a more or less selective uptake of certain photoensitizers by precancerous or cancerous tissue [1, 12] (Fig. 5.1).

5.2 Clinical Aspects in Classification of Photosensitizers

PDT is an intrinsically *selective* therapy, in the sense that some photoactive substances accumulate more in degenerate than in the normal tissue. Such an accumulation, together with a precise application of light, determine how discriminating PDT can be in distinguishing between degenerate and healthy tissue with respect to inflicting damage. It has to be remembered that the selective enrichment in the target tissue depends not only on the photosensitizer, but also on differences in cell composition and compartmentalization. In contrast, the extent to which optical energy is channeled into oxygen activation is a physical quantity that, in analogy to the absorption spectrum, is characteristic for each individual substance and depends on the particular optical wavelength in question [20, 23, 31].

The photosensitizers that are of interest regarding current and future clinical applications can be classified and exploited according to their different chemical, physical, and pharmacokinetic qualities. The same major aim, the selective generation of singlet oxygen in the tumor cells and their destruction, is fundamentally valid for all photosensitizers.

As far as topical PDT is concerned, prominent photosensitizers include the thiazin dyes methylene blue and toluidine blue, and the protoporphyrin IX precursor δ-aminolaevulic acid.

5.2.1 Substances

5.2.1.1 Dyes

The thiazine dyes contain a triple ring system and represent a widely used class of photosensitizer which are topically applied on mucous membranes, e.g., in dentistry, where the destruction of bacteria via PDT without significant side effects is currently being researched clinically. They are also used to treat superficial lesions of mucous membranes in the field of ENT and dentistry, e.g., leukoplakia, where long remission rates have been achieved. Methylene blue (Fig. 5.2) is soluble in water, and has a broad absorption band in the red area of the spectrum with a maximum, depending to an extent on the solvent, around 665 nm. Toluidine blue is very similar, but a maximum that corresponds to somewhat shorter wavelengths, around 625 nm. Being water soluble, it cannot pass easily through biological membranes, and finds use in topical but not in systemic PDT. Another since decades well-known substance with a high PDT-potential is Indo-Cyano-Green (ICG). All substances have the great advantage of nearly no dark toxicity. But due to their elimination by the liver they can use only topical or in case of ICG just at the first pass [13, 33].

5.2.1.2 Tetrapyrroles

The substances most frequently used in systemic PDT are the family of tetrapyrroles, which belong to the *first generation* photosensitizers (Fig. 5.3). The chlorins, which form one of the groups of the *second generation* photosensitizers

Fig. 5.2 Methylene blue

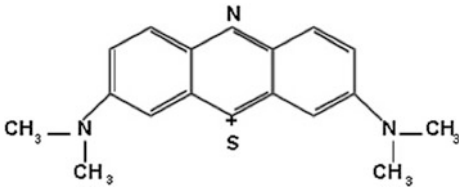

Fig. 5.3 Classification of Photosensitizer

and are in essence reduced porphyrins, are finding increasing use. Bacteriochlorophyll derivates and pheophorbides, stable derivates of chlorophyll varieties that are found in bacteria, are related to the porphyrins and are simple to produce. Phthalocyanins and naphthalocyanins, which are azaporphyrin derivates, show high tumor selectivity, are simple to synthesize and are very stable. They are also associated with a high yield of reactive oxygen species. Porphyrins are the most frequently used photosensitizers in PDT, and their well-established effectiveness makes them the standard for the newer substances [9, 11, 21]. In 1913 Meyer-Betz conducted the first documented clinical trial in the modern history of the PDT in the form of a self experiment with i.v. injection of hematoporphyrin. A wealth of experience has since been gathered with porphyrins, and because of their efficacy and low intrinsic toxicity, they make up most of the photosensitizers in current clinical use. Ubiquitous in nature, the decades since 1913 have seen improvements with respect to the chemical and photophysical qualities. The aims of present developments include progress regarding the

- selectivity, i.e., specificity, through better retention in degenerate than in healthy tissue
- clinical response
- side effects
- depth of the tumor tissue which can be handled efficiently
- monitoring and control of the therapy.

5.2.2 Pharmakokinetics

Knowledge of the pharmakokinetics of a photosensitizer is of essential importance for an optimal therapy planning. This includes determining the best time to irradiate and the adopting the correct strategy regarding the most important side effects, for example, the photo sensibilization of the skin or the retina, in their anticipation. This will of course be based to a large extent on field experience, but a good idea of the dynamics of the transportation and distribution of the photosensitizer between the various compartments, including the blood and liquor as well as the individual organs, is indispensable. Most of our knowledge about the

tissue distributions of photosensitizers comes from animal experiments, though the analysis of sera from patients also provides essential information on transportation phenomena. In vitro studies on the binding of photosensitizers to albumin and other proteins in blood, and the *exchange* of substances between the various vehicles involved, e.g., between albumin and lipoproteins, also serve to shed light on these matters. [10, 18, 29]

5.2.2.1 Photosensitizer Delivery and Transportation

It appears that hydrophilic substances, including hematoporphyrin and porphyrins substituted with hydrophilic side groups, are transported generally with albumin, the hydrophobic ones in lipoproteins, including LDLs. The selective uptake (Fig. 5.4) of certain photosensitizers could then be partly explained by an increased expression of LDL receptors by tumor cells, which can depend on proliferation. However, the distribution will depend on the dose used, as well as the homogeneity of the photosensitizer. HpD, for example, corresponds to a mixture of oligomers, and when, applied intravenously, a significant portion forms aggregates in blood, even though most becomes bound to albumin. The distribution profile can be complicated by transfers from albumin-bound photosensitizer to lipoproteins.

5.2.2.2 Tissue Uptake: The Problem of Targeting

The accumulation in a tissue occurs both through passive mechanisms, such as an intrinsically high membrane affinity and leakiness in the tumor vasculature. Active ones, such as the selective uptake of photosensitizer in the cells through carrier

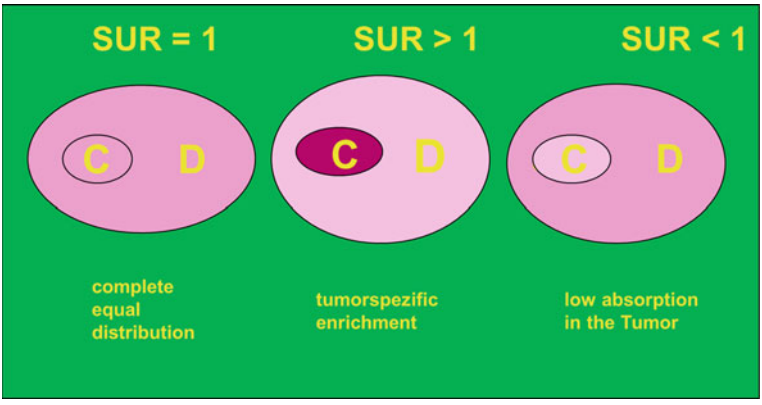

Fig. 5.4 Specific uptake ratio ($SUR = C/D$). C = Photosensitizer-concentration per g tissue. D = Photosensibitizer-dosage per kg body-weight

systems, can also play a role. For example, experiments involving ^{14}C-labeled hematoporphyrin derivative [6], revealed triexponential kinetics for the clearance from the blood, the excretion of the majority of the substance in the faeces and the accumulation in organs of the reticuloendothelial system, e.g., the liver and spleen. The last fact was interpreted as pointing to the possible involvement of macrophages in the process of tissue uptake.

Apart from the possibility of a direct uptake of photosensitizer, precursors in the sense of prodrugs can be given, for example, δ-aminolaevulic acid, that are taken into the cell and then converted to the active form, which would be protoporphyrin IX in the given example. Photosensitizers (such as phthalocyanins) can be bound to carrier molecules such as lipoproteins or antibodies before injection. This offers the possibility of increasing the selective uptake by the targeted tissue and, for hydrophobic substances, of allowing an intravenous application in the first place [8].

The distribution at the cellular level itself is an additional and crucial factor that needs to be taken into account in trying to understand the patterns of damage that PDT can inflict. Thus, hydrophilic photosensitizers are found to be concentrated primarily in lysosomes and in the cytoplasma, hydrophobic ones on the other hand in the various membrane systems, for example, those of the mitochondria, the endoplasmatic reticulum, and the cell membrane itself [22]. One can very well imagine for the sake of argument, for instance, that the destructive effects of a high rate of ROS generation restricted to the lysomes of a cell may be nowhere as deletirious as a significantly lower rate located in the nucleus or the mitochondrial membranes.

It should, therefore, be clear that the proper and comprehensive concept of a *target* should not simply be taken to mean an organ, a cell or some part of a cell. The aim is ultimately not simply selective *uptake* but rather selective *cell death*.

Passive accumulation mechanisms can include the delayed breakdown of the photosensitizer into photochemically ineffective metabolites and its delayed clearance from the tissue.

5.2.2.3 Administration Route

Dyes can be only administered topically except the ICG. But even in this dyes the mucosal penetration capability on one hand; on the other hand the standing time of the jelly is not long enough for a passive penetration so the capsulation with liposomes is used.

ALA can be administered topically and systemic by intestinal resorption. In both cases not the drug itself works but only the intracellular produced and in dysplastic/malignant cells higher and longer retained PPIX.

Principally, all the other PS can be administered topically or systemic. But for the majority of these substances due to great molecule the skin and the mucous membrane are a barrier for resorption (Fig. 5.5).

Here are strong intraepithelial dysplasias without any vascularisation (IENIII/CIS) topical substances the drug of choice. But with thicker lesions the penetration

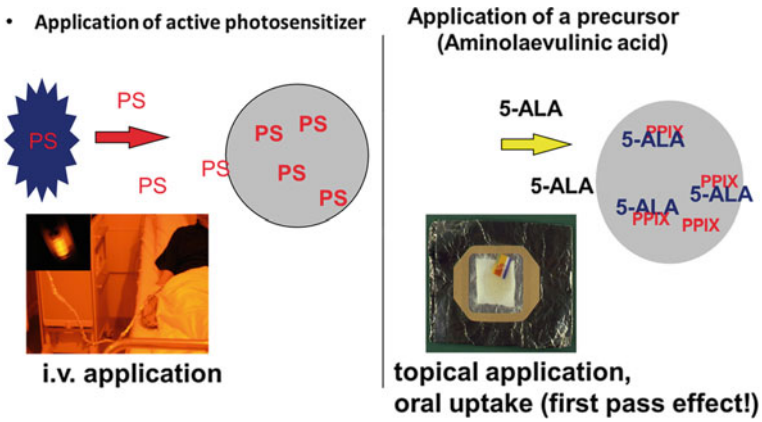

Fig. 5.5 Application forms

of these topical substances is not safe enough and with vascularisation and stroma formation the indication change to systemic photosensitizers. Here, we have beside the more or less specific accumulation in the tumor cells the secondary effect of destruction of the tumor vessels.

General one can say:

The more dysplasia/CIS with no vascularization—the more topical.

The more tumor with stroma and vascularization—the more systemic

5.2.2.4 Elimination

Photosensitizer elimination occurs via the liver and kidneys. Measurements on the elimination in faeces and urine with animals point to haematoporphyrin as being essentially hepatically eliminated. Interestingly, certain phthalocyanins appear to be eliminated to a very significant extent in the urine. The ratio of excreted photosensitizer concentration in urine to that in the faeces is not constant, probably reflecting shifts in the distribution between the various blood and tissue compartments.

In discussing the elimination, the plasma clearance also has to be considered. This will generally not show a simple exponential fall in plasma concentration, but rather a multicomponent behavior with components having half-lives between a few days and over a month. Another aspect in systemic photosensitizers is the accumulation time.

From the aspect of patients care a short acting PS with short unwanted skin sensitivity seems the best one. But with this advantage one get two other limitations:

The specific uptake ratio (SUR) depends by the interacting time—the longer—the higher the PS in the target tissue in relation (not necessarily the absolute concentration) to the surrounding tissue and the short time window for irradiation.

5.2.2.5 Vascular Damage and Hypoxia

In PDT, effects that are not specific to degenerate cells can also play an important role in tumor control. Almost all photosensitizers employed at this time, including the hematoporphyrins, have a high affinity to the endothelium of blood vessels. Therefore, as could be expected, one of the regular consequences of PDT is a destruction of blood vessels. In fact, the effects on the vasculature are essentially the very first ones seen. Inflammatory reactions, with edema, vasoconstrictive and vasodilatative phases and hemorrhagic necrosis [25]. This can have a considerable impact on the overall results. Such an effect could well be disadvantageous near diffusely infiltrating tumors, because of the risk of extensive necrosis and excessive soft tissue destruction. Since an adequate tumor selectivity in this respect is not given, the effects of the PDT on the healthy tissue would have to be minimized by an exact planning of the irradiation field. However, this unselective process can also have certain advantages:

- tumor regions with a poor microcirculation, and which therefore would not be capable of taking up sufficient photosensitizer for a selective effect, may also be controlled, and
- even an adequate perfusion in the irradiated volume may be reduced so much, that tumor cells which may have been only reversibly damaged through the PDT nevertheless die.

A very clear disadvantage of the resulting acute hypoxia is the loss of the key component oxygen to the process of PDT itself. This line of thought leads to the possibility that fractionation is at least as important to PDT as it is to radiotherapy, on condition that the hypoxia induced both by vascular occlusion and the activation of oxygen by photosensitizer is reversible.

As far as the damage to the vasculature through PDT using, among others, hematoporphyrin derivative seems to depend strongly on the level of photosensitizer in the blood [16].

5.3 Light Source

5.3.1 Influence of Spectral Range

In the spectral range from UV light to the deep infrared, the penetration depth of light in tissue grows with increasing wavelength (Fig. 5.6). On this basis alone, the excitation of a photosensitizer at the longest possible wavelength would generally be advantageous. Limitations are imposed by the discrete (line) nature of the photosensitizer absorption spectra. With hematoporphyrin derivates, currently the most frequently employed photosensitizers, an optical wavelength of approximately 635 nm is generally used. This corresponds to the absorption peak lying

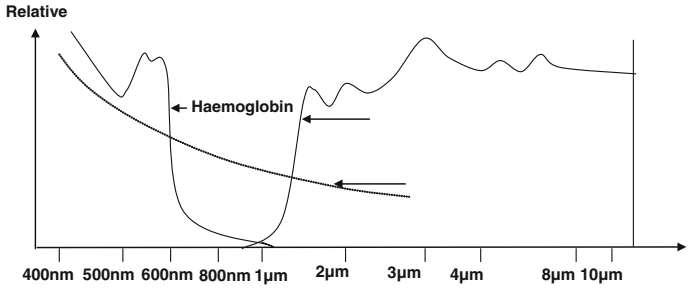

Fig. 5.6 Relative absorption of light by water and the pigment hemoglobin

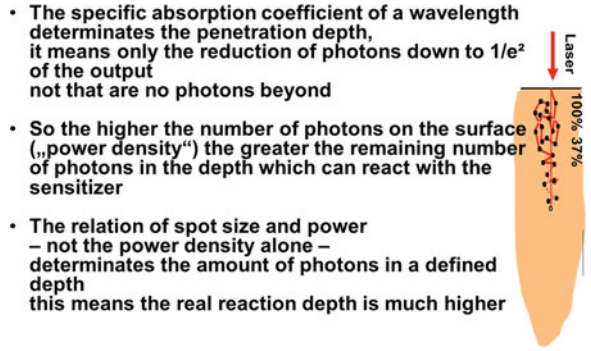

Fig. 5.7 Influence of photon flux

furthest in the red. In in vivo experiments, measurements show that the penetration depth of light at such a wavelength is approximately 1 cm. Clinical results, however, show that damage to the targeted tissue can occur to a depth of several centimetres (Fig. 5.7). This results by the fact that the so-called "penetration depth" means only the reduction of the irradiated power density on the surface is reduced in a given depth to $1/e^2$. It means not that beyond are no photons. So the higher the amount of Photons in a collimated beam the higher the remaining photons in a given depth (="reaction depth"). The limit is the maximum power density on the surface to avoid secondary damages (see Sect. 4.4). Nevertheless, this restriction regarding the penetration means that the use of PDT is limited to that of superficial lesions, for example, superficial precancerous lesions or tumors, or the palliative treatment of cutaneous metastases. Deeper lying tissue would have to be treated by means of an interstitial PDT. A central aim of current research is the development of photosensitizers which can be usefully employed at longer wavelengths [2, 14, 19].

There are specific indications, for instance, the treatment of a Barrett esophagus or bladder cancer, for which light with a shorter wavelength, such as provided by the argon or KTP-laser, is employed. Its wavelength of 514 nm or 534 nm, respectively, also corresponds to one of the absorption peaks of hematoporphyrin derivates. This, however, represents the exceptional deliberate use of a restriction

in the light penetration. The idea lying behind this method is to avoid damage to deeper lying structures. Nevertheless, it demonstrates how PDT can be modulated through the tailored choice of the wavelength used. PDT did start in the ancient Egypt with sunlight, got the first scientific upturn in the beginning twentieth century with introduction of high power electric arc lamps. But all these light sources emit incoherent non-collimated multi-wavelength light so the application was limited. With introduction of the LASER as a coherent, collimated, and monochromatic light source in the 70th the next upturn happened. But the question is is LASER necessary. The coherence is the condition for diagnostic, e.g., in OCT as the name says, but in therapy not. If in future 2-photon activation in PDT will happen is not yet clear.

The monochromaticity is a "conditio sine qua non," due to reduction of unwanted side effects of non-active wavelength in conventional light—the introduction of multispectral flash lamps ("IPL") once again is a roll backwards into the 20th of the twentieth century.

5.3.2 *Influence of Collimation*

The collimation of LASER allows the coupling into fibers for endoscopic or interstitial application. But for large field irradiation the Gaussian distribution would cause inhomogeneous irradiation and needs special fiber end-faces. One aspect of collimation is the calculable forward photon scattering so that thicker lesions can be irradiated. With introduction of high power LED we have a new situation. The LED emits a narrow band of light which is for a specific PS-activation precise enough. Furthermore, due to formation of a large number of LED's in one unit a large field irradiation is possible. But in two aspects one has to take into account:

Due to the non-collimation the influence of the distance to the power density is much greater than by LASER so only flat surfaces can be irradiated with controlled parameters.

The other aspect is that with non-collimation the forward-scattering is reduced and we have more backscattering with a higher under-surface intensity (Fig. 5.8). This must not be good or bad, it is a fact. In strong intraepithelial lesions by LEDs the underlying tissue is preserved against unwanted irradiation, but thicker lesions cannot irradiated in their full thickness with remaining tumor cells.

5.3.3 *Light Access Route*

Due to the fact that Laser light can be transmitted by fibers not only the surface can be irradiated even any operation field and intracorporal regions. In case of skin lesions and mucosa near natural orificiae a direct irradiation can happen, in the

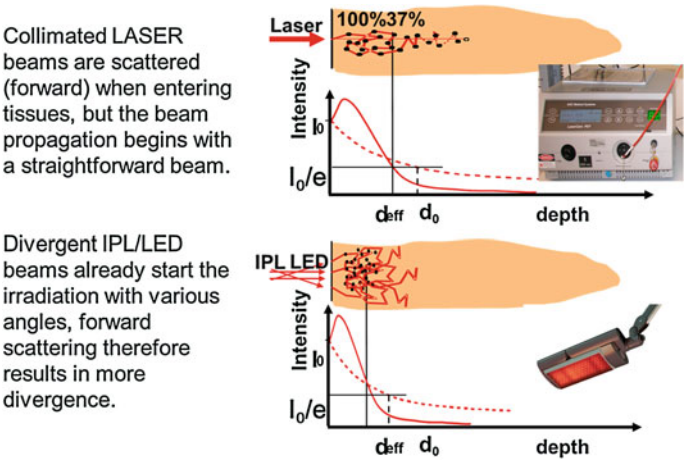

Fig. 5.8 Why do LASER penetrate deeper?

same way in intraoperative situs like neurosurgery. Here, even it is very important to control the beam parameters. The light transport in the fiber follows the Gaussian intensity profile. This means that in the center of the beam one has a much higher number of photons/power density than in the periphery. In focused beams one has to take into account that after the focus the beam is divergent the more, the smaller the focus. To overcome these problems special light distribution systems are necessary (Fig. 5.9).

Fig. 5.9 Choice of access

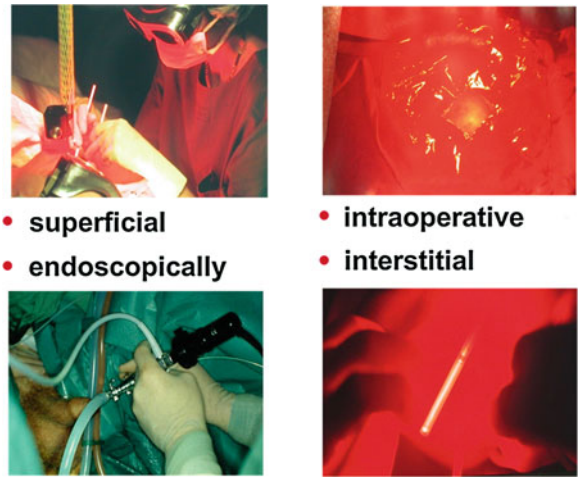

5.3.4 Light Applicator Systems

Focussed light application plays only in ophthalmology an important role for the treatment of senile macula degeneration. In all other application a large field or diffuse irradiation is necessary. For a well-marked irradiation of a surface is instead a bare fiber—due to the above-explained problems—the applicator of choice a so-called "Microlens" fiber. With a lens at the fiber end the primary divergent and Gaussian beam gets a homogenious power density over the whole surface. This allows a precise calculation of the irradiation parameters. Due to the flexibility of these applicators they even can be used in endoscopy. But for homogenious irradiation in longer hollow organs or for interstitial applications from interstitial thermotherapy well-known diffuse light applicators are in use (Fig. 5.10).

5.4 Perioperative Management

5.4.1 Photosensitization

The photosensitization of the skin, the most important side effect of PDT with porphyrins, corresponds to that known from experience with other photoactive substances such as antibiotics, phytotherapeutic agents and cosmetics. Depending

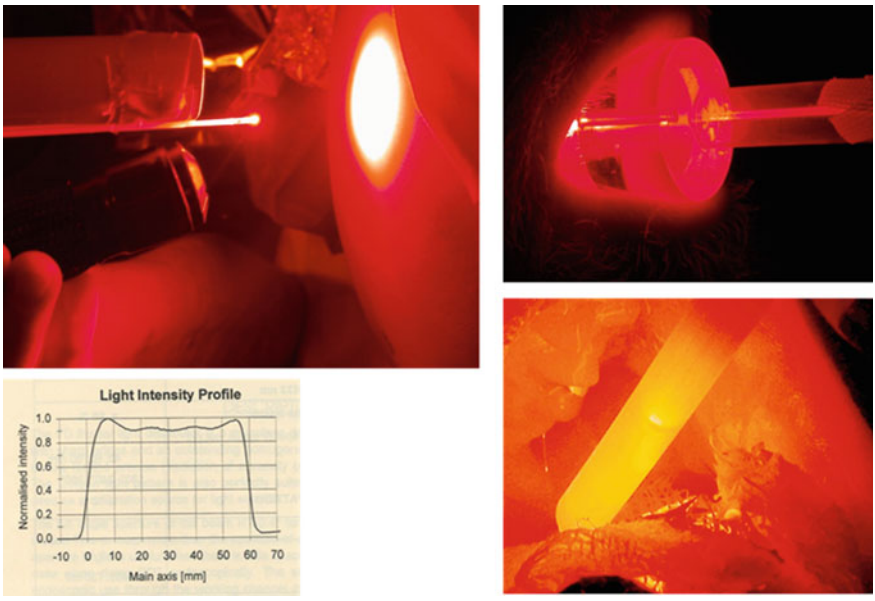

Fig. 5.10 Applicators

on the sensitizer used and the degree of exposure to light, this sensitization can take on an appearance ranging from a simple polymorphous light dermatosis (sun allergy) up to a serious epidermolysis or necrosis such as seen with congenital erythropoetic porphyria. The basic mechanism of this porphyria corresponds exactly to photodynamic therapy. As a rule, such skin irritations are short-lived, and permanent scars occur only in cases of absolute disregard of protective measures.

The same risk happens for the cornea and retina. [7, 30]

One possible solution is to take the patients in the dark for this photosensitization time. But, e.g., in some tetrapyrroles the skin photosensitization time can take several days. On the other hand, just these patients are often with palliative cancer therapy where the life quality is a very important aspect. Here is the yellow light of the Sodium vapor lamp—well-known as a street lamp—a perfect solution. Nearly, all Photosensitizers have an excitation gap in the yellow. On the other hand, our eyes have the highest sensitivity for the visual process just in this wavelength. This means that with low illumination which cannot cause any skin or retinal photosensitization the patients have the full visual capacity to read books, hygienic purposes in the bathroom including use the shower. With daily skin spectroscopy the total amount of PS in the skin can be measured and by a light step the risk for phototoxic reactions can be reduced.

5.4.2 Metabolic Disorders

The major part of the metabolism and elimination of hematoporphyrin derivates takes place in the liver. However, a poor liver function does not automatically represent a contraindication for the application of these substances, since their use displays a large therapeutic width, due to their low intrinsic toxicity. In patients with liver malfunctions, the possibility of a considerably lengthened and intensified photosensitization should be taken into account.

5.4.3 Immune Reactions

The allergic potential of a photosensitizer depends on its basic chemical structure. The hematoporphyrins generally have such a potential, which, however, is very dependent on the method of preparation and purification. Modern preparations, such as dihematoporphyrin ether (DHE: Photofrin II®) or hematoporphyrin derivate (HpD), have such a high degree of purity that reports about allergic reactions represent the exception. HpD has, for instance, been added in significant concentrations to several geriatric compounds for many years. This naturally represents a potential risk of photosensitization that has hardly been considered, but there has as yet been no notable number of accounts concerning allergic incidents.

5.4.4 Temperature and Pain Management

Due to the normally low power density in principle during PDT no rise in temperature happens (Fig. 5.11). But for deeper reaction depth a higher power density (photon flux) at the surface is necessary. This can cause a power density above 300 mW/cm^2 at which an overheating can happen. To reduce this effect a surface cooling either with cold air or ice cube is necessary.

But another situation even needs surface cooling: In ALA-PDT there is a burning sensation which is not related to an increasing temperature. This is caused by direct activation of PPIX in the C nerve fibers [3]. This mimics burning without any high temperature. This effect will be enhanced due to the fact that for instance in Basalioma the content in C-nerve fibers is greater than in normal skin (Fig. 5.12). This can be detected even in diagnostic ALA-fluorescence [4].

To overcome this effect even a cold air cooling is useful but here not to cool down an overheating but to depolarize the nerve fibers so they cannot react to the Laser irradiation. But this works not in all patients so sometimes regional anesthesia (local infiltration is without any effect!) or general anesthesia is necessary. But also some systemic photosensitizers can cause severe pain. The HpD is painless, but some photosensitizers in the family of Chlorins induce severe pain also in endoscopic and interstitial therapy. The effect is not yet clear but all they have a higher penetration depth (Fig. 5.13) [5].

5.5 Clinical Indications

The indication in treatment of solid tumors is mainly under palliative aspects in surgical primarily not resectable tumors or local recurrences and metastasis without any other therapeutical option like chemotherapy or radiotherapy [16, 26, 27] (Fig. 5.14). The reason is that with a surgical R0-resection in nearly all tumor entities the best 5y-life rates are obtainable. But in this tumor surgery another indication of PDT comes more important. After R0-resection direct intraoperative a PDT is performed to irradiate the tumor bed to increase the primary radicality without unnecessary defects. So the intention is similar to the intraoperative radiation. But one problem is the photosensitivity of the tissue to the operation or endoscopic light source. This is the reason that today only in neurosurgery the intraoperative ALA-PDT is routine.

But with increasing of patients with Human Papilloma Virus infections the virus induced dysplasias, e.g., in anogenital and ENT-regions increases. An early detection before an invasion starts is necessary (Fig. 5.15). One has to remember that dyplasias are a chronical disease. So we cannot prevent all the times recurrences. But we have to prevent the transition from a non-infiltrating dysplasia to an early invasive cancer [23]. Here, PDT is a curative tool for these diseases, e.g., because PDT is repeatable without any risk of resistance against this therapy. And with

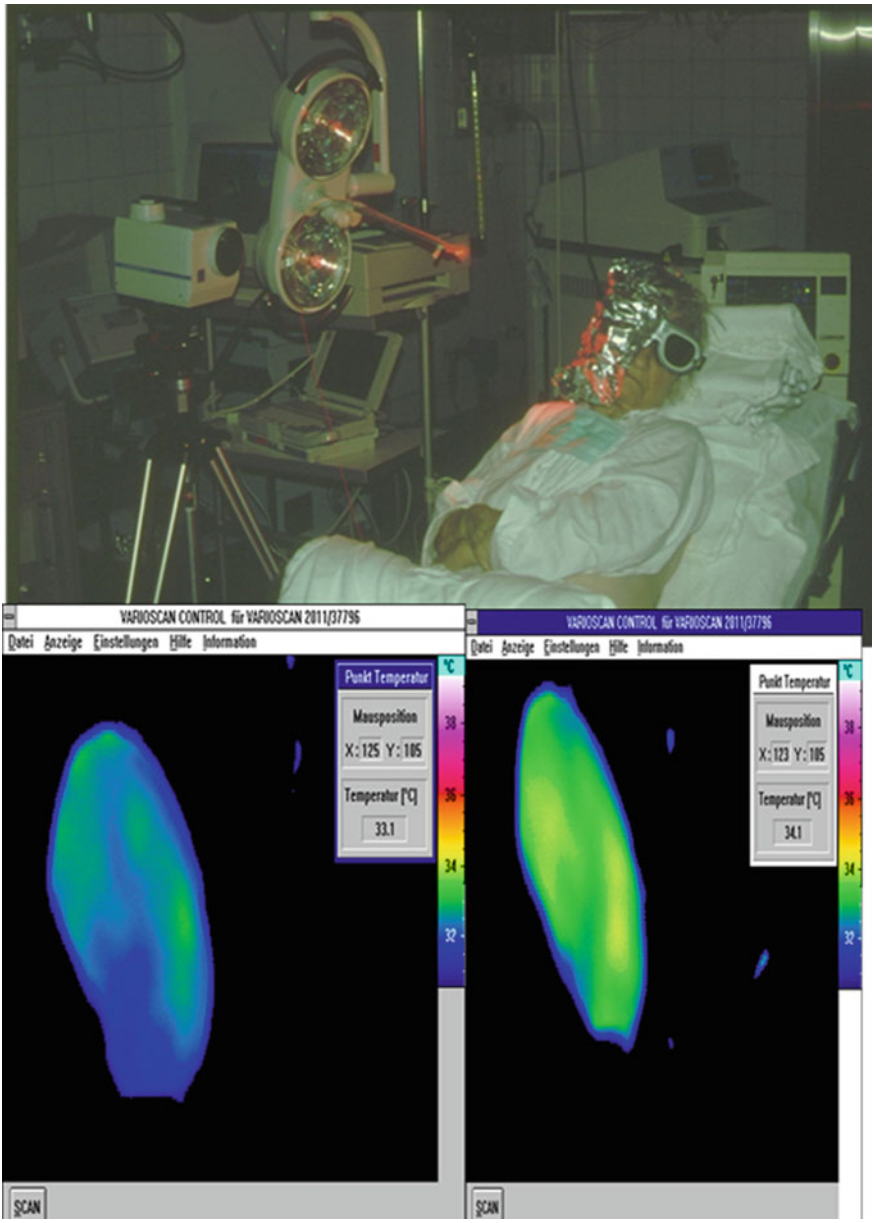

Fig. 5.11 Intraoperative temperature control with thermography. No rise in temperature is detected

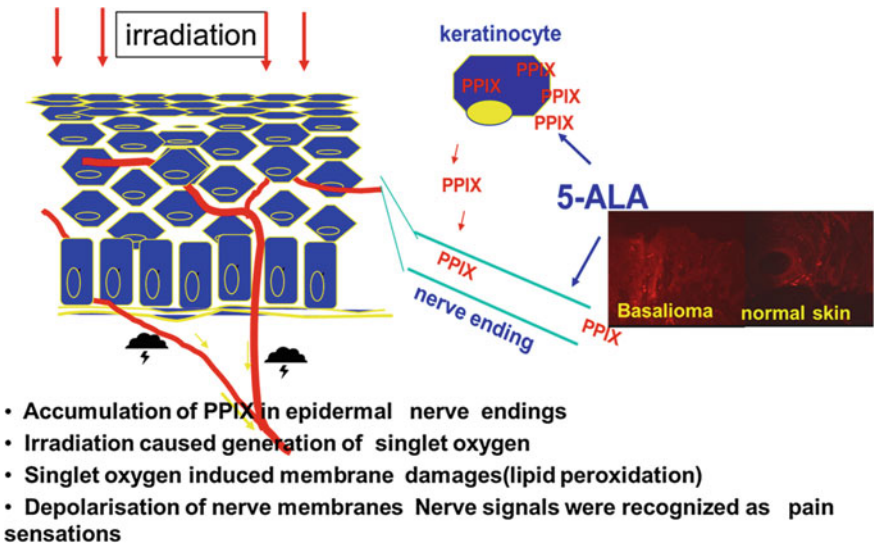

Fig. 5.12 Mechanism of PPIX uptake or generation in epidermal nerve endings

Fig. 5.13 Intraoperative cool air therapy for depolarization of C nerve fibers

increasing success in research of multiphoton fluorescence, Raman spectroscopy and OCT particularly in endoscopy these lesions and an invasion can be detect early [15, 28, 32, 34].

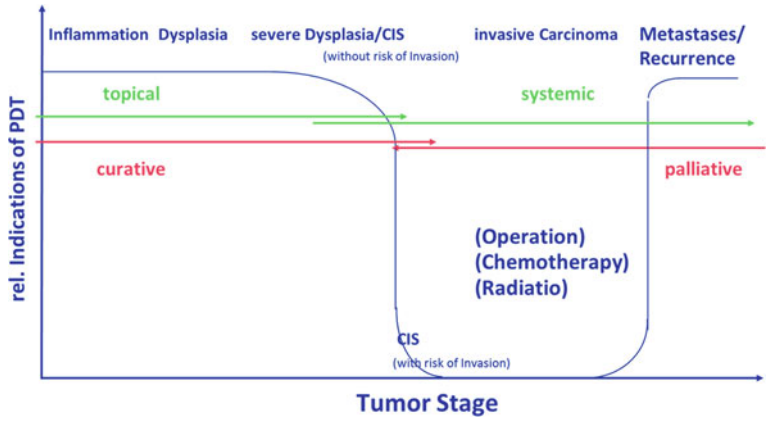

Fig. 5.14 relative clinical importance of PDT

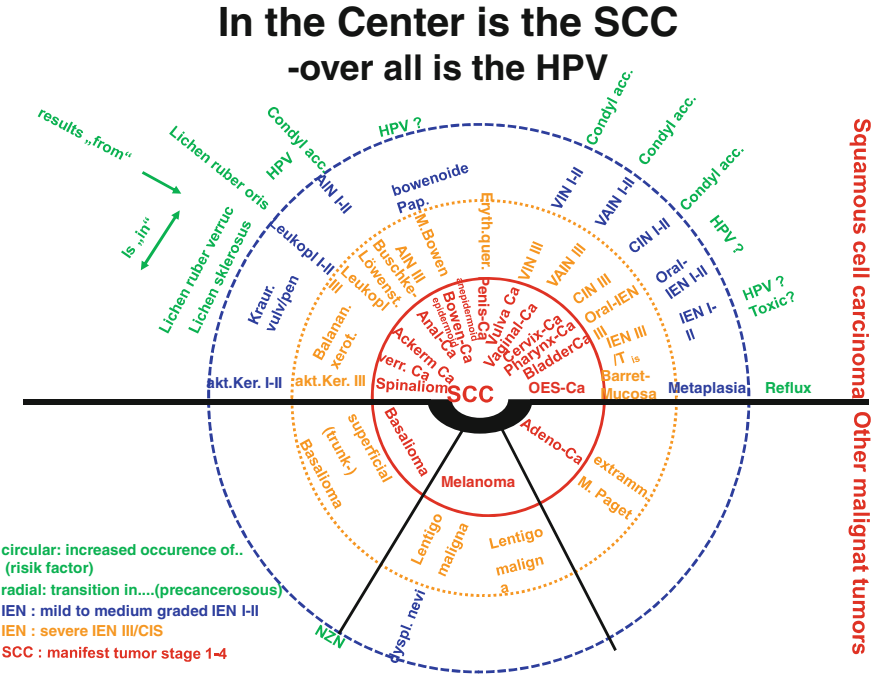

Fig. 5.15 Precancerous diseases and diseases with higher risk of malignancy

But with photosensitizers with increasing remaining in the vascular systems more benign indications start. The latest but now the major indication is at this time the age-related macula degeneration. Due to the fact that the used BPD has normally a good penetration into tissue and a low intravascular remaining potential

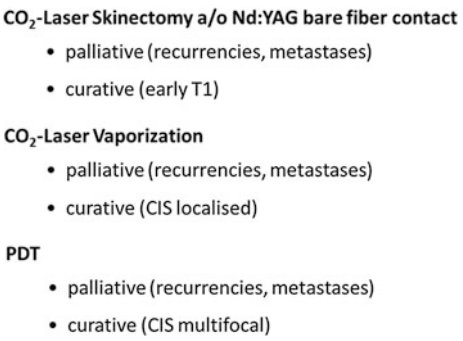

Fig. 5.16 Therapy modalities in laser tumor therapy

here a capsulation with liposomes are necessary. Because this coupling is in the blood not stable, within few minutes after application the Laser activation is necessary to avoid damage of the retinal epithelium. Longer experiments started in the treatments of congenital vascular tumors like infantile hemangioma and in vascular malformation especially port wine stains. But even after more than 20 years research we are at this field before a broad application. The same is in the treatment of inflammatory skin diseases. The psoriasis was one of the oldest application for PDT in non-malignant diseases but could not come to routine. At this time the most field of clinical research is now the treatment of severe acne. But comparative studies did show either severe skin photosensitivity which strained the patients more than the disease. In combination with pulsed Dye-Laser the additional effect to Laser alone is minor so at this time it is not clear if PDT will have a real success for this indication. In treatment of warts and condylomatas without dysplasias the PDT for virus eradication could not show any success. This is easy to explain the metabolism and proliferation in warts and non-dysplastic condylomas is better than in the surrounding tissue so no specific effect can happen. But has the cell itself change to dysplasia the PDT again is the tool of choice (Fig. 5.16).

5.6 Irradiation Protocol

Besides the right choice of the best Photosensitizer (e.g., topical/systemic, lipo-/hydrophilic, long-acting/short acting) and right choice of light source much more important is the irradiation protocol (Fig. 5.17). Here, we have to calculate separately the Laser parameters power, beam diameter, irradiation duration, furthermore irradiation at which time after ps-adminisration, total dosis, and sequence.

In general one can say:

The thicker the tumor—the higher the power density—possibly with shorter irradiation time

– **depending by the total volume**

Kreisfläche

Dosimetrie Kreisfläche						Dosimetrie Kreisfläche MICROLENS							Laser	MYTEST	* 0.9
PDT						PDT							0,5	0,47	0,423
MICROLENS		'Bitte Parameter eingeben				Pat:							1	0,92	0,828
		P Laser		T Laser		Laser:							1,5	1,34	1,206
		3,213	W	1600	sec	Faser:							2	1,79	1,611
						Sens:							2,5	2,23	2,007
						Charge:							3	2,73	2,457
						Applikation:	00:00:00						3,5	3,18	2,862
					Gesamt	Beginn Laser:							4	3,57	3,213
						Ende Laser:									
						Anaesthesie:									

	cm	cm	cm2	W/cm2	J/cm2		cm	cm	cm2	W/cm2	J/cm2	W	s	Laser			
Lokalisation	D	r2	A	PD	ED	Lokalisation	Durchmesser	r2	A	PD	ED	P	t	W		Bemerkungen	
	0,9	0,20	0,64	5,05	8080,83	17 links Untersch. (Knie)	4,5	5,08	15,90	0,15	100,42	2,457	650	3			
	1	0,25	0,79	4,09	6545,47	9 (a-c) links inframammär	8	16,00	50,27	0,06	102,27	3,21	1600	4		9a BCC	b-c AK
	1,5	0,56	1,77	1,82	2909,10												
	2	1,00	3,14	1,02	1636,37												
	2,5	1,58	4,91	0,65	1047,28												
	3	2,25	7,07	0,45	727,27												
	3,5	3,06	9,62	0,33	534,32												
	4	4,00	12,57	0,26	409,09												
	4,5	5,06	15,90	0,20	323,23												
	5	6,25	19,63	0,16	261,82												
	5,5	7,56	23,76	0,14	216,38												
	6	9,00	28,27	0,11	181,82												
	6,5	10,56	33,18	0,10	154,92												
	7	12,25	38,48	0,08	133,58												
	7,5	14,06	44,18	0,07	116,36												
	8	16,00	50,27	0,06	102,27												
	8,5	18,06	56,75	0,06	90,59												
	9	20,25	63,62	0,05	80,81												
	9,5	22,56	70,88	0,05	72,53												
	10	25,00	78,54	0,04	65,45												

Seite 1

Fig. 5.17 Excel calculation sheet for multiple lesions

The more superficial—the lower the power density—possibly with longer irradiation time

– **depending by the total volume**

Even the cooling influences not only the pain sensation and/or thermal side effects but also the ROS-production. Due to the capillary spasm by cooling the microcirculation is in the overlying tissue reduced which causes a lower oxygen concentration with lower singlet oxygen production. But on the other hand we know that a lower oxygen concentration due to reduced microcirculation can produce –OH radicals.

Another aspect is the beam diameter. At lower power density at the edges there is the risk that not enough singlet oxygen for cell death is produced so there is the risk of remaining tumor cells. So it is important even with "Microlens" irradiation to calculate the beam diameter greater than the lesion and cover the surrounding tissue with aluminum foil or zinc ointment to protect against unwanted irradiation. This means that an irradiation system Laser or diode-lamps need a reserve capacity.

For the daily clinical process the following PDT-protocols [35] have been shown useful:

5.6.1 Conventional

This is the most used protocol in PDT and for the majority of indications suitable (Fig. 5.18).

Fig. 5.18 Conventional protocol

One Drug—one wavelength—one irradiation

The requirements for this procedure are:

- high specific PS accumulation
- tumor thickness in the region of penetration depth

The aim for the patient is:

- easy handling
- treatment of large areas in one session

But this procedure has some disadvantages:

- long sessions
- sometimes pain full

In actinic keratosis, superficial basalioma and Bowens disease without risk of Bowen carcinoma procedure is the therapy of choice and can be combined intraoperative with surgical techniques like CO_2-Laser vaporization

5.6.2 Recovery

This protocol is, e.g., for topical ALA-preparations where after a delay time new PPIX is produced in the dysplastic cells.

One Drug—one wavelength—two/m irradiations

The requirements for this procedure are:

- active or passive late accumulation

The aim for the patient is:

- detection of remaining tumor cells
- supra selective destruction
- lower risk of overdosage

But this procedure has some disadvantages:

- multiple sessions
- reliable patients

In the meantime the patient has to be protected against artificial or sunlight and on the next morning a spetroscopie is necessary to count the amount of new PPIX-concentration

5.6.3 *Fractionated*

For this protocol there are two indications:

One is the situation of microcirculation which not allows to irradiate in one session (Fig. 5.19).

But another indication can be the patient itself. In very old and/or reduced patents make sometime sense to divide the irradiation on two sessions for recovery of the patient

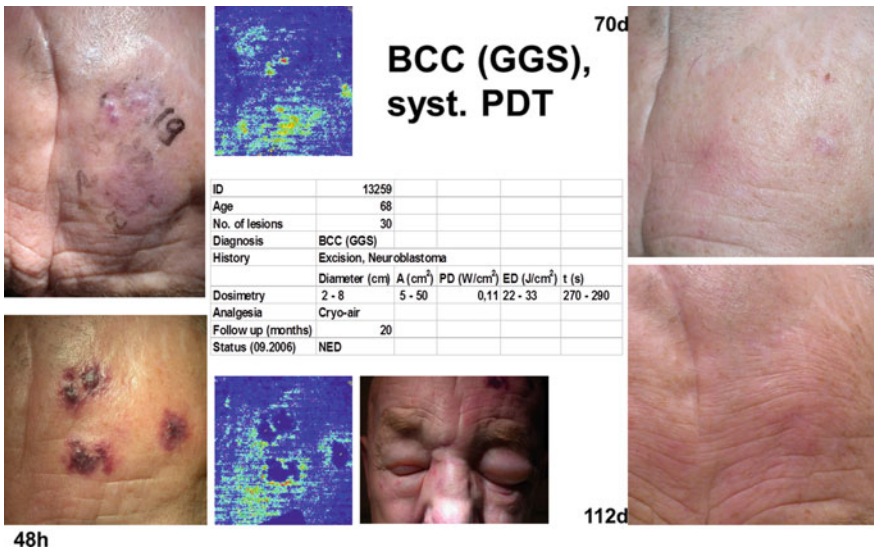

Fig. 5.19 Fractionated protocol. In the Laser Doppler investigation there is reduction of the microcirculation so the irradiation is stopped to avoid necrosis. After 24 h normalization occurs and the second pass happened

One Drug—one wavelength—two/m irradiations

The requirements for this procedure are:

- long interacting PS
- defined PS metabolism

The aim for the patient is:

- reduced risk of massive tissue necrosis (in the first pass)
- deeper penetration by reduced shielding (following passes)
- reduced risk of low dose PDT

But this procedure has some disadvantages:

- multiple sessions
- reliable patient

5.6.4 Boostering

This protocol has particularly advantages in disseminated and/or deeper lesion like recurrences and metastases (Fig. 5.20). Two aspects are important:

One is that PS-concentration in the overlying tissue like metastases shields the deeper parts of the tumor so it cannot be treated in one session.

The other aspect is that remain tumor cells in the surrounding where treated before they growth to new metastases.

One Drug—one wavelength—two/m cycles

The requirements for this procedure are:

Fig. 5.20 Boostering protocol. The second turn was performed approximately 3 month later

- defined PS metabolism
- no undetected PS surplus

The aim for the patient is:

- enhanced destruction of remaining tumor cells
- preserving of tissue in between

But this procedure has some disadvantages:

- strong protocol
- long skin photo senzitation time

5.6.5 Piggy-Back

This protocol is especially important in endoscopy where tissue cannot protect against unwanted irradiation but tumor cells are in different tissues. Here, one can use the different penetration depth of different wavelength, so with the longer wavelength a direct irradiation of visible parts is possible without the risk of unattended irradiation of the underlying muscle for instance and with the shorter wavelength a full space irradiation can be performed

One Drug—two wavelengths—one irradiation

The requirements for this procedure are:

- two absorption max for Quantum yield
- relevant wl in different tumor thickness

The aim for the patient is:

- complete destruction of superficial and deeper tumor cells in one session
- preserving unaffected soft tissue, e.g., musculature

But this procedure has some disadvantages:

- high technical infrastructure required
- specific Laser safety measurements

5.6.6 Sandwich

This protocol uses the fact that pharmacologic different PS have the same activation wavelength. So in one session, for instance, a topical PS like ALA for dysplasia and a systemic PS for early invasive carcinoma can be used simultaneously. This is particularly helpful in diseases where clinically a discrimination is not easily possible. Here, the substances find specifically their target.

Two drugs—one wavelength—one irradiation

The requirements for this procedure are:

- specific enrichment for each PS
- no photon or oxygen quenching

The aim for the patient is:

- simultaneous irradiation of intraepithelial dysplastic cells and
- solid tumor with stroma and vascularization

But this procedure has some disadvantages:

- exact planning for systemic drug delivery and topical application
- sometimes only under general anesthesia due to pain

5.7 Conclusion

PDT is a clinical procedure which follows all medical requirements for any other medical procedure:

It needs a strong indication

It needs a patient adjusted protocol and

It needs an intraoperative control and if necessary intraoperative changing of the procedure.

But with this principles PDT is an important and reliable part of therapeutical techniques

References

1. Alberts B, Bray D, Johnson A, Lewis J, Raff M, Roberts K, Walter P (1998) Essential Cell Biology, Garland
2. Algermissen B, Jamil B, Osterloh K, Berlien HP (1997) Detection of oxygen-based radicals using electron spin resonance under PDT conditions. In: SPIE Proceedings December
3. Algermissen B, Osterloh D, Philipp CM, Berlien H (2003) Management of ALA-PDT induced pain sensations. Med Laser Appl 18(1):57–64
4. Algermissen B, Berlien HP, Haas N (2004) Basal cell carcinomas in port-wine stains treated with thorium X. Acta Derm Venereol 84(6):475
5. Algermissen B, Hermes B, Henz BM, Müller U, Berlien HP (2002) Laser-induced weal and flare reactions: clinical aspects and pharmacological modulation. Br J Dermatol 146(5):863–868
6. Bellnier D, Ho K, Pandey RK, Missert J, Dougherty TJ (1989) Distribution andelucidation of the tumor-localizing component of hematoporphyrin derivative in mice.Photochem Photobiol. 50:221–228
7. Blum FH (1964) Photodynamic action and diseases caused by light. Hafner, New York
8. Chan W-S, Marshall JF, Lam GYF, Hart IR (1988) Tissue uptake, distribution and potency of the photoactivatable dye chloraluminium sulfonated phthalocyanine in mice bearing transplantable tumors. Cancer Res 48:3040–3044

9. Dolphin D (ed) (1987) The Porphyrins 3. Academic Press
10. Dressler C, Ismail MS, Nowak C, Berlien HP (1995) Pharmacokinetics of the far red absorbing octa-alpha-butyloxy-zinc phthalocyanine in Lewis lung carcinoma bearing mice. In: SPIE Proceedings, Jan 1995
11. Dressler C, Ismail MS, Stroebele S, Berlien HP (1995) Absorption spectroscopic analysis of the pharmacokinetics of octa-alpha-butyloxy-zinc phthalocyanine in Lewis lung carcinoma-bearing mice. In: SPIE Proceedings, Mar 1995
12. Förster Th (1946) Energieumwandlung und Fluoreszenz. Naturwissenschaften 6:166
13. Fox MA (1986) Advances in Photochemistry. Volman DH, Hammond GS, Gollnick K (eds), vol 13, p 237
14. Giering K, Dressler C, Herter R, Berlien HP (1996) Photobleaching of the photosensitizers octa- <alpha> -butyloxy-zincphthalocyanine and 132-hydroxy-bacteriopheophorbide-a-methylester. In: SPIE Proceedings, Jan 1996
15. Göppner D, Mechow N, Liebscher J, Thiel E, Seewald G, Buchholz A, Gollnick H, Philipp CM, Schönborn KH (2012) High-resolution two-photon imaging of HE-stained samples in dermatohistopathology—a pilot study on skin tumours. Photonics Lasers Med 1(2):133–140
16. Henderson BW and Donovan JM (1989) Release of prostaglandin E2 from cells by photodynamic treartment in vitro. Cancer Res 49:6896–6900
17. Ismail MS, El-Shehry AH, Berlien HP (1998) Laser-induced thermotherapy (LITT) for treatment of local recurrences in patients with breast cancer. In: SPIE Proceedings Laser-Tissue Interaction, Tissue Optics, and Laser Welding III, vol: 3195, January 1998
18. Ismail MS, Dressler C, Röder B, Berlien HP (1998) 13(2)-hydroxy-bacteriopheophorbide a methyl ester pharmacokinetics measurements with fluorescence versus absorption spectroscopy. Is there a difference? J Clin Laser Med Surg 16(4):203–210
19. Jamil B, Algermissen B, Osterloh D, Philipp CM, Berlien HP (2002) Qualitative differences in the generation of activated oxygen species by Photosensitizers used in pdt medical laser application 17(1)
20. Jori G (1989) Photosensitizing compounds: their chemistry, biology and clinical use. Wiley, Chichester, pp 78–86
21. Kessel D (1986) Porphyrin-lipoprotein association as a factor in porphyrin localization. Cancer Lett 33:183–188
22. Kongshaug M, Moan J, Brown SB (1989) The distribution of porphyrins with different tumor localizing ability among human plasma proteins. Br J Cancer 59:184–188
23. Moser JG (ed) (1998) Photodynamic tumor therapy 2nd and 3rd generation Photosensitizers. Harwood Academic Publishers, Switzerland
24. Müller U, Philipp CM, Fleige B, Berlien HP (2003) Laser therapy of vulval and cervical dysplasias. Med Laser Appl 18(2)
25. Nelson JS, Liav LH, Orenstein A, Roberts WG, Berns MV (1988) Mechanism of tumor destruction following photodynamic therapy with hematoporphyrin derivative, chlorin and phthalocyanine. J Natl Cancer Inst 80:1599–1605
26. Philipp CM, Rohde E, Berlien HP (1995) Nd: YAG laser procedures in tumor treatment. Semin Surg Oncol 11(4):290–298
27. Philipp CM, Rohde E, Waldschmidt J, Berlien HP (1994) Laser-induced thermotherapy of benign and malignant tumors controlled by color-coded duplex sonography. In: SPIE Proceedings, Dec 1994
28. Philipp CM, Müller U, Urban P, Berlien HP (2008) Potential of systemic photosensitizers for PDT of skin malignancies. In: SPIE Proceedings, 2 May 2008
29. Roeder B, Dressler C, Fuchs B, Berlien HP (1994) Pharmakokinetics of 132-hydroxy-bacteriopheophorbide: a methyl ester studied by fluorescence spectroscopy on Lewis lung carcinoma bearing mice. In: SPIE Proceedings, Mar 1994
30. Salet C, Moreno G (1990) New trends in photobiology. Photosensitizazion of mitochondria. Molecular and cellular aspects. J Photochem Photobiol, B 5:133–150
31. Srinivasan R, Ors JA (1978) Organic photochemistry with 6.7-eV photons: bicyclo [n. 1.0] alkanes and tricyclo [3.2. 1.02, 4] octane. J Amer Chem Soc 100:7089

32. Stroebele S, Dressler C, Ismail MS, Berlien HP (1995) Optimized fluorescence diagnosis of tumors by comparing five-ALA-induced xenofluorescence and autofluorescence intensities of a murine tumor/nontumor tissue system cultivated on the CAM. In: SPIE Proceedings, Dec 1995
33. Wayne RP (1988) Principles and applications of photochemistry. Oxford University Press, Oxford
34. Ziolkowska M, Philipp CM, Liebscher J, Berlien HP (2009) OCT of healthy skin, actinic skin and NMSC lesions. Med Laser Appl 24(4):256–264
35. Ziolkowska M, Philipp CM, Mueller U, Urban P, Berlien HP (2013) Clinical adjusted photodynamic therapy. Optik Photonik 8(1):42–44

Chapter 6
Photochemical Internalization: A Novel Technology for Targeted Macromolecule Therapy

Kristian Berg, Anette Weyergang, Marie Vikdal, Ole-Jacob Norum and Pål Kristian Selbo

Abstract Photochemical internalization (PCI) is a novel technology for release of endocytosed macromolecules into the cytosol. The technology is based on the use of photosensitizers located in endocytic vesicles that upon activation by light induces a release of macromolecules from their compartmentalization in endocytic vesicles. PCI has been shown to enhance the biological activity of a large variety of macromolecules and other molecules that do not readily penetrate the plasma membrane, including type I ribosome-inactivating proteins (RIPs), gene-encoding plasmids, adenovirus, oligonucleotides, and the chemotherapeuticum bleomycin. PCI has also been shown to enhance the treatment effect of targeted therapeutic macromolecules. The results show that PCI can induce efficient light-directed delivery of macromolecules into the cytosol, indicating that PCI may have a variety of useful applications for site-specific drug delivery, e.g., in gene therapy, vaccination, and cancer treatment. Our studies also indicate that PCI of bleomycin is superior to PDT in targeting the tumor periphery and that this is partly the cause of the improved treatment effect of PCI as compared to PDT.

K. Berg (✉) · A. Weyergang · M. Vikdal · P. K. Selbo
Department of Radiation Biology, Norwegian Radium Hospital,
Oslo University Hospital, Oslo, Norway
e-mail: kristian.berg@rr-research.no

A. Weyergang
e-mail: anette.weyergang@rr-research.no

M. Vikdal
e-mail: marie.vikdal@rr-research.no

P. K. Selbo
e-mail: selbo@rr-research.no

O.-J. Norum
Department Orthopedic Oncology, Oslo University Hospital, Oslo, Norway
e-mail: oleno@ous-hf.no

M. H. Abdel-Kader (ed.), *Photodynamic Therapy*,
DOI: 10.1007/978-3-642-39629-8_6,

6.1 Introduction

The utilization of macromolecules in therapy of cancer and other diseases is becoming increasingly relevant to successful tumor therapy. Recent advances in molecular biology and biotechnology have made it possible to improve targeting and design of cytotoxic agents, DNA complexes, and other macromolecules for clinical applications. To achieve the expected biological effect of these macromolecules, in many cases, internalization to the cell cytosol is crucial. Macromolecules are frequently prohibited from penetrating cell membranes, are instead, endocytosed and without any active intervention become degraded by hydrolytic enzymes in the lysosomes. Thus, at an intracellular level, the most fundamental obstruction for cytosolic localization of therapeutic macromolecules is the membrane-barrier of the endocytic vesicles [1]. Photochemical internalization (PCI) is a novel technology for release of endocytosed macromolecules into the cytosol. PCI has been shown to potentiate the biological activity of a large variety of macromolecules and other molecules that do not readily penetrate the plasma membrane [2, 3]. PCI may be utilized for treatment of most solid tumors and the first phase I clinical trial with PCI of bleomycin [4] for several cancer indications, including SCC of the Head and Neck, sarcomas, and breast carcinoma metastasis to the skin, have recently been completed with encouraging results (unpublished data).

In many cancers, local recurrence (LR) is almost inevitable and no efficient local cure is available, e.g., malignant brain tumors and malignant pleural mesothelioma. PDT and PCI may be used for local as well as systemic control of cancer. Here, the principle of PCI using PCI of immunotoxins as examples and their impact on invasive cancer, the tumor vasculature and antitumor immunity will be discussed.

6.2 Background

Photodynamic therapy (PDT) is a promising modality (4) approved for cancer treatment (mainly skin (basal cell carcinoma (BCC) and AK), lung, esophagus, and bladder) world-wide. PDT is based upon light activation of a compound, named photosensitizer (PS), which has a preferential retention in tumor tissues. Light exposure of the photosensitizers with visible light generates reactive oxygen species (ROS), where singlet oxygen is considered as the most important, and thereby induces cytotoxic effects in the light exposed area (Fig. 6.1). PSs have no side effect in the absence of light. PDT-induced cellular damage is dependent on the physico-chemical properties of the photosensitizer. It is well-known that upon administration some photosensitizers localize to the endosomes and lysosomes of the cell. Light exposure of some of these photosensitizers (such as $TPPS_{2a}$, $TPCS_{2a}$ (Amphinex®), and $AlPcS_{2a}$) has been shown to damage the membrane of the endocytic vesicles without inducing severe cytotoxicity [5, 6]. This is in contrast to

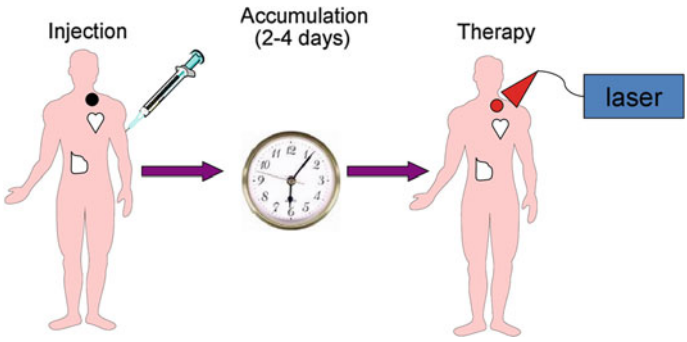

Fig. 6.1 Schematic description of the treatment procedure for PDT is also utilized by PCI. In the clinical PCI procedure today bleomycin is injected prior to the light exposure

other methods developed to induce endo-lysosomal damage, where the treatment is cytotoxic or exert low efficacy and/or specificity.

Although a molecule is unable to penetrate the plasma membrane, it is still taken up into the cell by means of endocytosis, either by receptor-mediated or adsorptive endocytosis or by pinocytosis. Endocytosed molecules are further transported to late endosomes and lysosomes where they are degraded. Drugs, with intracellular targets, that are not able to penetrate the plasma membrane will be degraded in the endocytic vesicles and will not exert any therapeutic effects. As described above, PDT with selected PSs has been shown to damage the endo-lysosomal membrane without inducing severe cytotoxicity and may therefore be utilized for cytosolic release of endocytosed drugs before they are degraded (Fig. 6.2). This method, Photochemical internalization (PCI) has been shown to increase the effect of ribosome-inactivating protein (RIP) toxins from plants, immunotoxins, genes (in both plasmids and viruses), peptide nucleic acids (PNA), siRNA, peptides (for vaccination), doxorubicin, and bleomycin [3]. Experiments have been performed in many cell lines (>80) and 10 tumor models derived from all major cancers and shown to exert a synergistic effect in all cases. The results show that PCI can induce efficient light-directed delivery of macromolecules into the cytosol, indicating that PCI may have a variety of useful applications for site-specific drug delivery, e.g., in gene therapy, vaccination, and cancer treatment.

Although the PCI technology has been developed for intracellular delivery of therapeutic macromolecules some chemotherapeutic agents accumulate in endocytic vesicles probably due to their size and/or charge. Bleomycin is a highly used chemotherapeutic agents for several cancer indications, but is also known for accumulating in endocytic vesicles [7]. The therapeutic effect of bleomycin is limited and lung fibrosis is a severe side effect frequently observed after accumulated doses bleomycin. However, after entering the cytosol bleomycin has been found highly cytotoxic and it has been estimated that only approximately 500 molecules is sufficient to kill a cell [8, 9]. PCI of bleomycin has been shown to improve the cytotoxic effect of bleomycin both in vitro and in vivo [4] and used in

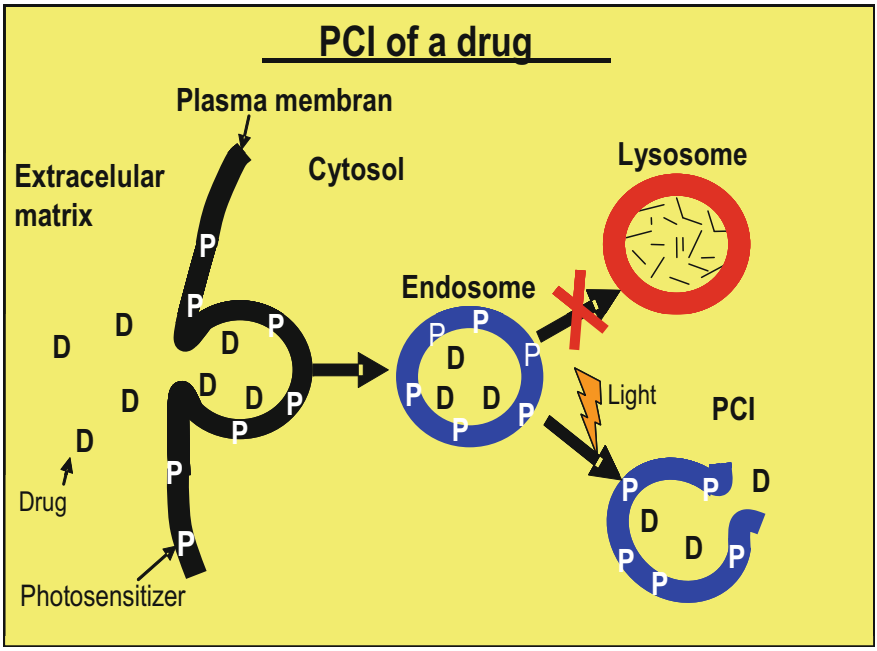

Fig. 6.2 Schematic description of the PCI technology

a phase I clinical trial that showed promising results. A benefit might be a reduced adverse effect of PCI of such chemotherapeutic agents if the therapeutic window can be increase and lower doses of cytotoxic chemotherapeutics can be administrated. In the clinical trial bleomycin was injected only once with a standard bleomycin dose.

6.3 PCI of Ribosome-Inactivation Protein Toxins and Immunotoxins as an Example of Therapeutic Macromoleculesfor Potential Clinical Use

A variety of plant RIPs have been shown to enzymatically inhibit ribosomal activity and are therefore highly cytotoxic to mammalian cells. These RIPs are endocytosed, but only a small fraction (5 % less) of molecules are successfully translocated through the Golgi apparatus to the cytosol where the toxins inhibit ribosomal protein synthesis eventually killing the cell. PCI may be used to increase both the efficacy and specificity of these toxins. There are two groups of RIPs, type I and type II. Type II RIPs, like ricin, consist of 2 polypeptide chains, one cytotoxic A-chain with N-glycosidase activity and one B-chain which binds to the cell surface. Type I RIPs, like gelonin, agrostin, and saporin, lack the B-chain and are

therefore poorly taken up and translocated to the cell cytosol. Hence, the cytotoxic effect of these protein toxins without linking any targeting moiety is absent or very low. A considerable cytotoxic effect of type I RIPs has been shown in combination with PCI, both in vitro and in vivo [10].

The development of monoclonal antibodies (mAbs) has been a revolution in cancer treatment, and several mAbs are today approved for clinical use. Treatment resistance is often a problem in mAbs-treatment. The drug response can, however, be increased by binding the mAbs to cytotoxic compounds, such as protein toxins, forming immunotoxins (ITs). The historical problems with first and second generation ITs are largely solved by the use of recombinant DNA technology where chimeric proteins consisting of the fv-fragment of an antibody and a protein toxin are constructed [11]. Antibodies or antibody fragments can be replaced with other targeting molecules like cytokines or growth-factors (e.g., IL-2, EGF, and VEGF). One of the advantages of using RIP-based ITs in cancer treatment is that these molecules are highly toxic when they enter the cytosol of the cell. It is estimated that as few as 1-10 RIP molecules in the cytosol is sufficient to kill a cell. However, there are some disadvantages of using protein toxins for the treatment of solid tumors, such as (1) limited penetration through the malignant tissue; (2) expression of neutralizing antibodies due to repeated injections of the IT; (3) uptake of the IT in normal cells causing side effects such as vascular leak syndrome (VLS), hemolytic-uremic syndrome, and damage on other organs which express the target-antigen on the cell surface. Since RIP-based ITs are unable to penetrate the membranes of endocytic vesicles, targeting fusion toxins based on type I RIPs are thought to induce less side effects than type II based ITs. PCI, as described below, can be used to activate type I RIP-based ITs by a photochemical release of the protein toxin into the cytosol of a cell. This activity is induced only in the tissue that is exposed to light and consequently, the dose limiting adverse effects of the IT is highly reduced. Recently, we demonstrated that PCI of the melanoma targeting fusion toxin MELscFv-rGel strongly augmented the therapeutic effect of MELsvFc-Gel in vitro and synergistic effects were also achieved in vivo [12]. This is the first in vivo study that documents therapeutic effects of PCI of a targeting macromolecule after systemic administration. Of particular interest, compared to other studies where ITs are injected multiple times, the IT was administered only once in this study.

6.4 Impact of PCI on the Tumor Cells, the Vasculature, and the Immune System

PDT is known for exerting its effect through targeting the parenchyma (tumor cells), the vasculature, and the immune system (Fig. 6.3). An in vivo-ex vivo assay has shown that PCI of bleomycin may target both the tumor cells and the vasculature (unpublished results).

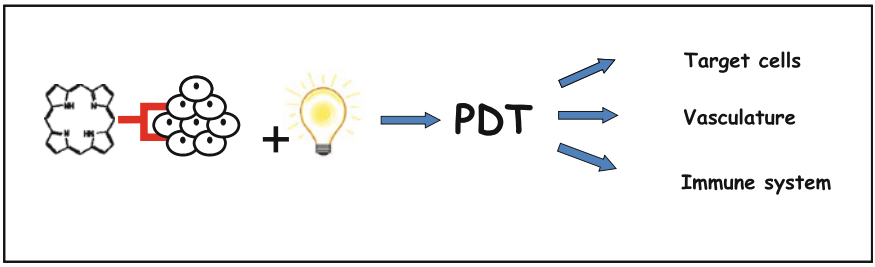

Fig. 6.3 Schematic description of PDT and the main therapeutic effects. The PS associates with the target tissue, e.g., tumor, and upon exposure to light absorbed by the PS induces several therapeutic effects

6.4.1 PCI: Therapeutic Effects on Invasive Cancers

The infiltrative growth of many cancers frequently results in local recurrences (LRs) as well as metastasis and is therefore a major challenge in cancer treatment. The rates of LR and metastasis vary from cancer to cancer and are in general dependent on the pathological anatomical diagnosis and local anatomical considerations [13].

PDT is currently under clinical investigation as an adjuvant to surgery when a safe surgical resection margin cannot be obtained. However, although increased survival time has been observed by PDT performed on the surgical cavity local recurrences are frequently observed. Our recent results with an invasive tumor model in athymic mice indicate that this is due to resistance of the transitional zone (periphery) of the tumor to PDT, while PCI is much more efficient in eradicating this zone [14]. This has been shown by performing PDT and PCI of BLM on the cavity after marginal surgical resection of invasive HT1080 fibrosarcoma xenografts [15]. PDT was found to be completely inactive on the residual tumor cells, while PCI strongly prevented tumor growth after surgery.

6.4.2 PCI: Vascular Targeting

The treatment effect of PCI in vivo has until recently been assumed to be due to targeting of the tumor parenchyma cells and that the enhanced therapeutic effect as compared to PDT to be due to induction of necrosis in deeper tissue layer than by . However, our recent results utilizing the invasive HT1080 fibrosarcoma model indicate that the PS $AlPcS_{2a}$ is also localized in the endothelial lining of the vasculature and most likely is the cause of the vascular shutdown observed shortly (2 h) after light exposure (from Gd-DPMA based MRI) [15]. The vascular shutdown was complete, except for the tumor periphery that appeared unaffected. There were no differences between PDT and PCI of bleomycin in this respect.

However, bleomycin is a slow acting chemotherapeuticum and is not expected to exert any therapeutic effect shortly after administration. It has recently been shown by an in vivo-ex vivo assay that the vasculature in the periphery is also targeting by PCI of bleomycin (unpublished data). PCI may, therefore, on this basis be used to target both the tumor parenchyma cells as well as the vasculature of the tumor.

A large number of clinical anti-angiogenesis studies have been established for the therapy of cancer. Proteins important for the regulation of angiogenesis include vascular endothelial growth factor A (VEGF-A), FGF, TNF-α, EGF, HIF-1α, and IL-8. VEGF-A is one of the major mediators in tumor angiogenesis and binds the receptors VEGFR-1 and VEGFR-2 on vascular endothelial cells. VEGFR-2 is presumed to be the most important receptor mediating the proangiogenetic effects of VEGF in solid tumors. Several types of drugs (tyrosin kinases, siRNA, Mabs, and soluble receptors) targeting the VEGFR-2 or downstream signaling pathways are under development for clinical use. A fusion protein consisting of VEGF-A (isoform VEGF121) and recombinant gelonin, VEGF121-rGel has been shown to induce cytotoxic effects on cells expressing VEGFR-2 [16]. The therapeutic effect of VEGF121-rGel is, however, limited by toxicity to normal cells. PCI should therefore be a proper approach to strengthen the therapeutic effect and specificity of VEGF121-rGel-based therapy. Recent studies indicate that PCI of VEGF121-rGel on VEGFR2 stably transfected PAE endothelial cells (KDR cells) induces a strong synergistic cytotoxicity in vitro (unpublished data).

6.4.3 Antitumor Immunity by PDT and PCI

A significant increase in the infiltration of $CD8^+$-T cells is reported in the tumor of PDT responsive patients compared to patients that to not respond to the treatment [17]. In addition, preclinical studies demonstrate that PDT induces inflammatory and immunologic responses. PDT leads to an immediate accumulation of neutrophils in the affected tissue followed by an increase of mast cells and monocytes that have implications for the treatment effect. Preclinical reports also indicate that PDT may have a vaccinating effect [18]. We have therefore initiated a study to explore vaccinating effects of PDT and PCI using a CT26.CT25 mouse colon carcinoma xenograft model growing subcutaneously in athymic and thymic mice. Our data show that no tumors grow upon reinjections of tumor cells in thymic mice 0-2 months after CR of PDT and PCI (unpublished data). This is highly encouraging and indicates antitumor immunity of therapies using PCI photosensitizers.

6.5 Conclusions

PCI is highly efficient in improving internalization of macromolecules. Substantial site-direction of the treatment can be obtained by the need for light activation and in some diseases, such as in solid cancers, the preferential retention of the

photosensitizer in the diseased areas. This dual selectivity will reduce damage of the normal surrounding tissue. An additional selectivity is obtained when the macromolecule of interest is bound to a tumor seeking ligand or antibody. Most technologies developed so far are useful for internalization of only one group of compounds, while PCI has been shown to act efficiently in internalization of a large variety of macromolecules and may be useful for internalization of different macromolecules simultaneously. The method can be combined with most other means for generating site- and tissue-specificity.

References

1. Varkouhi AK, Scholte M, Storm G, Haisma HJ (2011) Endosomal escape pathways for delivery of biologicals. J Control Release 151:220–228
2. Berg K, Selbo PK, Prasmickaite L, Tjelle TE, Kjølsrud S, Rodal GH, Anholt H, Sandvig K, Moan J, Gaudernack G, Fodstad Ø, Rodal SK, Høgset A (1999) Photochemical internalization. A novel technology for site-specific delivery of macromolecules into cytosol. Cancer Res 59:1180–1183
3. Selbo PK, Weyergang A, Høgset A, Norum OJ, Berstad MB, Vikdal M, Berg K (2010) Photochemical internalization provides time and space controlled endo-lysosomal escape of therapeutic molecules. J Control Release 148:2–12
4. Berg K, Dietze A, Kaalhus O, Høgset A (2005) Site-specific drug delivery by photochemical internalization enhances the antitumor effect of bleomycin. Clin Cancer Res 11:8476–8485
5. Høgset A, Prasmickaite L, Selbo PK, Hellum M, Engesæter BØ, Berg K (2004) Photochemical internalisation in drug and gene delivery. Adv Drug Deliv Res 56(1):95–115
6. Berg K, Nordstrand S, Selbo PK, Tran DTT, Angell-Petersen E, Høgset A (2011) Disulfonated tetraphenyl chlorin ($TPCS_{2a}$), a novel photosensitizer developed for clinical utilization of photochemical internalization. Photochem Photobiol Sci 10:1637–1651
7. Pron G, Mahrour N, Orlowski S, Tounekti O, Poddevin B, Belehradek J Jr, Mir LM (1999) Internalisation of the bleomycin molecules responsible for bleomycin toxicity: a receptor—mediated endocytosis mechanism. Biochem Pharmacol 57:45–56
8. Poddevin B, Orlowski S, Belehradek Jr J, Mir LM (1991) Very high cytotoxicity of bleomycin introduced into the cytosol of cells in culture. Biochem Pharmacol 42:S67–67
9. Silve A, Leray I, Mir LM (2012) Demonstration of cell membrane permeabilization to medium-sized molecules caused by a single 10 ns electric pulse. Bioelectrochemistry 87:260–264
10. Selbo PK, Sivam G, Fodstad Ø, Sandvig K, Berg K (2001) In vivo documentation of photochemical internalization, a novel approach for site specific cancer therapy. Int J Cancer 92:761–766
11. Pastan I, Hassan R, Fitzgerald DJ, Kreitman RJ (2006) Immunotoxin therapy of cancer. Nat Rev Cancer 6:559–565
12. Selbo PK, Rosenblum MG, Cheung L, Zhang W, Berg K (2009) Multi-modality therapeutics with potent anti-tumor effects: photochemical internalization enhances delivery of the fusion toxin scFvMEL/rGel. PLoS ONE 4(8):e6691
13. Clarke M, Collins R, Darby S et al (2005) Effects of radiotherapy and of differences in the extent of surgery for early breast cancer on local recurrence and 15-year survival: an overview of the randomised trials. Lancet 366(9503):2087–2106
14. Norum O-J, Gaustad J-V, Angell-Petersen E, Rofstad1 EK, Peng Q, Gierckskey KE, Berg K (2009) Photochemical internalization of bleomycin is superior to photodynamic therapy due to the therapeutic effect in the tumor periphery. Photochem Photobiol 85:740–49

15. Norum OJ, Giercksky KE, Berg K (2009) Photochemical internalization as an adjunct to marginal surgery in a human sarcoma model. Photochem Photobiol Sci 8:758–762
16. Mohamedali KA, Kedar D, Sweeney P, Kamat A, Davis DW, Eve BY, Huang S, Thorpe PE, Dinney CP, Rosenblum MG (2005) The vascular-targeting fusion toxin VEGF121/rGel inhibits the growth of orthotopic human bladder carcinoma tumors. Neoplasia 7:912–920
17. Abdel-Hady ES, Martin-Hirsch P, Duggan-Keen M, Stern PL, Moore JV, Corbitt G, Kitchener HC, Hampson IN (2001) Immunological and viral factors associated with the response of vulval intraepithelial neoplasia to photodynamic therapy. Cancer Res 61:192–196
18. Gollnick SO, Vaughan L, Henderson BW (2002) Generation of effective antitumor vaccines using photodynamic therapy. Cancer Res 62(6):1604–1608

Part IV
Oncological Applications

Chapter 7
PDT in Dermatology

Carsten M. Philipp

7.1 Introduction

Skin is the largest organ of the human body. Usually, it is easy accessible for topical application of drugs and light dosimetry is easy due to the rather flat appearance in a first approximation. On the other hand a larger number of skin diseases cover a larger area or show multifocal appearance, which favors regional or large field therapies and impedes surgical interventions. As scar formation is another and today highly unwanted result of surgery, the widespread use of PDT in dermatology is a necessary consequence.

According to the World Health Organization (WHO), between two and three million people in the world develop white skin cancer (nonmelanoma skin cancer, NMSC) every year [1]. According to the German Cancer Society 120 of 100,000 inhabitants in Germany are affected yearly with NMSC. Of these, 100 cases are basal cell carcinoma (BCC), which makes it the most frequently occurring malignant skin tumor, followed by squamous cell carcinoma (SCC). Actinic keratosis (AK) is a premalignant lesion and can lead to SCC [2].

Historically, PDT started with dermatological application. The first documented in the modern times treatment was done by Von Tappeiner and Jesionek who treated BCC with topically applied Eosin and light in 1904. They discovered the effect of Eosin staining and light on living cells in 1899, when they studied some protozoon species (paramecia), some were exposed to light others were not accidentally. The light exposed samples died and the concept was born. They also defined the term PDT as "interaction by a fluorescent dye and light and oxygen to produce a cytotoxic effect", which is not precise with regard to today's knowledge, but was revolutionary at the time of the authors [3–5].

The use of psoralene containing topicals and exposure to sunlight is even much older and dates back several thousand years to the ancient history of mankind.

C. M. Philipp (✉)
Ev. Elisabeth Klinik Berlin, Abt. Lasermedizin, Berlin, Germany
e-mail: cmphilipp@dglm.org

M. H. Abdel-Kader (ed.), *Photodynamic Therapy*,
DOI: 10.1007/978-3-642-39629-8_7,

Documented in several ancient books as the *Atharavaveda* (1400 BC, India) or the *Papyrus Ebers* (1550 BC, Egypt) it was a common treatment for vitiligo and psoriasis in India, Egypt, and Greece. Today this therapy is known as PUVA-therapy, which significantly differs from PDT regarding the involved mechanisms but has in common that a drug is activated by light.

The first systemic application of porphyrin was described by Hausmann in 1911 who injected porphyrin into mice and Meyer-Betz who self injected hematoporphyrin and exposed himself to light on a sun deck during a bus ride in 1912 [6, 7]. The effect was obviously a phototoxic reaction with severe swelling of light exposed skin at head and hands, which fortunately recovered after some days. The photographs of this experiment are legendary. Although topical PDT is most common today, systemic PDT plays an important role for advanced skin tumors and skin metastases, e.g., of breast cancer.

7.2 Photosensitzers for Topical PDT

7.2.1 5-ALA/PpIX

The very first attempts to topical PDT were performed by Tappeiner and his group at the Pharmacological Institute of the Ludwig-Maximilians-University in Munich between 1903 and 1905, when they used eosin, fluorescein, acridine orange, and other dyes to treat "ulcus rhodens," ulcerated basal cell carcinoma, and other tumors of the skin, including the problem of "lupus vulgaris", the cutaneous tuberculosis, which was of high importance at that time [8, 9].

The application was usually topical, but also injection of the dyes into the tumors was reported for sensitization and irradiation with artificial light from an arc lamp was used. Today dyes as methylene-blue, toluidine-blue-O, and indocyanine green are in the focus of research e.g., for applications in dental medicine (periodontal diseases) as they act as bactericide disinfectant when used in combination with light.

Penetration of those rather small dye molecules into tissues e.g., skin with its barrier the stratum corneum is much better than of larger molecules as porphyrins which came into favor as photosensitizers for PDT after the description by Hausmann and Meyer-Betz in the early 19th century. But topical application of porphyrins failed, due to their poor penetration of the skin barrier and the topical PDT was left as a treatment modality, maybe also due to the growing possibilities of radiotherapy which dominated the nonsurgical skin tumor treatment for decades.

The solution of this problem was found in 1990 by Kennedy and Pottier who demonstrated that a small molecule, 5-aminolevulinic acid (ALA), easily penetrates into the skin [10, 11].

ALA is a precursor of heme, it is not a photosensitizer by itself but it is quickly metabolized to another precursor of heme, the protoporphyrin IX (PpIX) via the intrinsic cellular heme-biosynthetic pathway. Exogenous administration of ALA bypasses the natural regulation that heme exerts on ALA synthesis, which leads to increased production of PpIX [12]. PpIX has been found to preferentially accumulate in tumor as compared with normal cells. This phenomenon can be explained by differences in heme-biosynthetic pathway between nonmalignant and malignant cells. It has been shown that decreased activity of ferrochelatase [13–16] and limited availability of iron [17] in tumor cells contribute to increased PpIX accumulation. Enhanced activity of enzymes leading to production of PpIX, such as ALAD, UROD, or PBGD [13, 18] has also been observed in tumor cells.

PpIX is a strong photosensitizer, which assembles in mitochondria of tumor cells leading to their damage after light exposure (Fig. 7.1). Usually, about 4–6 h after administration of ALA, when PpIX has been already synthesized, target cells are exposed to light, which leads to excitation of the photosensitizer and formation of $^1O_2$ that exerts cytotoxic effects [19, 20].

5-Aminolevulinic acid for dermatologic applications is available in different formulations throughout the world today. Brand names are Metvix®, Alacare®, Alasens® Levulan® Kerastick®, Ameluz® with differing concentrations and carriers.

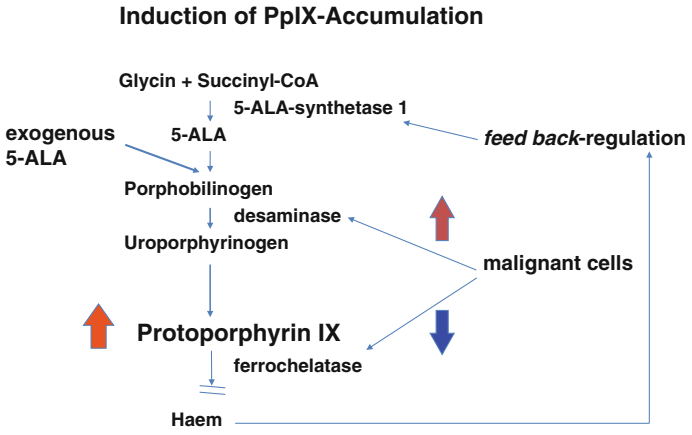

Fig. 7.1 Pathway of PpIX-accumulation in dysplastic and cancerous cells Although all enzymes involved in the heme-biosynthetic pathway are necessary, only two of them: ALAS1 and ferrochelatase are considered to be rate-limiting. Normally, the activity of ALAS1, is regulated by heme through the negative feedback mechanism. Normally, the feedback mechanism leads to the production of PpIX in such amounts that can be efficiently converted to heme by ferrochelatase. Exogenous administration of ALA bypasses the natural regulation that heme exerts on ALA synthesis, which leads to increased production of PpIX. The efficacy of ferrochelatase is then too low to convert excessively produced PpIX to heme, which results in the accumulation of PpIX within cells. About 4–6 h after administration of ALA, when PpIX is already synthesized, target cells are exposed to light, which leads to excitation of the photosensitizer and formation of 1O2 that exerts cytotoxic effects [20]

Levulan® is also known under the name Aladerm. Alasens® is a formulation from Russia, which might be used orally or topical. All products have approval for the treatment of non-hyperkeratotic actinic keratosis (AK) grade I and II at least in the countries of origin. Metvix® additionally is approved for noninvasive superficial squamous cell carcinoma (Morbus Bowen, MB), superficial basal cell carcinoma (sBCC) and nodular basal cell carcinoma (nBCC) in combination with prior curettage in Europe. Explicit excluded is the treatment of morpheic (morpheaform) BCC. Whether the treatment of nodular BCC with topical photosensitizers makes any sense or not should be evaluated in studies to come, today in our clinic we do not treat nodular BCC with topical PDT if they extend more than one millimeter into the skin. Reason for this limitation is not the penetration of the drug but the lack of control the tumor in its full extend with optical coherence tomography (OCT), which will be discussed later in this article. Penetration depth of the mentioned ALA formulations, e.g., Metvix®, within the given times is expected to be between 2 and 3 mm in non-hyperkeratotic skin.

Already to use formulations are somewhat expensive. But there is a free recipe for an ALA-thermogel by Professor Dr. Christel Müller-Goymann from the Institut für Pharmazeutische Technologie der Universität Braunschweig available at the internet which could easily be prepared by a pharmacist and all components can be obtained by the pharmacist also [21] (Table 7.1).

The components should be weighted and stirred together with 1,450 rpm in an unguator for 90 s. During the exothermic reaction a gel may be formed that becomes liquid again if cooled down below 12 °C. Preferably cooled water should be used, as else the gel may becomes too sticky for stirring it properly. The preparation should be stored only shortly and always in a cold place (6–8 °C) as the amino component is not stable in the dissolved form. It is possible to produce a larger amount of the base and add the active component (5-aminolevulinic acid) shortly before use. The ALA-thermogel should be applied when it is still cold and liquid. In contact with skin it turns into a gel that would not run off from the site.

If you want to use this recipe please make sure not to violate possible restrictive laws regarding the use of free formulated prescription drugs in the country you are working in. In Germany, it is common to make prescriptions for topical ointments e.g., in dermatology or ENT with a composition of ingredients which is not available as a patented drug formulation. Every medical doctor can write a

Table 7.1 Components of ALA-thermogel [21]

Component	g/100 g
5-aminolaevulinic acid	10.00
Poloxamer 407 (Pluronic® F127)	18.00
Isopropyl alcohol	11.25
Dimethylisosorbid	11.25
Medium-chain triglycerides(Miglyol® 840)	4.50
Water	45.00

personalized prescription and if the pharmacist is able to produce it then he becomes liable for the proper composition of the drug and the MD who is using it becomes liable for its use including unwanted side effects.

7.2.2 Penetration Enhancement

Compared to the large porphyrin molecules ALA is a small molecule and penetrates skin faster and deeper. Nevertheless, the application time of a solution of ALA in water or base cream would be much longer as suggested in the fact sheets for the above-mentioned brand formulations. The bioavailability is somewhat crucial for compliance of both patients and clinician, and it is important for marketing. But a higher bioavailability also reduces unwanted side effects due to a lower concentration of the active drug necessary and a higher selectivity. Furthermore, during longer permeation times the active substance may be changed by polymerization or other chemical changes.

All brand formulations use special pharmacological features to enhance the penetration of the skin barrier. The active ingredient of Metvix® is the methyl ester of 5-aminolaevulinic acid (MAL, MAOP). It is less polar and therefore penetrates the stratum corneum in a higher rate compared to the more hydrophilic substance. Ameluz® employs patented nanostructures to enhance the permeability of the skin. Other options to increase the permeation would be the use of dimethyl sulfoxide (DMSO) and ethylene-diamine-tetraacetic acid (EDTA) in the base of the formulation. For the ALA-thermogel a 7.5-fold increase in comparison with base cream DAC, and a 19.5-fold increase compared to water containing hydrophilic ointment was described [22].

It is clinical practice to remove strong hyperkeratotic layers prior to the application of ALA. A mechanical curettage, erbium laser ablation, or fractionated techniques may be used. Forster reported a strong increase of fluorescence increase and a deeper penetration of ALA after erbium laser ablation of the stratum corneum [23]. Less sophisticated microneedle pretreatment has shown to improve the permeability of the skin as well [24] and iontophoresis proved to be effective in increasing the transport for MAL, but both techniques increase the efforts, complexity and possible risks of the procedure also [25]. These attempts show that penetration of the drug and the gradient of concentration are of major concern and the limiting factor for topical PDT, as light of the usually applied wavelength for therapy (635 nm) shows a rather deep penetration into tissues and theoretically could be applied up to any total energy.

7.2.3 Other Topical Photosensitizers

Fosgel®, Foslip® and Fospeg® contain Temoporfin (mTHPC) a chlorin which is marketed as Foscan® for systemic applications. Fosgel®/Foslip® contains mTHPC bound to conventional liposomes, Fospeg® consists of mTHPC bound to pegylated liposomes. Chlorins are potent photosensitizers, but relatively large molecules. The first reports on Foslip® in 2006 and 2007 in animal models where promising [26, 27]. The evaluation may continues [28] but clinical studies are not reported so far and the formulation is not commercially available, yet it is not announced at the website of biolitec®, the company that distributes Foscan®.

Another promising topical photosensitizer is indocyanine green (ICG) currently under evaluation for the treatment of periodontal diseases and acne [29, 30]. Other indications including basal cell carcinoma or cholangiocarcinoma showed less favorable results compared to other photosensitizers and were left. Actually, there is no concurrent topical photosensitizer to ALA and its derivative MAL in clinical relevant use.

7.3 Systemic Photosensitizers

Most of PDT applications in dermatology are based on topical application of ALA and its derivatives. This might be understandable from the dermatological view, but it is all but logical from the view of an oncologist. It is limiting PDT to benign diseases, epithelial dysplasia and very superficial tumors, which should be not necessarily the limit. At a certain stage in tumor development vascular growth into and nutrition of the tumor masses becomes evident. As the amount of accumulated photosensitizer decreases with the depth in topical application critical regions may be not or insufficiently sensitized. In this situation, a photosensitization via a systemic route should be considered as a possible and maybe superior compared to topical application. Today, clinically relevant systemic photosensitizers are based on two substances, hematoporphyrin (HPD) or chlorin. The major disadvantage of both substances is their general photosensitization of skin after systemic administration. Nevertheless, a high specific uptake ratio with an efficient contrast between solid skin tumors and surrounding healthy skin can be obtained at a certain time interval, which is substance specific and ranges between hours in case of chlorine-e6 (Fotolon®, not commercially available today, APOCARE Pharma) to one or two days in HPD (Photofrin®, Pinnacle Biologics) and even longer in mTHPC (Foscan®, Biolitec).

7.4 Fluorescence Diagnostics: Clinical Aspects

7.4.1 Fluorescence Diagnostics

PpIX is a strong photosensitizer but it also shows a bright red fluorescence with center wavelengths of 636 and 700–710 nm when excited with blue light of usually 405 nm (380–440 nm). As it requires the presence of an added fluorophore this type of fluorescence is named xenofluorescence in contrast to autofluorescence from tissue-specific fluorophores. The clinical use of PpIX-fluorescence goes far beyond dermatological applications, it is used to delineate the borders of gliomas after oral uptake of Gliosan® as well as of bladder tumors after local installation of Hexvix®. Special pharmacological formulations again help to allow optimized accumulation in tissue-specific tumors and surroundings. But whatever formulation is used, the fluorescence is of PpIX and shows the characteristic red fluorescence and all the other typical features and shortcomings, e.g., strong photobleaching and lack of discrimination power between dysplasia and inflammation. Usually, a two-dimensional image is generated by excitation with a blue light source and applicable filters for endoscopes or cameras or simply goggles that cut off the blue light to enhance the visual effect. The first commercially available system was the D-light®-system by Storz for use in urology. Today numerous systems exist, each with special features for its specific use. In endoscopy, e.g., for imaging of bronchial dysplasias, the comparison of the autofluorescence and xenofluorescence images is often use to overcome the shortcomings of PpIX-fluorescence imaging. All of the endoscopic systems may be used in dermatology, but excitation is also possible with a woodlight lamp. For documentation a usual CCD or CMOS camera equipped with a cut off filter for blue light (for example: HOYA, K2 yellow) is applicable (Figs. 7.2, 7.3).

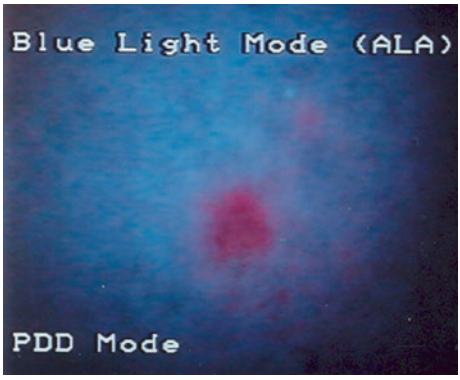

Fig. 7.2 PPIX-fluorescence in sBCC (D-light). Image of a typical PpIX-fluorescence in a superficial BCC, as the lesion is clearly demarcated the fluorescence is sharp

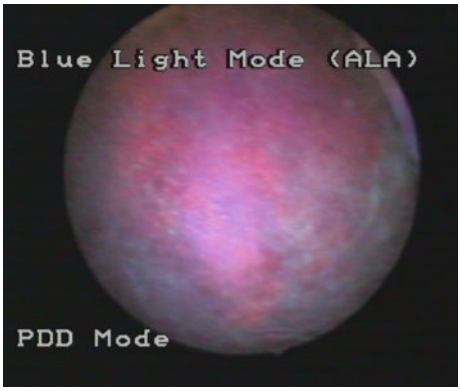

Fig. 7.3 PPIX-fluorescence in AK (D-light). Image of a typical PpIX-fluorescence in actinic keratosis, as often the AK is situated in a region of more or less solar damaged skin, the whole area displays a strong signal

7.4.1.1 In motley pictures little clarity, much error and a grain of truth… (Goethe, Faust I)

The problem with image reception is their powerful reflection in our brains. As clinicians we believe what we see, and very often we do not think about the real significance of those impressive images.

To interpret those images of fluorescence properly, we have to recognize three basic truths:

1. Excitation with blue light always affects only the very superficial layers in depths that range rather in micrometers than in millimeters.
2. Our eyes are not made for an objective assessment as they enhance low intensities in recognition and have only weak discrimination ability for high intensities above a certain level in order to maximize the information.
3. Our eyes are usually not able to discriminate a red of 636 nm from 670 nm and visual recognition underlies numerous inter individual differences.

Therefore, it is nearly impossible to judge if fluorescence is weak or strong by the visual aspect. Neither it is possible to decide if the particular fluorescence we see is of PpIX or another substance. Camera systems, e.g., of specially designed fluorescence cameras make things usually even worse, as they are constructed (built) to enhance weak signals and the colors of a display usually cannot be trusted.

Finally, there is only one message left that could be stated if we see the "red": There is any red fluorescence at the surface.

One possible option to increase the contrast is to expose the sensitized region to a small amount of light (even white light). Photobleaching of PpIX will lead to a decay of the signal and superficially fluorescence will be wiped out, while higher concentrations of PpIX remain to discriminate more severe lesions with higher grades of dysplasia. But care has to be taken, that photobleaching does not wipe out all the fluorescence. Overall, it is not a significant and reproducible option.

Another way is to use a calibrated fiber spectroscopic system with integrated excitation and detection fibers and map the region of interest. If application of

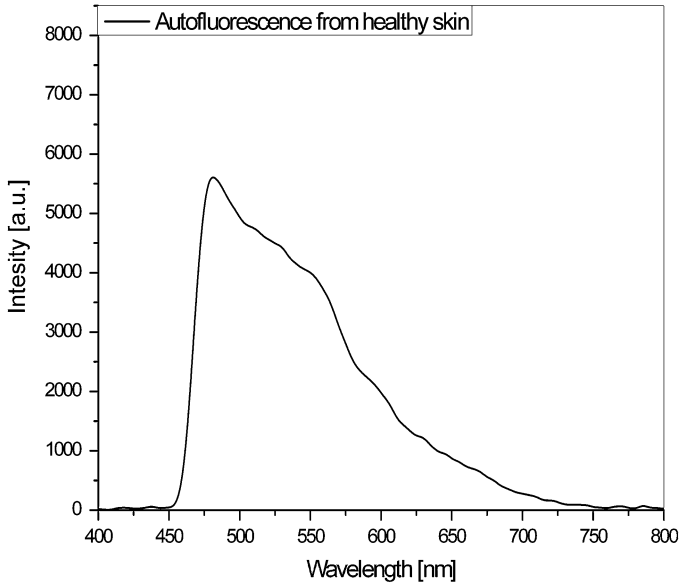

Fig. 7.4 Fluorescence from native healthy skin (autofluorescence). The curve resembles different parts of fluorescence, in the blue to yellow range usually some autofluorescence (flavins, NaDH) is detected, while in the red region fluorescence is weak. If there would be any significant fluorescence in the red, it could be due to a hidden porphyria of the patient

ALA is standardized with regard to cleaning of the region, removal of hyperkeratosis, amount of substance per area, time of incubation, and parasitic light protection, the intensity of the resulting peak correlates with the content of PpIX and therefore allows relative measurements of PpIX amount in tissues. It also allows discrimination between red fluorescence from PpIX and other fluorophores, which might occur after ALA application (Figs. 7.4, 7.5, 7.6).

The typical curve changes during the irradiation, the typical peaks decreases in correlation with the delivered amount of photons/energy due to the photobleaching effect and a new peak occurring at 670 nm which indicates the production of photoproducts of PpIX, e.g., photoprotoporphyrin (PPP) (Fig. 7.7).

7.4.2 Recovery Fluorescence

In some cases (usually deeper lesion, e.g. BCC) a secondary increase of the PpIX-signal at 636 nm is detected after 24 h when the lesion was covered with light protection shields in the meantime but without further application of ALA (Fig. 7.8) and corresponding fluorescence images after photosensitization, after irradiation and after 24 h (Fig. 7.9a–c).

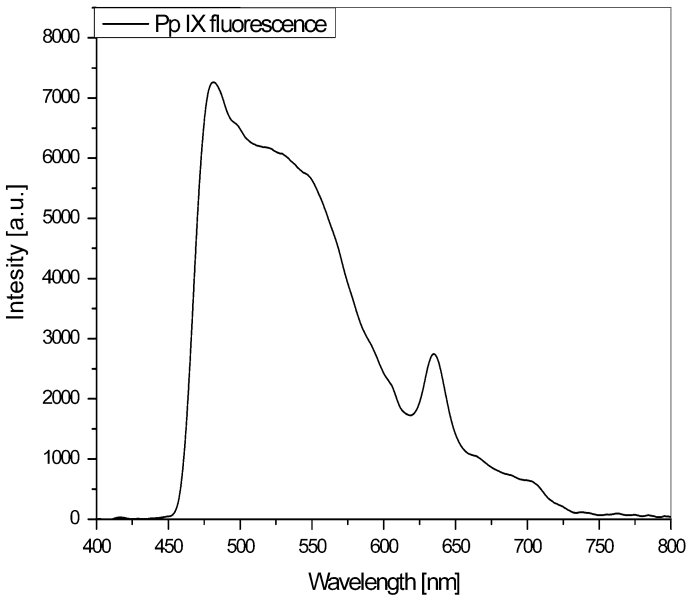

Fig. 7.5 Fluorescence from ALA incubated healthy skin after 6 h application time. The curve resembles different parts of fluorescence, in the blue to yellow range usually some autofluorescence (flavins, NaDH) is detected, while in the red region fluorescence is weak. Usually, the curve is comparable with the curve of native skin, some small peak at 636 nm may be visible, e.g., shortly after ALA removal and prolonged application time (as here)

The generation of photoproducts in ALA-PDT is well-known [31–34]. Usually, the major components are photoprotoporphyrin (PPP) and other chlorins, which are responsible for the shifts of the typical fluorescence peaks from 636 and 700–710 to 670 nm (Fig. 7.7). Thus, the finding of a recovery fluorescence at 636 nm after 24 h may suggest: (a) an excess amount of ALA in the NMSC lesions and surrounding tissues, (b) a deeper penetration of ALA with extended incubation times, (c) a local persistence of viable cells, able to continue the production of PpIX after first irradiation.

Excess amount of the precursor drug aminolevulinic acid is an intended safety measure. It is common to apply much higher amounts of the prodrug as possibly needed, to ensure a sufficient supply and therefore a sufficient generation of the active photosensitizer PpIX. The formulation we have used contained 20 % 5-ALA in Tylose® gel, 10 % 5-ALA in the ALA-Thermogel and the ready to use formulation Metvix® contains 16 % methylated ALA on a cream base.

A well-known microscopic technique (fluorescence recovery after photobleaching, FRAP) uses the fluorescence recovery to measure the lateral diffusion properties of various membrane or cytoplasmic constituents [35]. The kinetic of fluorescence re-appearance was experimentally used to study the diffusion of methylated ALA and PpIX [36]. Usually, penetration of a drug into skin follows gradient concentrations and time is an important factor for deeper penetration.

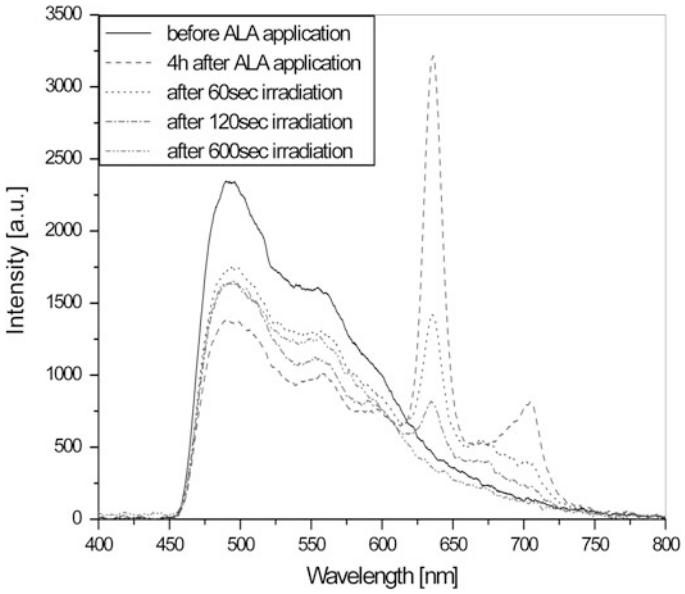

Fig. 7.6 Fluorescence from ALA incubated AK with typical pronounced PpIX-fluorescence peaks, the curves resembles different parts of fluorescence, in the blue to yellow range usually some autofluorescence (flavins, NaDH) is detected, while in the red region the signal of PpIX is depicted after sensitization with a dominant peak at 636 nm and a smaller peak at 700 nm. After irradiation of 60, 120, and 600 s, respectively, the peaks decrease, PpIX is bleached

Excess presence of 5-ALA in the region, in and around the lesion to be treated, may allow a transport (active or passive) toward the diseased cells after primary consumption by the production of PpIX during the incubation time and consecutive photobleaching during the first irradiation. During photobleaching, the gradient of concentrations of 5-ALA between the surrounding tissue, acting as reservoirs, and the lesion increases and another transport of 5-ALA is started. Else it may be discussed, if PpIX produced in the surrounding tissues may be transported by diffusion to the lesions. But usually, we found a sharp demarcation with blue-red contrast between lesions and surroundings in the 2D-fluorescence control by means of D-Light system, indicating low PpIX-levels in the surroundings 24 h after the first irradiation.

If some cells, e.g., in deeper layers of the lesion [37] may not have received lethal doses of drug or light at time of the first PDT, these cells bear the risk of a recurrence of the lesion. This requires high attention as it is clinically not acceptable. Remnant cells may continue further PpIX generation or accumulation if ALA or PpIX is or become available. Hence, repeated light exposures should increase the efficacy of ALA-PDT [38].

Bacteria are always present in human skin. They may offer different pathways for the generation of fluorescent derivatives of ALA. Their short cell cycle and migration capabilities allow rapid (re)invasion of necrotic tissues at the lesions

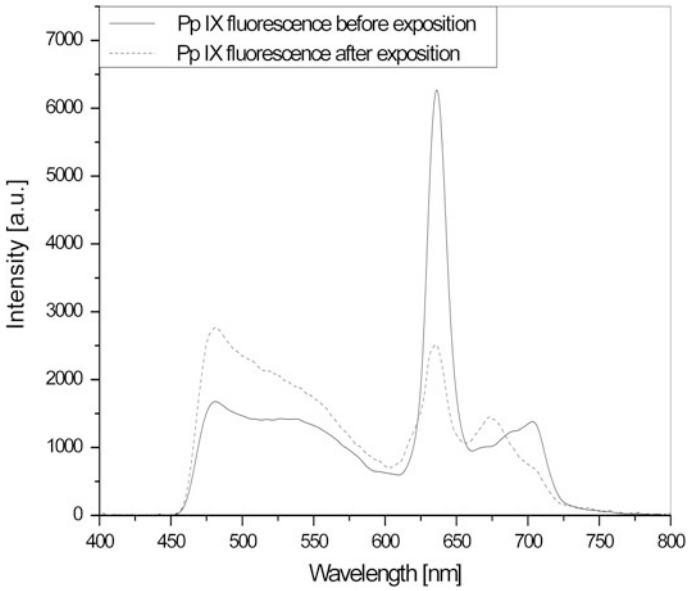

Fig. 7.7 Fluorescence from ALA incubated AK after irradiation with decreased PpIX-fluorescence peak and increase of fluorescence at 670 nm indicating the production of photoproducts of PpIX, e.g., photoprotoporphyrin (PPP)

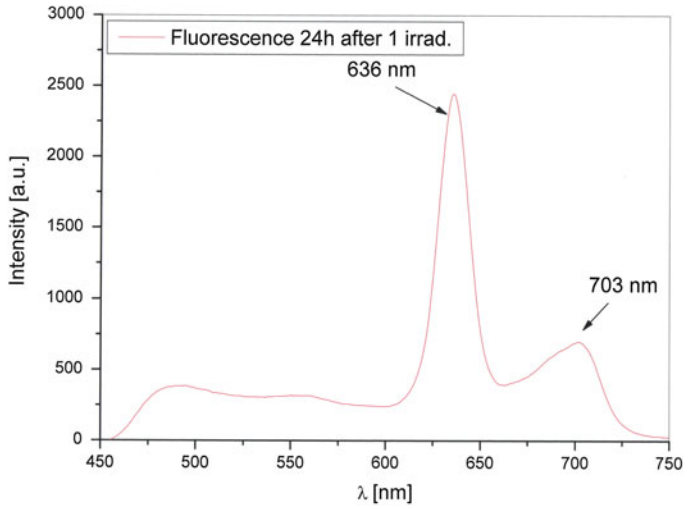

Fig. 7.8 Fluorescence from ALA incubated AK after irradiation and after a time interval (24 h) while covered with light shielding dressing and "recovery" fluorescence in the red region

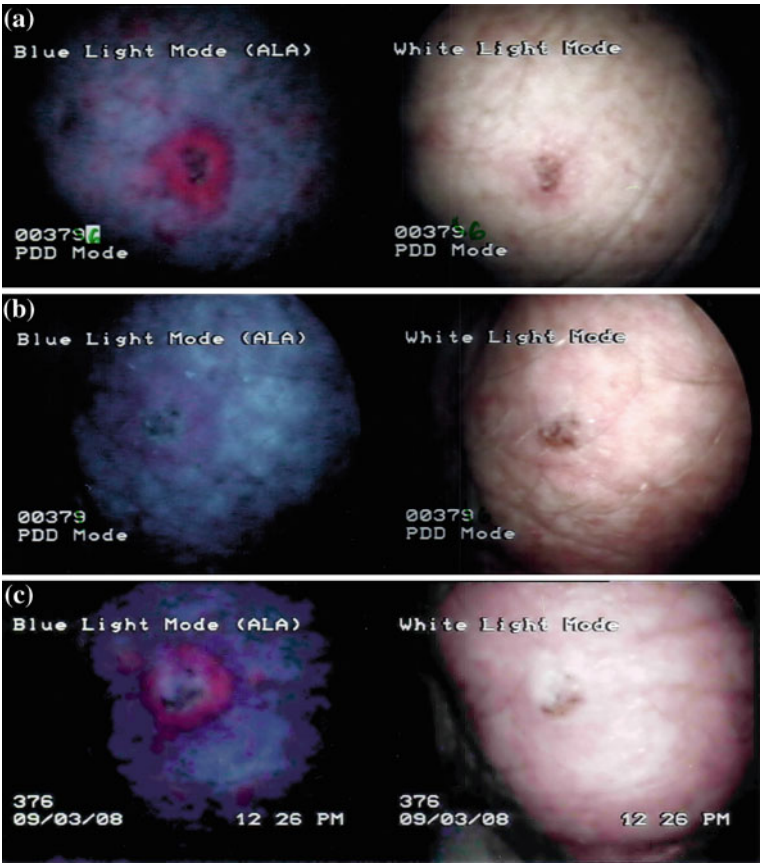

Fig. 7.9 **a–c** (*please mount the three images together)* Fluorescent images (D-light) of a BCC-lesion, **a** after photosensitization, **b** after primary irradiation, **c** after 24 h with light shielding dressing. Figure 7.9a,b correspond with Fig. 7.6 (loss of fluorescence during irradiation) and Fig. 7.9c corresponds with Fig. 7.8 (recovery fluorescence after 24 h)

site, even after local eradication by PDT. Water soluble porphyrins were found after irradiation of bacterial cultures incubated with ALA with a fluorescence peak of 618–620 nm [39]. As this wavelength hardly can be discriminated from 636 nm by 2D fluorescence imaging, it could be falsely interpreted as recovery fluorescence of PpIX if no spectral analysis is done.

7.4.3 Endpoint of Irradiation

The lack of fluorescence is often used as endpoint of irradiation. After all, this is not an ideal guide as the excitation with blue light does not affect the deeper layers

of the dysplastic tissues or tumors, and remaining PpIX would not be detected. Shallow bleaching could lead to an early interruption of treatment and persistence of deeper portions of the diseased tissues, which still could be sensitized. Insertion of spectroscopic fibers and interstitial mapping of the PS-concentration would be an alternative but is not practicable. We use a precomputed light overdose in PpIX-PDT instead. Neither the photosensitizer (which in case of PpIX is consumed during the procedure) nor the light itself is harmful. Exposure of not sensitized volumes does not lead to additional damage and already lethally irradiated cells have to be regarded as dead. Therefore, an overdose above the decay of superficial fluorescence is advocated. On the other hand, if there is still fluorescence detectable after the calculated and delivered dose of light, the irradiation should be continued.

7.5 Light Sources for PDT, Dosimetry

There is a long discussion about the proper light sources for PDT. It is relatively easy to acknowledge that endoscopic guided and interstitial PDT requires lasers, as the transport of the light into the body is the bottleneck and this can easily be handled only with lasers. To irradiate the surface of a body one could also use tungsten filament, xenon arc, metal halide, and fluorescent lamps or LED, probably OLED in the near future (Ambulight®), and of course lasers. Even daylight has been successfully used in the treatment of low grade AK [40–43].

What would be the best choice then? As always, this cannot be answered finally at present and prospective and for all indications in the same way. For topical PDT in dermatology, it seems to be rather not very important which light source is used as penetration of ALA into the tissues and subsequent PpIX generation is the limiting factor. Always the total light dose should be administered in a homogenous fashion over the area. This is usually realized by LED-arrays (and OLED's, organic LED) and lasers with flat top profile fiber applicator. The calculation of dose and power density is easy, as all light emitted is light of the proper wavelength (usually 635 +−5 nm for porphyrins including PpIX) and the area is described by a circle. In LED the emission range is wider but still covers the typical red absorption peak of PpIX, the irradiated area usually is larger and square. Lamps emit a rather inhomogenous spectrum of different wavelengths and only a portion is effective in PDT, consequently the total irradiation dose has to be much higher and the duration of irradiation is usually of longer duration and side effects may increase. During the lifetime of a lamp, the emission spectrum may change and repeated calibration is necessary. Additionally used filters add further problems as cooling and wear. As LEDs have become widely available, the use of lamps is decreasing. A typical LED array is Aktilite® which was designed by Photocure® for the use with Metvix® with a recommended energy density of 37 J/cm^2. Next step in clinical applications is an battery powered OLED, mounted to a plaster that is applied directly on the diseased and sensitized tissues, allowing an low-power density and long exposure

times to achieve a total energy density of about 50 J/cm^2 (Ambulight®) for self-administered light for PDT by the patient. The current state (year 2013) of development is reflected in a report of the National Institute for Health and Clinical Excellence [44].

During the development of modern PDT, dye lasers have played a dominant role as light sources. Only with lasers it was possible to calculate and deliver the required energy at certain wavelengths for the numerous often preclinical photosensitizers, each with a specific absorption peak. Those dye lasers usually were tunable, a single laser could be tuned to a requested wavelength within a certain range. Today, diode lasers with fixed wavelength have totally replaced those bulky, expensive, and hard to handle devices in the clinical work. Usually, 635 nm is used with PpIX and HPD, 652 or 665 nm are used with different chlorins. As fiber applicators used to apply lasers may be chosen from a wide variety of emission profiles (flat top profile, cylindrical, ball shaped, interstitial, …) they can be adopted to all clinical needs of the different clinical fields of PDT. Active calculation of the irradiation parameters is necessary with lasers. Power density (PD, W/cm^2) should be kept below 200 mW/cm^2 as a higher PD leads to unwanted thermal effects. There is a theoretical advantage of higher power densities in deeper lesions, especially if systemic photosensitizers are used. In case of higher PD, an efficient cooling of the tissues is mandatory. The dose for PpIX-PDT depends on the indication and the photosensitizer and ranges between 37 and 200 J/cm^2.

7.6 Treatment Protocols

7.6.1 Topical PDT with ALA Induced PpIX

In our clinic, the indication for topical PDT in AK and BCC is based on routinely performed OCT investigations of the tumors. If a tumor exceeds one millimeter in thickness, we usually do not settle the indication for topical PDT, only tumors that can be imaged in full are regarded as suitable, other may be treated surgically or with systemic PDT. After careful cleaning and disinfection and removal of hyperkeratotic epithelium the baseline autofluorescence of the tumor is measured using a fibre spectrometer followed by the application of the prodrug. For topical PDT, we use either Metvix® or ALA-Thermogel in our clinic. A single layer of cotton compress acting as grid is used in larger areas to ensure homogenous distribution of the substance, e.g., in larger areas. The area is covered with adhesive plastic foil (Tegaderm™) and a second light shielding plaster made of aluminum foil and Mepore®. After usually 3 h of application time, the prodrug is removed and the light shielding dressing is replaced again for at least 1 h. During this “incubation time” more PpIX is produced in the tumor while surrounding skin clears from surplus PpIX; hence increasing the contrast between dysplasia or tumor and surrounding skin. Directly prior to exposure with light of 635 nm the

light shielding dressing is removed and PpIX-fluorescence is measured, again with a fiber spectrometer and optionally fluorescent images are taken for documentation purposes. In patients with multiple lesions, the light shielding dressing is kept in later to treat sites and only removed prior to irradiation, in order to avoid photobleaching with sub-therapeutic light doses.

One of the major disadvantages of PpIX-PDT is the pain that is developing shortly after the start of irradiation. Pain reception differs inter-individually within a wide range; nevertheless, most of the patients require an analgetic treatment at least with a mild stream of cooled air. Local anesthesia without suprarenin may be used but usually regional anesthesia is more effective and is preferred also because of less local interaction with blood supply and the avoidance of increased interstitial pressure in the treatment region. In case the irradiation site is localized at the head, sufficient eye protection with metal shields is applied; else a laser safety goggle offers safe eye protection for the patient.

The required light dose is applied either with a laser (Biolitec®) equipped with a flat top profile applicator (microlens®) or the Aktilite® LED with a dosimetry according to the type of disease. After the calculated energy is delivered, PpIX-fluorescence is measured again and in case of lack of fluorescence the treatment is completed with a petrolatum ointment and wound dressing. In case of residual fluorescence at 636 nm the irradiation is continued. Usually, we then add another 50 % of the intended light dose and measure fluorescence again, and so on. Benign lesions are usually irradiated with a lower light dose, which usually is fixed and remaining fluorescence requires no higher doses.

In critically thick lesions, e.g., in some of basal cell carcinoma and Bowens disease, we use a light shielding wound dressing after the irradiation to avoid bleaching of possible newly produced PpIX. In such lesions, we measure fluorescence with the fibre spectrometer on the next day, usually about 16–18 h after the first exposure. In case of presence of "recovery" fluorescence, the irradiation is repeated with the same irradiation parameters as on day one. Four to six weeks after PDT patients are called in and carefully examined clinically and by means of OCT and punch biopsy if necessary. In case of persistence of lesions a second treatment is performed.

7.6.2 PDT with Systemic Photosensitizers

In some situations a systemic PDT is required. Some of the patients are referred from the tumor board after other therapeutic options (e.g., radiotherapy, surgery) have been excluded due to individual circumstances or in case of recurrences after primary first-line treatment. Usually in such cases the intention to treat is palliative, but in dermatologic indications the results may be curative. With growing experience, we have started to offer systemic PDT for dermatologic tumors with deeper portions in elective indications and if topical PDT is not suitable.

The patients are lab checked for porphyria and renal and liver function. At day one of the systemic photosensitization, the patients are hospitalized and receive the photosensitizer intravenously after taking spectroscopic baseline measurements from the tumor site and surrounding tissues. The choice of the photosensitizer is influenced mainly by tumor type and volume. Patient and treatment rooms are equipped with a yellow ambient light of low intensity which does not lead to skin irritation but provides enough light for orientation and even reading of books or newspapers. During the accumulation time of the photosensitizer in the tumor repeated spectroscopic measurements are performed. Typically, the peaks in the curves are less pronounced and the contrast between tumor and surrounding tissues is less compared to PpIX-sensitization. This measurements help to detect the time of maximum photosensitization of the tumor. Usually, this will be 4 h after Fotolon® or 48 h after Photofrin® administration.

At appropriate time the patient is transported to the treatment room, where the irradiation site is prepared by using light shielding dressings for the surrounding tissues and a mask that leaves the irradiation site free for exposure with the laser of the specific wavelength for the photosensitizer, usually 635 nm for Photofrin® and the deeper penetrating 665 nm for Fotolon®. Other irradiation wavelengths as 532 nm are possible in case a more shallow reaction is required. Further detailed information about possible wavelengths and wavelength combinations, as well as differentiated irradiation protocols may be found in the chapter: "Implementation of Laser Technologies in Clinical PDT". In treatment with Fotolon® the total dose is delivered in one treatment session; Photofrin® allows a second irradiation after 24 h if necessary or planned, as the clearance from tumor and patient is much slower compared to Fotolon®. In general, the light dosimetry in systemic PDT is more important for the result/side effect ratio as compared with topical PDT where an overexposure is nearly not possible, whereas a light overdose in systemic PDT may lead to increased side effects on surrounding tissues.

The required type of anesthesia is more depending on the tumor and tumor site as on the photosensitizer, ranging from none to general anesthesia. After the calculated light dose is delivered the patient is brought to his room at the ward and stays there for the time necessary to diminish the photosensitization of the skin. During this time (usually two days in Fotolon® and three to four days in Photofrin®), spectroscopic readings are performed at usually light exposed sites (forehead) and sites usually shielded from light (inside upper arm) to detect the appropriate time for discharge from the hospital. Careful instruction of the patient regarding light protection is mandatory. The time and extend of post-PDT light protection may vary with regard to the photosensitizer applied.

7.7 Indications/Limitations

7.7.1 Premalignant and Malignant Lesions

7.7.1.1 Actinic Keratosis

The majority of topical PDT is applied in actinic keratosis. Another treatment option is cryotherapy. In a number of studies, the results of both treatment options are compared with the result of comparable clearing rates at a high level (80–90 %) but a better esthetic result in PDT [45–49]. Compared to Imiquimod a higher cure rate in grade II lesions was found [50], and Topical PDT has been reported to be equally effective in transplant recipients [51]. The most frequent side effect except burning pain sensation was temporary hyper-pigmentation. Erythema, skin edema, crusting, and exfoliation should not be regarded as side effects they rather have to be seen as intended effects of the treatment. The pain related to irradiation is reported to be stronger with higher power density.

7.7.2 Bowens Disease (Morbus Bowen, Intraepithelial Squamous Cell Carcinoma)

In Bowen's disease, the SCC is present within the epidermis and has not breached the basement membrane. If left untreated, the disease can invade the dermis (invasive SCC) and there is then the potential of metastases. Approximately 3 % of cases will develop into invasive disease [52]. Treatment options include surgery, cryotherapy, curettage, radiotherapy, and topical therapies using 5-FU or imiquimod. In a long-term follow-up comparison of topical PDT with cryotherapy and 5-FU treatment a significant better result was found in the PDT-group with 68 % complete response rate after 2 years and 82 % after 1 year [53]. Less favorable results with a higher relapse rate over the time were reported in 2012 for the treatment of high grade anal intraepithelial neoplasia (AIN) with systemic PDT [54]. This is in concordance with own observations, but must be seen with regard to the background of the usually HPV-related development of AIN and of a high co-infection rate of these patients with HIV.

7.7.3 Basal Cell Carcinoma (BCC)

Basal cell carcinoma is the most common form of skin cancer, predominantly located in the head and neck areas indicating a strong correlation with excessive UV exposure. BCC is generally slow growing and locally invasive and may take a variety of clinical appearances such as nodular, cystic, superficial, morpheic, ulcerated,

or pigmented. Treatment options for BCC include surgical excision, curettage, cryosurgery, surgical laser, radiotherapy, imiquimod, topical 5-FU, and PDT.

In superficial BCC, an almost complete response to PDT is reported by nearly all authors. A better esthetic outcome is uniformly observed in PDT, when compared with surgery or cryotherapy [55]. In nodular BCC, the data for primary complete response are in favor for surgery. Also the long-term recurrence rate seems to be higher (14 %) in topical PDT, even if primary curettage is employed [56]. Some authors found comparable results between PDT with fractionated irradiation and surgery [57]. Effects and side effects are comparable to treatment of AK, nevertheless the BCC lesions are usually smaller and show a sharper demarcation as AK which is often composed by different grade lesions with generalized actinic changes of the surrounding skin.

A sustained cure rate between 87 and 94 % depending on photosensitizer dose and irradiation protocol was reported by Betz et al. after PDT with low to regular drug dose PDT with systemic Foscan®-PDT and a mean follow-up of 42 months in 117 patients with 460 lesions. Besides the variations in the study on drug dose, total fluence of light delivered, drug-light interval the higher recurrence rates were seen in recurrent BCCs [58].

7.7.4 Cutaneous T Cell Lymphoma (CTLC, Mucoisis Funguides)

Several investigations have appraised PpIX-PDT as a prospective modality for CTCL. Its benefit for CTCL is considerably modest, and it is generally reserved as forth-line therapy. While PDT is efficient for patch/plaque stage of MF, PpIX-PDT is not useful for the tumor stage of CTCL, due to insufficient penetration of photosensitizer and light [59]. It may be useful for resistant cases of localized plaques, particularly in the head and neck region [60].

7.7.5 Benign Lesions

7.7.5.1 Warts

Attempts to treat warts with PDT date back to the first topical application of ALA by Kennedy, which was not effective [61]. In a more recent study, ALA-PDT was applied for a maximum of four times versus placebo resulting in 87 % clearance versus 17 % in the placebo group [62]. These results show that ALA-PDT in combination with a sufficient keratolysis is an alternative in the treatment of recalcitrant warts. Pain is also reported during the treatment; therefore, the benefit is questionable as flashlamp pumped pulsed dye laser treatment is at least equally effective after keratolysis and less time consuming.

7.7.6 Genital Warts

HPV-induced genital warts show an increasing incidence and present considerable problems both for the individual and the health care system. Recurrence rates between 20 and 50 % are reported after surgical CO2-laser therapy, other therapies are even less effective. With a high rate of intra-vaginal and intra-anal involvement other therapies (imiquimod, podophyllin-toxin) are usually limited. There are a larger number of single institution reports on smaller numbers of patients with genital warts with variable response rates [63], but due to the at least partially strong hyperkeratosis a complete topical photosensitization is rather questionable. We have found a weak and not reproducible accumulation of PpIX in genital warts in patients with both AIN and genital warts, who where sensitized for AIN treatment in "sandwich-PDT".

7.7.7 Acne

After first emphatic reports on the treatment of acne with PpIX-PDT more recent studies revealed equally good results after repeated treatments but also disclosed the high rate of severe side effects as pain, erythema, skin edema, transient hyperpigmentation, sometimes even blistering or an acute exacerbation [64]. However, as the basic therapeutic concept seems to be effective other modified treatment protocols may reduce the rate and severity in the future.

7.7.8 Skin Rejuvenation

The efficacy of topical PDT for rejuvenation of photoaged skin has been demonstrated in several studies. Photosensitizer concentration, application and incubation times, light sources (often IPL), light dose, and number of treatments vary between the studies and differ significantly from those in topical PDT for premalignant and malignant diseases. An excellent overview has been published recently by Kohl and Karrer [65].

7.7.9 Cutaneous Leishmaniasis

Cutaneous leishmaniasis is a parasitical disease which appears after single or multiple skin lesions after infection with some of the subspecies of the intracellular parasite Leishmania. It presents a common health problem and standard treatments are often ineffective. The systemic variant is called Kala-Azar. Clinical reports have shown promising results from PpIX-PDT as a treatment for cutaneous leishmaniasis. But more recent basic studies revealed an unspecific action by destruction of host cells and lack of antiparasitical effect [66, 67].

7.7.10 Others

Topical PpIX-PDT is also mentioned in the literature as treatment option for granuloma anulare, sebaceous gland hyperplasia, hidradenitis suppurativa, and lichen sclerosus. The number of patients treated in each group is relatively small and final assessment of the efficacy not possible today.

7.8 Control of Indications and Results with Optical Coherence Tomography

Topical PDT is limited to superficial diseases. To settle the diagnosis of an actinic keratosis usually clinical criteria are efficient but with higher grade of dysplasia the risk of development of Bowens disease increases. If the photosensitization would not reach the deeply located portions the therapy would miss the most important part of the disease. Usually biopsies are required to proof the diagnosis, but there remains some uncertainty with regard to right site for the biopsy. A comparable situation exists in the treatment of BCC, e.g., in nodular BCC.

Optical coherence tomography (OCT), established in ophthalmology, has more recently become an option for imaging of the dermal structures with faster and deeper reaching systems. OCT allows the reconstruction of images from the upper skin layers, much the same as ultrasound does, but with a much higher spatial resolution. It can be used to illustrate single layers and their vertical and horizontal expansion. Imaging depth is usually about 1 mm but is dependent on the specific properties of the tissues [68–72]. It is neither able to image single cells, nor a grade of dysplasia at the present state of development.

The SR-OCT system (Thorlabs) we have used includes a broadband superluminescent diode (SLD). The particular SLD radiates at 930 nm and has a 95 nm spectral bandwidth, which yields a maximum imaging depth of approximately 1.6 mm and an axial resolution of 10 μm in skin. The lateral resolution varies with the tissues between 10 to 15 μm. In all displayed pictures the OCT image grasps 2 mm horizontally and 1 mm vertically. The SLD is fiber-coupled to a Michelson interferometer. The interference signal, from the sample and reference arm reflections, is coupled back into the same fiber and is redirected by the fiber optic coupler to a high-speed spectrometer. The spectrum exhibits peaks and troughs, and the period of such a modulation is proportional to the optical path difference (OPD) in the interferometer [73]. If multilayered objects such as tissue are imaged, each layer imprints its own modulation periodicity depending on its depth (OPD), with the amplitude of the spectrum modulation proportional to the square root of the reflectivity of that layer. A CCD camera can be used to transform the optical spectrum into an electrical signal which exhibits ripples of different frequencies. A fast Fourier transform (FFT) of the spectrum of the CCD signal translates the periodicity of the channeled spectrum into peaks of different frequency, related to

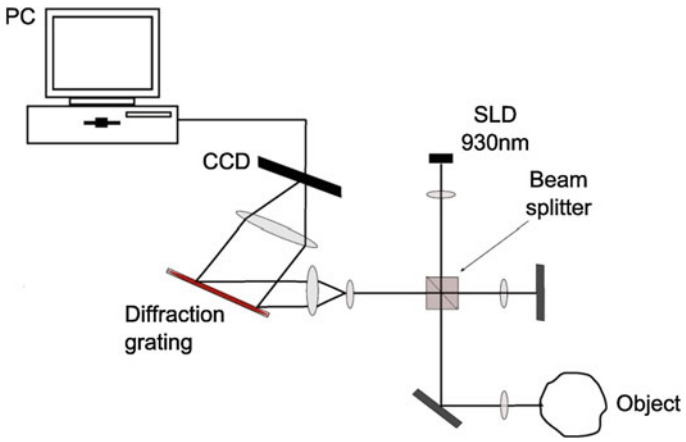

Fig. 7.10 OCT, schematic

the path imbalance (Fig. 7.10). Immersion with Instillagel® was used to reduce surface reflection for optimized images by index matching.

In terms of optical properties the upper layer of the epidermis, the stratum corneum, is a smooth reflecting surface and some of the incident light will be scattered by its multiple layers of keratin. The lower layer of the epidermis is built up of proliferating cells and is usually more transparent. The dermis consists mainly of cells, collagen, and elastic fibers with a hydrocolloid surrounding and blood vessels. It also bears adjacent skin structures such as hair follicles and sebaceous glands. Each of these structures shows typical three dimensional patterns of cellular aggregation and will be displayed in the OCT images with regard to their optical properties, i.e., difference in refractive index compared to adjacent tissues. The base is formed by the subcutis with larger blood vessels, sweat glands, and nerves for the upper skin layers as well as the hypodermic fat and connective tissue, which may be displayed also.

The OCT can produce images of the layers of skin and their changes (AK) as well as dermal tumors (BCC) and display their vertical and horizontal dimensions proportionally. The imaging depth is slightly variable and depends on the optical density, scattering, and absorption parameters of the tissues and may be distorted by hair or dust particles on the surface. However, below 1 mm the imaging quality decreases significantly with currently available systems.

In healthy skin, a good correlation between the images of histological samples and the two-dimensional OCT images was found. In diseased skin equivalents of typical gross histological features of changes in dermal layers, epithelial dysplasia as AK and BCC and could be found in OCT images [74]. Although the spatial resolution in turbid media is less than in air and does not allow the observation of cellular features or thin layers (e.g., the basal membrane) the different skin layers can clearly be distinguished [75] by currently available OCT systems. We therefore use OCT routinely as investigative tool in the clinical evaluation of actinic

Fig. 7.11 Clinical image of AK

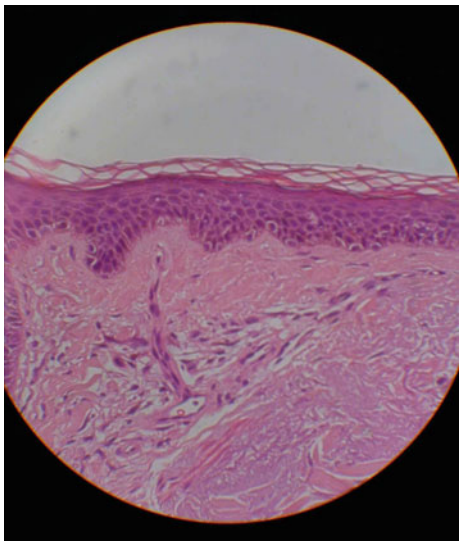

Fig. 7.12 Histopathology of AK

keratosis and NMSC lesions, both for settling the indication for either topical or systemic PDT and for control of the post-PDT outcome.

7.8.1 OCT Imaging of Actinic Keratosis

The actinic keratosis is a potential preliminary stage of Bowen's disease and may develop into a SCC. It usually appears in sun exposed skin areas, e.g., nose, forehead, temples, backs of the hand, ears. AK appears as a well-defined, reddened skin area with epithelial alterations (Fig. 7.11). Histopathology of AK shows an acanthosis and a thickened or watery stratum corneum or ulceration (Fig. 7.12). In this sample of a AK, the thickened stratum corneum is visible as a bright line in OCT (Figs. 7.13, 7.14). The epithelium is broad and with a brighter and more condensed aspect when compared to healthy skin; the dermal layer appears as a

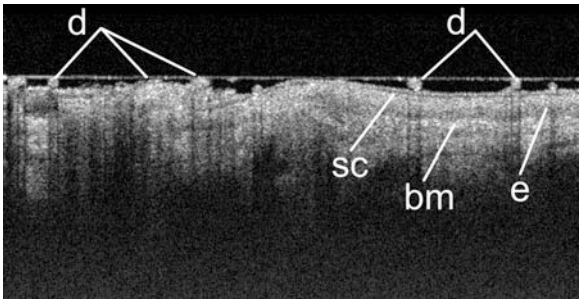

Fig. 7.13 OCT of AK at the hairy head (*d* dandruff, *sc* stratum corneum, *e* epithelium, *bm* level of basal membrane)

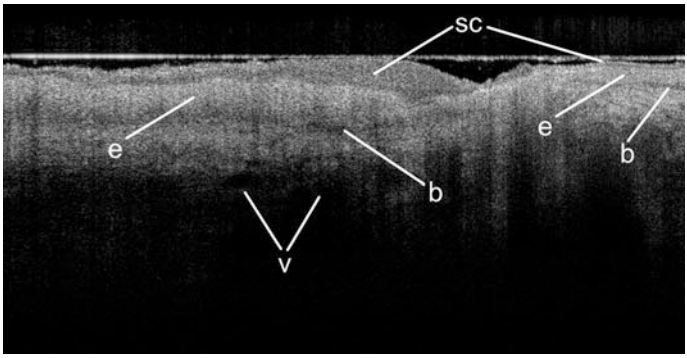

Fig. 7.14 OCT image of AK with hyperkeratosis (*left*) and ulceration (*right*)

relatively thin band with a bright signal (high lucidity). In Fig. 7.13, the image taken from the scalp, dandruff is visible on top of the stratum corneum. Figure 7.14 shows partially on the right side erosive AK (right) and hyperkeratotic rim (left), erosive AK may display different patterns. However, as single cells are not displayed due to the lack of resolution in OCT imaging the grade of dysplasia can only be assessed by secondary pattern changes.

7.8.2 OCT Imaging of Bowen's Disease

Bowen's disease is an intraepithelial SCC (carcinoma in situ). Invasion into deeper skin layers is possible and has to be excluded before local treatment as metastases are possible in the invasive disease. This skin tumor is also promoted by UV-light, chemical materials (e.g., arsenic) or certain viruses (HPV). BD appears as a red or white demarcated skin area (Fig. 7.15) with hyperkeratosis and may ulcerate in later phases of the disease. In histopathology an irregular epidermal layer is found with hyperkeratosis and acanthosis and an irregular thickness with portions reaching deep into the dermis (Fig. 7.16).

Fig. 7.15 Clinical image of Bowens disease

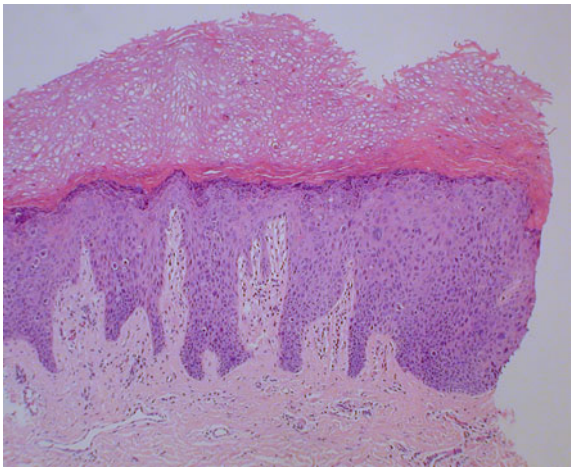

Fig. 7.16 Histopathologic image of Bowens disease

Comparison of the histopathological image with the OCT image (Fig. 7.17) shows a good correlation for the appearance of the thickened stratum corneum and the upper layers of the epidermis. The loss of visualization of the dermal epidermal junction due to the thickness of the upper layers is a significant sign. The plane of the basal membrane is not depicted in the obtained OCT image as it fades into black for deeper layers.

In non-hyperkeratotic lesions or after removal of the hyperkeratosis the transformation into Bowens disease is depicted by irregular portions of the epithelial layer that penetrate through the region of the basal membrane into the corium. These regions, once depicted by OCT, may be evaluated in the near future by 2-photon-microscopy (2PM, TPM), another optical method that provides 3D insight views of cells and at the same time allows spectroscopic, time resolved fluorescence or Raman spectroscopy measurements with a single instrument. A new device that could obtain images comparable to sectional histology combined with the mentioned properties was described by Göppner et al. recently [76].

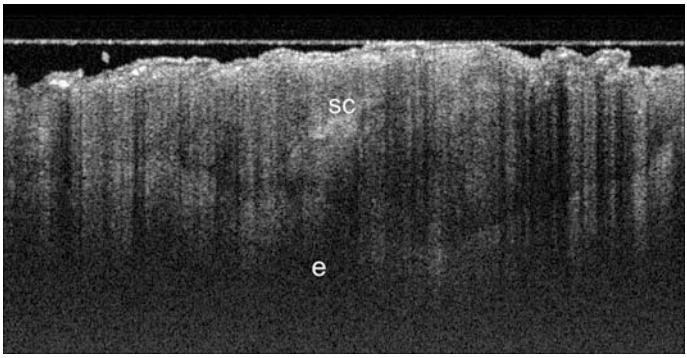

Fig. 7.17 OCT image of hyperkeratotic Bowens disease

Fig. 7.18 Clinical image of a solid BCC at the nose

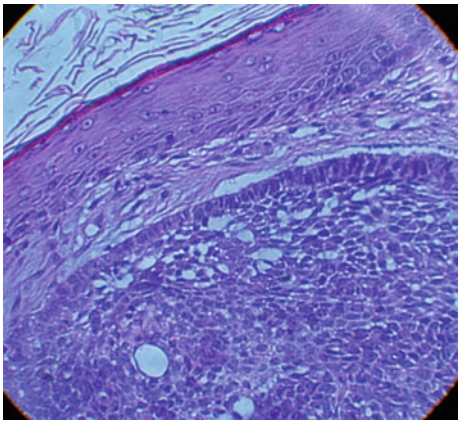

Fig. 7.19 Histopathological image of the sam tumor as in Fig. 7.18

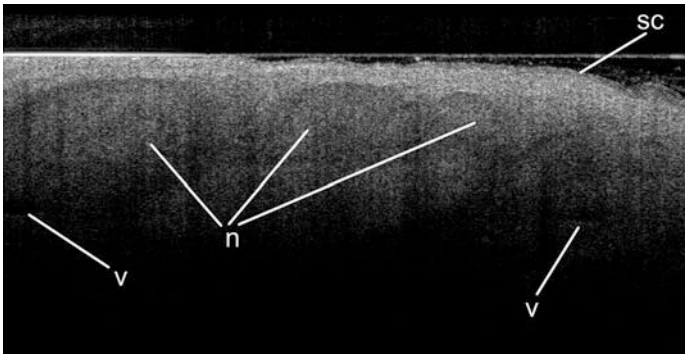

Fig. 7.20 OCT image of solid BCC displaying the typical nodules (n) located below the epidermis with the stratum corneum (sc) and small vessels (v)

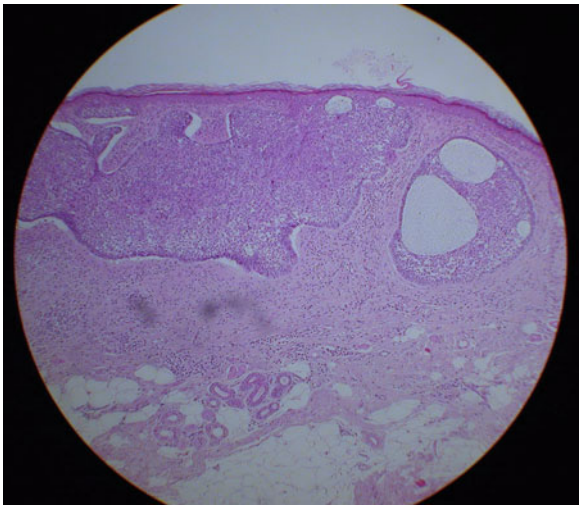

Fig. 7.21 Histopathological image of a cystic BCC

7.8.3 OCT Imaging of Basal Cell Carcinoma

Basal cell carcinoma is an infiltrative and destructive growing tumor, usually without metastasis. The most frequent cause for the development of the BCC is UV-light damage, in particular with light skin types. Basically, three types of BCC can be distinguished: the superficial, nodular, and morpheic form, although the German guidelines discriminate between 10 types. Figure 7.18 shows the clinical appearance of a solid BCC, Fig. 7.19 the histological preparation of a sample from the same tumor. The OCT image (Fig. 7.20) is characterized by nodular structures in the dermis.

Even cystic formations in cystic BCC can be found in the corresponding OCT image (Figs. 7.21, 7.22). A clinical image of a morpheic BCC at the thorax is

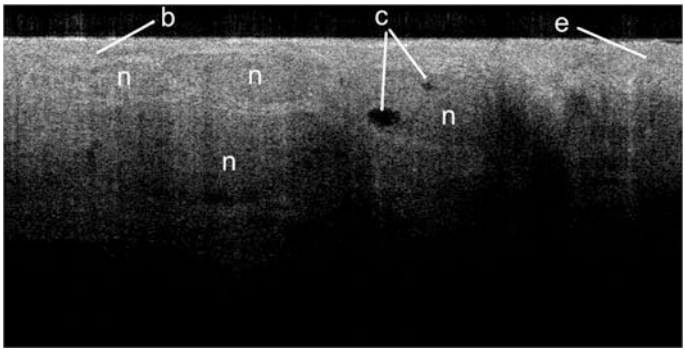

Fig. 7.22 OCT image of cystic BCC, (*n* nodular structures of BCC, *C* cysts, *e* epithelial layer, *B* plane of the basal membrane)

Fig. 7.23 Clinical image of morpheic BCC

Fig. 7.24 Histopathological image of the morpheic BCC in Fig. 7.23

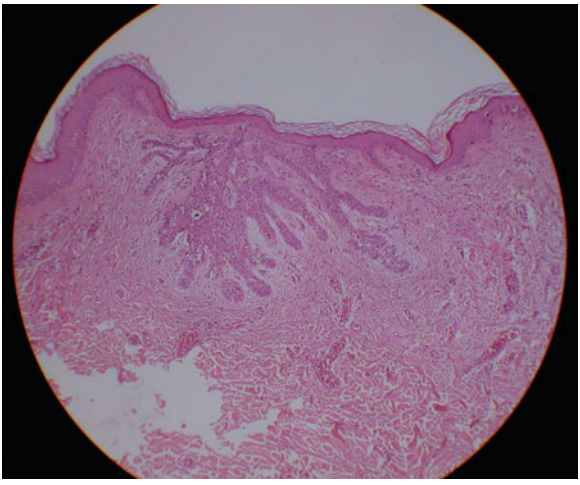

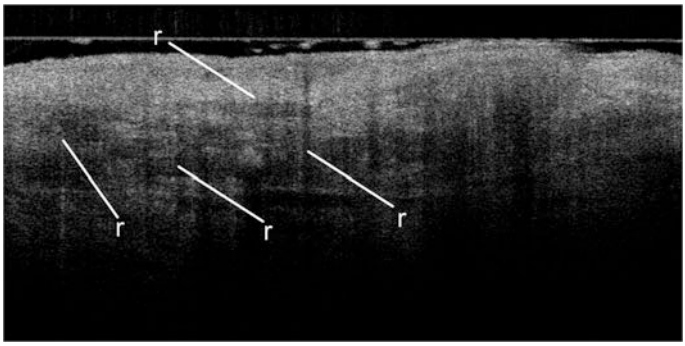

Fig. 7.25 OCT image of the same morpheic BCC as in Figs. 7.23 and 7.24, (*r* BCC structures)

given in Fig. 7.23, the corresponding histopathological image (Fig. 7.24) shows the multiple small extensions of the tumor, which correspond to the dark subepithelial structures in the OCT image (Fig. 7.25).

7.9 Conclusion

In conclusion PDT is not a "promising technique" but a substantial part of dermatologic-oncology practice. The concept of a prodrug that is converted to the active substance preferably by tumors allows a high contrast between diseased and surrounding tissues and makes this therapy easy to handle and safe. Currently, most of the applications are related to low grade superficial lesions, but with potentially upcoming new systemic photosensitizers and improvement of noninvasive imaging of skin tumors larger tumors will come in reach and the success story will continue.

Acknowledgments I would like to thank all my coworkers in clinical and experimental PDT in our clinic and in particular to Maria Ziolkowska, Friederike Hirsch and Max Klomsdorff who prepared the grafics and OCT-images for this article.

References

1. http://www.who.int/uv/health/uv_health2/en/index1.html
2. http://www.krebsgesellschaft.de/pat_ka_hautkrebs_definition,107793.html
3. von Tappeiner H (1900) Ueber die Wirkung fluorescierende Stoffe auf Infusiorien nach Versuchen von O Raab. Munch Med Wochenschr 47:5
4. Raab O (1900) Ueber die Wirkung Fluorescierender Stoffe auf Infusorien. Z Biol 39:524–546

5. Tappeiner H von, Jodlbauer A (1907) Die Sensibilisierende Wirkung Fluorescierender Substanzen. *Untersuchungen über die Photodynamische Erscheinung* FCW, Vogel Leipzig
6. Hausmann W (1911) Die sensibilisierende Wirkung des Hamatoporphyrins. Biochem Z 30:276–316
7. Meyer-Betz F (1913) Untersuchungen über die Biologische (photodynamische) Wirkung des Hamatoporphyrins und anderer Derivative des Blut- und Gallenfarbstoffs. Dtsch Arch Klein Med 112:476–503
8. von Tappeiner H, Jesionek A (1903) Therapeutische Versuche mit fluorescierenden Stoffen. Munch Med Wochenschr 47:2042–2044
9. Jesionek A, von Tappeiner H (1905) Zur Behandlung der Hautcarcinome mit fluorescierenden Stoffen. Arch Klin Med 82:223
10. Divaris DX, Kennedy JC, Pottier RH (1990) Phototoxic damage to sebaceous glands and hair follicles of mice after systemic administration of 4-aminoevulinic acid correlates with localized protoporphyrin IX fluorescence. Am J Pathol 136:891–897
11. Kennedy JC, Pottier RH, Pross DC (1990) Photodynamic therapy with endogenous protoporphyrin IX: basic principles and present clinical experience. J Photochem Photobiol, B 6:143–148
12. Collaud S, Juzeniene A, Lange N (2004) On the selectivity of 5-aminolevulinic acid-induced protoporphyrin IX formation. Curr Med Chem Anticancer Agents 4:301–316
13. Hinnen P, de Rooij FW, van Velthuysen ML, Edixhoven A, van Hillegersberg R, Tilanus HW, Wilson JH, Siersema PD (1998) Biochemical basis of 5-aminolaevulinic acid-induced protoporphyrin IX accumulation: a study in patients with (pre)malignant lesions of the oesophagus. Br J Cancer 78:679–682
14. Krieg RC, Fickweiler S, Wolfbeis OS, Knuechel R (2000) Cell-type specific protoporphyrin IX metabolism in human bladder cancer in vitro. Photochem Photobiol 72:226–233
15. Hefti M, Holenstein F, Albert I, Looser H, Luginbuehl V (2011) Sesceptibility to 5-aminolevulinic acid based photodynamic therapy in WHO I meningioma cells corresponds to ferrochelatase activity. Photochem Photobiol 87:235–241
16. Ohgari Y, Nakayasu Y, Kitajima S, Sawamoto M, Mori H, Shimokawa O, Matsui H, Taketani S (2005) Mechanisms involved in delta-aminolevulinic acid (ALA)-induced photosensitivity of tumor cells: relation of ferrochelatase and uptake of ALA to the accumulation of protoporphyrin. Biochem Pharmacol 71:42–49
17. Stout DL, Becker FF (1990) Heme synthesis in normal mouse liver and mouse liver tumors. Cancer Res 50:2337–2340
18. Navone NM, Polo CF, Frisardi AL, Andrade NE, Battle AM (1990) Heme biosynthesis in human breast cancer-mimetic "in vitro" studies and some heme enzymic activity levels. Int J Biochem 22:1407–1411
19. Wachowska M, Muchowicz A, Firczuk M, Gabrysiak M, Winiarska M, Wańczyk M, Bojarczuk K, Golab J (2011) Aminolevulinic acid (ALA) as a prodrug in photodynamic therapy of cancer. Molecules 16:4140–4164
20. Collaud S, Juzeniene A, Lange N (2004) On the selectivity of 5-aminolevulinic acid-induced protoporphyrin IX formation. Curr Med Chem Anticancer Agents 4:301–316
21. http://www.dermotopics.de/german/ausgabe1_09_d/DIP1_09_d.htm
22. Grüning N, Müller-Goymann CC (2008) Physicochemical characterisation of a novel thermogelling formulation for percutaneous penetration of 5-aminolevulinic acid. J Pharm Sci 97:2311–2323
23. Forster B, Klein A, Szeimies RM, Maisch T (2010) Penetration enhancement of two topical 5-aminolaevulinic acid formulations for photodynamic therapy by erbium: YAG laser ablation of the stratum corneum: continuous versus fractional ablation. Exp Dermatol 19:806–812
24. Mikolajewska P, Donnelly RF, Garland MJ, Morrow DI, Singh TR, Iani V, Moan J, Juzeniene A (2010) Microneedle pre-treatment of human skin improves 5-aminolevulininc acid (ALA)- and 5-aminolevulinic acid methyl ester (MAL)-induced PpIX production for

topical photodynamic therapy without increase in pain or erythema. Pharm Res 27:2213–2220
25. Lopez RF, Bentley MV, Delgado-Charro MB, Salomon D, van den Bergh H, Lange N, Guy RH (2003) Enhanced delivery of 5-aminolevulinic acid esters by iontophoresis in vitro. Photochem Photobiol 77:304–308
26. Johansson A, Svensson J, Bendsoe N, Svanberg K, Alexandratou E, Kyriazi M, Yova D, Gräfe S, Trebst T, Andersson-Engels S (2007) Fluorescence and absorption assessment of a lipid mTHPC formulation following topical application in a non-melanotic skin tumor model. J Biomed Opt 12:034026
27. Alexandratou E., Kyriazi M, Trebst T, Gräfe S, Yova D (2007) Photodynamic therapy of non melanoma skin cancer murine model by topical application of a novel mTHPC liposomal formulation. In: Proceedings SPIE 6632, Therapeutic Laser Applications and Laser-Tissue Interactions III, 66320 V, 03 July 2007
28. Scheglmann D, Fahr A, Gräfe S, Neuberger W, Albrecht V (2011) Temoporfin and its liposomal formulations Foslip and Fospeg—Properties and behavior. Photodiagnosis and Photodynamic Therapy 8(2):195
29. Boehm TK, Ciancio SG (2011) Diode laser activated indocyanine green selectively kills bacteria. J Int Acad Periodontol 3(2):58–63
30. Tuchin VV, Genina EA, Bashkatov AN, Simonenko GV, Odoevskaya OD, Altshuler GB (2003) A pilot study of ICG laser therapy of *acne vulgaris*: photodynamic and photothermolysis treatment. Lasers Surg Med 33(5):296–310
31. König K, Schneckenburger H, Rück A, Steiner R (1993) In vivo photoproduct formation during PDT with ALA-induced endogenous porphyrins. J Photochem Photobiol, B 18(2–3):287–290
32. Dysart JS, Patterson MS (2006) Photobleaching kinetics, photoproduct formation, and dose estimation during ALA induced PpIX PDT of MLL cells under well oxygenated and hypoxic conditions. Photochem Photobiol Sci 5(1):73–81
33. König K, Wyss-Desserich MT, Tadir Y, Haller U, Tromberg B, Berns MW, Wyss P (2006) Modifications of protoporphyrin IX fluorescence during ALA-based photodynamic therapy of endometriosis. Med Laser Appl 21(4):291–297
34. Theodossiou T, MacRobert AJ (2002) Comparison of the photodynamic effect of exogenous photoprotoporphyrin and protoporphyrin IX on PAM 212 murine keratinocytes. Photochem Photobiol 76(5):530–537
35. Department of Biology, Davidson College, Davidson, NC 28035. Fluorescence recovery after photobleaching (FRAP). <http://www.bio.davidson.edu/Courses/Molbio/FRAPx/FRAP.html>
36. Moan J, Ma L, Iani V, Juzeniene A (2005) Influence of light exposure on the kinetics of protoporphyrin IX formation in normal skin of hairless mice after application of 5-aminolevulinic acid methyl ester. J Invest Dermatol 125(5):1039–1044
37. Orenstein A, Kostenich G, Malik Z (1997) The kinetics of protoporphyrin fluorescence during ALA-PDT in human malignant skin tumors. Cancer Lett 120(2):229–234
38. Van der Veen N, De Bruijn HS, Star WM (1997) Photobleaching during and re-appearance after photodynamic therapy of topical ALA-induced fluorescence in UVB-treated mouse skin. Int J Cancer 72(1):110–118
39. Dietel W, Pottier R, Pfister W, Schleier P, Zinner K (2007) 5-Aminolaevulinic acid (ALA) induced formation of different fluorescent porphyrins: a study of the biosynthesis of porphyrins by bacteria of the human digestive tract. J Photochem Photobiol, B 86(1):77–86
40. Attili SK, Lesar A, McNeill A, Camacho-Lopez M, Moseley H, Ibbotson S, Samuel ID, Ferguson J (2009) An open pilot study of ambulatory photodynamic therapy using a wearable low-irradiance organic light-emitting diode light source in the treatment of nonmelanoma skin cancer. Br J Dermatol 161(1):170–173
41. Brancaleon L, Moseley H (2002) Laser and non-laser light sources for photodynamic therapy. Lasers Med Sci 17(3):173–186

42. Wiegell SR, Haedersdal M, Philipsen PA, Eriksen P, Enk CD, Wulf HC (2008) Continuous activation of PpIX by daylight is as effective as and less painful than conventional photodynamic therapy for actinic keratoses; a randomized, controlled, single-blinded study. Br J Dermatol 158:740–746
43. Wiegell SR, Hædersdal M, Eriksen P, Wulf HC (2009) Photodynamic therapy of actinic keratoses with 8% and 16% methyl aminolaevulinate and home-based daylight exposure: a double-blinded randomized clinical trial. Br J Dermatol 160:1308–1314
44. http://www.nice.org.uk/guidance/MTG6
45. Fayter D, Corbett M, Heirs M, Fox D, Eastwood A (2010) A systematic review of photodynamic therapy in the treatment of pre-cancerous skin conditions. Barrett's oesophagus and cancers of the biliary tract, brain, head and neck, lung, oesophagus and skin. Health Technol Assess 14:37
46. Kaufmann R, Spelman L, Weightman W, Reifenberger J, Szeimies RM, Verhaeghe E et al (2008) Multicentre intraindividual randomized trial of topical methyl aminolaevulinate-photodynamic therapy vs. cryotherapy for multiple actinic keratoses on the extremities. Br J Dermatol 158:994–999
47. Szeimies RM, Karrer S, Radakovic-Fijan S, Tanew A, Calzavara-Pinton PG, Zane C et al (2002) Photodynamic therapy using topical methyl 5-aminolevulinate compared with cryotherapy for actinic keratosis: a prospective, randomized study. J Am Acad Dermatol 47:258–262
48. Morton C, Campbell S, Gupta G, Keohane S, Lear J, Zaki I et al (2006) Intraindividual, right-left comparison of topical methyl aminolaevulinate-photodynamic therapy and cryotherapy in subjects with actinic keratoses: a multicentre, randomized controlled study. Br J Dermatol 155:1029–1036
49. Freeman M, Vinciullo C, Francis D, Spelman L, Nguyen R, Fergin P et al (2003) A comparison of photodynamic therapy using topical methyl aminolevulinate (Metvix) with single cycle cryotherapy in patients with actinic keratosis: a prospective, randomized study. J Dermatol Treat 14:99–106
50. Sotiriou E, Apalla Z, Maliamani F, Zaparas N, Panagiotidou D, Ioannides D (2009) Intraindividual, rightleft comparison of topical 5-aminolevulinic acidphotodynamic therapy vs. 5% imiquimod creamfor actinic keratoses on the upper extremities. J EurAcad Dermatol Venereol 23:1061–1065
51. Dragieva G, Prinz BM, Hafner J, Dummer R, Burg G, Binswanger U et al (2004) A randomized controlled clinical trial of topical photodynamic therapy with methyl aminolaevulinate in the treatment of actinic keratoses in transplant recipients. Br J Dermatol 151:196–200
52. Cox NH, Eedy DJ, Morton CA (1999) Guidelines for management of Bowen's disease. British association of dermatologists. Br J Dermatol 141:633–641
53. Morton C, Horn M, Leman J, Tack B, Bedane C, Tjioe M et al (2006) Comparison of topical methyl aminolevulinate photodynamic therapy with cryotherapy or Fluorouracil for treatment of squamous cell carcinoma in situ: results of a multicenter randomized trial. Arch Dermatol 142:729–735
54. van der Snoek EM, den Hollander JC, Aans JB, Sterenborg HJ, van der Ende ME, Robinson DJ (2012) Photodynamic therapy with systemic meta-tetrahydroxyphenylchlorin in the treatment of anal intraepithelial neoplasia, grade 3. Lasers Surg Med 44(8):637–44
55. Szeimies RM, Ibbotson S, Murrell DF, Rubel D, Frambach Y, de Berker D et al (2008) A clinical study comparing methyl aminolevulinate photodynamic therapy and surgery in small superficial basal cell carcinoma (8–20 mm), with a 12-month follow-up. J Eur Acad Dermatol Venereol 22:1302–1311
56. Rhodes LE, de Rie MA, Leifsdottir R, Yu RC, Bachmann I, Goulden V et al (2007) Five-year follow-up of a randomized, prospective trial of topical methyl aminolevulinate photodynamic therapy vs surgery for nodular basal cell carcinoma. Arch Dermatol 143:1131–1136

57. Berroeta L, Clark C, Dawe RS, Ibbotson SH, Fleming CJ (2007) A randomized study of minimal curettage followed by topical photodynamic therapy compared with surgical excision for low-risk nodular basal cell carcinoma. Br J Dermatol 157:401–403
58. Betz CS, Rauschning W, Stranadko EP, Riabov MV, Volgin VN, Albrecht V, Nifantiev NE, Hopper C (2012) Long-term outcomes following Foscan®-PDT of basal cell carcinomas. Lasers Surg Med 44(7):533–540
59. Edstrom DW, Hedblad MA (2008) Long-term follow-up of photodynamic therapy for mycosis fungoides. Acta Derm Venereol 88(3):288–290
60. Debu A, Bessis D, Girard C, Du Thanh A, Guillot B, Dereur O (2013) Photodynamic therapy with methyl aminolaevulinate for cervical and/or facial lesions of folliculotropic mycosis fungoides: interest and limits. Br J Dermatol 168(4):896–898
61. Kennedy JC, Pottier RH, Pross DC (1990) Photodynamic therapy with endogenous protoporphyrin IX: basic principles and present clinical experience. J Photochem Photobiol, B 6:143–148
62. Fabbrocini G, De Vita V, Monfrecola A (2010) Photodynamic therapy with 20% topical 5-Aminolaevulinic Acid or Placebo for the treatment of common therapies-resistant plantar warts: a randomised double-blind trial. J Egypt Women Dermatol Soc 7(2):81–86
63. Szeimies RM, Schleyer V, Moll I, Stocker M, Landthaler M, Karrer S (2009) Adjuvant photodynamic therapy does not prevent recurrence of condylomata acuminata after carbon dioxide laser ablation—A phase III, prospective, randomized, bicentric, double-blind study. Dermatol Surg 35(5):757–764
64. Itoh Y, Ninomiya Y, Tajima S et al (2001) Photodynamic therapy of acne vulgaris with topical delta-aminolaevulinic acid and incoherent light in Japanese patients. Br J Dermatol 144:575–579
65. Kohl EA, Karrer S (2012) Photodynamic skin rejuvenation. Photonics and Lasers in Medicine 1:27–33
66. Gardlo K, Horska Z, Enk CD, Rauch L, Megahed M, Ruzicka T, Fritsch C (2003) Treatment of cutaneous leishmaniasis by photodynamic therapy. J Am Acad Dermatol 48(6):893–896
67. Akilov OE, Kosaka S, O'Riordan K, Hasan T (2007) Parasiticidal effect of delta-aminolevulinic acid-based photodynamic therapy for cutaneous leishmaniasis is indirect and mediated through the killing of the host cells. Exp Dermatol 16(8):651–660
68. Welzel J, Lankenau E, Birngruber R, Engelhardt R (1997) Optical coherence tomography of the human skin. J Am Acad Dermatol 37(6):958–963
69. Steiner R, Kunzi-Rapp K, Scharffetter-Kochanek K (2003) Optical coherence tomography: clinical applications in dermatology. Med Laser Appl 18(3):249–259
70. Gambichler T, Orlikov A, Vasa R, Moussa G, Hoffmann K, Stücker M, Altmeyer P, Bechara FG (2007) In vivo optical coherence tomography of basal cell carcinoma. J Dermatol Sci 45(3):167–173
71. Mogensen M, Morsy HA, Thrane L, Jemec GB (2008) Morphology and epidermal thickness of normal skin imaged by optical coherence tomography. Dermatology 217(1):14–20
72. Mogensen M, Nürnberg BM, Forman JL, Thomsen JB, Thrane L, Jemec GB (2009) In vivo thickness measurement of basal cell carcinoma and actinic keratosis with optical coherence tomography and 20-MHz ultrasound. Br J Dermatol 160(5):1026–1033
73. Jenkins FA, White HE (1957) Fundamentals of optics. McGraw-Hill, New York
74. Ziolkowska M, Philipp CM, Liebscher J, Berlien H-P (2009) OCT of healthy skin, actinic skin and NMSC lesions. Med Laser Appl 24(4):256–264
75. Mogensen M, Joergensen TM, Nürnberg BM, Morsy HA, Thomsen JB, Thrane L et al (2009) Assessment of optical coherence tomography imaging in the diagnosis of non-melanoma skin cancer and benign lesions versus normal skin: observer-blinded evaluation by dermatologists and pathologists. Dermatol Surg 35(6):965–972
76. Göppner D, Mechow N, Liebscher J, Thiel E, Seewald G, Buchholz A, Gollnick H, Philipp CM, Schönborn K-H (2012) High-resolution two-photon imaging of HE-stained samples in dermatohistopathology—A pilot study on skin tumours. Photonics Lasers Med 1(2):133–140

Chapter 8
Photodynamic Diagnosis and Therapy for Brain Malignancies from the Bench to Clinical Application

Herwig Kostron

Abstract Glioblastomas are the third most common cause of cancer death in patients between 15 and 35 years. Photodynamic diagnosis (PDD), fluorescence guided tumour resection (FGR) and photodynamic therapy (PDT) is undergoing intensive clinical investigations as adjuvant treatment for malignant brain tumours. Besides many reports on clinical phase I/II trials for PDT for malignant brain tumours, there are only few controlled clinical trials. Variations in treatment protocols make the evaluation scientifically difficult; however, there is a clear trend towards prolonging median survival after one single photo dynamic treatment as compared to standard therapeutic regiments. According to a met-analysis the median survival for primary glioblastoma multi-forme WHO IV after PDT was 22 months and for recurrent GBM 9 months as compared to standard conventional treatment which is 15 and 3 months, respectively. Fluorescence-guided resection of the tumour demonstrated significant greater reduction of tumour burden. The combination of PDD/FGR and intra operative PDT ("to see and to treat") offers an exciting approach to the treatment of malignant brain tumours. Photodynamic treatment supported by observational studies with combined total of $> 1{,}000$ patients and 3 controlled trials in GBMs. PDT was highly selective, safe, significantly improved good quality survival and delayed tumour relapse ($p < 0.001$). The following chapter provides an overview on the current clinical data of PDT as well as photosensitisers, technical developments and indications for photodynamic application in neurosurgery.

Keywords Photodynamic therapy · Photodynamic diagnosis · Fluorescence guided resection · Neurosurgery · Malignant brain tumour · Photofrin® · 5-ALA · FOSCAN® · FOTOLON

H. Kostron (✉)
Department of Neurosurgery, University Innsbruck, Innsbruck, Austria
e-mail: praxis@saggen10.at

M. H. Abdel-Kader (ed.), *Photodynamic Therapy*,
DOI: 10.1007/978-3-642-39629-8_8,

8.1 Introduction

The incidence of malignant brain tumours varies from 4/100.000 to 14/100 with an increase up to 70/100.000 in the elderly population above 65 years [1]. Glioblastomas are the third most common cause of cancer death in patients between 15 and 35 years old. Malignant brain tumours carry a lethal prognosis with a median survival of 15 months for grade IV tumours [1–3] (Table 8.1). The 5-year survival is under 1 %.

Surgery is the first and most important step in the treatment of malignant gliomas and remains the mainstay in therapy. However, radical resection is hardly possible due to infiltration into normal brain parenchyma. Recurrences occur 95 % locally within 2 cm from the initial site and arise from tumour cells (guerrilla or satellite cells) embedded in the area of oedematous or normal brain adjacent to tumour (brain adjacent to tumour region "BAT") [2]. For almost 30 years, Photodynamic therapy (PDT) has been used to treat malignant brain tumours and is further under intensive clinical investigations as adjunctive treatment for malignant brain tumours [2–5]. Since photosensitisers are accumulated in pathological brain tissue to a higher extent than in normal brain parenchyma, subsequent activation by light produces a variety of cytotoxic oxidative reactions which induce selective tumour destruction [6, 7]. Therefore, PDT offers more selectivity as compared to chemo and radiotherapy and seems to be a logical concept for brain tumours infiltrating into normal brain.

Clinical studies demonstrated a benefit for the patients treated with PS-mediated PDT in terms of prolongation of median survival time as well as quality of life [2, 5, 7–10].

Fluorescence guided delineation had been under investigation to distinguish normal from pathological brain tissue with fluorescine and tetracycline or auto fluorescence [11–13], however, the sensitivity and specificity were too low to be of clinical significance for neurosurgery. Modern intraoperative imaging techniques such as MRT, CT, neuronavigation and ultrasound are expensive tools and—which is very important in clinical use—do not calculate the brain shift during operation. The fluorescence properties of photosensitisers such as HPD, 5-Amino-Leavulinic-Acid (5-ALA) and chlorine compounds such as meta-TetraHydroxyPhenylChlorin (mTHPC) and Fotolon (Clorine e 6) are used for photodynamic diagnosis (PDD)

Table 8.1 outcome of malignant gliomas WHO gradings, therapeutic strategies [1]

Histology WHO	Therapy	Recurrence time	Median survival
Glioblastoma multiforme WHO IV (GBM)	Surg, CHT, XRT	6 months	15 months
Anaplastic Astrocytoma WHO III (AA)	Surg, CHT, XRT	18 months	3 years
Astrocytoma II	Surg, XRT	3 years	6 years
Astrocytoma I	Surg,	8 years	10 years

Surg surgery, *XRT* radiotherapy, *CHT* chemotherapy

and FGR has been established in various clinical applications and in neurosurgery [11–17]. This intraoperative PDD allows a "real-time" optical delineation of normal and malignant tissue which facilitates intraoperative orientation and allows fluorescence guided resection (FGR) which results in a more radical resection. This translates directly in a significant longer survival [4, 15, 17]. This was also combined with PDD and PDT involving two sensitizers; one sensitizer for diagnosis (ALA) and one for treatment (Fotofrin) [17, 18].

Intraoperative mTHPC mediated PDD followed by intraoperative PDT has been reported in recurrent glioblastoma multi-forme with promising results [15–17]. Simultaneous intraoperative PDT involving only one sensitizer offers a logical supplement to PDD according to the KOSTRON slogan "to see and to treat" [15].

This review analyses the available data and draws the future potential of PDD and PDT for its application in neurosurgery.

8.2 Basics: Photosensitisers, PDT Mechanisms, Effect on Normal Brain

8.2.1 Photosensitisers

Photosensitisers used for brain tumours require a different profile than for e.g. superficial tumours. The tumour burden in the brain is much larger and radical resection is hardly possible because of infiltration of tumour into normal brain tissue of 2 cm and deeper.

The ideal neurosurgical sensitizer should have (a) A high selectivity for tumour and tumour cells and should cross the blood brain barrier (BBB) and target also tumour cells embedded in normal brain tissue (guerrilla cells); (b) Photo activation in the near infrared range and beyond; (c) Strong fluorescence properties; (d) High quantum yield; (e) No systemic toxicity with no or only short lasting sensitisation of the skin [19]. The photosensitizer of first generation Hematoporphyrin derivative (HPD) is a complex mixture of various porphyrins [20, 21], which was used for most of the basic experimental work and almost exclusively in the clinical brain tumour studies. HPD has its optimum absorption between 628 and 635 nm and allows a penetration depths up to 5 mm depending on the tissue. The dose in clinical use is 2 mg/kg injected intravenously. Energies required are ranging from 60 to 260 J/cm^2. The ratio of the concentration in tumour to normal brain ranges from 2.5 to 4:1 and in animal experiments it ranges up to 12:1. In human GBM the concentrations vary significantly from 1.46 to 4.00 μg/g wet weight. The concentration in the BAT region ranged from 0.6 to 1.2 μg/g. In this series the amount of PS correlated positively with the survival of the patients [7]. Light sensitisation of the skin was observed for up to 8 weeks.

Meso-tetra-hydroxyphenyl-chlorin (mTHPC, Tempoforin, FOSCAN®) has been used as second generation sensitizer with a higher tumour to brain ratio in humans of 10:1 at a dose between 0.05 and 0.15 mg/kg and light doses of 20 J/cm^2

[15, 16, 22–24]. The ratio in the BAT region is around 1:20. Clinical results of FGR mediated by mTHPC followed by intraoperative PDT have demonstrated a significant benefit for survival in recurrent malignant gliomas [15]. Light sensitisation of the skin was observed for 4 weeks.

5-Aminolevulinic acid (ALA) induced protoporhyrin IX produces excellent fluorescence for diagnostic purposes and is activated at 635 nm. Sufficient cell kill of superficial tumours such as bladder and skin tumour is achieved at energies of up to 100 J/cm^2 [14, 23, 25]. The ratio of ALA concentration in tumour to normal brain is around 4:1. Currently there is a phase I/II trial for PDT mediated by ALA under investigation [26]. A randomised phase III trial investigating the effect of ALA (GLIOLAN®) mediated FGR demonstrated a higher incidence of radical tumour removal than under white light, which translated also in a progression free survival but did not influence overall survival [14]. Skin phototoxicity after ALA application is only few to 24 h after instillation.

Bacteriochlorine, Benzoporphyrin (BPD), boronated porphyrins, Chloraluminium-phthalocyanine (AlClPc), Fotolon (clorine e6), hypericin, methylene blue, Tin Ethyl purpurin (SnET2) and texaphrin are further sensitizers with great potential for its use in brain tumour surgery [27–31].

8.2.2 PDT-Mechanisms

The mechanisms of PDT are based on photo-oxidative reactions and depend strongly on the type of photosensisers, light dose regime and investigated tumour cells, the pathology, the absorbance and chemistry of the sensitizer and the incubation time [6, 8, 10, 19].

Over the past years, many different pathways of PDT-mediated cytotoxicity were found at the molecular level. Besides the primary vascular damage and direct cellular effect [7], further cytotoxic mechanisms are mediated by cytokine modulation and autophagy [32]. Transforming growth factor, fibroblastic growth factor, interleukin-1 and interleukin-6 but also PDGF and TNF play a role in mediating the photo-oxidative cytotoxic process [33, 34]. Interleucin-6, an autoendocrine stimulator for glial tumours, is significantly reduced in cell cultures after PDT [35, 36]. Oxidative stress activates early response genes further modulates apoptosis depending on the cell lines employed [37]. Since porphyrins are incorporated in lipoproteins, the low-density-lipoprotein receptor pathway is one important factor for the selective accumulation of porphyrins by glial tumour cells express significant amounts of LDL–lipoprotein receptor related protein.

One other contribution to cytotoxic efficacy might be the inhibition of migration of human glioma cells [38]. All these above mechanisms outlined above could contribute to the PDT effect exceeding the depths penetration of the activating light (bystander effect). More details of the mechanisms of PDT are found in this book at Chaps. 2 and 3.

8.2.3 *Effect of PDT on Normal Brain*

Despite a high selectivity of PS towards tumour cells, injury to normal glial and neurones had been observed in the normal brain [6, 19, 23, 31]. This damage depends on the type of sensitizer used, the concentration of sensitizer, time interval of sensitisation to light exposure and light density. An important part plays the blood–brain-barrier which protects the normal brain from toxic substances. Whereas the blood–brain-barrier does not exist within the tumour, and the surrounding oedema, this barrier is well intact in the brain embedding tumour island [23, 24]. However, the evidence is mostly derived from experimental work. HPD is taken up by normal brain in a dose depending fashion varying from 0.2 μg/g to 1.2/g μg wet weight brain tissue at a dose of 10 and 20 mg HPD/kg bodyweight. Twenty mg/kg and 100 J cause death of the animals due to severe swelling. Fluorescence diagnosis demonstrated the presence of the sensitizer mostly along the fibre bundles of the white matter. Upon light activation first break down of blood–brain barrier, swelling of astrocytes and neurones are observed. After 2 days coagulation necrosis occurs in a dose dependent fashion at concentrations higher than 5 mg HPD [7, 11, 25]. Intra tumoral or intra parenchymal instillation of the sensitizer does not exhibit selectivity; however, the higher doses resulted in higher tissue concentrations which again created a greater toxicity. Experimental studies used high doses of HPD whereas at clinical relevant doses of 2.0 mg to 5 mg/kg only few reports described morphological changes in the normal human brain [7, 33].

Focal necrosis around the vessels 24 h after intra-arterial injection was found in only one series [7], whereas oedema post PDT was described by almost all authors. Muller reported a significant increase of intracranial pressure despite avoiding hyperthermia effects [39]. After stereotactic PDT cerebral oedema was observed in most of the cases. The amount of postoperative swelling correlates with the residual tumour volume, so the tumour resection has to be performed to the outmost possible extent [7, 39].

8.3 Interaction of PDT with Chemotherapy and Radiotherapy

In 2000 Temozolemide was introduced as highly effective chemo therapy for malignant brain tumours and constitutes now the golden standard in conjunction with surgery and ionising radiation [40, 41]. Steroids (like dexamethasone) are widely used in neurosurgery for the treatment of tumour-associated oedema and might decrease the uptake of PS into the tumour cells [7].

However, this varies strongly within the various cell lines and tumour. Doxorubicin e.g. potentiates therapeutic efficacy of mTHPC-mediated PDT significantly when given after light irradiation, but to a lesser extent when given prior [42]. There are no reported clinical data on the interaction of PDT and chemotherapy.

PDT might be of advantage in the treatment of tumours not responding to chemotherapy because cells which express multi drug resistance features are less likely to be cross-resistant to PDT [43]. The combination of PDT and targeted drugs, such as VGF, PDGF, EGFR as well as factors enhancing apoptosis and phagocytoses enhance or potentiate the efficacy of PDT [44–46]. A promising approach is the combination of Bleomycin and Photochemical internalisation (PCI) in various clinical indications [47–49].

8.3.1 Interaction of PDT and Ionising Radiation

Ionising radiation is a standard therapy in the postoperative course after surgery of malignant brain tumours [1, 4, 40]. The interaction of HPD-mediated PDT and ionising radiation was investigated in a rat gliosarcoma model 9L. After intraperitoneal injection and low doses of HPD an additive effect of both treatment modalities could be observed, whereas direct injection with high intra tumoral concentration and high light doses of 120 J/cm^2 and 4 Gy resulted in significant greater response indicating a potentiating mechanism. The effect was more pronounced when PDT was followed by XRT within 30 min [50]. The underlying mechanism is thought to be the inhibition of the potential lethal damage induced by PDT. In a more recent study, employing human glioma spheroids study it was shown that gamma radiation and PDT interact in a synergistic manner only if both light fluence and gamma radiation dose exceed approximately 25 J cm^{-2} and 8 Gy, respectively [51].

In an early series at the authors institution patients with de novo glioblastomas were treated with one single dose of 4 Gy of electrons within 30 min after PDT [7]. The results remained unchanged to that ones without immediate x-radiation treatment; therefore, this treatment protocol were not continued. Radiotherapy was commenced in addition in all de novo patients within 10 days after surgery and PDT. We did not see any side effects from this radiotherapy. There were also no side effects reported in the 5-ALA-mediated PDD/FGR trial where ionising radiation of 60 Gy was commenced within 4 weeks after sensitisation [7].

There is a recent feasibility report of the combination of stereotactic radio surgery and PDT in brain tumours which showed a synergistic effect and gave promising results [52].

8.4 Instrumentation

Initial work was performed with argon dye laser systems or xenon arc lamps with adequate filtering. Now LEDs and diode lasers are available in almost all desired wavelengths and are much reliable and cost effective. Laser light delivery in Neurosurgery has become the state of the art and interstitial PDT has become

possible. Light delivery and dosimeter is a critical point in PDT and especially in neurosurgery with no ideally geometrical shaped or superficial lesions and irregular and large volumes must be treated [53, 54].

An inflatable balloon is employed to facilitate dosimetry. In general the cavity or the balloon is filled with a 0.1 % concentration of intra-lipid solution or plane water to achieve a homogeneous light distribution [7, 39]. The superficial light delivery is performed mostly by bare fibres or spheroids. Interstitial light application is performed by cylindrical fibres at power density of 250 to 350 mW/cm^2 without producing carbonisation at the fibre tip. The placements of up to 6 fibres are done by 3D planning and stereotactic methods [40–42, 55, 56]. Repetitive PDT treatments were given using 100 J/cm^2 of a Diode Laser at 630 nm [57, 58]. Important parameters such as fluence rate, sensitizer fluorescence intensity, and changes in local blood oxygen saturation can be measured with the same fibres that deliver the therapeutic light [59].

8.5 Photodynamic diagnosis and Fluorescence Guided Resection

At the beginning of the photodynamic story, PDT was strongly driven forward to improve the results in the treatment of various cancer entities and brain tumours, since there was no other effective treatment. Since the late 90 the fluorescence aspects of photodynamics became more important. Besides phototoxic properties, the fluorescence abilities of the photosensitiser are used for optical discrimination of normal and malignant tissue allowing intraoperative PDD and FGR thus minimising residual tumour [11]. Intraoperative fluorescence is induced by UV light (370–440 nm). The induced fluorescence light is collected by a dual optical fibre to a CCD camera and a spectroscopy. Normal white light illumination of the surgical microscope can be switched to blue light excitation with simultaneous observation by the naked eye. The induced fluorescence could be seen direct through the observer light path. Standard neurosurgical microscopes (Zeiss, Leica) have been adopted for fluorescence detection [11, 16, 17, 60]. Reduced dose of Foscan is under clinical examination (Kostron personal comm).

8.6 Methods and Patients

The indications for PDT are primary and recurrent malignant brain tumours. Slow growing tumours such as low-grade astrocytomas or other benign lesions are not taking up sufficient concentrations of photosensitisers. Tumours which are not protected by the blood brain barrier (BBB) are a good indication for PDD/PDT such as Scull base tumours or tumours of the pituitary gland. There are similar findings in maxillofacial tumour patients [61]. Most recent case reports include

Table 8.2 Metastasis, malignant meningeomas and recurrent pituitary tumours

Author	Number of patients	Histology	Median survival
Eljamel 2008 [17, 65]	103	Various[a] braintumors	13 mo for GBM
Muller 2006 [39]	112	HGG	11 mo
Kaneko 2008 [62]	90	GBM	18.5 mo
		AA	36.2 mo
Kostron 2006 [7, 15]	116	GBM	19 mo
		Recur GBM	9 mo
Stylli 2006 [63]	350	GBM	24.3 mo
		Recurr GBM	16 mo
		AA	76.7
Pichlmeier 2006 [14]	243	GBM	GBM cr 16.7
			GBM ic 11.8

GBM Glioblastoma multiforme WHO IV
AA Anaplastic Astrocytoma WHO III
HGG High-grade glioma WHO IV and WHO III
GBM cr GBM with complete resection > 95 %
GBM ic GBM with incomplete resection
[a] *Various braintumours* GBM, metastasis, meningeomas, pituitary tumour

patients suffering from metastasis, malignant meningeomas and recurrent pituitary tumours (Table 8.2) [62, 63].

The patients were treated with a variation of PS, such as various formulations of HPD (HPD, Photofrin I, DHE, Photofrin II, Photosan 3 or mTHPC. In order to utilise PS also for intraoperative diagnostics Photofrin and 5-ALA are combined [5, 60, 62, 63] or mTHPC for both indications [15, 16]. Photolon has equal properties but there are only mostly experimental and few favourable clinical data are published [31].

The following protocol for PDT is generally accepted. The patients are sensitised with HPD (Photofrin) 2, 5 mg/kg or with Foscan® 0.15 mg/kg BW 24 to 48 h prior to a standard craniotomy [7, 15, 17]. Steroids are withdrawn 2 to 3 days prior to sensitisation, so far tolerated. A standard craniotomy is performed and after maximal tumour resection under white light the resection is continued with intraoperative PDD and under fluorescence guidance.

Nowadays, PDT is performed by diode lasers emitting at the required wavelengths. The light is delivered by bare fibres coupled into a modified balloon system, by a spherical distributor or by a 20 mm long cylinder for interstitial treatment. The power density for surface illumination varies depending on the lasers used. For interstitial treatment the power density ranges from 250 to 350 mW. For treatments of HPD-mediated PDT the light dose was increasing from 20 J/cm^2 for the first patients to the standard dose of up to 250 J/cm^2.

Residual tumour in functional areas can be treated by interstitial PDT which is performed at a power density of 250–350 mW/sec to a total dose of 150 J. The light dose for the mTHPC sensitised patients was 20 J/cm^2 and the interstitial

therapy was performed at a power density of 350 J/cm^2 to a dose of 20 J/cm^3. The fibres are placed according to preoperative 3D planning by means of neuronavigation or by stereotactic means [15, 62]. After the operation the patients were kept in ambient room light. After mobilisation the patients were slowly exposed to normal sunlight to allow pigmentation of the skin. A light metre was provided for the patients to control light exposure. The patients were followed by clinical exams and MRI/CT scans every 3 months [15].

8.7 Clinical Trials and Results

Since 1980 more than 1,000 patients had been treated meanwhile world-wide [7, 39, 62–64] (Table 8.2). This number is relatively low as compared to the amount of patients treated with lung, bladder or skin cancers. The reason might be that the incidence of brain tumours is lower and their treatment more complicated since it requires highly sophisticated surgery and instrumentation. In general the patients were sensitised with HPD-Photofrin in various formulations and only one trial used mTHPC as sensitizer [15]. The majority of the patients were sensitised parenterally and few patients received intra tumoural or intra-arterial sensitisation [7].

Light irradiation was performed with photo radiation lamps, dye laser, gold vapour KTP dye laser and diode lasers. Patients presenting with primary glioblastomas underwent 45 Gy of irradiation within 4 weeks after PDT. The light dose was initially low at 70 to 180 J/cm^2 which was finally increased to 240 J/cm^2 in the majority of the patients. Most of the patients underwent standard craniotomies and open tumour resection [7]. Stereotactic approach was chosen by several other authors [7, 26, 56]. Muller observed complete response with excellent survival in cases where a cystic geometric tumour cavity allowed a very homogeneous light distribution [39].

The results of the reported cases of high-grade tumours are difficult to evaluate because the histology are in general not detailed. High-grade gliomas consisting of WHO grade IV and grade III gliomas are often pooled but they have a significantly different prognosis with 15 months vs. 36 months, respectively.

8.7.1 Primary Glioblastoma

Primary glioblastoma were initially treated with various formulations of HPD 24–72 h prior to treatment. These patients received in addition conventional radiotherapy of total 55–60 Gy as well as chemotherapy (Temozolemide). Photofrin® is now easily commercially available. The median time to progression was 13 months. Patients with recurrences after PDT underwent retreatment with PDT without any other treatment. Their median survival was 10 months. There was no adverse effect from a second photosensitization and photo radiation [7].

The total median survival of primary glioblastomas in the compiled series was 19 months (range 9–27 months).

In the Canadian phase III study 112 patients were treated with PDT and adjuvant radiotherapy of 45 Gy. The median survival was 9 months. Furthermore, at this institution a randomised phase III was conducted enrolling 77 primary GBM which underwent whether surgery plus PDT and XRT or surgery and XRT. The results were not significant with a median survival of 11 months vs. 8 months, respectively [39]. A similar result was reported enrolling 31 patients which had a median survival of 13 months after FGR and PDT as compared to 6 months in the controls [17].The largest series enrolling more than 350 high-grade gliomas was reported by Stilly 2006 in an uncontrolled trial [63]. Primary gliomas received 45 Gy in addition and reached a median survival of 27 months. Eljamel conducted an innovative randomised trial combining FGR and metronomic PDT, which yielded significant better results as compared to the control group [17].

Recurrent glioblastomas: Thirty-nine patients with recurrent glioblastomas were treated photodynamically because of treatment failures. The median time to first recurrence without any other treatment was 7 months and the median survival time after PDT was 9 months (range 3–18 months). Fourteen patients were re-operated after 12 months having presented with a first recurrence. No further treatment was commenced. These patients suffered another recurrence within 3 months. After a third surgical procedure and PDT the median time to recurrence was 6 months (3–8 months) [7].

Stylli reported a median survival of 18 months for patients with recurrent high-grade gliomas and PDT [63]. Muller reported 64 recurrent glioblastomas which underwent a dose escalation in a randomised phase III trial. Patients receiving more than 1,700 J had a median survival of 9.2 months, whereas those receiving less than that had a survival of 6, 6 months [39].

Kaneko had treated 90 patients mostly bearing glioblastomas with a median survival of 18 months [62]. Fifteen recurrent glioblastomas were treated by multiple interstitial fibres which were based on a computed 3D image and stereotactically placed interstitial fibres. The light dose was 100 J/cm^2 with median survival of 6 months or a light dose of up to 400 J/cm [55, 56], (Figs. 8.1, 8.2)

High-grade gliomas WHO III: Over 120 recurrent anaplastic astrocytomas were treated photodynamically with energies varying from 45 to 175 J/cm^2 with a median survival of 56 months (range 36, 0 to 76, 7 months). Malignant mixed oligo-astrocytomas and ependymomas had a 2 year survival of 37 and 75 %, respectively [5, 7, 39, 62, 63].

Brain tumours of other origin: Malignant meningiomas were treated with light dose up to 260 J/cm^2 and the median survival was 6, 15 and 23 months, respectively.

Pituitary tumours: These are benign tumours, however, when they recur they produce anatomical malignancy. Thirty patients suffering from recurrent pituitary tumours were treated in combination with fluorescence-guided localisation and resection because of repeated recurrence and treatment failures. All cases

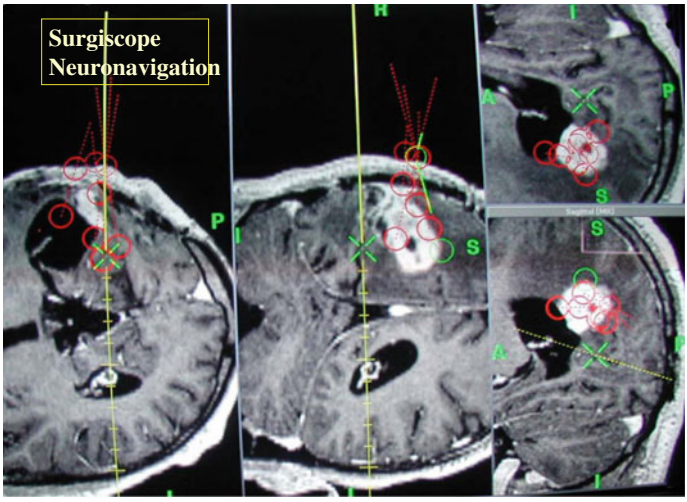

Fig. 8.1 Pre-operative planning for stereoactic PDT treatment after FOSCAN mediated fluorescence guided resection

Fig. 8.2 Operative setting for stereotactic fibre insertion for PDT

responded favourable all showing no progression or recurrence of tumours for 2, 5 years [64].

Metastasis: There are 46 reported cases of metastasis of various origins. All except of melanoma metastasis showed complete or partial response and patients usually died to systemic progress with local control.

8.7.2 MTHPC-Mediated PDT

Twenty-four patients with primary or recurrent GBM were enrolled in this trial and demonstrated a median time to progression of 4 months and a median survival time of 9 months [15].The patients with metastasis demonstrated complete tumour control in 2 cases for up to 28 months, 2 were progressing 6 months after treatment and were lost to follow up. One scull base tumour demonstrated a complete response with a follow up of 24 months; the other relapsed within 7 months. All patients tolerated mTHPC-mediated treatment well; one patient suffered swelling of the treated area. Two patients experienced severe toxic reaction to sunlight due to unintentional exposure to direct sunlight requiring conventional treatment.

One patient was treated with a malignant nerve sheath tumour of the scull base and the tumour recurred 12 months after treatment.

8.7.3 Photodynamic diagnosis and Fluorescence Guided Resection 4.9

Maximal tumour resection is directly correlated with a longer survival [1, 2, 4, 39] which can be facilitated by intra operative PDD and FGR. Five-ALA (GLIOLAN®) is given orally at 20 mg/kg BW 3 to 4 h prior to surgery or also FOSCAN® 0.15 mg/kg BW whether 24 or 96 h prior to surgery. A randomised phase III trial proved that FGR mediated by 5-ALA results in a significant higher amount of almost complete resection than without, which translated in greater survival of 16.7 versus 11.8, respectively [60]. Foscan-mediated PDD and FGR was investigated in recurrent GBM and compared to a cohort of paired patients. The histological specimens of fluorescent tissue correlated to a sensitivity and specificity of 89 and 96 %, respectively [16, 22]. Complete resection was achieved in 68 % as compared to 35 % in the control group which was demonstrated by MRI within 48 h after surgery. These latter patients underwent immediate PDT after FGR tumour resection was accomplished. The results were significantly longer in the treatment group with 9 months as compared to the matched pair group, which lived 3 months in the median [15]. Since tumour grows invasively also functional areas such as speech, motor function or psychic function, complete resection cannot be performed in order not to harm the patient. In such cases, interstitial PDT can be performed in those functional areas [18, 55, 56]. Care has to be taken not to harm the patients since an impaired neurological status (KPI < 60 %) correlates with a shorter overall survival [1], (Figs. 8.3, 8.4), (8.5)

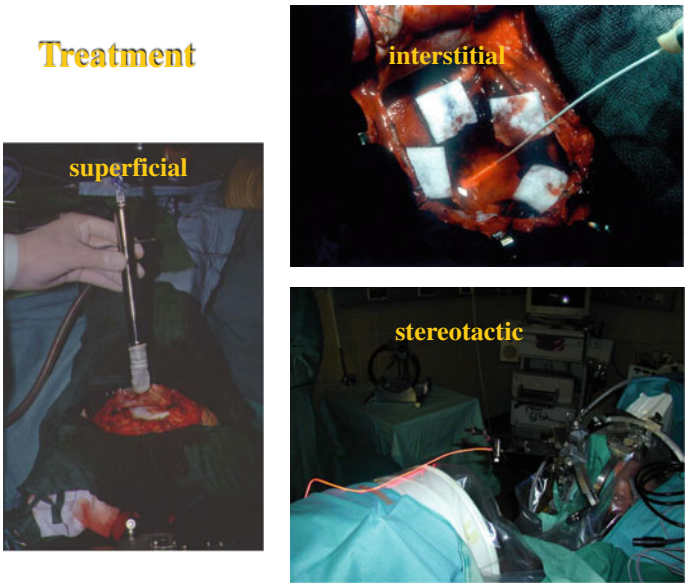

Fig. 8.3 Typical intraoperative PDT treatment; clockwise: intracavitary balloon treatment; interstitial treatment with laser fibres in place; stereotactic treatment

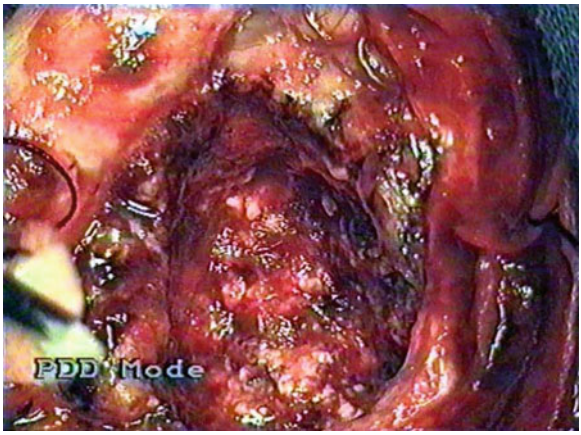

Fig. 8.4 Post-operative resection cavity with no hint of residual tumour, note the whitish area at one o'clock

8.8 Discussion

The purpose of this review is to summarise the current available data on brain tumours which underwent photodynamic-mediated therapies, which includes FGR/PDD and PDT. Because of variations in the treatment protocols of each individual investigator, the data are hardly comparable. There are two randomised

Fig. 8.5 Post-operative PDD, note the clear fluorescence derived from FOSCAN at one o′clock

phase III trials, one trial with paired controls and 15 uncontrolled trials in comparison with historical controls.

The largest series currently comes from Melbourne which recruited more than 350 patients presenting with high-grade gliomas, the majority being recurrent tumours [63]. The median survival for primary glioblastomas undergoing Photofrin-mediated PDT (180–240 J/cm^2) and 45 Gy of radiation was 24 months, anaplastic gliomas WHO III had a median survival of 76, 7 months, respectively. Recurrent gliomas demonstrated a 16 months median survival after PDT as compared to historical controls which lived in the median 12 months.

Muller reported on two randomised controlled phase III studies with primary as well as recurrent on high-grade gliomas which were sensitised with 2 mg Photofrin 12–36 h prior to operation [39]. This randomised Phase III study enrolling 43 primary glioblastomas in the treatment arm and 33 patients in the control showed a trend towards prolonged survival with a difference of 3 months; however, the numbers were too small to show statistical significance. The comparison high to low dose light radiation did not show a difference in survival, whereas a previous study reported significant better results. Patient undergoing PDT greater than 1,700 J had a survival of 9.2 months as compared to 6.6 months who were treated with a lower dose than 1,700 J. A high light dose was always associated with a longer survival.

The results for primary glioblastomas at our own institution showed a median survival of 19 months and for patients suffering from recurrent tumours 9–6 months, which is significantly longer as the natural lifespan and up to same as with high cost chemotherapy demonstrating the PDT affectivity and efficiency. Direct intra-tumoural or selective intra-arterial injection performed in few patients resulted in a high intra-tumoural PS concentration; however, the results were not improved as compared to intravenous sensitisation [7]. Photosensitiser kinetics depends on the tumour blood flow and oxygenation of the tumour is highly inconsistent within tumour entities and varies significantly in in vivo and in vitro

models [23, 24] The concentration of the sensitizer varied significantly among the tumours even in tumours of the same histology [7, 25].

After PDT the relapses always recur locally and there is no difference in the patterns of recurrence as after conventional treatment modalities. The reason of the recurrences is multiple. In comparison to tumours localised elsewhere in the body, brain tumours exceeds 100 cm^3 and more. Even after most radical resection, tumour cells embedded in the normal brain might escape PDT. This BAT area is often the site of tumour recurrence. At this critical area a low light dose and low sensitizer dose coincidence. To overcome this problem and to circumvent the BBB the sensitizer were injected directly into the tumour cavity resulting in significant higher intra-tumoural concentration; however, the clinical results were not improved. Muller irradiated patients within 12 h after sensitisation to prevent the rapid washout of sensitizer at the BAT region [39]. Therefore, most likely a low penetration of activating light seems to be the most realistic reason for recurrences on that site [25]**.** In the opposite, interstitial radiation improved depth penetration to about 2 cm and dosimetry at this critical area, but this also did not improve the results [15, 55, 56, 59]. The best results were actually achieved by Stylli and Kaye using high dose of superficial irradiation [63]. Different approaches in varying light delivery, timing of light delivery, varying photosensitiser concentrations and also drugs changing the micro-environment of the tumour had been investigated which will induce and prolong different photochemical and phototoxic reactions. Metronomic or multiple treatment sessions after one time sensitisation with Photofrin has been reported with favourable effects. Multiple investigations are currently performed to elucidate metronomic PDT [57, 58].

Ionising radiation was applied to the patients whether almost simultaneously or consecutively within 4 weeks after PDT. There was no observed adverse interaction between these two modalities. In a most recent trial, there was a significant advantage reported for PDT followed by immediate intraoperative radiation [50, 52]. A synergistic response of hyperthermia with PDT was observed when was delivered simultaneously or within 30 min after PDT [65], however, there is no clinical relevance of hyperthermia in neurooncology. Of greater importance in neurooncology might be the fact that PDT does not induce resistance to chemotherapy and might be effective in tumours expressing multidrug resistant features [43]. PDT in combination of targeted therapies changing the molecular signature of the tumour cells could further improve the treatment response [36, 42, 44–46]. However, the interactions of PDT with current standard treatment modalities such as ionising radiation and chemotherapy is by far not yet fully elucidated and investigated. The use of carrier systems such as liposomal encapsulated photosensitizers or PCI enhances selectivity and the PDT-mediated cytotoxic effects significantly [47, 49]. Vector enhanced delivery of non-viral or viral vectors are further promising approaches to enhance the selectivity and effectivity of PDT [66, 67].

PDT-specific side effects were considered as mild responding to conservative treatment with only short impairment of the patients. Besides the prolonged skin sensitivity for Photofrin and Foscan, increased intracranial pressure was reported

from various centres [15, 39]. A reversible diencephalic syndrome and neuropathy was reported during PDT of the middle cerebral fossa most probably due to hyperthermic effect to the midline structures [68, 69], however, this did not impair the patient's outcome.

ALA-(GLIOLAN®)-mediated FGR has been approved in various countries and is considered as standard in resection for high-grade brain tumours [60]. However, despite the visualisation of the tumourous tissue the limitations in resection are functional structures such as speech, motor and intellectual function. Therefore, immediate treatment of the residual tumour in such areas is a logical concept "see and to treat", which was emphasised by Kostron in 1998 [11].

Foscan-mediated PDD/FGR has the advantage of only one drug performing also very efficiently PDT [15], whereas ALA-mediated FGR needs the addition of a second sensitizer such as Photofrin to perform PDT [17, 18]. However, it could be demonstrated that ALA-PDT induces significant apoptosis [37] and immune mediators [35, 38]. Currently a pilot study investigates PDT-mediated 5-ALA following FGR [26].

The development of instrumentation has to be, however, as intensive as for sensitizers. Light dosimetry is critical for PDT response and under dosing might often be the cause for therapeutic failures. On-line dosimetry could prevent such failures [59]. Computer aided planning with 3D reconstruction of the remaining tumour and an exact planning of dosimetry, which can be archived by multiple stereotactic interstitial fibres placed by neuronavigation systems, should be considered mandatory for treating brain lesions [54–56].

The prime indications of PDT in neurosurgery are infiltrating high-grade gliomas. Pituitary tumours, spinal tumours, cystic lesion at the scull base and scull base tumours and metastatic lesions are also good indications in second line therapy. Low-grade gliomas demonstrate a significant longer survival and may be not good candidates for PDT. Also tumours in delicate areas such as brain stem must be excluded from PDT, whereas it can be used interstitially for example in the motor strip or other functional areas without impairing function [15, 19]. Novel indications are scull base tumours and tumour in the field of ENT [61, 70] as well as osseous tumour such as metastasis of the vertebrae or bone at the scull base [71].

The sensitizers in clinical practice such as Photofrin, 5-ALA and Foscan show efficacy in regard to cytotoxicity and gave proof of principle of the effect of PDT in neurooncology. Photodynamic treatment supported by several observational studies with combined total of $> 1{,}000$ patients and 3 RCT used PDT in GBMs. PDT was highly selective, safe, significantly improved good quality survival, and delayed tumour relapse ($p < 0.001$). Fluorescence image-guided surgery for maximum safe surgical resection achieves complete resection in > 65 % and prolongs tumour free survival ($p < 0.001$).

PDT is currently offered in only a few selected centres, although it is gaining acceptance as adjunctive treatment modality to conventional cancer therapies. The clinical potential and implementation of PDD and FGR has brought general PDT to a wider acknowledgement to the neurosurgical community and will increase the

awareness in neurosurgery. The data show that PDT especially in combination with PDD/FGR is a safe and an effective treatment for a second line therapy in neurooncology and has the potential to be the fourth mainstay in neurooncology besides surgery, chemo and radiotherapy.

References

1. Lacroix M, Abi-Said D, Fourney DR, Gokaslan ZL, Shi W, DeMonte F, Lang FF, McCutcheon IE, Hassenbusch SJ, Holland E, Hess K, Michael C, Miller D, Sawaya R (2001) A multivariate analysis of 416 patients with glioblastoma multiforme: prognosis, extent of resection, and survival. J Neurosurg 95:190–198
2. Kostron H (2010) Photodynamic diagnosis and therapy and the brain. Methods Mol Biol 635:261–280
3. Eljamel S (2010) Photodynamic applications in brain tumors: a comprehensive review of the literature. Photodiagn Photodyn Ther 7(2):76–85
4. Bechet D, Mordon SR, Guillemin F, Barberi-Heyob MA (2012) Photodynamic therapy of malignant brain tumours: a complementary approach to conventional therapies. Cancer Treat Rev. doi:10.1016/j.ctrv.2012.07.004
5. Eljamel SM (2008) Brain photodiagnosis (PD), fluorescence guided resection (FGR) and photodynamic therapy (PDT): past, present and future. Photodiagn Photodyn Ther 5:29–35
6. Castano AP, Demidova TN, Hamblin MR (2004) Mechanisms in photodynamic therapy: part one—photosensitizers, photochemistry and cellular localization. Photodiagn Photodyn Ther 1:279–293
7. Kostron H, Obwegeser A, Seiwald M (1996) PDT in neurosurgery; a review. J Photochem Photobiol, B 36:157–168
8. Fayter D, Corbett M, Heirs M, Fox D, Eastwood A (2010) A systematic review of photodynamic therapy in the treatment of pre-cancerous skin conditions, Barrett's oesophagus and cancers of the biliary tract, brain, head and neck, lung, oesophagus and skin. Health Technol Assess 14(37):1–288
9. Patrice T, Olivier D, Bourre L (2006) PDT in clinics: indications, results, and markets. J Environ Pathol Toxicol Oncol 25(1–2):467–485
10. Stylli SS, Kaye AH (2006) Photodynamic therapy of cerebral glioma—A review, Part I—A biological basis. J Clin Neurosci 13:615–625
11. Kostron H, Zimmermann A, Obwegeser A (1998) MTHPC-mediated photodynamic detection for fluorescence guided resection of brain tumors. Surgical-assist systems. In: Bogner SM, Charles ST, Grundfest WS, Harrington JA, Katzir A, Lome LS, Vannier MW, von-Hanwehr R (eds) SPIE proceedings-series. International-biomedical-optics-society, SPIE vol 3262. pp 259–264
12. Bogaards A, Varma A, Zhang K, Zach D, Bisland SK, Moriyama EH, Lilge L, Muller PJ, Wilson BC (2005) Fluorescence image-guided brain tumour resection with adjuvant metronomic photodynamic therapy: pre-clinical model and technology development. Photochem Photobiol Sci 4:438–442
13. Kennedy JC, Marcus SL, Potier RH (1996) Photodynamic therapy and photodiagnosis using endogenous photosensitisation induced by 5-aminolevulinic acid (ALA): mechanism and clinical results. J Clin Laser Med Surg 15:289–304
14. Pichlmeier U, Bink A, Schackert G, Stummer W (2008) Resection and survival in glioblastoma multiforme: an RTOG recursive partitioning analysis of ALA study patients. Neuro Oncol 10:1025–1034
15. Kostron H, Fiegele Th, Akatuna E (2006) Combination of FOSCAN® mediated Fluorescence Guided Resection and Photodynamic Treatment as new therapeutic concept for Malignant Brain Tumors. Laser Med 24:285–290

16. Zimmermann A, Ritsch-Marte M, Kostron H (2001) mTHPC-mediated photodynamic diagnosis of malignant brain tumors. Photochem Photobiol 74:611–616
17. Eljamel MS, Goodman C, Moseley H (2008) ALA and Photofrin® Fluorescence-guided resection and repetitive PDT in glioblastoma multiforme: a single centre Phase III randomised controlled trial. Lasers Med Sci 23:361–367
18. Kaneko S, ShírasakaT, Yoshimuzi T, Fujimoto S,Yamouchi T,Yoshimoto T, Tokuda K, Kashiwaba T, Kohama Y (2002) Fluorescence diagnosis and PDT using two types of photosensizer. In: Recent progress on clinical and basic research of ALA, Proceedings of 2nd international ALA symposium, Fukuoka, pp 17–24
19. Jori G (1996) Tumour photosensitizers: approaches to enhance the selectivity and efficiency of photodynamic therapy. J Photochem Photobiol, B 36:87–93
20. Allison RR, Downie GH, Cuenca R, Hu XH, Carter JH, Sibata CH (2004) Photosensitizers in clinical PDT. Photodiagn Photodyn Ther 1:27–42
21. Kessel D (2004) Photodynamic therapy: from the beginning. Photodiagn Photodyn Ther 1:3–7
22. Kostron H, Obwegeser A, Jakober R, Zimmermann A, Rueck A (1998) Experimental and clinical results of mTHPC (Foscan®)—mediated photodynamic therapy for malignant brain tumors. Optical methods for tumor treatment and detections: mechanisms and techniques in photodynamics therapy VII. In: Dougherty TJ (ed) International-society-for-optical-engineering, SPIE, vol 3247. Bellingham WA, pp 40–45
23. Obwegeser A, Jakober R, Kostron H (1998) Uptake and kinetics of C-14 labeled m-THPC and 5-ALA in C-6 rat glioma model. Br J Cancer 78:733–738
24. Mannino S, Molinari A, Sabatino G, Ciafrè SA, Colone M, Maira G, Anile C, Arancia G, Mangiola A (2008) Intratumoralvs systemic administration of meta-tetrahydroxyphenylchlorin for photodynamic therapy of malignant gliomas: assessment of uptake and spatial distribution in C6 rat glioma model. Int J Immunopathol Pharmacol 21(1):227–231
25. Johansson A, Palte G, Schnell O, Tonn JC, Herms J, Stepp H (2010) 5-Aminolevulinic acid-induced protoporphyrin IX levels in tissue of human malignant brain tumors. Photochem Photobiol 86(6):1373–1378
26. Beck TJ, Kreth FW, Beyer W, Mehrkens JH, Obermeier A, Stepp H, Stummer W, Baumgartner R (2007) Interstitial photodynamic therapy of non-resectable malignant glioma recurrences using 5-aminolevulinic acid induced protoporphyrin IX. Lasers Surg Med 39:386–393
27. Ritz R, Daniels R, Noell S, Feigl GC, Schmidt V, Bornemann A, Ramina K, Mayer D, Dietz K, Strauss WS, Tatagiba M (2012) Hypericin for visualization of high grade gliomas: first clinical experience. Eur J Surg Oncol 38(4):352–360
28. Rovers JP, Schuitmaker JJ, Vahrmeijer AL, Van-Dierendonck JH, Terpstra OT (1998) Interstitial photodynamic therapy with the second-generation photosensitiser bacteriochlorin in a rat model for liver metastases. Br J Cancer 77:2098–2103
29. Cole CD, Liu JK, Sheng X, Chin SS, Schmidt MH, Weiss MH, Couldwell WT (2008) Hypericin-mediated photodynamic therapy of pituitary tumors: preclinical study in a GH4C1 rat tumor model. J Neurooncol 87(3):255–261
30. El-Zaria ME, Ban HS, Nakamura H (2010) Boron-containing protoporphyrin IX derivatives and their modification for boron neutron capture therapy: synthesis, characterization, and comparative in vitro toxicity evaluation. Chemistry 16(5):1543–1552
31. Shliakhtsin SV, Trukhachova TV, Isakau HA, Istomin YP (2009) Pharmacokinetics and biodistribution of Photolon (Fotolon) in intact and tumor-bearing rats. Photodiagn Photodyn Ther 6(2):97–104
32. Kessel D, Oleinick NL (2009) Chapter 1 initiation of autophagy by photodynamic therapy. Methods Enzymol 453:1–16
33. Kamoshima Y, Terasaka S, Kuroda S, Iwasaki Y (2011) Morphological and histological changes of glioma cells immediately after 5-aminolevulinic acid mediated photodynamic therapy. Neurol Res 33(7):739–746
34. Coupienne I, Fettweis G, Rubio N, Agostinis P, Piette J (2011) 5-ALA-PDT induces RIP3-dependent necrosis in glioblastoma. Photochem Photobiol Sci 10(12):1868–1878

35. Kammerer R, Buchner A, Palluch P, Pongratz T, Oboukhovskij K, Beyer W, Johansson A, Stepp H, Baumgartner R, Zimmermann W (2011) Induction of immune mediators in glioma and prostate cancer cells by non-lethal photodynamic therapy. PLoS ONE 6(6):e21834
36. Zhan Q, Yue W, Hu S (2011) Effect of photodynamic therapy and endostatin on human glioma xenografts in nude mice. Photodiagn Photodyn Ther 8(4):314–320
37. Inoue H, Kajimoto Y, Shibata MA, Miyoshi N, Ogawa N, Miyatake S, Otsuki Y, Kuroiwa T (2007) Massive apoptotic cell death of human glioma cells via a mitochondrial pathway following 5-aminolevulinic acid-mediated photodynamic therapy. J Neurooncol 83(3): 223–231
38. Etminan N, Peters C, Ficnar J, Anlasik S, Bünemann E, Slotty PJ, Hänggi D, Steiger HJ, Sorg RV, Stummer W (2011) Modulation of migratory activity and invasiveness of human glioma spheroids following 5-aminolevulinic acid-based photodynamic treatment. Laboratory investigation. J Neurosurg 115(2):281–288
39. Muller PJ, Wilson BC (2006) Photodynamic therapy of brain tumors—A work in progress. Lasers Surg Med 38:384–389
40. Stupp R, Hegi ME, Gilbert MR, Chakravarti A (2007) Chemoradiotherapy in malignant glioma: standard of care and future directions. J Clin Oncol 25:4127
41. Stupp R, Mason WP, van den Bent MJ, Weller M, Fisher B, Taphoorn MJB, Belanger K, Brandes AA, Marosi C, Bogdahn U, Curschmann J, Janzer RC, Ludwin SK, M.Sc Gorlia T, Allgeier A, Lacombe D, Cairncross JG, Eisenhauer E, Mirimanoff RO (2005) European organisation for research and treatment of cancer brain tumor and radiotherapy groups and the national cancer institute of Canada clinical trials group. Radiotherapy plus concomitant and adjuvant. Temozolomide for glioblastoma. N Engl J Med 10:987–996
42. Kirveliene V, Grazeliene G, Dabkeviciene D, Micke I, Kirvelis D, Juodka B, Didziapetriene J (2006) Schedule-dependent interaction between Doxorubicin and mTHPC-mediated photodynamic therapy in murine hepatoma in vitro and in vivo. Cancer Chemother Pharmacol 57:65–72
43. Hornung R, Walt H, Crompton NE, Keefe KA, Jentsch B, Perewusnyk G, Haller U, Köchli OR (1998) m-THPC-mediated photodynamic therapy (PDT) does not induce resistance to chemotherapy, radiotherapy or PDT on human breast cancer cells in vitro. Photochem Photobiol 68:569–574
44. Chen Bin, Pogue BW, Hoopes PJ, Hasan T (2005) Combining vascular and cellular targeting regimens enhances the efficacy of photodynamic therapy. Int J Radiat Oncol Biol Phys 61:1216–1226
45. Ferrario A, Rucker N, Wong S, Luna M, Gomer ChJ (2007) Survivin, a member of the inhibitor of apoptosis family, is induced by photodynamic therapy and is a target for improving treatment response. Cancer Res 67:4989–4995
46. Fanuel-Barret D, Patrice T, Foultier MT, Vonarx-Coinsmann V, Robillard N, Lajat Y (1997) Influence of epidermal growth factor on photodynamic therapy of glioblastoma cells in vitro. Res Exp Med 197:219–233
47. Norum OJ, Selbo PK, Weyergang A, Giercksky KE, Berg K (2009) Photochemical internalization (PCI) in cancer therapy: from bench towards bedside medicine. J Photochem Photobiol, B 96(2):83–92
48. Hirschberg H, Zhang MJ, Gach HM, Uzal FA, Peng Q, Sun CH, Chighvinadze D, Madsen SJ (2009) Targeted delivery of bleomycin to the brain using photo-chemical internalization of Clostridium perfringens epsilon prototoxin. J Neurooncol 95(3):317–329
49. Mathews MS, Blickenstaff JW, Shih EC, Zamora G, Vo V, Sun CH, Hirschberg H, Madsen SJ (2012) Photochemical internalization of bleomycin for glioma treatment. J Biomed Opt 17(5):058001
50. Kostron H, Swartz MR, Miller DC, Martuza RL (1986) The interaction of hematoporphyrin derivative, light, and ionizing radiation in a rat glioma model. Cancer 57(5):964–970
51. Madsen SJ, Sun CH, Tromberg BJ, Yeh AT, Sanchez R, Hirschberg H (2002) Effects of combined photodynamic therapy and ionizing radiation on human glioma spheroids. Photochem Photobiol 76:411–416

52. Lyons M, Phang I, Eljamel S (2012) The effects of PDT in primary malignant brain tumours could be improved by intraoperative radiotherapy. Photodiagn Photodyn Ther 9(1):40–45
53. Mang TS (2004) Lasers and light sources for PDT: past, present and future. Photodiagn Photodyn Ther 1:43–48
54. Mang TS (2008) Dosimetric concepts for PDT. Photodiagn Photodyn Ther 5:217–223
55. Krishnamurthy S, Powers SK, Witmer P, Brown T (2000) Optimal light dose for interstitial photodynamic therapy in treatment for malignant brain tumors. Lasers Surg Med 27:224–234
56. Kaneko S, Kobayashi H, Kohama Y (1999) Stereotactic intratumoral photodynamic therapy on malignant brain tumors. Abstract, international symposium on photodynamic therapy in clinical practice, Innsbruck
57. Bisland SK, Lilge L, Lin A, Rusnov R, Wilson BC (2004) Metronomic photodynamic therapy as a new paradigm for photodynamic therapy: rationale and preclinical evaluation of technical feasibility for treating malignant brain tumors. Photochem Photobiol 80:222–230
58. Hirschberg H, Sørensen DR, Angell-Petersen E, Peng Q, Tromberg B, Sun CH, Spetalen S, Madsen S (2006) Repetitive photodynamic therapy of malignant brain tumors. J Environ Pathol Toxicol Oncol 25:261–279
59. Thompson MS, Johansson A, Johansson T, Andersson-Engels S, Svanberg S, Bendsoe N, Svanberg K (2005) Clinical system for interstitial photodynamic therapy with combined on-line dosimetry measurement. Appl Opt 1:4023–4031
60. Stummer W, Pichlmeier U, Meinel T, Wiestler OD, Zanella F, Reulen HJ (2006) Fluorescence-guided surgery with 5-aminolevulinic acid for resection of malignant glioma: a randomised controlled multicentre phase III trial. Lancet Oncol 7:392–401
61. Abbas S, Jerjes W, Upile T, Vaz F, Hopper C (2012) The palliative role of PDT in recurrent advanced nasopharyngeal carcinoma: case series. Photodiagn Photodyn Ther 9(2):142–147
62. Kaneko S (2008) A current overview: photodynamic diagnosis and phtodynamic therapy using 5-ALA in neurosurgery. JJSLSM 29:135–146
63. Stylli SS, Kaye AH (2006) Photodynamic therapy of cerebral glioma—A review Part II—Clinical studies. J Clin Neurosci 13:709–717
64. Marks PV, Belchetz PE, Saxena A, Igbaseimokumo U, Thomson S, Nelson M, Stringer MR, Holroyd JA, Brown SB (2000) Effect of photodynamic therapy on recurrent pituitary adenomas: clinical phase I/II trial–an early report. Br J Neurosurg 14:317–325
65. Triesscheijn M, Baas P, Schellens JHM, Stewart FA (2006) Photodynamic therapy in oncology. Oncologist 11:1034–1044
66. Sakai M, Fujimoto N, Ishii K, Nakamura H, Kaneda Y, Awazu K (2012) In vitro investigation of efficient photodynamic therapy using a nonviral vector; hemagglutinating virus of Japan envelope. J Biomed Opt 17(7):078002
67. Park EK, Bae SM, Kwak SY, Lee SJ, Kim YW, Han CH, Cho HJ, Kim KT, Kim YJ, Kim HJ, Ahn WS (2008) Photodynamic therapy with recombinant adenovirus AdmIL-12 enhances anti-tumour therapy efficacy in human papillomavirus 16 (E6/E7) infected tumour model. Immunology 124(4):461–468
68. Varma AK, Muller PJ (2008) Cranial neuropathies after intracranial Photofrin-photodynamic therapy for malignant supratentorial gliomas-a report on 3 cases. Surg Neurol 70(2):190–193
69. de Carvalho AC, Zhang X, Roberts C, Jiang F, Kalkanis SN, Hong X, Lu M, Chopp M (2007) Subclinical photodynamic therapy treatment modifies the brain microenvironment and promotes glioma growth. Glia 55(10):1053–1060
70. Jerjes W, Upile T, Betz CS, El Maaytah M, Abbas S, Wright A, Hopper C (2007) The application of photodynamic therapy in the head and neck. Dent Update 34:478–486
71. Burch S, London C, Seguin B, Rodriguez C, Wilson BC, Bisland SK (2009) Treatment of canine osseous tumors with photodynamic therapy: a pilot study. Clin Orthop Relat Res 22:44–47

Chapter 9
Photodynamic Therapy for Thoracic Oncology

Keyvan Moghissi and Ron R. Allison

Abstract Photodynamic Therapy (PDT) continues to evolve in the management of thoracic malignancies. The relative simplicity of this treatment, in combination with reliable tumour ablation, has allowed for function sparing treatment to become a reality for a worldwide audience. Of particular importance is the ability of PDT to offer primary or palliative therapy to a cohort of patients who may otherwise be without good treatment options. Most important is that PDT fits well into the current multidisciplinary approach to cancer care as PDT compliments surgery, chemotherapy and radiation therapy. This can only help our patients in their fight against the scourge known as cancer.

9.1 Introduction

The architecture of the chest is based on two bony pillars; one in front, the sternum, and the other behind, the vertebral column. The pillars are connected by a series of ribs. The bony framework of the chest thus constructed resembles that of a cage, the thoracic cage, which is covered with muscles, connective tissues and skin. The breasts are, in effect, a pair of glands within the anterior chest wall.

The thoracic cavity is comprised of three compartments:

- Two laterals, the pleural spaces, each of which accommodates one lung.
- The middle space, the mediastinum (mediastinal space), containing the heart and its great vessels.

K. Moghissi (✉)
The Yorkshire Laser Centre, Goole, UK
e-mail: kmoghissi@yorkshirelasercentre.org

R. R. Allison
20th Century Oncology, Greenville, NC, USA
e-mail: rallison@rtsx.com

M. H. Abdel-Kader (ed.), *Photodynamic Therapy*,
DOI: 10.1007/978-3-642-39629-8_9,

- The oesophagus and a number of other structures such as the thymus glands and a network of lymphatic vessels and intercalating nodes.

The three spaces within the chest are separated from one another by membranes which curtain them off into compartments.

The tissue component of any of the organs and structures within the thoracic cavity, and/or the chest wall, may develop malignant neoplastic changes, some of which are amongst the most important cancers in terms of incidence, difficulty of treatment and mortality. Lung cancer has the highest rank in incidence and death rate by cancer in men. The breast is the top of the list in women. Four cancers are particularly significant both from the point of view of relative inadequacy of the so-called standard cancer therapy methods: surgery, chemotherapy and radiotherapy, and also from the perspective of Photodynamic Therapy (PDT), these are:

1. Lung cancer
2. Oesophageal cancer
3. Mesothelioma
4. Breast cancer

9.2 PDT Mechanisms in Thoracic Oncology

The modus operandi of PDT is the activation of a photosensitiser (PS) by a light of specific wavelength. Oxygen is an important third party whose presence is essential in generating cytotoxic agents, notably singlet oxygen, which induces death of the treated cell. In the laboratory situation this is called the Photodynamic Reaction (PDR) or *Photodynamisch Wirkung* by the German discoverer of the process [1].

The mechanism of PDR in the laboratory setting is discussed amply elsewhere in this book. Translation of PDR to a clinical situation related to thoracic malignancies needs some elaboration.

As currently practiced clinical PDT in the thoracic region requires application of a photosensitizing agent, which is allowed time to accumulate in the tumour bed and also to clear normal tissues. Intense illumination is then applied as exclusively as possible to the tumour bed. The light energy activates the photosensitizing agent allowing for creation of the PDR which is highly toxic to the tumour and surrounding vasculature.

To better understand this complex interaction of drug, light and reaction pertaining to thoracic tumours we will elaborate on each of these three critical components.

Photosensitisers (PSs): By definition these are natural or synthetic substances that can create, what is termed, a "type II photochemical reaction". The end result is creation of singlet oxygen species which is a highly toxic free radical that can destroy cellular function. PSs may also create a type I reaction which results in toxic peroxidation. As will be detailed, many PS may also fluoresce which plays a great role in thoracic PDT [2–6].

Whilst thousands of structures may behave as a PS, only a handful have been approved for use in clinical PDT. Most are derivatives of porphyrins or dyes, both of which allow for high production of the type II reaction and generally also for fluorescence capability. For thoracic PDT several PS have become commercially available [2]. Potential benefits and consequences for these PS in thoracic PDT are now briefly detailed.

- *Photofrin*: This is the oldest and most common PS and remains the standard against which all newer PS are compared. Photofrin is a mixture of various hematoporphyrins and is available worldwide. The drug is infused, usually at 2 mg/kg, in an outpatient setting. About 48 h is allowed for the PS to concentrate in the tumour and clear normal tissue. Then illumination may be undertaken with highly reliable ablation of lesions within the treatment region. Photofrin is not the most rapid producer of the type II reaction so clinical treatment time is about 10–20 min per lesion. The treatment is generally painless. Unfortunately, Photofrin remains in most tissues, including the skin, for 4–6 weeks post infusion so sunlight precautions are critical to prevent severe sunburn during this period.
- *MACE*: This is a synthetic chlorin (plant porphyrin) that produces a high level of reaction so that treatment time can be only a few minutes. The drug also achieves high levels of tumour concentration only a few hours after infusion meaning that treatment can occur on the same day, which is very convenient. Photosensitivity remains for several weeks. Usually 3 mg/kg is infused.
- *Foscan*: This synthetic chlorin is the most potent of the current photosensitizers, where treatment of only a minute or two per lesion is required. However, because it is so potent, reflected light may have enough energy to activate the PS which can lead to treatment of inappropriate anatomy. Importantly, after the drug is infused into the patient, even room light may cause a severe photosensitivity reaction in exposed skin. Patients must, therefore, be kept in a dark room for the first 24 h after PS infusion (0.15 mg/kg). Treatment initiates about 4 days (96 h) post infusion. The treatment itself is relatively painful and anaesthesia should be considered.
- *ALA*: This is a pro-drug that is enzymatically converted to an active PS: PPIX. ALA has found utility in PDT since it can be formulated as a cream for skin PDT or as a pill for systemic PDT. In cream form ALA does not penetrate tissue deeply so it is an excellent therapy for superficial cutaneous lesions. Treatment can be the same day as cream application, but 24–48 h is required for systemic therapy (20 mg/kg oral dose). ALA can also be very painful during illumination.

Light Sources [7]: Each PS has its own characteristic intensity (fluence) and wavelength for activation; these are not interchangeable. Therefore, appropriate illumination equipment is required for each particular photosensitizer. The PS used in thoracic oncology activates in the red light spectrum (600 nm or greater). Red light penetrates tissues to perhaps 1 cm or more; so many endobronchial, oesophageal and cutaneous lesions are amenable to PDT illumination though those that are bulky may require several PDT sessions for treatment success. As will be

discussed, the light source may also be implanted into a bulky tumour. The goal in all cases is to achieve the correct intensity of light to the entire tumour, so that the PS can be activated for lesion destruction. However, the clinician does not want to illuminate regions without tumour as this will result in excess morbidity. Currently, light delivery comes in two categories. First are fibreoptics with diffusing tips which illuminate in all directions. Second are microlens fibreoptics which are forward illuminating, like a flashlight. Depending on availability and the clinical situation either or both fibreoptics may be employed in treatment. The light source itself may vary from intense incandescent or fluorescent bulbs to lasers. Currently, lasers are preferred as they can offer the optimal intensity and wavelength of light tuned to a particular PS. Recently, light emitting diodes, which are less expensive, have become available for many photosensitizers.

Photodynamic Reaction: This is the accumulation of light energy transfer to the photosensitizer. Upon successful activation by appropriate light energy and wavelength the PS will produce singlet oxygen. These singlet oxygen species are highly destructive. Tumour cell membranes and organelle membranes will be injured or destroyed leading to programmed cell death (apoptosis) and/or necrosis. In both cases tumour tissue can be eradicated but, clinically, the mechanism of cell death may be of importance. [4–6] Apoptotic death results in tumour dissolution with re-absorption. In contrast, necrotic death pathways result in release of cellular contents which may lead to cytokine release and immune response. This may have ramifications as this regional and immune response may lead to additional normal tissue injury, termed the bystander response. Similarly, singlet oxygen will also injure and destroy vascular membranes as the PS also accumulates here. This will lead to rapid loss of blood flow, stasis and clotting. The loss of blood supply will significantly enhance the ability of PDT to achieve complete ablation of tumour.

PS also accumulates, though to a lesser degree, in surrounding normal tissue. Therefore, it is critical to minimise illumination to these regions in order to avoid normal tissue injury. In clinical reality this is almost impossible to do as tumour and normal tissues intercalate. Yet by accurate and focal illumination normal tissue injury can be minimised.

Upon illumination the PDR occurs rapidly. During treatment, visible lesions turn dusky, hypoxic and often leak exudate. At the completion of the illumination session the physician should have visual confirmation of these changes. Normal surrounding tissue will also react, but less briskly. Significant tumour and normal tissue slough are a possibility, followed by healing. This tissue slough is generally of little consequence, except endobronchially when tissue slough can lead to pulmonary obstruction. To prevent this, all patients must undergo repeat bronchoscopy 48 h post PDT for pulmonary toilet [8, 9].

Fluorescent Detection: As the PS loses energy it can emit detectable light, termed fluorescence. Intentionally, fluorescing the PS by using lower energy light is termed fluorescent detection or photodiagnosis (PD). As PS accumulates in tumour, by intentionally fluorescing the tumour region it is possible to better demarcate lesions as well as detect lesions that were not visually obvious. Fluorescence is, therefore, a useful clinical tool to improve PDT both by localising the

regions to illuminate and also avoiding regions not requiring PDT. Further, loss of fluorescence after PDT treatment is correlated with treatment success and is thus a good means to assess if a lesion requires additional PDT after initial treatment illumination [4–6].

Clinical Procedure: For all patients it is extremely important to understand that skin photosensitivity initiates at PS application, not treatment. Patients who cannot abide by photosensitivity precautions should not be offered PDT.

As light source placement is critical to success, this is generally the most difficult aspect of PDT. Endobronchial or oesophageal lesions may be treated endoscopically in the vast majority of cases. The clinician should illuminate the entire lesion with as homogeneous an illumination as possible. Under-illumination will not create a sufficient PDR for success. Over-illumination may lead to unnecessary morbidity particularly to nearby normal tissues. For non-bulky lesions the clinicians may, if possible, choose between a diffuser and microlens. The lens may be focused on the tumour, minimising normal tissue illumination. [10, 11] The diffuser usually will lie over the tumour regions. Whilst this will maximise tumour illumination it also exposes surrounding normal tissues to the full light dose. In bulky lesions illumination may be more difficult due to anatomical issues. Here, diffusing fibres are often used inserted into the tumour mass to illuminate from the inside out. As most diffuser fibres will break upon excessive pressure, in these situations the tumour may be "opened" by tools such as the biopsy needle or use of laser to core an opening.

More peripheral lesions may be approached endobronchially by using magnetic guidance or through a VATS procedure. In all cases the concept is to try to bring the treatment light to an appropriate position to illuminate the tumour bed [12, 13].

Diffuse regions such as mesothelioma may require additional expertise for appropriate illumination. In these situations multiple lesions of fairly large volume may be treated, therefore, multiple lasers may be required. Further, to improve light distribution additional substances such as emulsion may be applied. This is further described in the Malignant Pleural Mesothelioma (MPM) Sect. 9.5.6.

Cutaneous lesions occurring in the chest wall have many treatment options. PDT can play a role since it can ablate lesions of various histologies including metastatic tumours. In each instance it is important to ensure that all lesions are homogeneously illuminated. As some patients may have 30–40 lesions, a system to ensure this, as well as the appropriate equipment is critical. This is further described in the chest wall involvement by local recurrence of breast cancer, of this text [14, 15].

It must be emphasised that in clinical situations the tools and parameters to assess the results of PDT are not similar to those which are used in the laboratory or even in some in vivo experiments which effectively measures PDR. That is to say that, in practice, laboratory and experimental work may not translate to the outcome in patients.

9.3 Lung Cancer (Bronchial carcinoma)

9.3.1 Introduction

Lung cancer has been one of the most important therapeutic challenges of the twentieth century. The development of pulmonary surgery culminating in the first pneumonectomy by Graham and Singer in 1933 [16] was hailed as the road to a new era of lung cancer treatment which could lead, it was hoped, to reversal of the poor outcome of the disease known for centuries. Unfortunately, in the following years, this proved not to be the case.

In 2008 some 1.6 million people were diagnosed as having lung cancer in the world. In the same year 1.3 million died from the disease [17]. Advances in surgery, radiotherapy and chemotherapy, referred to as standard cancer treatments, in the past 50 years have not translated to a significant amelioration of the outcome for lung cancer sufferers. Clearly, new methods of detection and a change of treatment ethos must seriously be considered in order to improve the situation.

9.3.2 Development of Broncho-Pulmonary Cancer

It is generally acknowledged that lung cancer develops in a stepwise fashion. This implies that, in response to different carcinogens, gradual aberrations occur in the molecular and genetic makeup of normal broncho-pulmonary cells. Initially, these changes are not reflected in the morphology of the affected cells. Continuation of carcinogenic exposure leads to microscopic morphological alterations of the affected cells at first characterised by "metaplasia". The next gradual steps in carcinogenesis become a crescendo of abnormal changes of the morphology and aggressive cell division from metaplasia, through various grades of dysplasia, to carcinoma in situ. As the name suggests, carcinoma in situ is a localised and superficial neoplastic lesion of bronchial epithelia which, as yet, has not penetrated deep below the mucosal surface. Deeper involvement beyond the epithelial surface results in yet further deterioration of the cells and tissues subjected to carcinogenesis. Local invasion and expansion results in lymphatic and extra pulmonary metastatic involvement and true generalised neoplastic disease. This sequence of events, initiated with molecular changes of the cells and ending with full blown invasive cancer and generalised neoplastic disease, has important diagnostic and therapeutic relevance.

Firstly, at the earliest stage of molecular events and even in the dysplastic morphological stages, cessation of the carcinogenic stimulus and local treatment can allow reversal of the process and a return to normal. At carcinoma in situ and local invasion stage interventional bronchoscopic methods specific to cancer, including lasers and PDT, may eradicate the disease. The success of local therapy methods, including surgical resection, becomes improbable as the tumour crosses the boundaries of "localness".

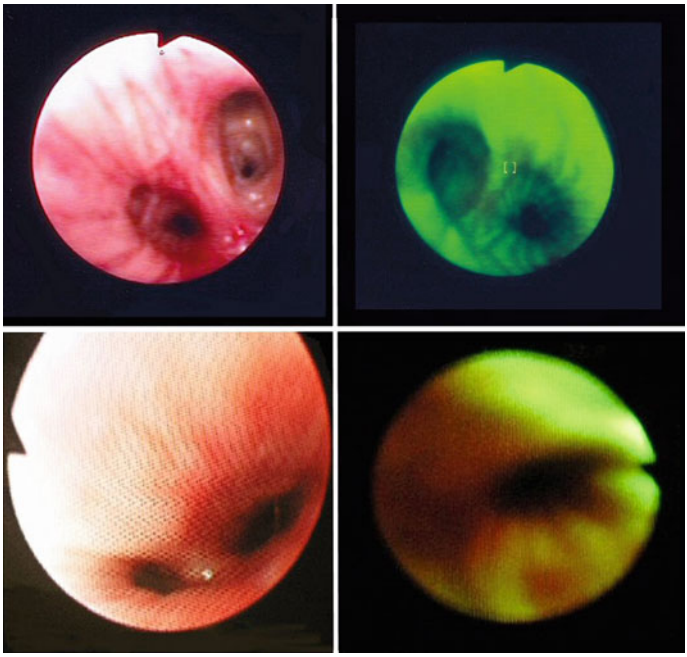

Fig. 9.1 **a** Appearance of normal bronchial mucosa at *white light* bronchoscopy. **b** Appearance of same area using *fluorescence light* (note *homogenous green*). **c** Appearance of *left lower* lobe bronchial mucosa at *white light* bronchoscopy. **d** Appearance of same area using *fluorescence light* (note *reddish brown* colour of early cancer)

An early diagnosis of molecular changes can be made using molecular/genetic methods identifying "markers". There are as yet no specific and reliable molecular markers for the early detection of lung cancer. However, bronchial pre and early neoplastic morphological changes may be visualised through bronchoscopic examination, particularly when a fluorescence method (autofluorescence bronchoscopy—AFB) is used instead of ordinary white light bronchoscopy [18, 19].

Standard bronchoscopic examination of the bronchial tree uses an electric generated (white) light which can reveal a tumour when it causes a raised mass of 2–3 mm. In contrast AFB, using a monochromatic light in the region of blue-ultraviolet wavelength, has several times more possibility of localising a superficial lesion, such an intra epithelial neoplasia and carcinoma in situ [18, 20] (Fig 9.1a, b, c, d).

9.3.3 Classification of Lung Cancer

Classification is a way of grouping different types of lung cancer into categories, allowing understanding and providing a universal language for communication amongst scientists and clinicians.

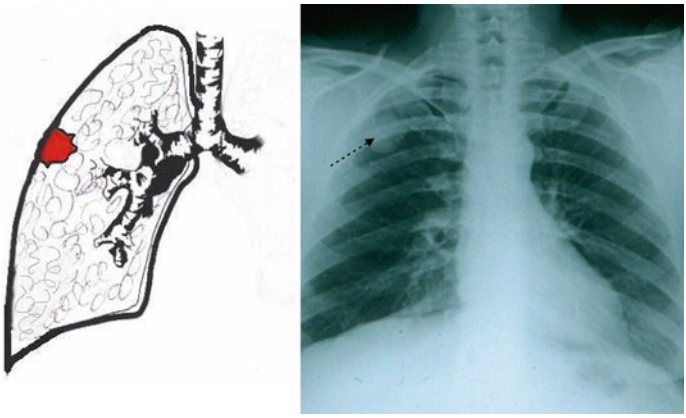

Fig. 9.2 Peripheral lung cancer: **a** diagram, **b** chest x-ray appearance

- *Histological classification* [21]: Lung cancers are classified according to their histological characteristics. The World Health Organisation (WHO) recognises principal histological types, squamous-cell carcinoma, adeno-carcinoma, large cell and small cell varieties. The three main histological types, other than small cell carcinoma, are collectively referred to as non-small cell lung cancer (NSCLC).
- *Topographical classification*: This is based on the area within the lung where the tumour has initially originated. In this respect some tumours (60 %) start within the airway (bronchial tree) and these are known as central type tumours. Some other tumours initiate in the substance of the lung; these are known as peripheral lung cancer (Fig. 9.2a, b).
- *Stage* (*TNM*) *classification* [22]: This is the most important of all classifications which arranges the cancer according to size and extent of local and distant spread and then attempts to correlate these parameters to survival outcome within a given treatment spectrum. By convention the stage classification uses acronyms: T (for tumour) its size and location graded by numbers 1–4, N (for lymph node involvement) and numbered from 1 to 3 according to location in the chest and M (for distant metastases) numbered according to their location and numbered 1–3.

TNM classification allows clinicians and pathologists to place a given cancer within a chart and give a rough prognosis; thus, bringing about a universal understanding. For instance a patient with a T4, N2, M2 lung cancer indicates an advanced cancer locally with serious lymph node spread and metastatic component.

9.4 PDT for Lung Cancer

After a long period of gestation and much laboratory work, clinical PDT emerged from the laboratory and became a therapeutic reality; in fact, it was over 30 years ago that the Japanese thoracic surgeon Hyata and colleagues at the Tokyo Medical University [23] carried out the first bronchoscopic PDT in a patient with early stage bronchial carcinoma who was otherwise unfit for surgical resection. The patient survived over 4 years, completely cancer free, and died from unrelated causes. During the 1980s and 1990s a considerable volume of work was carried out throughout the world. These clinical studies were responsible to define the indications and refine the methodology.

9.4.1 PDT Indications in Lung Cancer

Traditionally, at least during the past 60 years, the standard treatment for lung cancer has been formulated under the trio of surgery, radiotherapy and chemotherapy, solo or in concert. Progress in science and technology has allowed a number of newer methods to enter into the field of therapy of which the most promising in the past 25–30 years has been PDT.

It must be emphasised that PDT, like surgery, is essentially a local therapy and its use in lung cancer should be considered as local ablation of the tumour. It can, however, be used in conjunction with chemo-radiation to achieve local and general effects just as is the case for surgical resection of cancer.

PDT indications in lung cancer are:

1. In locally advanced endobronchial tumours. In such cases an endobronchial exophytic tumour causes collapse of an entire lung, or a major part of it, through blockage of the air conducting system. The role of PDT in these cases is to necrose the tumour allowing opening of the blocked airway [7, 24].
2. In early stage superficial endobronchial cancers in patients ineligible for surgical resection. PDT is used in such cases with curative intent [10, 25, 26].
3. In recurrent or metachronous tumours after previous major lung resection. This is an important indication of PDT since neither further surgery nor chemo-radiation would be of benefit, even if the patient was otherwise fit. This is because residual pulmonary function is impaired proportionally to the extent of the resection. Likewise, chemo-radiation, by inflicting collateral injury to the normal lung, further compromises the already impaired pulmonary function.
4. In peripheral lung tumours when the patient is unfit or unwilling to undergo surgical resection including minimal access surgery such as Video-Assisted Thoracoscopic surgery (VATS) [12, 13].

9.4.2 Methodology

- Pre-sensitisation: For all lung cancers, pre-sensitisation is carried out by IV administration of the drug. The PS licenced and most commonly used (at least in the western world) is Photofrin® (Porfimer Sodium).
- Illumination: Two types of illumination are used:

(a) Interstitial in which the cylindrical diffuser of the delivery fibre is placed within the mass of the tumour (Fig. 9.3).
(b) Surface illumination in which light exposure is carried out by placing the diffuser in proximity of the lesion (for example within the lumen of the bronchus). Alternatively, a delivery fibre with a forward projection is used (microlens) (Fig. 9.4).

The methodology in practice is summarised in Fig. 9.5

Bronchoscopic PDT is carried out under general anaesthetic using the rigid and/or flexible bronchoscope. The delivery fibre is introduced through the biopsy channel of the flexible bronchoscope Fig. 9.6 [7, 24, 27]. For bulky tumours the interstitial method of illumination is used employing 630 nm laser light. After appropriate exposure (standard of 200 J/cm) clearing is carried out. This involves removal of the necrotic tissues and debris followed by thorough bronchial washing with saline solution.

For superficial, early stage endobronchial tumours, surface illumination is used delivering 150–200 J/cm of the lesion according to thickness of the tumour (if this is known by imaging). Such patients with early cancer are usually submitted to surgical resection which is considered as the treatment of choice when their general condition and pulmonary function allow the undertaking.

About 2–3 h after recovery from the anaesthetic the patient can be discharged from the hospital.

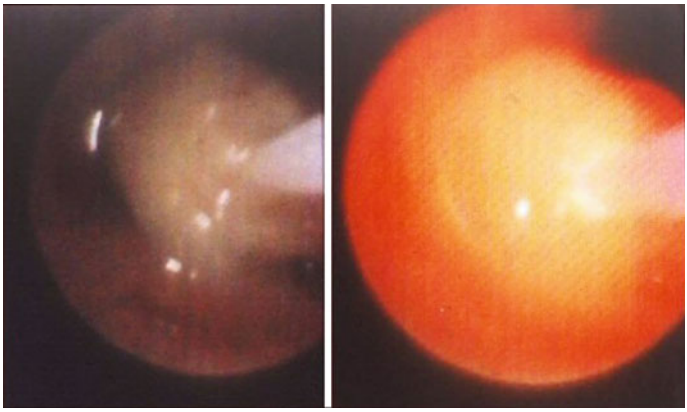

Fig. 9.3 Interstitial illumination: *left* fibre in the tumour with laser light off, *right* the same with the laser light on

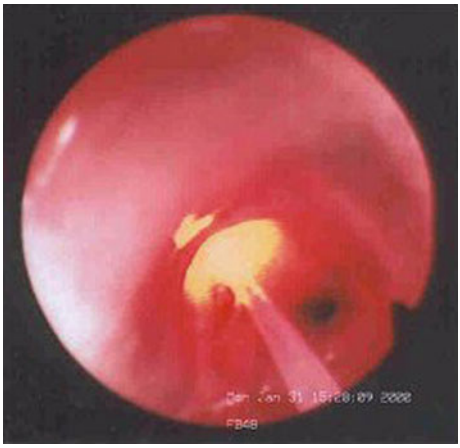

Fig. 9.4 Forward (superficial illumination)

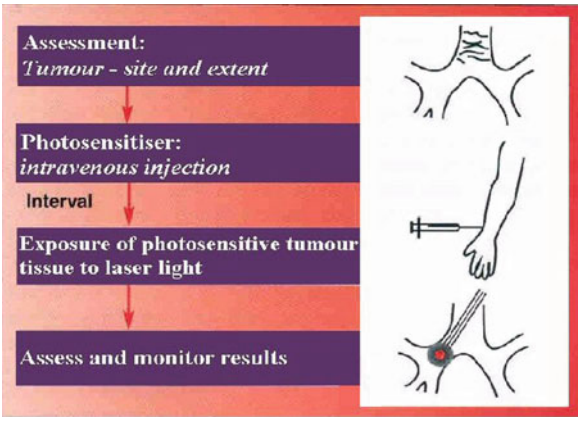

Fig. 9.5 Scheme of bronchoscopic PDT

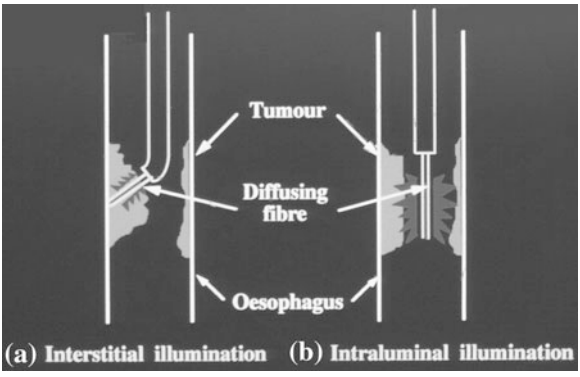

Fig. 9.6 Endoscopic (oesophagoscopy) illumination: *left* interstitial, *right* intraluminal

9.4.3 Results of PDT in Lung cancer

- Locally advanced:
  A number of authors have shown that PDT achieves its aim of palliation in patients who have significant endoluminal obstruction caused by exophytic tumour, particularly in the major airway (main stem or lobar bronchus). Symptomatic relief, both in terms of improvement in breathing and reduction of dyspnoea index, discontinuation of repeated chest infection, haemoptysis, cough and haemptysis.
  Symptomatic improvement is proportionate to re-canalisation of the airway, clearing of chest x-ray and improved spirometry [7, 23, 27, 28].
- Early superficial:
  There are a number of publications clearly indicating that in early neoplastic endobronchial lesions, long-term complete remission/response follows bronchoscopic PDT. Japanese clinicians, who from the start concentrated their efforts on treating such early cancers, offer PDT in selected patients as the primary treatment of choice on par with surgery. In effect they show that the results of PDT compare with the best results of surgical resection in patients with early stage endobronchial tumours [25, 27].
  Other workers, including this author, demonstrate that 5 years survival in such tumours is 65–67 % [10]. However, if the non-cancer deaths were to be taken into consideration the figure reaches to 70 %. In a highly selected patient population an 80 % five years survival has been reported [29, 30].
- Peripheral lung cancer:
  There is not much experience in the use of PDT in the substance of the lung. Such tumours cannot be accessed for illumination bronchoscopically. Some authors have used a trans-cutaneous approach under CT imaging [12]. Our group, with a small number of cases, advocates using a thoracoscopic approach under vision [13].

9.5 PDT for Cancer of the Oesophagus and Barrett's Dysplastic Mucosal Lesions

9.5.1 Introduction

Cancer of the oesophagus is one of the most distressing conditions which, worldwide, affects nearly 462,000 people annually and causes death in some 406,500 [17]. At its early stage, the condition escapes diagnosis since its initial symptoms are non-specific and, in many, by the time the disease is suspected and diagnosed, surgical resection and reconstruction, which is the treatment of choice, cannot be applied with curative intent. In effect over 50 % of cases are inoperable at presentation and of these at most 20 % will have an early stage cancer suitable

for surgery with curative intent [31]. However, 75–80 % of patients with stage I (mucosal cancer) could have a chance of 5 years or more survival when operated by an experienced team. [32–34].

Over the past 50 years the standard method of treatment for oesophageal cancer has been formulated, by tradition and experience, to be the trio of surgery, radiotherapy and chemotherapy in different combinations. In the absence of a validated screening programme for early detection, and despite the considerable advances in diagnostic methods, and in each of the three standard treatment methods, the outcome from the patient's perspective has hardly changed and remains poor. For every 100 patients diagnosed, only 10–15 will have a chance of surviving more than 5 years. However, the concerns and problems for clinicians involved in the treatment of oesophageal cancer, do not totally relate to early diagnosis of the disease for which surgical resection remains the mainstay of therapy. Therapeutic and management problems relate to finding the best therapy which can be applied to the overall majority of patients who, at presentation, are at an advanced stage of the disease which is not oncologically suitable for operation, and for the cohorts who are oncologically suitable for surgical treatment but otherwise inoperable because of their general condition and/or comorbidity.

In the mid twentieth Century a number of minimally invasive methods of treating cancer of the oesophagus became available with the aim of relieving dysphagia, which is distressing and eventually responsible for nutritional deficiencies. Being unable to swallow solids or liquids and, in the course of time even saliva, for patients with advanced oesophageal cancer is distressing enough. The inability to ingest medications (including analgesics) is an added therapeutic problem not shared with many other equally distressing cancers.

From its inception PDT became one of the important methods of therapy for patients with severe dysphagia caused by the protrusion of tumour into the oesophageal lumen. Although PDT was initially used for symptom relief in these patients, in the course of time a number of other indications of PDT for oesophageal cancer evolved.

9.5.2 Current Indications of PDT in Oesophageal Cancer

PDT indications in oesophageal cancer are:

1. Locally advanced disease.
2. Early stage cancer.
3. Miscellaneous indications of PDT in Oesophageal cancer.

9.5.2.1 PDT in Locally Advanced Cancer of the Oesophagus

This concerns cases in which the tumour presents as a mass protruding within the lumen of some part of the oesophagus causing dysphagia (swallowing difficulties)

of different scales, usually III–IV (I being difficulty with solids and IV being total dysphagia even to saliva) [35]. Many such patients will have lymph node involvement and possibly metastases in the liver and other organs. The primary aim of treatment is palliation of dysphagia allowing patients to swallow normal consistency food or at least up to and including semi-solids.

9.5.2.2 PDT for Early Stage Cancer

Patients with early oesophageal cancer usually do not have endoluminal lesions; therefore, they do not present with dysphagia at the initial phase of the development of their tumour. In fact they may be asymptomatic and have been diagnosed in the course of investigations for indistinct upper gastro-intestinal tract symptoms, perhaps during a fortuitous endoscopy and biopsy for a different condition. In the normal way such patients are good subjects for resectional surgery following further investigation. Nevertheless, oesophagectomy is a major undertaking and some patients will be ineligible for the surgical treatment. In this cohort of patients, PDT has an important indication and is a worthwhile undertaking [36].

9.5.2.3 Miscellaneous Indications of PDT in Oesophageal Cancer

This group includes a number of heterogeneous indications:

(a) Local recurrence at the site of anastomosis after oesophagectomy and reconstruction of the upper alimentary tract.
(b) PDT for blockage of oesophageal stent by tumour re-growth.
(c) PDT as salvage for local failure after chemo-radiation therapy (RCT).

9.5.3 Methodology [37, 38]

- Pre-sensitisation: Review of the literature indicates that an overall majority of clinicians consider that the preferred methodology for PDT of oesophageal cancer is systemic (IV) administration of PS followed by laser light illumination. Most clinicians, including the authors, use Photofrin (Porfimer sodium) which is administered 24–72 h prior to endoscopic illumination. Photofrin is activated by 630 nm light which is delivered through an optical fibre, endoscopically delivered.
- Endoscopic Illumination:

(a) For most locally advanced tumours with a bulky mass of exophytic lesion, the interstitial method of illumination is carried out (Fig 9.6). Using this method the cylindrical diffusing end of the light delivery fibre is inserted into the mass of tumour. This permits a regular delivery of the light within a radius of 7–10 mm.

In cases where the mass of the tumour is involved circumferentially in the oesophageal wall, illumination will have to be intraluminal as shown in Fig. 9.6.

Experience has shown that a light dose of 200 Joules/cm is appropriate for optimal illumination. This is made up of 400 mW for the length of the lesion.

(b) Illumination for superficial mucosal lesions is usually carried out via intraluminal illumination. Although the standard dose is indicated by many of the clinicians and scientists to be 200 J/cm of the lesion, in practice this can be 100–150 J/cm of lesion as, in most cases, there are planned or unplanned areas of illumination overlap.

Whilst clearly it is possible to perform endoscopic illumination in patients under topical anaesthetic and sedation, we prefer to carry out the procedure under general anaesthetic. This allows better control by the operator and focusing on the illumination process rather than the comfort of the patient. Oesophagoscopic PDT is usually undertaken as a day case procedure.

9.5.4 Results of Endoscopic PDT for Oesophageal Cancer

Adverse events:

- Death attributed to PDT is extremely rare.
- Uncommon adverse events reported in the literature are pain and oesophagitis which may last for a few days leading to ulceration and haemorrhage.
- Haemorrhage, requiring blood transfusion, and perforation are extremely rare.
- Photosensitivity skin reaction (burn) is the commonest of the adverse events. However, the incidence is dependent of the type of the PS used and the level of experience and management skill of the PDT team. On the whole Photofrin needs a lengthier clearance time from the body and skin than ALA. However, the range of photosensitivity skin reaction reported in the literature for Photofrin® PDT is reported to be between 0 and >35 %. At the Yorkshire Laser Centre, where the majority of PDT cases use Photofrin®, photosensitivity in its milder form has never been >5 % and for the past 2–3 years was 0 %.
- Stricture formation is the most serious of complications. Its incidence is reported to be higher in patients undergoing PDT with the use of Photofrin® (about 23 %) than for ALA (about 8 %). The records of the YLC related to stricture following PDT in early cancer and Barrett's mucosa with HGD stands at 8 %.

9.5.4.1 Results in Locally Advanced Disease

The aim of these cases is palliation of symptoms, essentially that of dysphagia. Necrosis of the obstructing tumour allows recanalisation thus permitting amelioration of swallowing. Figure 9.7 shows the change of dysphagia scale 6 weeks

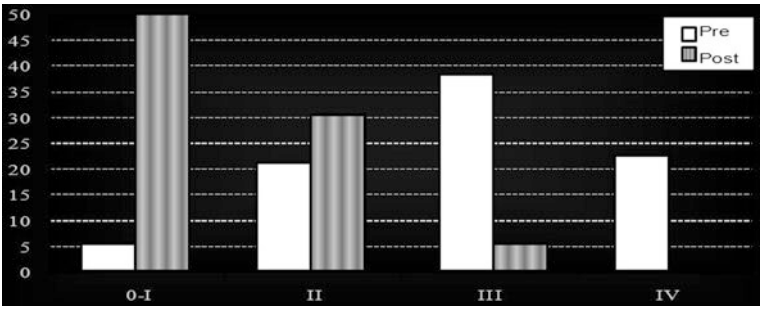

Fig. 9.7 Changes in dysphagia scale resulting from endoscopic PDT in locally advanced cancer of the oesophagus

after endoscopic PDT in large series of patients [37, 39, 40]. The relief of dysphagia is accompanied by improvement in performance status and nutritional status of patients. Although only a small proportion of patients with bulky endoluminal tumour will have complete response in the pathological sense, with macroscopic and microscopic evidence of clearance of the tumour, after endoscopic PDT the majority have important partial response allowing the passage of solid and liquid through the oesophagus to the stomach. Objectively this can be shown by endoscopic examination and contrast study.

9.5.4.2 Results of Endoscopic PDT in Early Stage Cancer

The aim of PDT in early stage cancer as previously stated is survival benefit, a true oncological treatment of an early stage cancer in patients who are ineligible for surgical resection. This is an area of increasing interest since oesophagectomy, which is the prime option for such patients, may not be a practical proposition for some whose general condition puts them into the category of inoperability because of the prohibitive risk of surgery in their case.

Personal experience and the review of the relevant literature indicate that PDT can achieve the expected long survival [41, 42]. In a group of 40 patients with clinical stage I oesophageal cancer who were ineligible for surgical resection on account of high operative risk and important co-morbidity, over 50 % survived 5 years or more; if non-cancer mortality were to taken into account, the figure rose to over 60 %. Similar results have been reported by other authors [42–44].

9.5.4.3 Miscellaneous Indications of PDT

(a) Local recurrence after oesophagectomy and reconstruction can be due to a variety of reasons, such as microscopic involvement of the oesophageal margin of resection, pre-existing high grade dysplasia (HGD) degeneration to

carcinoma, co-existence of cancer with HGD, missed or misinterpreted biopsy specimen, and true de novo development of tumour at the site of the anastomosis. All large published series show a few of such cases which can pose therapeutic dilemma [31, 45–48]. PDT is a suitable method of therapy for these patients.

(b) PDT for blockage of oesophageal stent by tumour re-growth: Over and under growth of tumour above or below the stent is not unusual. Not is in-growth of tumour within the coils of some uncovered stents. In either circumstance, PDT is a very suitable method to be used for re-canalisation of the lumen of the stent [39, 41].

(c) PDT as salvage for local failure after chemo-radiation therapy: this concerns two categories of patients:

- Patients who are offered chemotherapy to down-stage their cancer prior to surgery. A number of such patients, either by intention or due to deterioration of their general, haematological and/or nutritional state cannot complete the treatment, or even the chemotherapy part of the package. These patients are difficult to treat and PDT is another indication which can help at least some with better quality of life (QOL) and survival.
- Some patients with early cancer are offered, or opt to have CRT instead of or in addition to surgery. Failure of treatment means that they are at risk of expansion or upgrade of the cancer to higher stage. PDT is shown to be an effective mode of therapy in such patients [49, 50].

9.5.5 PDT in Barrett's Oesophagus

9.5.5.1 Introduction

Barrett's oesophagus refers to a condition in which a variable length of the mucosal lining of the lower part of the oesophagus (over 3 cm above the gastro-oesophageal junction) is covered by columnar epithelium of either gastric or intestinal type instead of the usual squamous variety (Fig. 9.8). Norman Barrett, a British thoracic surgeon, who initially described the condition, thought that the abnormal mucosa was congenital in origin [51]. It later became apparent that the abnormal mucosal lining was an acquired occurrence resulting from gastro-oesophageal reflux [52, 53]. When such a columnar (metaplastic) epithelial-lined mucosa is repeatedly exposed to gastric content with its high acid component, by episodes of gastro-oesophageal reflux, mucosal injuries characterised by inflammation, ulceration and scarring may develop. In some cases, over time, the injured cells of the mucosa start a stepwise morphological pattern with parallel behavioural changes. These changes are referred to as dysplasia which can be of different degree; namely low, moderate and high grade. Morphological and

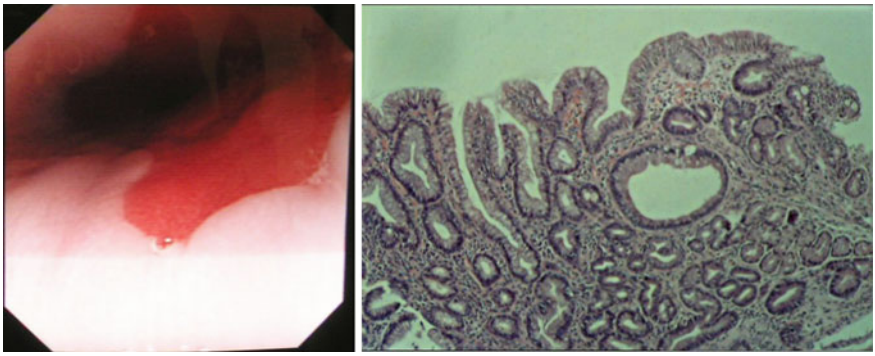

Fig. 9.8 *Left* oesophagoscopic appearance of metaplastic Barrett's mucosa (*white area* normal squamous epithelial oesophageal mucosa, *red area* metaplastic columnar mucosa). *Right* histology of a biopsy showing metaplastic intestinal Barrett's mucosa

histological crescendo changes are akin to what have already been described in the section of lung cancer under Development of Lung cancer. In short, Barrett's metaplastic mucosa is predisposed to changes which could progress to HGD. In terms of cellular abnormalities this approaches an early cancer (adenocarcinoma) of the oesophagus.

It is generally accepted that patients with metaplastic Barrett's mucosa have a slightly higher risk of developing oesophageal cancer than the normal population. However, by the time the mucosal transformation reaches to HGD, the possibility of cancer formation is considerably greater. Indeed, based on experience, some authors [45–48, 54] including these authors, believe that 30–40 % of patients diagnosed with Barrett's mucosa with HGD are harbouring an early intra-mucosal or even sub-mucosal cancer.

It, therefore, follows that many surgeons consider that persistence of HGD in a long segment of Barrett's mucosa warrants investigation and oesophagectomy and reconstruction of the oesophagus. Others argue that such a major undertaking is only justified in cases showing histologically proven characteristics of cancer in a biopsy sample.

The advent of PDT as an oncological therapeutic method has only expanded the debate.

9.5.5.2 Indications of PDT in Barrett's Oesophagus

It is generally agreed that patients with metaplastic mucosa but without HGD should be followed up by endoscopic surveillance and treated with anti-reflux medication and/or surgical procedure to prevent continuing reflux of the gastric content into the oesophagus with its unpleasant symptomology. Without an anti-reflux procedure, the frequency of such surveillance is debatable.

In the case of Barrett's mucosa with HGD, therapeutic opinions are divided. Many experienced surgeons would opt for surgical resection and reconstruction of

the oesophagus in young and fit patients, arguing that Barrett's Mucosa with HGD is a carcinoma in waiting if it is not already a cancer [45, 46]. Others believe that it is unjustifiable to undertake the major operation of oesophagectomy, with its operative mortality and post-operative morbidity, ignoring considerable advances made in recent years in endoscopic therapeutic methods. Should the operative strategy be adopted, surgery should be undertaken by a team with experience and high throughput [54]. They prefer to resort to suppression of gastric acid content by proton pump inhibitor (PPI) medication and continuing surveillance. PDT has introduced a third therapeutic option allowing a high proportion of patients to be treated endoscopically. The personal experience of these authors suggests that:

- One should consider the surgical option in a fit patient with HGD associated with long standing Barrett's mucosa. Alternatively, in such a patient, one could carry out one endoscopic PDT cycle and later re-evaluate the situation endoscopically and with appropriate imaging (CT scan).
- Depending on the level of response to endoscopic PDT, one may continue with a further cycle if downgrading of dysplasia has occurred.
- When, and if, there is no change in the grading of dysplasia, surgical resection should be considered unless there is a high risk of operative mortality and/or post-surgical morbidity such that affects the QOL.

9.5.5.3 Methodology

- Pre-sensitisation: *Photofrin*® is the most frequently employed PS in BO. It is administered at the dose of 2 mg/kg body weight intravenously. 5-ALA has been used by some investigators in varying dose 20–60 mg/kg body weight taken orally. Foscan (mTHpc) has also been tried in a small number of patients at the dose 0.15 mg/kg/bw [55].
- Illumination: Light is delivered via an optical fibre which is placed into the lumen. Some authors use a nude diffuser end of the optical fibre directly into the lumen. Others use a fabricated balloon or applicators which have been tested in respect of their light transmission. The light dose depends on the type of applicator and the PS being used as well as the experience of the operator.

9.5.5.4 Results

Complete response:

Eradication of HGD is the aim of all endoscopic procedures including PDT with whichever PS. Review of the literature places the success rate in large series between 20 and 77 % after a year. Despite many trials, randomised or otherwise, the position of PDT in Barrett's mucosa with HGD must be viewed as a method

which can be used in selected patients by clinicians experienced with all aspects of the treatment of the condition.

In the absence of convincing evidence, the choice of PS should be that with which the operating practitioner is familiar and can achieve the best results and used in the context of clinical trials protocol.

Finally, on the subject of Barrett's mucosa, we believe that since metaplastic mucosa is in the first place produced by gastro-oesophageal reflux, an anti-reflux operation and/or non-surgical mechanism should always be considered as part of the endoscopic treatment package.

9.5.6 PDT in Diffuse Malignant Pleural Mesothelioma

9.5.6.1 Introduction

The pleura is a thin membrane which envelops the lung, covering its external surface (visceral pleura) and then reflects on itself as one continuous sheet to cover the inner surfaces of the chest wall (parietal pleura). It is smooth and shiny and its function is to facilitate movement of the lungs during respiration and to prevent friction when the lungs change their volume and come into contact with the chest wall during inspiration and expiration.

Diffuse MPM is a slow growing tumour which arises from mesothelial cells which, in turn, are the basic structural cells of the pleura. The tumour spreads locally in all directions to involve the whole of the pleural membrane of the inner chest wall (parietal pleura) as well as the outer surfaces of the lung (visceral pleura) (Fig. 9.9). Distant metastases are uncommon. MPM is essentially a local

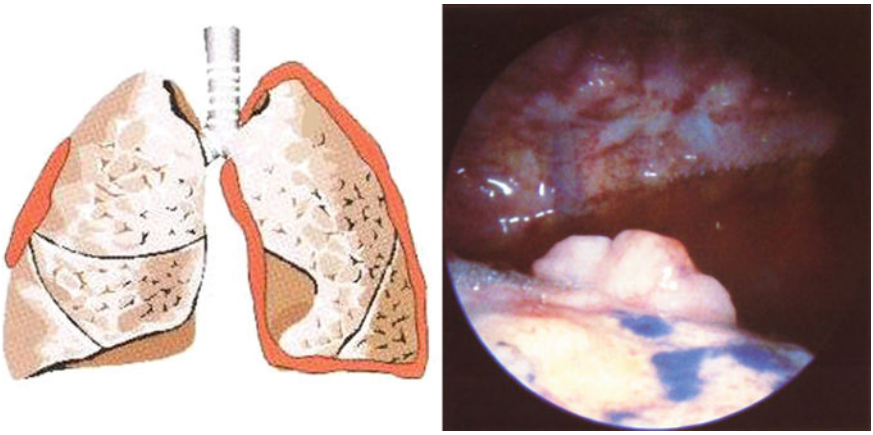

Fig. 9.9 *Left* schematic diagram showing the involvement of the *right* lung and the *inner left* chest wall by diffuse malignant pleural Mesothelioma (*MPM*). *Right* thoracoscopic view of the pleural space showing involvement of the chest wall (*bottom*) and the lung involvement (*top*) by MPM

disease and the cause of death usually relates to respiratory insufficiency. The characteristic gross appearance of the "en bloc" pleura-pulmonary resection or post-mortem specimen is one of encasement of a compressed lung beneath a thick and rigid sheet of tumour resembling a spongy cake (the lung) covered all around by thick layers of icing (pleural tumour).

The disease is usually caused by exposure to asbestos dust or fibres and manifests itself after a long period (sometimes >30 years) after exposure. Its insidious evolution over many months makes early diagnosis an incidental finding based on a high index of suspicion.

Symptoms are gradual, initially presenting with increasing shortness of breath due to the development of diffusely thickened pleural membrane thus encasing the underlying lung which is practically crushed under the unyielding and hard sheet of mesothelioma. Pleural effusion, associated with pain, appears as the disease progresses.

Diagnosis is reached by radiology and biopsy of the pleural membrane and cytological examination of the pleural fluid.

Treatment:

There is no generally agreed standard treatment for MPM. When treated for symptom relief and with supportive measures, the median survival for a patient with MPM is variously reported to be between 6 and 17 months [55–57] depending on the stage of disease at presentation. Thus far, none of the standard cancer therapy methods, when used in their single modality protocol, have shown to significantly influence the outcome of the disease over and above its natural history and what is achieved through non-specific supportive treatment [58–62]. Therefore, effort is being made to develop multi-modal regimes [63, 64]. Surgical treatment of total or partial de-bulking, forms the fundamental part of multi-modal therapy. Extra pleural pleura-pneumonectomy was introduced in the 1950s. However, surgical operation and adjuvant chemo-radiotherapy have shown to offer survival benefit [65, 66].

Early in the development of PDT, its potential to treat a wide variety of malignant tumours were investigated by Dougherty et al. [67]. Considering that MPM is essentially a localised disease and that PDT is also essentially a local treatment, it seems reasonable to use PDT to treat MPM.

9.5.6.2 Role of PDT in MPM

The role of PDT in MPM is evolving and, so far, much effort has been directed towards establishing credible methodology. Review of the literature [68] indicates that PDT has been tried intra-operatively (SURG-IOP-PDT) in conjunction with surgery ± chemo-radiation therapy. In effect all investigators have carried out: a ***surgical procedure*** followed by ***an intra-operative PDT*** and have introduced chemo-radiation before or following the "Surgery-PDT duo".

The basic structure of the Surgery-and Intra-Operative PDT (SURG-IOP-PDT) protocol is based on:

- Administration of the PS is prior to surgery.
- Operation scheduled to be carried out at an optimal time between drug administration and illumination, appropriate to the particular PS.
- Surgical operation with the objective of *de-bulking*; excision of the visible tumour partially or totally macroscopically at operation.

A variety of surgical operations have been used within the Surg-IOP-PDT ensemble: partial pleurectomy (decortications), radical pleurectomy (RP), simple pleuro-pneumonectomy (resection of the lung and pleura) en-block, and radical pleuro-pneumonectomy (excision of the lung, pleura, diaphragm, and pericardium).

Tri-modality treatment involving radical extra pleural pneumonectomy, radiotherapy and chemotherapy which was championed by Sugarbaker and colleagues [69], has received enthusiastic reception by some thoracic surgeons [70, 71]. However, in the last few years, the idea of Tri-modality has been abandoned by many in favour of the principle of pulmonary parenchyma preservation to which PDT is added with/without chemo-radiation component [68]. Yet it is still with tri-modality treatment that the best survival outcome is achieved, though with the penalty of long hospitalisation and an inferior QOL.

Friedberg recently published some interesting results showing that following parenchyma-saving surgery of RP (macroscopic clearance of tumour) and PDT, there is advantage of better QOL than that offered by more radical surgery added to by survival benefit [72, 73].

The struggle to find a solution to MPM treatment goes on within and without the framework of PDT. Review of the literature concerned with the use of PDT in MPM [68] and further updates [73] suggest that PDT does have a role for this disease.

9.5.6.3 Methodology

Pre-sensitisation:

Photofrin® (Porfimer Sodium) has been used most frequently at the dose of 2 mg/kg/bw in a majority of cases. Foscan® (mTHPC) has also been tried in a few series but with more complications [68].

Illumination:

The choice of light source is not an issue since each PS has its defined light with specific wavelength which activates the PS. However, the major issue resides with the device(s) that can be used to deliver the light and to distribute it within the vast and multi-facetted hemithorax, destroying the tumour and preserving the rest of the structure. Both theoretically and practically, there are a number of major issues to be resolved concerning uniform illumination. In this regard some manufacturers have been working to develop fibreoptic fabrics to better distribute the light within the thorax.

Light dose is yet another unresolved issue:

The latest in the unceasing efforts to develop PDT in MPM is reflected in a recent publication by Friedburg [74] in which 38 patients with MPM underwent RP and intra-operative PDT. A total of 35 also received systemic therapy. The median overall survival for patients with epithelial subtypes of cancer was nearly 3 years. This was despite the fact that these overall survival results did not translate to improved progression-free survival. This might, however, be attributed to the conservation of the lung in patients undergoing RP and IOP, instead of pleura-pneumonectomy.

What transpires from a review of the literature is that RP ± IO PDT is attended by survival benefit even when the disease-free period had not been improved.

9.6 PDT for the Chest Wall Recurrence of Breast Cancer

PDT is sometimes employed for chest wall recurrence from breast cancer [14, 15]. This usually applies to some patients with a biopsy proven tumour that is actively progressing locally on the chest wall despite previous attempts at salvage with various chemotherapeutics, further surgery and additional radiation therapy. At that point treatment options are very limited. Lesions that are not controlled will enlarge, become painful, fester and ulcerate often with a foul smell, leading to a diminished QOL. PDT may be an option.

Amongst the earliest trials with Photofrin PDT were patients with cutaneous recurrence from breast cancer. Various drug and light doses were delivered. It was evident that the usual 2 mg/kg was able to ablate these lesions but wound healing was difficult, probably due to the patient undergoing previous extensive surgery, chemo and radiation. Several investigators then employed lower drug doses; 0.8 mg/kg appeared to offer a high degree of efficacy in terms of lesion ablation and, as important, at this dose wound healing was to be expected. Essentially, for chest wall recurrence from breast cancer, low dose Photofrin PDT replaces a non-healing, tumour-infested wound with a wound that is sterilised of tumour and will eventually heal.

It is important to select patients carefully and to evaluate the depth and the extent of cancer infiltration. The length of time it takes to heal appears to relate to the volume of tissue requiring PDT as well as the volume of the actual tumour. Often these lesions are multifocal and may become confluent, requiring a large volume of skin to be illuminated. In these cases wound healing may take weeks if not months. Small-defined cutaneous lesions (<1 cm) can heal rapidly, so earlier intervention will improve the outcome for PDT in this group of patients. Unfortunately, most patients are considered for PDT after they have failed all other options and their lesions may be too large for PDT to offer a high chance of

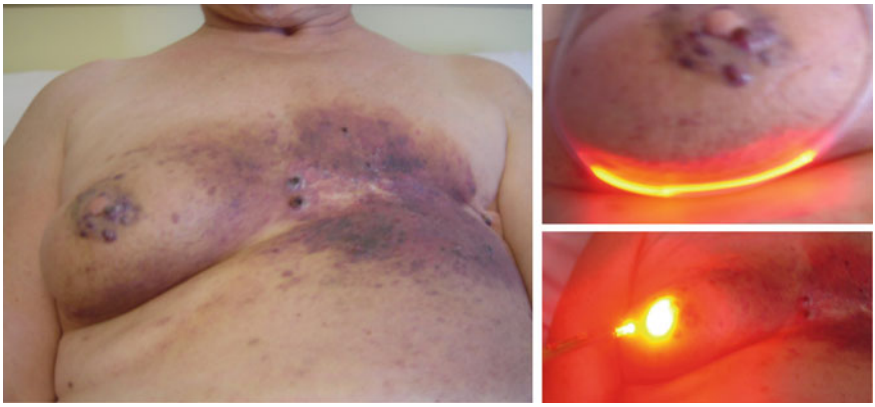

Fig. 9.10 *Left* patient with recurrence of breast cancer following chemo/radiation. The *left breast* has been removed and the *right breast* shows tumour around the mamilla and submammary area. *Right* top and *bottom* show simultaneous illumination using two lasers for the *right breast* tumours

success. In selected individuals several PDT sessions may be required. Further, for patients who have responded well to PDT but have developed new cutaneous lesions, additional PDT sessions are possible and often successful.

As these patients often have multiple and large volumes requiring illumination it is critical to have the appropriate equipment and staff. This might require multiple lasers and microlens available for therapy (Fig. 9.10). With Photofrin PDT these out-patient treatments may stretch many hours and nursing must be available. A means to demarcate the area requiring therapy and also an ability to annotate which areas have been illuminated is also a necessity. A map of the treatment volume, as is often employed in Dermatology, is suggested. Appropriate eye protection for patient and staff is mandatory.

Generally, by the end of the PDT sessions, cutaneous lesions take on a dusky appearance and also begin to weep. Within 48 h most lesions appear necrotic. Often an eschar will form over larger volumes of illuminated tissue. In many cases a slow but steady healing will take place. Less intervention to the wounds is best. Most patients should be given a weeks supply of narcotic pain medication, though in many cases after PDT, the chest wall is less painful as the tumours involutes.

Given the relative complexity of treatment, the requirement for multiple lasers and staffing issues, chest wall PDT requires a multidisciplinary approach to encompass not only therapy but also the healing of these often extensive, highly symptomatic lesions. The use of PDT for primary treatment of breast cancer is possible but should be part of an IRB approved treatment protocol as this is not considered standard care.

References

1. Von Tappeiner H (1904) Jodlbrauer Auber die wirkung der photodynamischen stoffe auf protozoenund enzyme. Arch Klin Med 80:427–487
2. Allison RR, Downie GH, Cuenca R, Hu XH, Childs CJH, Sibata CH (2004) Photosensitizers in clinical PDT. Photodiagn Photodyn Ther 1:27–42
3. Castano AP, Demidova TN, Hamblin MR (2004) Mechanisms in photodynamic therapy: part one—photosensitizers, photochemistry and cellular localization. Photodiagn Photodyn Ther 1:279–293
4. Castano AP, Demidova TN, Hamblin MR (2005) Mechanisms in photodynamic therapy: part two—cellular signalling, cell metabolism and modes of cell death. Photodiagn Photodyn Ther 2:1–23
5. Demidova TN, Hamblin MR (2005) Mechanisms in photodynamic therapy: part three—photosensitizer, pharmacokinetics, biodistribution, tumour localization and modes of tumour destruction. Photodiagn Photodyn Ther 2:91–106
6. Allison RR, Moghissi K (2013) Photodynamic therapy (PDT): PDT mechanisms. Clin Endosc 46:1–6. http//dx.doi.org/10.5946/ce.2013.46.1.24
7. Mang TS (2004) Lasers and light sources for PDT: past, present and future. Photodiagn Photodyn Ther 1:43–48
8. Moghissi K, Dixon K, Stringer MR, Freeman T, Thorpe A, Brown S (1999) The place of bronchoscopic Photodynamic Therapy in advanced unresectable lung cancer; experience with 100 cases. Eur J Cardiothorac Surg 15:1–6
9. Allison RR, Moghissi K, Downie G, Dixon K (2011) Photodynamic therapy (PDT) for lung cancer. Photodiagn Photodyn Ther 8:231–239
10. Moghissi K, Dixon K, Thorpe JAC, Stringer MR (2007) Photodynamic therapy in early central lung cancer: a treatment option for patients ineligible for surgical resection. Thorax 62:391–395
11. Moghissi K, Dixon K (2008) Update on the current indications, practice and results of photodynamic therapy (PDT) in early central lung cancer (ECLC). Photodiagn Photodyn Ther 5:10–18
12. Okunaka T, Kato H, Tsutsui H et al (2004) Photodynamic therapy for peripheral lung cancer. Lung Cancer 43:77–82
13. Moghissi K, Dixon K, Thorpe JAC (2003) A method of video-assisted thoracoscopic photodynamic therapy (VAT-PDT). Interact Cardiovasc Thorac Surg 2:373–375
14. Allison RR, Mang T, HewsonG, Sneider W, Dougherty T (2001) Photodynamic therapy for chest wall progression from breast cancer is an under utilised treatment modality. Cancer 1(91):1–8
15. Cuence RE, Allison RR, Sibata C, Downie GH (2004) Breast cancer with chest wall progression, treatment with photodynamic therapy. Ann Surg Oncol 11(3):322–327
16. Graham E A, Singer JJ (1933) Successful removal of an entire lung for carcinoma of the bronchus. J Am Med Assoc 101:1371–1374
17. Jemal A, Bray F, Center HM, Farley J, Ward E, Forman D (2011) Global cancer statistics. CA Cancer J Clin 61:69–90
18. Lam S, Kennedy T, Unger M et al (1998) Location of bronchial epithelial neoplastic lesions by fluorescence bronchoscopy. Chest 113:696–702
19. Stringer MR, Moghissi K (2004) Photodiagnosis and fluorescence imaging in clinical practice. Photodiagn Photodyn Ther 1:9–12
20. Moghissi K, Dixon K, Stringer MR (2008) Current indications and future perspective of fluorescence bronchoscopy: a review study. Photodiagn Photodyn Ther 5:238–246
21. WHO International histological classification of tumours (1982) No 1 Histological typing of lung cancer. 2nd edn. Am J Clin Pathol 77:123–136
22. Sobin LH, Gospodarowicz MK, Wittekind C (2009) TNM classification of malignant tumours (7th revised ed). Wiley-Blackwell, New Jersey

23. Hayata Y, Kato J, Konaka C, Ono J, Takizawa N (1982) Haematoporphyrin derivative and laser photoradiation in the treatment of lung cancer. Chest 81(269):277
24. McCaughan JS Jr, Williams TE (1997) Photodynamic therapy for endobronchial malignant disease: a prospective fourteen year study. J Thorac Cardiovasc Surg 114:940–946
25. Kato H (1998) Photodynamic therapy for lung cancer: a review of 19 years experience. J Photohem Photobiol 42:96–99
26. Kato H, Harada M, Ichinose S, Usuda J, Tsuchida T, Okunaka T (2004) Photodynamic therapy (PDT) of lung cancer: experience of the Tokyo Medical University. Photodiagn Photodyn Ther 1:49–55
27. Moghissi K, Dixon K (2003) Is bronchoscopic photodynamic therapy a therapeutic option in lung cancer: a review. Eur Respir J 22:535–541
28. Ross P Jr, Grecula J, Bekaii-Saab T et al (2006) Incorporation of photodynamic therapy as an induction modality in non small cell lung cancer. Lasers Surg Med 38:881–889
29. Endo C, Miyamoto A, Sakurada A, Aikawa H, Sagawa M, Sato M et al (2009) Results of long term follow up of photodynamic therapy for roentgenographically occult bronchogenic squamous cell carcinoma. Chest 136:369–375
30. Hayata Y, Kato H, Furuse K, Kusonoki Y, Suzuki S, Mimura S (1996) Photodynamic therapy of 169 early stage cancer of the lung and oesophagus: a Japanese multi-centre study. Laser Med Sci 11:255–259
31. Sharpe DA, Moghissi K (1996) Resectional surgery in carcinoma of the oesophagus and cardia: what influences long term survival? Eur J Cardiothorac Surg 10:359–364
32. Moghissi K (1992) Surgical resection for stage I cancer of the oesophagus and cardia. Br J Surg 79:935–937
33. Wang GQ, Jiao CG, Chang FB, Fang WH, Song JX, Lu N, Lin DM, Xie YQ, Yang L (2004) Long term results of operation for 420 patients with early squamous cell esophageal carcinoma discovered by screening. Ann Thorac Surg 77:1740–1744
34. Wang GQ, Jia CG, Song JX, Fang WH, Lu N, Lin DM, Zie YQ, Zhang JH, Wei WQ (2008) Diagnosis and long term results of surgical resection of early cardiac adenocarcinoma. Zhonghua Wait Ke Za Zhi 46:1045–1047
35. Moghissi K, Hornshaw J, Teasdale PR (1977) Enteral nutrition in carcinoma of the oesophagus treated by surgery; nitrogen balance and clinical studies. Nr J Surg 64:125–128
36. Moghissi K (2012) Where does PDT fit within the oesophageal cancer treatment jigsaw puzzle? JNCCN 10(Supplement):S1–S4
37. Moghissi K, Dixon K, Thorpe JAC, Stringer MR (2000) The role of photodynamic therapy (PDT) in inoperable oesophageal cancer. Eur J Cardiothorac Surg 17:95–100
38. Moghissi K, Dixon K, Stringer M, Thorpe JAC (2009) Photofrin PDT for early stage oesophageal cancer: long term results in 40 patients and literature review. Photodiagn Photodyn Ther 6:159–166
39. McCaughan JS Jr, Williams TE Jr, Bethel BM (1985) Palliation of oesophageal malignancy with photodynamic therapy. Ann Thorac Surg 40:113–120
40. Yoon HY, Cheon YK, Choi HJ, Shim CS (2012) Role of photodynamic therapy in the palliation of obstructing esophageal cancer. Korean J Intern Med 27:278–284
41. Moghissi K, Dixon K (2003) Photodynamic therapy in oesophageal cancer: a surgical view of its indications based on 14 years experience. Technol Cancer Res Treat 2:319–326
42. Lecleire S, di Fiore F, Antonietti M, Ben-Soussan E, Hochain P, Lerebours E, Michel P, Ducrotte P (2008) Non-operable patients with superficial esopahgeal cancer treated by photodynamic therapy after chemoradiotherapy have more severe complications that patients treated in primary intent. Am J Gastroenterol 103:2215–2219
43. Fouralis CN, Thorpe JAC (2006) Photodynamic therapy (PDT) in Barrett's oesophagus with dysplasia or early cancer. Eur J Cardiothorac Surg 29:30–34
44. Corti L, Skarlatos J, Boso C et al (2000) Outcome of patients receiving photodynamic therapy for early oesophageal cancer. Int J Radiat Oncol Biol Phys 1:419–424

45. Sujendran V, Sica G, Warren B, Maynard N (2005) Oesophagectomy remains the gold standard for treatment of high grade dysplasia in Barrett's esophagus. Eur J Cardiothorac Surg 28:763–766
46. Tharavei C, Hagen JA, Peters JH, Portale G et al (2006) Predictive factors of coexisting cancer in Barrett's high grade dysplasia. Surg Endosc 20:439–443
47. Williams VA, Watson TJ, Herbella FA, Gellarsen O et al (2007) Oesophagectomy for high grade dysplasia is safe, curative and results in good alimentary outcome. J GastroIntest Surg 11:1989–1997
48. Konda VI, Ross AS, Ferguson MK, Hart JA, Lin S et al (2008) Is the risk of concomitant invasive oesophageal cancer in high grade dysplasia in Barrett's oesophagus over estimated? Clin Gastroenterol Hepatol 6:159–164
49. Yano T, Muto M, Minashi K, Kojina T et al (2012) Photodynamic therapy as salvage for local failure after chemo-radiotherapy in patients with esophageal squamous cell carcinoma: a phase II study. Int J Cancer 131:1228–1234
50. Khanghra SK, Greenwald BD (2013) Endoscopic management of esophageal cancer after definitive chemo-radiotherapy. Dig Dis Sci Epub ahead of print, 17 Jan 2013
51. Barrett NR (1950) Chronic peptic ulcer of the oesophagus and oesophagitis. Br J Surg 38:175–182
52. Allison PR, Johnstone AS (1953) The oesophagus lined with gastric mucous membrane. Thorax 8:87–101
53. Moghissi K (1991) The enigma of Barrett's oesophagus: putting the record straight. Eur J Cardiothorac Surg 5:13–16
54. De Palma GD (2012) Management strategies of Barrett esophagus. World Gastr0-enterolog 18(43):6216–6225. doi: 10.3748wjg.v18.143.6216
55. Dunn JM, Mackenzie GD, Banks MR, Mosse CA, Haidry R, Green S, Thorpe S, Rodrigues-Justo M, Winstanley A, Novelli MR, Bown SG, Lovat LB (2012) A randomised controlled trial of ALA vs Photofrin photodynamic therapy for high-grade dysplasia arising in Barrett's oesophagus. Lasers Med Sci Epub ahead of print, 15 Jun 2012
56. Brenner J, Sordillo PP, Magill GB et al (1982) Malignant mesothelioma of the pleura. Review of 123 patients. Cancer 49:2431–2435
57. Antman KH, Shemin R, Ryan L (1988) Malignant mesothelioma: prognostic variables in a registry of 180 patients. The Dane-Fabre Cancer Institute and Brigham and Women's Hospital experience over two decades 1965–1985. J Clin Oncol 6:147–153
58. Huncharek M, Kelsy K, Mark EJ et al (1996) Treatment and survival in diffuse malignant pleural mesothelioma: a study of 83 cases from the Massachusetts General Hospital. Anticancer Res 16:1265–1268
59. Harvey JC, Erdman C, Pisch J et al (1996) Diffuse malignant mesothelioma: options in surgical treatment. Comp Ther 21:13–19
60. Chahinian AP, Pajack TF, Holland JF et al (1982) Diffuse malignant mesothelioma, prospective evaluation of 69 patients. Ann Intern Med 96:746–755
61. Law MR, Hodson MR, Turner-Warwick M (1984) Malignant mesothelioma of the pleura: clinical aspects and symptomatic treatment. Eur J Resp Dis 64:162–166
62. Sternman DH, Kaiser LR, Albelda SM (1999) Advances in the treatment of malignant pleural mesothelioma. Chest 116:504–520
63. Keller SM (1995) Adjuvant therapy for malignant pleural mesothelioma (review). Chest Clin North Am 4:127–135
64. Sugarbaker DJ, Jaklitsch AT, Liptay MJ (1995) Mesothelioma and radical multi-modal therapy: who benefits? Chest 107(Supl):3455–3505
65. Aisner J (1995) Current approach to malignant mesothelioma of the pleura. Chest 107:332S–344S
66. Sugarbaker D, Garcia JP, Richards WG et al (1996) Extra pleural pneumonectomy in the multi modal therapy for malignant pleural mesothelioma: results of 120 consecutive patients. Ann Thorac Surg 224:288–296

67. Dougherty T, Kaufman JE, Goldfarb A et al (1978) A photoradiation for the treatment of malignant tumour. Cancer Res 38:2628–2635
68. Moghissi K, Dixon K (2005) Photodynamic therapy in the management of malignant pleural mesothelioma: a review. Photodiagn Photodyn Ther 2:135–147
69. Sugarbaker DJ, Jaklitsch MT, Bueno R et al (2004) Prevention, early detection and management of complications after 328 consecutive extrapleural pneumonectomies. J Thorac Cardiovasc Surg 128:138–146
70. Fevzi BH, Metintas M, Caglar H (2008) Trimodality treatment of malignant pleural mesothelioma. J Thorac Oncol 3:499–504
71. Scherpereel A, Astoul P, Baas P et al (2010) Guidelines of the European respiratory society and the European society of thoracic surgeons for the management of malignant pleural mesothelioma. Eur Resp J 35:479–495
72. Friedberg JS, Mick R, Culligan M et al (2011) Photodynamic therapy and the evolution of a lung-sparing surgical treatment for mesothelioma. Ann Thorac Surg 91:1738–1745
73. Friedberg JS, Culigan MJ, Mick R et al (2012) Radical pleurectomy and intraoperative photodynamic therapy for malignant pleural mesothelioms. Ann Thorac Surg 93:1658–1665
74. Friedberg JS, Culigan MJ, Mick R, Stevenson J, Hahn SM, Sterman D, Punekar S, Glatstein E, Cengel K et al (2012) Radical pleurectomy and intraoperative photodynamic therapy for malignant pleural mesothelioma. Ann Thorac Surg 93:1658–1665

Chapter 10
Photodynamic Therapy for Polypoidal Choroidal Vasculopathy

Patrycja Nowak-Sliwinska, Michel Sickenberg and Hubert van den Bergh

Abstract Photodynamic therapy (PDT) with Visudyne® was the first successful therapy for wet age-related macular degeneration (AMD). Clinical tests of PDT for wet AMD surprisingly showed a significantly better outcome for patients from Japan, Singapore, and China as compared to the results obtained on Caucasian patients. These differences pointed to the fact that patients with polypoidal choroidal vasculopathy (PCV), which is encountered more frequently in people with darker skin, had inadvertently been included among the AMD patients. As these two diseases are difficult to distinguish with the fluorescein angiography used in these trials, the switch to indocyanine green angiography (ICGA) then permitted the more specific and detailed study of PCV with Visudyne® therapy. The results of PCV treated with PDT turned out to be very good indeed, even though on the time scale of 1 year or more retreatment was needed in some patients. Anti-VEGF therapy by itself, however, did not show anywhere near the same benefit for treating PCV as was the case for the treatment of wet AMD. Recently, triple therapy with Visudyne®-PDT combined with anti-VEGF therapy and a steroid was found to give the best results for the visual acuity of patients with PCV. This chapter summarizes the data on PDT of PCV, and the effect of different combination therapies. Some of the pathological and genetic similarities and differences between PCV and wet AMD are also discussed.

Keywords Age-related macular degeneration · Antiangiogenic · Choroidal neovascularization · Optical coherence tomography · Polypoidal choroidal vasculopathy · Visudyne®-photodynamic therapy

P. Nowak-Sliwinska · M. Sickenberg · H. van den Bergh (✉)
Department of Chemistry, Ecole Polytechnique Fédérale De Lausanne, Lausanne, Switzerland
e-mail: Hubert.vandenbergh@epfl.ch

P. Nowak-Sliwinska
e-mail: Patrycja.Nowak-Sliwinska@epfl.ch

M. H. Abdel-Kader (ed.), *Photodynamic Therapy*,
DOI: 10.1007/978-3-642-39629-8_10,

Abbreviations

AMD	Age-related macular degeneration
AREDS	Age-related eye disease study
BCVA	Best-corrected visual acuity
BPDMA	Benzoporphyrin derivative monoacid ring A
CNV	Choroidal neovascularization
ELN	Elastin gene
ETDRS	Early treatment diabetic retinopathy study
ICGA	Indocyanine green angiography
IVTA	Intra-vitreal triamcinolone acetonide
OCT	Optical coherence tomography
PCV	Polypoidal choroidal vasculopathy
PED	Pigment epithelial detachment
pO_2	Partial pressure of oxygen
RPED	Retinal pigmented epithelium detachement
TTA	Triamcinolone acetonide
VDA	Vascular disrupting agent
VEGF-A	Vascular endothelial growth factor A
V-PDT	Visudyne®-photodynamic therapy

10.1 Introduction

Photodynamic therapy (PDT) was introduced in ophthalmology in the late 1990s as a clinical treatment for choroidal neovascularization (CNV) secondary to AMD [1]. PDT with Visudyne® as a photosensitizer was the first effective and safe treatment for subfoveal lesions, saving more than a million eyes from blindness.

CNV is encountered in patients with AMD, but also occurs in pathologic myopia, inflammation, angioid streaks, trauma, and choroidal rupture [2, 3]. Although wet AMD constitutes only a small fraction of AMD, it is the major cause of blindness of the elderly in the western world [4]. CNV often develops in the central part of the macula called the fovea, where the leaking vessels lead to edema, and finally scar tissue replacing the photoreceptors. The maintenance of healthy macular function is dependent on the integrity of the different layers of the retinal tissue in this region. These include the choroidal blood supply, Bruch's membrane, the retinal pigmented epithelium (RPE), the neural retina containing the photoreceptors, and the network of other cells which preprocess the optical signal before sending it via the ganglion cells, axons, and the optic nerve to the brain. The etiology of CNV secondary to AMD is not completely known. It has been proposed that the photoreceptor outer segments accumulate oxidative stress in the vision process, and then these outher segments are "partially" shed and are replaced. The shed outer segment fragment is then phagocytosed and destroyed by the neighboring RPE cells. Upon aging this process no longer functions optimally,

which leads to deposits of fatty material in and under the RPE. Such deposits, that may show up as colored spots during ophthalmoscopy, are called drusen. The decreased transport of oxygen, liquid, and nutrients through these lipophilic deposits leads to hypoxia, the induction of HIF-1α and VEGF-A and hence neoangiogenesis and vascular sprouting from the choroid into Bruch's membrane. Neovessels are frequently restricted to the area below the RPE and near Bruch's membrane. These are sometimes called "occult" CNV, as in fluorescein angiography they are more difficult to detect due mainly to the absorption of the excitation and emission wavelengths by the melanin in the RPE. However, the choroidal neovessels are sometimes capable of transgressing the RPE [2, 5, 6] thus making them more visible. These may be called "classic" neovessels. The newly formed blood vessels are pathologically and functionally abnormal, leaking lipids, fluid, and blood into the retina causing the edema and retinal thickening which is often associated with vision impairment. If this leakage extends over longer times it can lead to scar tissue in the retina and scotoma, i.e., dark regions in our central vision. The size and number of drusen can be correlated with disease progression and has been used as a predictor for patient outcome [7]. This pathology and its successful treatment by Visudyne®-photodynamic therapy (V-PDT) have been described extensively by our group and others [8–11].

Briefly, V-PDT is a treatment that utilizes the somewhat selective endothelial uptake of a photoactivatable compound in the CNV after i.v. injection of liposomal benzoporphyrin derivative monoacid ring A (BPDMA). Applied "standard" protocol of local light delivery (light dose of 50 J/cm^2, irradiance of 600 mW/cm^2 of 689 nm light over 83 s) produces a vaso-occlusive effect. Endothelial cell damage begins with the calcium influx into the cell. This provokes alterations in cytoskeletal components leading to cell shrinkage, loss of tight junctions between endothelial cells, and exposure of the vascular basement membrane [12]. Blood platelet aggregation after irradiation and their interaction with procoagulant extracellular matrix components comes with vessel constriction and eventually leads to thrombus formation [13]. The clinical results of AMD treatment trials involving PDT alone or in combination with other treatment modalities are described in detail elsewhere [14–24] and are summarized in Table 10.1.

While comparing the clinical trial results obtained in the identical AMD treatment, between Asian and Caucasian patients, it turned out, that the responses to PDT were better for Japanese patients (JAT trial) as compared to Caucasian patients (TAP trial) [25], see Fig. 10.1. Exactly, the same therapy in Japanese patients diagnosed with AMD gave better visual acuity gain then in the Caucasian patients also diagnosed with AMD [26–28]. Historically, with the use of ICGA atypical cases of AMD had been found, with a vascular network that terminates in polypoidal lesions. These lesions were called PCV. PCV was recognized for the first time in 1982 by Yannuzzi and colleagues as an uncommon hemorrhagic disorder of the macula [29]. Two years later similar changes named "posterior uveal bleeding syndrome" were observed by Kleiner et al. [30]. In 1985, Stern and colleagues characterized multiple, bilateral, serosanguineous retinal pigment epithelium (RPE) detachments occurring in the posterior segment in black woman [31].

Table 10.1 Summary of clinical trials with V-PDT for choroidal neovascularization

Study	Treatment regiment	Follow up period (months)	Results	Reference
TAP	Standard fluence V-PDT	24	V-PDT reduced the risk of moderate or severe vision loss in patients with CNV due to AMD	[15]
VIP	Standard fluence V-PDT (Northern America, Europe)	24	In the v-PDT group, VA improvement by at least five letters was observed in patients with CNV due to pathologic myopia	[14]
Lam et al.	Standard fluence V-PDT (Asian patients)	24	Median VA improvement was 1.7 lines, but the mean number of PDT retreatments required in the first 2 years was 2.3—lower than in the VIP study	[16]
ANCHOR	Ranibizumab (0.3 or 0.5 mg) standard fluence V-PDT	12	Ranibizumab was clearly superior to PDT with respect to both visual acuity (VA) and anatomic (lesion size and CNV leakage) efficacy outcomes	[18]
FOCUS	Ranibizumab 0.5 mg monthly; sham injections monthly +standard fluence V-PDT	24	Combination therapy was more effective than V-PDT alone and had a low rate of adverse events	[17]
PROTECT	Same-day standard fluence V-PDT +ranibizumab 0.5 mg	12	Improved VA, lesions were stabilized with minimal treatment required after month 3	[19]
MONT BLANC	Standard fluence V-PDT; ranibizumab 0.5 mg	12	VA improvements in the combination group are noninferior to a ranibizumab alone with three ranibizumab doses followed by injections on a monthly regimen	[20]
DENALI	Standard fluence V-PDT +ranibizumab 0.5 mg; reduced-fluence V-PDT +ranibizumab 0.5 mg; ranibizumab 0.5 mg	12	DENALI did not demonstrate noninferior visual acuity gain for V-PDT combination therapy compared with ranibizumab monthly monotherapy	[22]

(continued)

Table 10.1 (continued)

Study	Treatment regiment	Follow up period (months)	Results	Reference
RADICAL	Reduced[a] fluence V-PDT + within 2 h by ranibizumab (0.5 mg) + dexamethasone (0.5 mg);Reduced[b] fluence V-PDT +ranibizumab (0.5 mg) +dexamethasone (0.5 mg); ranibizumab only (0.5 mg)	24	*Significantly fewer retreatments required with combination therapies than with ranibizumab monotherapy!* Mean VA change from baseline was not statistically different among the treatment groups	[23]
TRIPLE THERAPY	Reduced[c] fluence V-PDT, 16 h later, dexamethasone (800 ug) + bevacizumab (1.5 mg)	9	Less than one-fourth of the patients treated with this regimen required additional treatment	[21]
	Standard fluence V-PDT + immediate injection of bevacizumab (1.25 mg) + TA (4 mg) + bevacizumab (1.25 mg) every 3 months	6	Short-term results of this study (at 6 months) showed low rate of retreatments, sustained CNV closure efficacy, and visual acuity improvement	[24]

CFT Choroidal foveal thickness; *PCV* poliploidal choroidal vasculopathy; Reduced[a] fluence: 25 J/cm^2 , 83 s, 300 mW/cm^2 at 689 nm; Reduced[b] fluence: 15 J/cm^2 , 83 s, 180 mW/cm^2 ; Reduced[c] fluence: 42 J/cm^2 , 300 mW/cm^2 ; Standard fluence: 50 J/cm^2 , 600 mW/cm^2 ; *TA* triamcinolone acetonide; *VA* visual acuity; *V-PDT* Visudyne® -photodynamic therapy

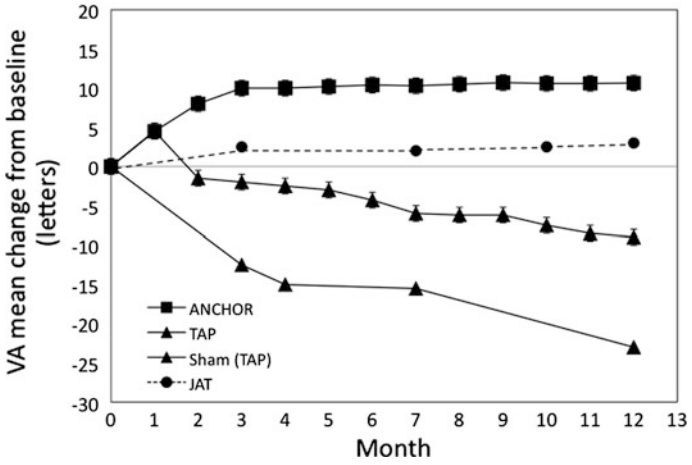

Fig. 10.1 Comparison of mean change of the visual acuity with different treatments in wet AMD. ANCHOR trial (PDT+ranibizumab), *JAT* and *TAP* trials (PDT). Month zero is the baseline

Five years later Yannuzzi and collaborators introduced the term "idiopathic PCV", since the observed pathogenesis of subretinal, polypoidal vascular lesions associated with hemorrhagic RPE detachments was at that time unknown [32]. It now became clear that the V-PDT trials on what had been identified by fluorescein angiography as AMD, had inadvertently included cases of PCV. The darker skinned patients have a higher percentage of PCV then their Caucasian counterparts, and the better visual acuity outcome in the JAT trial was thus mainly associated with more effective treatment of PCV as compared to AMD.

10.2 Clinical Appearance and Diagnosis of Polypoidal Choroidal Vasculopathy

PCV was often found to be the main vascular disorder in patients of pigmented races diagnosed with neovascular maculopathies, especially African-Americans and Asians. PCV is remarkably high in the Japanese population. PCV occurs in white patients [33], but to a lesser extent. Japanese clinical studies suggested that 54.7 % of the patients with neovascular AMD also have PCV [34]. This PCV is characterized by a branching vascular network originating from the inner choroid that terminates in polypoidal lesions [29]. The main clinical manifestation of PCV is the presence of serosanguineous RPE detachments in the region of the central macula or around the optic nerve. These lesions may bleed, causing vitreous hemorrhage, which potentially can lead to vision loss. Another feature is the presence of degenerated small arterioles and capillaries with a thickened basement membrane [35]. The polypoidal lesions range from small to large and perfusing

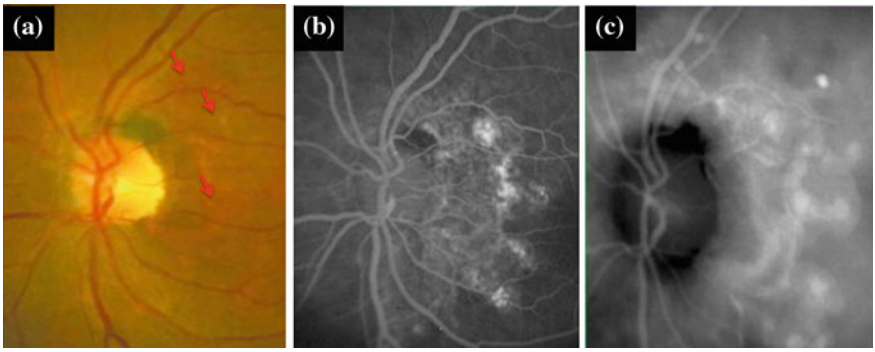

Fig. 10.2 Images of the first published patient, a 68-year-old African-American woman, with polypoidal choroidal vasculopathy (PCV). **a** Color fundus image with a hemorrhage. **b** Late phase of a fluorescein angiogram (*FA*) with patches of hyperfluorescence. **c** ICGA image showing classic polypoidal lesions 9 years later (Adapted from Imamura et al. 2010 [33])

branching inner choroidal vessels [36]. They are detectable mainly by means of ICGA, since the longer excitation and detection wavelengths, as compared to fluorescein angiography, can penetrate the RPE easier, allowing improved imaging. In early phase ICGA, PCV vessels are filled before retinal vessels and the area around polypoidal vessels remains hypofluorescent. Subsequently, small hyperfluorescent polyps become visible within the choroid. The late phase ICGA is associated with reversed fluorescence observations as compared to the early phase, i.e., the area surrounding the polypoidal lesions becomes fluorescent and the center of the lesions becomes hypofluorescent. In the very late stages of ICGA, the disappearance of fluorescence from the lesions is observed [37] (Fig. 10.2).

Another feature of the PCV is a hyalinization of choroid-based vessels. The latter refers to the replacement of smooth muscle tissue due to elevated intraluminal pressure or elastin coding gene (ELN) dysfunction [38]. Other histopathological features included plasma and/or fibrin exudation [39].

The reason for choroidal hyperpermeability as detected by ICG angiography in PCV is still not well known. High-resolution optical coherence tomography (OCT) images, giving a cross-sectional view of the retina and the choroid, showed that the polypoidal structures are located beneath the RPE [33, 40]. Subfoveal choroidal thickness is greater in eyes with choroidal hyperpermeability than that in eyes without it, in both wet AMD and PCV, whereas in eyes without choroidal hyperpermeability, the mean subfoveal choroidal thickness was greater in PCV than that in typical AMD [41].

While the branching vascular network may be quiescent in some cases of PCV, it can remain the main cause of leakage and exudation in other patients.

The presence of PCV in one eye generally indicates a high risk for bilateralism [29]. PCV is usually detected only after serosanguineous detachment of the RPE, or vitreous hemorrhage, but with less fibrous scarring compared to CNV [42, 43].

10.3 Discussion on Similarities and Differences Between PCV and Neovascular AMD

PCV associated with subretinal neovascularization was often misdiagnosed using fluorescein angiography as AMD [44, 45]. Moreover, it still remains somewhat controversial whether PCV represents a subtype of neovascularized AMD or a completely separate disorder.

Both diseases share some similarities, like laterality (bilateral), presence of CNV and some genetic background [44]; however only based on the differences, the proper diagnosis and treatment can be performed (see Table 10.2). Patients with PCV are mostly Asians or African-Americans and on the average they are younger than the patients diagnosed with AMD. Their eyes have considerably less, or even a complete lack, of drusen, which are a characteristic sign of AMD [44].

Although associated with multiple recurrent serosanguineous macular detachment, PCV is not linked to significant fibrous proliferation as is the case in end-stage neovascular AMD [46]. Choroidal thickness turns out to be different in the two disorders. As identified using enhanced-depth imaging OCT, i.e., by the measurement of the vertical distance from the Bruch's membrane to the innermost scleral layer [47], subfoveal choroidal thickness was thicker in the eyes with PCV, in contrast to the thinner choroid observed in eyes with AMD.

The relative importance of vascular endothelial growth factor (VEGF), an angiogenesis stimulator, and of pigment epithelium derived factor (PEDF), a protein that inhibits angiogenesis, both of which are expressed in choroidal neovascular membranes in the eyes with PCV and AMD, also appears to differ between the two diseases.

VEGF and PEDF were shown to be strongly expressed in vascular endothelial cells and retinal pigment epithelial cells of the excised subfoveal fibrovascular human CNV tissues [48]. The correlation in the expression of these two factors suggests their importance in the neovascularization process. Although the expression level of VEGF is increased in both pathologies as compared to the healthy eye, the VEGF level in PCV diagnosed eyes was considerable lower than in AMD eyes [49].

The genetics of PCV and AMD has been extensively studied [50, 51]. It was hypothesized that overexpression of high temperature required factor A1 (HTRA1) that controls the integrity of Bruch's membrane, facilitates the invasion of choroidal capillaries [52]. HTRA1 was found to be associated with both disorders, being about two-fold stronger in AMD than in PCV [52] in Asian patients. Another susceptibility gene in PCV seems to be the elastin gene (ELN), which is shown to be more associated with PCV than with AMD [38]. Moreover, the genes of complement factor H (CFH), HTRA1, and complement factor C2 were associated with both AMD, and PCV. The LOC387715 rs10490924, i.e., the gene which codes mitochondrial protein in photoreceptors, was found to be strongly associated with PCV and presented a different distribution in AMD and PCV [53]. LOC387715 rs10490924 correlates with vitreous hemorrhage, and also with the lesion size.

Table 10.2 Selected similar and differential features of AMD and PCV

Feature	AMD	PCV	Reference
Similarities			
Laterality	Bilateral		[29]
Appearance	Abnormal vasculopathy leading to serous exudation or vitreal hemorrhage		[33]
Angiogenesis factors	Increased level of VEGF		[64]
Treatment	Photodynamic therapy, anti-VEGF		[33]
Genetics	Complement factor H (CFH) High temperature required factor A1 (HTRA1)		[53]
Differences			
Location based on OCT	Intra Bruch's membrane	Beneath Bruch's membrane	[29]
ICGA late phase staining	Lesions located subfoveally Weaker hyperfluorescence with weaker margins	Lesions located peripapillary (Caucasians) and extrafoveally (Chinese); Late geographic hyperfluorescence	[44]
Choroidal thickness	Decreased	Increased	[47]
Fibrous proliferation	Yes	No	[42]
Vessels morphology	Small with ending branching polyps, less leaky vessels	Larger, leaky vessels	[82]
Drusen	Yes	Less or no drusen	[33]
Pulsations	No	Yes	[83]
Patient profile	European, American, elderly	African-American and Asian, younger then in AMD	[33]
Grading system	Based on the drusen size and number; (AREDS) classification	Based on the polyp location size and number	[36, 46]
VEGF and PEDF level	Increased	Increased, but lower than in AMD	[48]
Genetics	HTRA1, weaker association ELN down-regulation Complement factor 2 and factor B	HTRA1 ELN upregulation	[53]

10.4 Photodynamic Therapy in PCV

The most effective treatment for PCV is not yet well established for all cases. Early studies showed positive results using thermal laser photocoagulation [54–56]. Visudyne®-PDT (V-PDT) is clearly a safer treatment modality for subfoveal or juxtafoveal AMD and PCV due to the minimal damage done to the retina, and it has consequently been used very successfully in treating PCV.

In the clinical reports on V-PDT in PCV with a follow-up of about 1 year, preservation and improvement of visual acuity was achieved in more than 80 % of mostly Asian patients [26, 33, 57]. The summaries of the studies, which are discussed below, are presented in Table 10.3.

A prospective interventional study was performed in Japanese patients [26]. Based on ICGA, 36 eyes (39 %) were diagnosed with PCV and 54 eyes (58 %) with CNV secondary to AMD. Visual recovery after V-PDT was reported to be more favorable for the eyes with PCV (8 letters) than in those with AMD (7.0 letters). The VA improved (15 letters or more) in 6 % of the AMD patients, in 25 % of the PCV patients, and decreased (15 letters or more) in 31 % of the AMD patients and in 8 %, of the PCV patients. At 1-year fluorescein leakage was suppressed in 86 % of the PCV patients and 61 % of the AMD eyes. In conclusion, V-PDT resulted in superior results for treating PCV as compared to CNV secondary to AMD [26].

Spaide et al. [58], in 1 year retrospective review, reported on 16 patients with subfoveal PCV treated with V-PDT. The visual acuity improved in 9 (56.3 %) of the patients, and remained the same in 5 (31.3 %), and decreased in 2 (12.5 %) of the patients. There were no reported long lasting complications after the treatment. The mean change in visual acuity was an improvement of nearly 2.4 lines!

Promising results were also found in other studies in Japanese patients at 1 year after standard fluence PDT [27] or reduced-fluence V-PDT [28, 59]. In both studies PCV showed a significantly lower PDT frequency and greater improvement in the visual acuity than in the case of AMD, i.e., fewer PDT treatments per year were needed to obtain optimal results in the case of PCV than in the case of wet AMD. The recurrence period of PCV after PDT was clearly significantly longer than that in the case of AMD.

Even though all polypoidal lesions regress with PDT, its effect on branching does not seem to be permanent and thus recurrence of polypoidal lesions may occur in the long run. Another problem is the heterogeneous localization of the polyps, especially those in the peripapillary area, which is not always easily accessible for the laser light. Finally, repeated PDT may induce persistent choroidal atrophy.

In another example, during a 3-year follow-up period, a nonrandomized study was conducted involving eyes with newly diagnosed PCV, which were treated exclusively with V-PDT [60]. Patients were submitted to an average of 3.19 treatment sessions. In this study, approximately, 75 % of the treated eyes had no significant loss of vision, and 14.8 % showed significant improvement in visual acuity. Although the recurrences were frequent (59.3 % of the eyes at 3 years of follow-up), they responded well to retreatment, and were not associated with increased visual acuity loss.

Other limitations of PDT are a pigment epithelium detachment or the possibility of a large submacular hemorrhage. Hirami et al. retrospectively reviewed data for 91 eyes of patients who underwent PDT for the treatment of PCV [61]. In this study, during the follow-up period after PDT, postoperative subretinal hemorrhage was seen in 30.8 % of eyes. In 78.6 % of these eyes, the subretinal hemorrhage

Table 10.3 Summary of clinical trials with V-PDT alone or in combination with other treatment modalities in PCV

Treatment regiment/patient origin	Follow up period (months)	Results	Reference
Standard V-PDT/Japanese	12	VA improved (15 letters or more) in AMD and PCV by 6 and 25 %, respectively. Fluorescein leakage was suppressed in 86 % of PCV and 61 % of AMD eyes, respectively	[26]
Standard fluence V-PDT/ Japanese	24	VA preserved or improved in 79 % of eyes. Recurrence of polypoidal lesions in 64 % of eyes. An abnormal branching vascular network persisted in all subjects	[62]
Standard fluence V-PDT/ Japanese	19.2	Regression of the polypoidal lesions observed in 94 % of eyes. The branching vascular network remained in all eyes	[63]
Standard fluence V-PDT/ Japanese	12	Significantly better response to PDT in terms of VA improvement and effect durability	[27]
[a]Reduced-fluence V-PDT	12	Significantly lower PDT frequency and greater improvement in the visual acuity than AMD	[28]
Standard fluence V-PDT/ Japanese	12	The visual acuity improved in 56.3 % of patients, remained the same in 31.3 %, and decreased in 12.5 % and. No patient had any long lasting complication after the treatment	[58]
Standard fluence V-PDT/ European	36	75 % of the treated eyes had no significant loss of vision, and 14.8 % showed significant improvement in visual acuity	[60]
Standard fluence V-PDT + ranibizumab 0.5 mg in PCV/Asian	12	Complete regression of polypoidal lesions in combination therapy group	[71]
Standard fluence V-PDT + ranibizumab 0.5 mg	12	Mean BCVA change from baseline of 12.3 letters	[72]
Standard fluence V-PDT + bevacizumab 1.25 mg	12	Lower rate of post-PDT hemorrhage. Recurrence rate unchanged	[64]
Ranibizumab 0.5 mg + standard fluence V-PDT	12	Improved VA and reduced exudation	[66]
[a]Reduced-fluence V-PDT + bevacizumab 1.25 mg	12	Improved VA in 56 % treated eyes	[73]

(continued)

Table 10.3 (continued)

Treatment regiment/patient origin	Follow up period (months)	Results	Reference
[b]Reduced-fluence V-PDT+ranibizumab 0.5 mg	12	In 95 % of the eyes, best-corrected visual acuity remained stable or improved	[74]

[a] Reduced fluence: 25 J/cm^2 for 83 s
[b] Reduced fluence: 25 J/cm^2 for 70 s; Standard fluence: 50 J/cm^2 , 600 mW/cm^2 at 689 nm
VA visual acuity; *V-PDT* Visudyne® -photodynamic therapy

was absorbed without treatment. Although visual acuity was the same or increased in 81.8 % of eyes with subretinal hemorrhage alone, it decreased significantly in 50.0 % of the eyes with postoperative vitreous hemorrhage.

Akaza et al. with a follow-up of 24 months showed regression of the polypoidal lesions in 29 out of 31 eyes (94 %). However, recurrence of polypoidal lesions appeared in 10 of 29 eyes (34 %) and additional PDT was suggested. V-PDT could reduce the size of polypoidal lesions, but did not destroy them completely. Thus, the persistent branching vessels in the network are supposed to be at the origin of the new polypoidal lesions [62].

Similar results were obtained in another study with a follow-up of 19.2 months [63]. After initial V-PDT, the polypoidal lesions regressed in 94 % of eyes, but the branching vascular network remained in all eyes, and increased in size in 42 % of eyes.

Summarizing, PDT in CNV demonstrated very positive short- to medium-term results. Retreatment is necessary in many cases, but at a relatively low frequency. The observations reported above prompted the PDT field to search for efficient strategies to improve the efficiency and selectivity of V-PDT and reduce the treatment burden.

10.5 Combination Therapies in PCV

PDT in combination with other treatment modalities for neovascular AMD has been extensively investigated in in vivo models and in clinical trials by our group and by others [13, 64–66]. The closure of unwanted neovasculature by the combination of PDT with antiangiogenic compounds to prevent recurrent neovascularization, as well as with corticosteroids to prevent inflammation may provide an effective multilevel treatment for both AMD and PCV. Unique characteristics in the pathogenesis of PCV contribute to disease development and can be potential targets for intervention. To date, there is limited information on combination therapy for PCV that is refractory to anti-VEGF therapy. The exact role of VEGF in the pathogenesis of PCV remains to be elucidated. However, the recent studies

that show PCV being refractory to anti-VEGF therapy suggest that the development of PCV is less likely to be strongly dependent on VEGF-related pathways. Bevacizumab was found to decrease the amount of exudation associated with PCV, however, the results of this anti-VEGF monotherapy were not anywhere near as promising as those obtained in the treatment of AMD [33, 65, 67, 68], possibly due to the fact that in PCV one may deal with more mature vasculature than in the case of AMD.

Kokame et al., in a trial of monthly intravitreal ranibizumab (0.5 mg) injections for PCV, reported the stabilization of vision at 6 months in 12 eyes [69], as well as resolution of subretinal hemorrhage and a decrease in macular edema. Moreover, polypoidal lesions decreased in 33 % of eyes, but branching choroidal vessels were still present.

Presently, in order to investigate the safety and efficacy of a high dose ranibizumab (2.0 mg) in PCV patients, a phase II clinical trial (PEARL2) is recruiting patients [70]. The results are pending and are expected in 2013.

Due to the limited effectiveness of the anti-VEGF treatment by itself in PCV, combined therapy might be an option when persistent or recurrent exudative change is seen post-anti-VEGF treatments.

10.5.1 PDT and Anti-VEGF Targeting

In PDT of PCV, the mechanism of "selective" photothrombosis causes regression of the polyps and allows the gradual improvement of the pathological features. Combining PDT with an anti-VEGF agent can potentially create a synergistic effect that would (1) induce polyp regression, (2) reduce fluid leakage, and (3) reduce inflammation (see Fig. 10.3 a-h). There are several studies reporting promising results on PDT combined with anti-VEGF treatment. Selected trials are summarized below, as well as in the Table 10.3.

The EVEREST trial showed a 6-month efficacy of V-PDT in combination with ranibizumab for PCV. Complete regression of polypoidal lesions was achieved at 6 months in 77.8 % of the eyes after combination therapy, as compared to 71.4 % after PDT alone and 28.6 % after intravitreal injection of ranibizumab. At this time point the VA outcome of the 3 arms of this study was +10.9, +7.5, and +9.2 letters, respectively. However, at 24 month follow-up, 64 % of eyes treated successfully with V-PDT showed recurrence of polypoidal lesions [71].

In the study reported by Ruamviboonsuk et al. [72], 12 eyes diagnosed with PCV were treated with PDT combined with 3 monthly intravitreal injections of ranibizumab. The patients were monitored monthly with measurements of best-corrected visual acuity (BCVA) and OCT for 1 year. At that time point, the mean BCVA change from baseline was +12.3 letters and in all patients regression of polyps without recurrence was observed. This combination therapy, however, did not reduce the number of patients who required retreatment over 1 year follow-up, when compared to data in the studies of PDT alone (see Fig. 10.3 i).

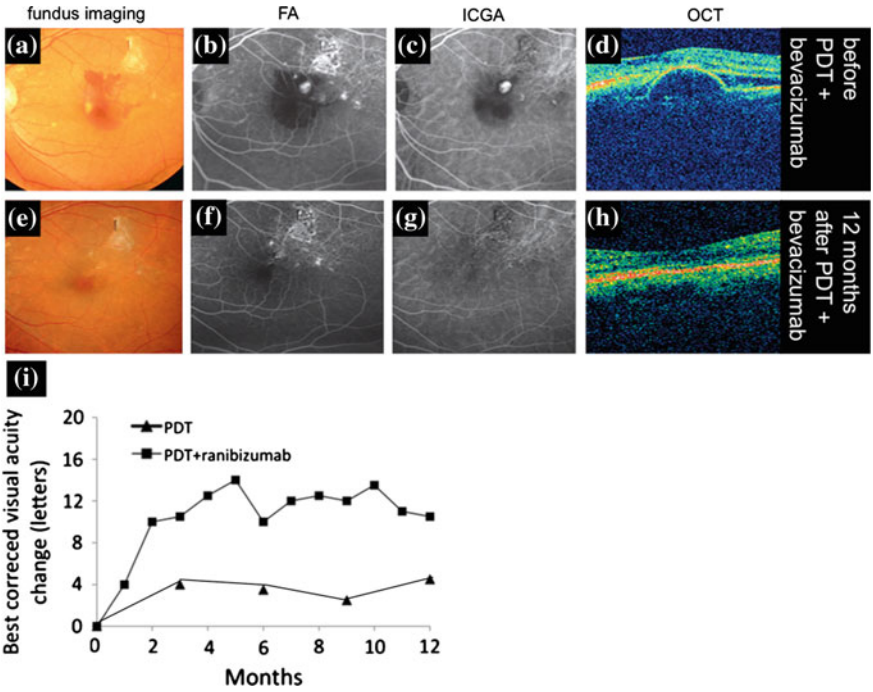

Fig. 10.3 PDT+ranibizumab treatment results in PCV. Representative images of the fundus (**a** and **e**), fluorescein angiography (**b** and **f**), indocyanine green angiography (**c** and **g**), and optical coherence tomography (**d** and **h**) before (**a**–**d**) and at month 12 post-treatment (**e**–**h**). **a** Fundus photo, at baseline, showing hemorrhagic retinal pigment epithelial detachment (*RPED*). **b** Fluorescein angiography (*FA*) presenting leakage with staining of the scar. **c** ICGA showing focal hyperfluorescence indicating an active polyp. **d** OCT showing RPED with subretinal fluid. **e** Fundus image at month 12, showing no recurrence of PCV. **f** Fluorescein angiography still showing no leakage with the staining of the scar. **g** ICGA showing no recurrence of the polyp with the vascular network identified. **h** OCT still showing resolution of the RPED and no subretinal fluid. **i** The mean best-corrected visual acuity change over time for PDT alone and PDT+ranibizumab treated patients in studies published before 2010 (Adapted from Raumviboonsuk et al. [72])

Also Gomi et al. reported superior results in PCV patients treated with PDT combined with intravitreal bevacizumab injection (1.25 mg) over patients treated with PDT alone. The rate of development of subretinal hemorrhage within 1 month from the initial treatment was significantly lower in the combined therapy group than in the PDT monotherapy group. Combined treatment decreased the rate of PDT-related hemorrhage but did not affect the recurrence of the lesions [64].

In a retrospectively reviewed study of 28 patients treated with 3 monthly intravitreal injections of ranibizumab (0.5 mg) and V-PDT performed 1 or 2 days after the initial injection of ranibizumab [66] and a follow up of 12 months, the mean visual acuity levels improved from 0.33 at baseline to 0.61. The mean improvement in BCVA from baseline was 2.65 lines and the central retinal thickness decreased by

two-fold. Combined intravitreal ranibizumab and V-PDT maintained or improved visual acuity and reduced the exudation without adverse events.

Reduced-fluence V-PDT (with a light dose of 25 J/cm^2 delivered over 83 s, and with an irradiance of 300 mW/cm^2) combined with intravitreal bevacizumab (1.25 mg) was reported recently by Sagong et al. [73] in 16 patients with PCV. At 12 months, the visual acuity improved in 56 % of the eyes by 3 lines or more, was stable in 37 % of eyes, and decreased in 1 eye because of the recurrence of polyps. Reduced-fluence PDT combined with bevacizumab for PCV seemed to be effective in improving vision and reducing complications. Similar promising results were reported recently using reduced-fluence V-PDT (light delivery over 70 s) followed 48 h later by intravitreal ranibizumab (0.5 mg) [74].

Summarizing, the combination therapy showed encouraging results including improved vision, the reduced incidence of subretinal hemorrhage, as well as the reduced recurrence of polyps when compared to PDT monotherapy for PCV.

10.5.2 PDT and Anti-inflammatory Strategies

PDT destroys existing neovessels effectively acting as a "CNV eraser", and can be combined with an anti-VEGF strategy aimed at inhibiting further neovessel growth and leakage, and corticosteroids, which will have an anti-inflammatory and anti-fibrosis effect. Thus, by affecting separate pathways, one may presume synergies that might lead to a better treatment outcome.

Whereas, promising results of PDT in combination with anti-inflammatory compounds were reported in AMD, e.g., [75], this treatment modality did not seem to be so efficient in PCV patients. A retrospective analysis of PCV patients who underwent V-PDT with or without intravitreal triamcinolone acetonide (IVTA), with follow-up of 2 or more years, was reported [76].Totally, 27 eyes were analyzed, with 12 eyes treated by PDT monotherapy and 15 eyes treated by combined PDT with IVTA. PDT reduced the risks of visual loss in patients with symptomatic PCV in the short term, but the effect was not sustained after 1 year. The adjunctive use of IVTA during PDT did not appear to result in additional benefit for treating PCV.

10.5.3 Triple Therapy

To date, we have found only one report with a long-term evaluation of the combination therapy involving V-PDT, anti-VEGF, and anti-inflammatory agents [77] in PCV. The gain of visual acuity was reported in almost 42 % of patients treated with the triple therapy, and only in 12 % in the V-PDT group. Moreover, in the triple therapy group, the retreatment-free period was longer and the vitreous

hemorrhage was reduced as compared to that in the V-PDT monotherapy group. Further long-term studies are necessary to optimize this very promising triple therapy protocol in PCV.

10.6 Conclusions and Future Directions

The current opinion for PCV treatment is based on clinical experience and a number of intermediate size and fairly large case series. A question that still remains is whether the more selective targeting of choroidal neovascular membranes would improve the therapeutic outcome of PDT leading to reduced retreatment rates [78]. The current use of PDT, both in AMD and PCV, is driven mainly by its combination with other treatment strategies affecting distinctly separate pathways. Additional problem when making treatment decisions in PCV management is the branching vascular network that supplies the polyps. The branching vascular network can continue to persist or even proliferate after thermal laser treatment or photodynamic ablation of the polyps, and thus may finally cause new leakage. Maybe when the polyps are located outside of the macula they might be efficiently destroyed by a thermal laser beam.

Another way to effectively and selectively close neovascularization is through treatment with vascular disrupting agents (VDAs) targeting tubulin. Tubulin is a protein dimer composed of α and β subunits that form microtubules, which are essential to cellular functions like mitosis, transport, and cytokinesis [79]. VDAs reversibly depolymerize the microtubules, leading to an instant shutdown of the blood vessels. Zybrestat (*Fosbretabulin,* Oxigene Inc.) is a small molecule combretastatin A4 phosphate prodrug that is converted to combretastatin inside endothelial cells. Once activated within the endothelial cells, it causes rapid collapse and necrosis of the vasculature. The compound is currently under development for the treatment of anaplastic thyroid cancer [80].

The FAVOR trial was a phase II study investigating the use of a single intravenous injection of Zybrestat at different doses (15–45 mg/m^2) compared to placebo in Asian patients with PCV, followed by imaging of the retina on days 2, 8, 15, and 28. The primary objective of the study was to observe a change in the number of polyps from baseline following the administration of Zybrestat. The data showed that Zybrestat was well tolerated. However, in the patients with decreased polyp activity, the reduction in subretinal fluid and retinal edema was insignificant [81].

In conclusion, PDT combined with anti-VEGF therapy and steroid represents, at this point of time, it seems, the best treatment modality for PCV. Larger clinical trials may help to further improve this treatment of PCV. Moreover, future molecular investigations will help to identify the genetic differences between PCV and AMD. This knowledge may then lead to the design of optimal personalized treatment strategies.

Acknowledgments The authors are grateful for financial support from Dr. J. Jacobi (to PNS).

Conflict of Interest The authors declare no conflict of interest.

References

1. Schmidt-Erfurth U, Miller J, Sickenberg M, Bunse A, Laqua H, Gragoudas E et al (1998) Photodynamic therapy of subfoveal choroidal neovascularization: clinical and angiographic examples. Graefes Arch Clin Exp Ophthalmol 236(5):365–374
2. Koh A, Lim TH, Au Eong KG, Chee C, Ong SG, Tan N (2011) Optimising the management of choroidal neovascularisation in Asian patients: consensus on treatment recommendations for anti-VEGF therapy. Singapore Med J 52(4):232–240
3. Koh S, Haimovici R (2004) In: Gragoudas ES, Miller JW, Zografos L (eds) Photodynamic therapy of ocular diseases. Lippincott Williams & Wilkins, Philadelphia
4. Ambati J, Ambati BK, Yoo SH, Lanchulev S, Adamis AP (2003) Age-related macular degeneration: etiology, pathogenesis, and therapeutic strategies. Surv Ophthalmol 48(3):257–293
5. Au Eong KG (2006) Age-related macular degeneration: an emerging challenge for eye care and public health professionals in the Asia Pacific region. Ann Acad Med Singapore 35(3):133–135
6. Coppens G, Spielberg L, Leys A (2011) Polypoidal choroidal vasculopathy, diagnosis and management. Bull Soc Belge Ophtalmol 317:39–44
7. Seddon JM, Reynolds R, Yu Y, Daly MJ, Rosner B (2011) Risk models for progression to advanced age-related macular degeneration using demographic, environmental, genetic, and ocular factors. Ophthalmology 118(11):2203–2211
8. van den Bergh H (2001) Photodynamic therapy of age-related macular degeneration: history and principles. Semin Ophthalmol 16(4):181–200
9. Nowak-Sliwinska P (2012) Anti-angiogenic treatment for exudative age-related macular degeneration: new strategies are underway. Current Angiogenesis 1(4):1–6
10. Schmidt-Erfurth U, Hasan T, Gragoudas E, Michaud N, Flotte TJ, Birngruber R (1994) Vascular targeting in photodynamic occlusion of subretinal vessels. Ophthalmology 101(12):1953–1961
11. Miller JW (2010) Treatment of age-related macular degeneration: beyond VEGF. Jpn J Ophthalmol 54(6):523–528
12. Stepinac TK, Chamot SR, Rungger-Brandle E, Ferrez P, Munoz JL, van den Bergh H et al (2005) Light-induced retinal vascular damage by Pd-porphyrin luminescent oxygen probes. Invest Ophthalmol Vis Sci 46(3):956–966
13. Weiss A, van den Bergh H, Griffioen AW, Nowak-Sliwinska P (2012) Angiogenesis inhibition for the improvement of photodynamic therapy: the revival of a promising idea. BBA Rev Cancer 1826(1):53–70
14. Blinder KJ, Blumenkranz MS, Bressler NM, Bressler SB, Donato G, Lewis H et al (2003) Verteporfin therapy of subfoveal choroidal neovascularization in pathologic myopia: 2-year results of a randomized clinical trial-VIP report no. 3. Ophthalmology 110(4):667–673
15. Kaiser PK (2006) Verteporfin therapy of subfoveal choroidal neovascularization in age-related macular degeneration: 5-year results of two randomized clinical trials with an open-label extension: TAP report no. 8. Graefes Arch Clin Exp Ophthalmol 244(9):1132–1142
16. Lam DS, Chan WM, Liu DT, Fan DS, Lai WW, Chong KK (2004) Photodynamic therapy with verteporfin for subfoveal choroidal neovascularisation of pathologic myopia in Chinese eyes: a prospective series of 1 and 2 year follow up. Br J Ophthalmol 88(10):1315–1319

17. Antoszyk AN, Tuomi L, Chung CY, Singh A (2008) Ranibizumab combined with verteporfin photodynamic therapy in neovascular age-related macular degeneration (FOCUS): year 2 results. Am J Ophthalmol 145(5):862–874
18. Brown DM, Kaiser PK, Michels M, Soubrane G, Heier JS, Kim RY et al (2006) Ranibizumab versus verteporfin for neovascular age-related macular degeneration. N Engl J Med 355(14):1432–1444
19. Schmidt-Erfurth U, Wolf S (2008) Same-day administration of verteporfin and ranibizumab 0.5 mg in patients with choroidal neovascularisation due to age-related macular degeneration. Br J Ophthalmol 92(12):1628–1635
20. Spitzer MS, Ziemssen F, Bartz-Schmidt KU, Gelisken F, Szurman P (2008) Treatment of age-related macular degeneration: focus on ranibizumab. Clin Ophthalmol 2(1):1–14
21. Augustin A (2009) Triple therapy for age-related macular degeneration. Retina 29(6):S8–S11
22. DENALI (2010) http://www.qltinc.com/newsCenter/2010/100615.htm
23. Hudson HL (2008) The RADICAL trial: exploring combination therapies. Retina Today 1:59–62
24. Yip PP, Woo CF, Tang HH, Ho CK (2009) Triple therapy for neovascular age-related macular degeneration using single-session photodynamic therapy combined with intravitreal bevacizumab and triamcinolone. Br J Ophthalmol 93(6):754–758
25. Japanese age-related macular degeneration trial (2003) 1-year results of photodynamic therapy with verteporfin in Japanese patients with subfoveal choroidal neovascularization secondary to age-related macular degeneration. Am J Ophthalmol 136(6):1049–1061
26. Gomi F, Ohji M, Sayanagi K, Sawa M, Sakaguchi H, Oshima Y et al (2008) One-year outcomes of photodynamic therapy in age-related macular degeneration and polypoidal choroidal vasculopathy in Japanese patients. Ophthalmology 115(1):141–146
27. Honda S, Imai H, Yamashiro K, Kurimoto Y, Kanamori-Matsui N, Kagotani Y et al (2009) Comparative assessment of photodynamic therapy for typical age-related macular degeneration and polypoidal choroidal vasculopathy: a multicenter study in Hyogo prefecture. Jpn Ophthalmol 223(5):333–338
28. Yamashita A, Shiraga F, Shiragami C, Ono A, Tenkumo K (2010) One-year results of reduced-fluence photodynamic therapy for polypoidal choroidal vasculopathy. Am J Ophthalmol 149(3):465–471 e1
29. Ciardella AP, Donsoff IM, Huang SJ, Costa DL, Yannuzzi LA (2004) Polypoidal choroidal vasculopathy. Surv Ophthalmol 49(1):25–37
30. Kleiner RC, Brucker AJ, Johnston RL (1990) The posterior uveal bleeding syndrome. Retina 10(1):9–17
31. Stern RM, Zakov ZN, Zegarra H, Gutman FA (1985) Multiple recurrent serosanguineous retinal pigment epithelial detachments in black women. Am J Ophthalmol 100(4):560–569
32. Yannuzzi LA, Ciardella A, Spaide RF, Rabb M, Freund KB, Orlock DA (1997) The expanding clinical spectrum of idiopathic polypoidal choroidal vasculopathy. Arch Ophthalmol 115(4):478–485
33. Imamura Y, Engelbert M, Iida T, Freund KB, Yannuzzi LA (2010) Polypoidal choroidal vasculopathy: a review. Surv Ophthalmol 55(6):501–515
34. Maruko I, Iida T, Saito M, Nagayama D, Saito K (2007) Clinical characteristics of exudative age-related macular degeneration in Japanese patients. Am J Ophthalmol 144(1):15–22
35. Okubo A, Sameshima M, Uemura A, Kanda S, Ohba N (2002) Clinicopathological correlation of polypoidal choroidal vasculopathy revealed by ultrastructural study. Br J Ophthalmol 86(10):1093–1098
36. Cackett P, Wong D, Yeo I (2009) A classification system for polypoidal choroidal vasculopathy. Retina 29(2):187–191
37. Spaide RF, Yannuzzi LA, Slakter JS, Sorenson J, Orlach DA (1995) Indocyanine green videoangiography of idiopathic polypoidal choroidal vasculopathy. Retina 15(2):100–110
38. Kondo N, Honda S, Ishibashi K, Tsukahara Y, Negi A (2008) Elastin gene polymorphisms in neovascular age-related macular degeneration and polypoidal choroidal vasculopathy. Invest Ophthalmol Vis Sci 49(3):1101–1105

39. Nakashizuka H, Mitsumata M, Okisaka S, Shimada H, Kawamura A, Mori R et al (2008) Clinicopathologic findings in polypoidal choroidal vasculopathy. Invest Ophthalmol Vis Sci 49(11):4729–4737
40. Iijima H, Iida T, Imai M, Gohdo T, Tsukahara S (2000) Optical coherence tomography of orange-red subretinal lesions in eyes with idiopathic polypoidal choroidal vasculopathy. Am J Ophthalmol 129(1):21–26
41. Jirarattanasopa P, Ooto S, Nakata I, Tsujikawa A, Yamashiro K, Oishi A et al (2012) Choroidal thickness, vascular hyperpermeability, and complement factor H in age-related macular degeneration and polypoidal choroidal vasculopathy. Invest Ophthalmol Vis Sci 53(7):3663–3672
42. Yannuzzi LA, Sorenson J, Spaide RF, Lipson B (1990) Idiopathic polypoidal choroidal vasculopathy (IPCV). Retina 10(1):1–8
43. Yannuzzi LA, Sorenson J, Spaide RF, Lipson B (1990) Idiopathic polypoidal choroidal vasculopathy (IPCV). 1990. Retina 32(Suppl 1):1–8 (2012 Feb)
44. Laude A, Cackett PD, Vithana EN, Yeo IY, Wong D, Koh AH et al (2010) Polypoidal choroidal vasculopathy and neovascular age-related macular degeneration: same or different disease? Prog Retin Eye Res 29(1):19–29
45. Lim LS, Mitchell P, Seddon JM, Holz FG, Wong TY (2012) Age-related macular degeneration. Lancet 379(9827):1728–1738
46. Jager RD, Mieler WF, Miller JW (2008) Age-related macular degeneration. N Engl J Med 358(24):2606–2617
47. Chung SE, Kang SW, Lee JH, Kim YT (2011) Choroidal thickness in polypoidal choroidal vasculopathy and exudative age-related macular degeneration. Ophthalmology 118(5):840–845
48. Matsuoka M, Ogata N, Otsuji T, Nishimura T, Takahashi K, Matsumura M (2004) Expression of pigment epithelium derived factor and vascular endothelial growth factor in choroidal neovascular membranes and polypoidal choroidal vasculopathy. Br J Ophthalmol 88(6):809–815
49. Tong JP, Chan WM, Liu DT, Lai TY, Choy KW, Pang CP et al (2006) Aqueous humor levels of vascular endothelial growth factor and pigment epithelium-derived factor in polypoidal choroidal vasculopathy and choroidal neovascularization. Am J Ophthalmol 141(3):456–462
50. Hayashi H, Yamashiro K, Gotoh N, Nakanishi H, Nakata I, Tsujikawa A et al (2010) CFH and ARMS2 variations in age-related macular degeneration, polypoidal choroidal vasculopathy, and retinal angiomatous proliferation. Invest Ophthalmol Vis Sci 51(11):5914–5919
51. Gotoh N, Nakanishi H, Hayashi H, Yamada R, Otani A, Tsujikawa A et al (2009) ARMS2 (LOC387715) variants in Japanese patients with exudative age-related macular degeneration and polypoidal choroidal vasculopathy. Am J Ophthalmol 147(6):1037–1041, 41 e1-2
52. Lee KY, Vithana EN, Mathur R, Yong VH, Yeo IY, Thalamuthu A et al (2008) Association analysis of CFH, C2, BF, and HTRA1 gene polymorphisms in Chinese patients with polypoidal choroidal vasculopathy. Invest Ophthalmol Vis Sci 49(6):2613–2619
53. Chen H, Liu K, Chen LJ, Hou P, Chen W, Pang CP (2012) Genetic associations in polypoidal choroidal vasculopathy: a systematic review and meta-analysis. Mol Vis 18:816–829
54. Yuzawa M, Mori R, Haruyama M (2003) A study of laser photocoagulation for polypoidal choroidal vasculopathy. Jpn J Ophthalmol 47(4):379–384
55. Nishijima K, Takahashi M, Akita J, Katsuta H, Tanemura M, Aikawa H et al (2004) Laser photocoagulation of indocyanine green angiographically identified feeder vessels to idiopathic polypoidal choroidal vasculopathy. Am J Ophthalmol 137(4):770–773
56. Costa RA, Navajas EV, Farah ME, Calucci D, Cardillo JA, Scott IU (2005) Polypoidal choroidal vasculopathy: angiographic characterization of the network vascular elements and a new treatment paradigm. Prog Retin Eye Res 24(5):560–586
57. Spaide RF, Martin ML, Slakter J, Yannuzzi LA, Sorenson J, Guyer DR et al (2002) Treatment of idiopathic subfoveal choroidal neovascular lesions using photodynamic therapy with verteporfin. Am J Ophthalmol 134(1):62–68

58. Spaide RF, Donsoff I, Lam DL, Yannuzzi LA, Jampol LM, Slakter J et al (2002) Treatment of polypoidal choroidal vasculopathy with photodynamic therapy. Retina 32(Suppl 1):529–535 (2012 Feb)
59. Yamashita A, Shiraga F, Shiragami C, Shirakata Y, Fujiwara A (2012) Two-year results of reduced-fluence photodynamic therapy for polypoidal choroidal vasculopathy. Am J Ophthalmol 18 Sep 2012
60. Leal S, Silva R, Figueira J, Cachulo ML, Pires I, de Abreu JR et al (2010) Photodynamic therapy with verteporfin in polypoidal choroidal vasculopathy: results after 3 years of follow-up. Retina 30(8):1197–1205
61. Hirami Y, Tsujikawa A, Otani A, Yodoi Y, Aikawa H, Mandai M et al (2007) Hemorrhagic complications after photodynamic therapy for polypoidal choroidal vasculopathy. Retina 27(3):335–341
62. Akaza E, Mori R, Yuzawa M (2008) Long-term results of photodynamic therapy of polypoidal choroidal vasculopathy. Retina 28(5):717–722
63. Wakabayashi T, Gomi F, Sawa M, Tsujikawa M, Tano Y (2008) Marked vascular changes of polypoidal choroidal vasculopathy after photodynamic therapy. Br J Ophthalmol 92(7):936–940
64. Gomi F, Sawa M, Wakabayashi T, Sasamoto Y, Suzuki M, Tsujikawa M (2010) Efficacy of intravitreal bevacizumab combined with photodynamic therapy for polypoidal choroidal vasculopathy. Am J Ophthalmol 150(1):48–54 e1
65. Lai TY, Chan WM, Liu DT, Luk FO, Lam DS (2008) Intravitreal bevacizumab (Avastin) with or without photodynamic therapy for the treatment of polypoidal choroidal vasculopathy. Br J Ophthalmol 92(5):661–666
66. Saito M, Iida T, Kano M (2012) Combined intravitreal ranibizumab and photodynamic therapy for polypoidal choroidal vasculopathy. Retina 32(7):1272–1279
67. Gomi F, Sawa M, Sakaguchi H, Tsujikawa M, Oshima Y, Kamei M et al (2008) Efficacy of intravitreal bevacizumab for polypoidal choroidal vasculopathy. Br J Ophthalmol 92(1):70–73
68. Tsujikawa A, Ooto S, Yamashiro K, Tamura H, Otani A, Yoshimura N (2010) Treatment of polypoidal choroidal vasculopathy by intravitreal injection of bevacizumab. Jpn J Ophthalmol 54(4):310–319
69. Kokame GT, Yeung L, Lai JC (2010) Continuous anti-VEGF treatment with ranibizumab for polypoidal choroidal vasculopathy: 6-month results. Br J Ophthalmol 94(3):297–301
70. Safety Study of High-Dose Ranibizumab for Polypoidal Choroidal Vasculopathy (PEARL2) (2010) http://clinicaltrials.gov/ct2/show/NCT01248117
71. Tsuchiya D, Yamamoto T, Kawasaki R, Yamashita H (2009) Two-year visual outcomes after photodynamic therapy in age-related macular degeneration patients with or without polypoidal choroidal vasculopathy lesions. Retina 29(7):960–965
72. Ruamviboonsuk P, Tadarati M, Vanichvaranont S, Hanutsaha P, Pokawattana N (2010) Photodynamic therapy combined with ranibizumab for polypoidal choroidal vasculopathy: results of a 1-year preliminary study. Br J Ophthalmol 94(8):1045–1051
73. Sagong M, Lim S, Chang W (2012) Reduced-fluence photodynamic therapy combined with intravitreal bevacizumab for polypoidal choroidal vasculopathy. Am J Ophthalmol 153(5):873–882
74. Ricci F, Calabrese A, Regine F, Missiroli F, Ciardella AP (2012) Combined reduced fluence photodynamic therapy and intravitreal ranibizumab for polypoidal choroidal vasculopathy. Retina 32(7):1280–1288
75. Saito K, Yamamoto T, Tsuchiya D, Kawasaki R, Haneda S, Yamashita H (2009) Effect of combined treatment with sub-Tenon injection of triamcinolone acetonide and photodynamic therapy in Japanese patients with age-related macular degeneration. Jpn J Ophthalmol 53(5):512–518
76. Lai TY, Lam CP, Luk FO, Chan RP, Chan WM, Liu DT et al (2010) Photodynamic therapy with or without intravitreal triamcinolone acetonide for symptomatic polypoidal choroidal vasculopathy. J Ocul Pharmacol Ther 26(1):91–95

77. Nakata I, Tsujikawa A, Yamashiro K, Otani A, Ooto S, Akagi-Kurashige Y et al (2012) Two-year outcome of photodynamic therapy combined with intravitreal injection of bevacizumab and triamcinolone acetonide for polypoidal choroidal vasculopathy. Graefes Arch Clin Exp Ophthalmol 25 Aug 2012
78. Madar-Balakirski N, Tempel-Brami C, Kalchenko V, Brenner O, Varon D, Scherz A et al (2010) Permanent occlusion of feeding arteries and draining veins in solid mouse tumors by vascular targeted photodynamic therapy (VTP) with Tookad. PLoS ONE 5(4):e10282
79. McKeage MJ, Baguley BC (2010) Disrupting established tumor blood vessels: an emerging therapeutic strategy for cancer. Cancer 116(8):1859–1871
80. Ni Z, Hui P (2009) Emerging pharmacologic therapies for wet age-related macular degeneration. Ophthalmologica 223(6):401–410
81. Study Evaluating the Safety and Response of Fosbretabulin in Asian Patients With Polypoidal Choroidal Vasculopathy (PCV) (2012) http://clinicaltrials.gov/ct2/show/NCT01023295
82. Green WR, McDonnell PJ, Yeo JH (1985) Pathologic features of senile macular degeneration. Ophthalmology 92(5):615–627
83. Yuzawa M, Mori R, Kawamura A (2005) The origins of polypoidal choroidal vasculopathy. Br J Ophthalmol 89(5):602–607

Part V
Non-Oncological Applications

Chapter 11
Functional Targeting of Bacteria: A Multimodal Construct for PDT and Diagnostics of Drug-Resistant Bacteria

Shazia Khan and Tayyaba Hasan

Scope

A multimodal construct that targets functionality unique to pathogens, but typically absent in mammals, is the focus of this chapter. A brief overview of antimicrobial photodynamic therapy (PDT) and targeting strategies is provided for context only, followed by the development of the functional targeting that is the substance of this chapter. Deeper reviews on PDT and antimicrobial PDT are topics of other chapters in this book, and other publications. The constructs termed β-lactamase enzyme-activated photosensitizer (β-LEAP)/β-lactamase enzyme-activated fluorophore (β-LEAF) and their potential applications and significance are described in the context of existing technologies. The conclusions with the current state of the art is that this methodology may provide a practical and rapid test for establishing the utility of antibiotics to specific infections, thus reducing the empirical use of these drugs and lowering the incidence of development of drug-resistant pathogens. A less developed aspect of the chapter is the potential for the use of these same constructs in PDT, where they can be used to eradicate lactamase-based drug-resistant bacteria that survive conventional antibiotic treatments, in addition to drug-sensitive bacteria. The chapter ends with a perspective on the broader potential of this platform in microbiology and parasitology.

S. Khan · T. Hasan (✉)
Wellman Center for Photomedicine, Massachusetts General Hospital,
Harvard Medical School, Boston, MA, USA
e-mail: thasan@mgh.harvard.edu

M. H. Abdel-Kader (ed.), *Photodynamic Therapy*,
DOI: 10.1007/978-3-642-39629-8_11, © Springer-Verlag Berlin Heidelberg 2014

11.1 Introduction

The emergence of drug-resistant bacteria poses a challenge to existing treatment strategies. The discovery of antibiotics was a major advance of the 20th century that revolutionized the management of infectious diseases and had a high impact on overall mortality rates worldwide. However, the overuse of antibiotics empirically has led to widespread incidence of drug resistance, where bacteria have devised various means to render antibiotics ineffective or evade their actions. The major mechanisms implicated in antibiotic resistance include enzymatic inactivation of antibiotics, altered target sites, decreased uptake and increased efflux of the antimicrobial agents [1]. Bacteria often employ multiple resistance factors concomitantly [2, 3].

Hospital-acquired infections (HAI) form a major portion of the antibiotic-resistant infections. The Centers for Disease Control and Prevention (CDC) estimates ~1.7 million HAI from bacteria, contributing to 99,000 deaths each year [4]. *Staphylococcus aureus*, including Methicillin-resistant *Staphylococcus aureus* (MRSA), is one of the leading causes of HAI. As per the Association for Professionals in Infection Control & Epidemiology, 1.2 million HAI are caused by *Staphylococcus* annually in the U.S. (2007). MRSA is the most common cause of ER skin infections (New England Journal of Medicine, 2006) and caused 89,785 infections and 15,249 deaths as per reports in 2008 (CDC, 2008). On an average, hospital costs increase ~$6,400 and hospital stay increases ~five days due to these infections (Healthcare Cost and Utilization Project Brief, 2007).

One of the treatment strategies has been to develop new antibiotics that can kill bacteria through different mechanisms. To this end, there have been five new classes of antibiotics since 1970—linezolid (2000) and daptomycin (2003) for systemic infections, mupirocin (1985) and retapamulin (2007) for topical infections, and the recent approval of fidaxomicin (2012) for the treatment of gut infections caused by *Clostridium difficile* [5]. The rate of introduction of new antibiotics, however, does not match up to increasing drug resistance.

Developing new treatment as well as diagnostic modalities, that can provide alternate treatment options and/or rapid information to guide therapy is vital. New methodologies being developed include an application of nanotechnology to deliver high payloads of antibiotics to bacteria using nanoparticles [6]; strategies to interfere with bacterial cell-to-cell communication through quorum sensing pathway to inhibit virulence and/or biofilm formation [7–9]; infection control using endolysins or virion-associated peptidoglycan hydrolases produced by bacteriophages, capable of digesting bacterial cell walls [10–12] and use of plant derived products and metal ions in conjunction with antibiotics [13].

11.2 Antimicrobial Photodynamic Therapy

Among emerging new approaches for management of bacterial infections is PDT, a photochemistry-based approach that has demonstrated efficacy against both drug-resistant and nonresistant pathogens. During PDT, light activation of certain photosensitizers (PS) results in formation of active molecular species, which are toxic to the surrounding cells and tissues [14]. Although PDT was discovered more than a century back as an antimicrobial [15, 16], its more recent application has been primarily for cancer treatment [17–19]. Renewed interest and developments in antimicrobial PDT or photodynamic antimicrobial chemotherapy (PACT) are fairly recent, accelerated by the advent of antibiotic resistance.

One of the advantages of PACT is that both antibiotic resistant and susceptible bacteria can be killed effectively [20–22]. Furthermore, so far there is no evidence of microbial resistance to PACT, even upon repeated application [23, 24]. This may be mainly because the mechanism of PDT-based killing/inhibition of microbial cells is different and relatively nonspecific compared to antibiotics, which tend to target specific components of the bacterial cell [25]. Additionally, PDT has broad spectrum of action, and the same PS can be used against bacteria, fungi and parasites.

PDT has shown promise in the pathogen control preclinically and clinically [14, 26]. This mode has been utilized to treat various tropical pathogen infections including leishmaniasis, trypanosomiasis and malaria, fungal infections and viruses, besides bacteria [27–41]. Different bacterial species, including *Mycobacterium bovis BCG*, *S. aureus*, *Escherichia coli, Acinetobacter baumannii* and *Helicobacter pylori* have been demonstrated to be susceptible to PDT [14, 42–50]. Furthermore, Phase II clinical trials have revealed encouraging results for PDT of leg ulcers and diabetic foot lesions [51]. Perhaps the most successful application of PDT thus far has been in dentistry. Pathogens in plaque have shown to be efficiently killed, and this modality also offers viable treatment options for periodontitis, as well as sterilization of endodontic root canals [26, 52–54]. Periowave, a photodisinfection technique developed by Ondine Biomedical (Vancouver, Canada) has been tested in five clinical trials and is available in Canada and some European countries, and is under review by the FDA currently (http://www.ondinebio.com/products/periowave). Helbo Photodynamic systems (Weis, Austria) and Denfotex Ltd (Inverkeithing, UK) have also developed PDT-based products for dentistry that have undergone clinical trials [53]. Ondine has developed other products as well for photodisinfection. These include MRSAid for eradication of bacteria in nasal passages, Exeloume for treating bacterial biofilms on inner surface of endotracheal tubes and Vitalwave to decolonize the birth canal to prevent transmission of HIV and other pathogens (www.ondinebio.com). MRSAid is in clinical trials and approved as a medical device in Canada, while Exelume and Vitalwave are in the prototype stage.

11.3 Targeted PDT

The active molecular species generated during PDT have multiple cellular targets [55]. This is advantageous because of the potential for broad use in bacteria with varied biology. However, on the flip side, other than the site of PS administration, passive preferential accumulation of the PS and light illumination interval, there is no mechanism for achieving selective destruction of bacteria [56]. This can result in damage to the healthy host tissue due to the nonspecific accumulation or concentration of PS [57]. Currently, most applications of PDT are limited to localized infections, where damage is controlled both by the slight preferential accumulation of the PS at infection site and by confining the volume of illumination. To make antimicrobial PDT more widely applicable, including both regional and systemic infections, targeted approaches that minimize collateral host damage need to be devised. The simplest approaches to such targeted PDT include localized light delivery/illumination and/or targeted PSs [14, 47, 58, 59].

To date, there have been only a few approaches for targeting antimicrobial PDT. Targeted photolysis is a method by which selectivity can be achieved. A moiety recognizing a cell surface marker, such as an antibody, hormone or cytokine can be used to target PS to cells to be killed. Monoclonal antibodies conjugated to PSs have been developed for specific and focused delivery for bacterial killing [60, 61]. Using liposomes for selective delivery of PS to bacterial cells is also possible, as the presence of negatively charged molecules like peptidoglycans, lipotechoic acid and lipopolysachcharides on the surface results in more negative charge in bacterial cells compared to host tissues [62, 63]. One study has demonstrated use of nanoparticles to achieve PS concentration in *Enterococcus faecalis* in a simulated dental infection [64]. Functionalization of polymeric nanoparticles is another method which may make it possible to target specific bacteria [65, 66].

11.4 Functional Targeting of Bacteria

A targeted approach that exploits functionality unique to bacteria, and absent in mammalian cells has been developed. This allows for exquisite selectivity between bacterial and host cells. The methodology, termed β-LEAP (β-lactamase enzyme-activated photosensitizer), is centered on a novel probe construct of the same name (β-LEAP), which capitalizes on the photophysical phenomenon of quenching and dequenching of certain PS. The PS can be quenched when in close proximity, decreasing probability of PS excited state transition, and hence there is decreased formation of active molecular species or fluorescence. β-LEAP is designed such that in the intact probe the PSs remain quenched. Upon cleavage of the β-LEAP probe by β-lactamase, free PSs capable of light-activated antimicrobial effects are released (Fig. 11.1). Here the chromophore serves as a PS, while in a parallel

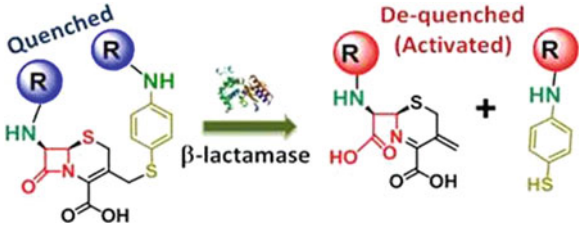

Fig. 11.1 β-LEAP quenching and dequenching. The photosensitizers (*R*) are statically quenched (*blue*) in the uncleaved construct, and hence inactive. When the β-lactam nucleus (*red ring*) is cleaved by β-lactamase, two free photosensitizer moieties that are potentially phototoxic (*red*) are released

approach, β-LEAF (β-lactamase enzyme-activated fluorophore), the chromophore is a fluorescing molecule that is used for diagnostic purposes. This is described subsequently.

The underlying concept involves synthesis of a photoactivable construct, which recognizes a unique target in bacteria. We focused on β-lactamase enzyme as a molecular target to use against bacteria. The bacterial enzyme β-lactamase that targets and cleaves the lactam ring of β-lactam antibiotics is a major resistance mechanism against β-lactam antibiotics. Production of β-lactamases is believed to be the first resistance mechanism developed against β-lactam antibiotics [67]. There is a wide array of β-lactamases with varying specificities and activities, found in both gram-positive and gram-negative bacterial species [68–70]. β-lactamase is an attractive target to use against bacteria, as this enzyme is absent in mammalian cells. This design and concept is extendable to other targets and pathogens.

11.5 β-LEAP and Targeted Antimicrobial PDT

The PS 5-(4'-carboxybutylamino)-9-diethylaminobenzo[a]phenothiazinium chlrodie (EtNBS-COOH) was shown to be a potent antimicrobial agent [71]. In β-LEAP, two EtNBS PSs are conjugated to a β-lactam ring containing cephalosporin derivative, 7-amino-3-chloromethyl-3-cephem-4-carboxylic acid p-methoxybenzyl ester (ACLE), via their free carboxy groups. β-LEAP shows ground-state quenching, and has nearly 5-fold lower fluorescence emission compared to EtNBS-COOH [47]. Homodimerization quenching, as seen here, has the added advantage of releasing two active PSs following probe cleavage, with potential for double the phototoxicity compared to a heterodimer or monomeric system.

This targeted use of PDT against resistant bacteria exploits a bacterial drug-resistance mechanism to activate the PS locally and specifically, affording greater selectivity [47]. β-LEAP was shown to be readily cleaved by *Bacillus cereus* penicillinase (a type of β-lactamase enzyme) with an enzyme concentration-dependent increase in fluorescence emission as a function of time (Fig. 11.2, [47, 72]).

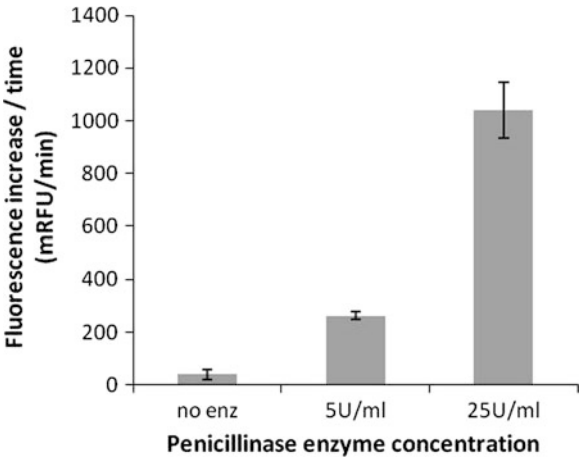

Fig. 11.2 Penicillinase cleaves β-LEAP resulting in fluorescence increase over time

Thus, with higher β-lactamase enzyme concentrations, more PS will be produced correspondingly. The antimicrobial effect of β-LEAP dependent PDT was demonstrated using MRSA clinical isolates [47]. The phototoxicity of β-LEAP and free EtNBS-COOH to human foreskin fibroblasts was compared, showing markedly lower toxic effects when the β-LEAP construct was used [47]. Co-cultures of MRSA and human foreskin fibroblasts showed more β-LEAP uptake in the resistant bacteria compared to human cells. Thus, β-LEAP can target lactamase producing bacteria selectively, with less damage to host tissue compared to a free PS.

This strategy and concept, where the bacteria's resistance mechanism is turned against it and utilized for therapy, represents a paradigm where PDT may be applied systemically, to target infections selectively and specifically. This therapeutic application looks promising based on this early work, and can be used in conjunction with standard antibiotic therapy and/or alone, to target both nonresistant and resistant bacteria. A potential limitation to this technique is that the timing of light delivery could be crucial. Enough time should have elapsed, allowing maximal release of free PS release due to β-lactamase action. At the same time, delays could result in diffusion of the cleaved product, reducing effectiveness of PDT at target infection site, as well increasing probability of nonselective host tissue damage. A better understanding of the pharmacokinetics and optimization of the time-point at which light should be applied following PS administration, as well as the duration of light application, can help circumvent these problems.

An application of this functional targeting of bacteria approach, where it may have an even greater impact, is as a rapid diagnostic tool, β-LEAF. In this context, the probe has a dual application—detection of the resistance biomarker β-lactamase and prediction of antibiotic susceptibility. These applications are described in detail below.

11.6 β-LEAF: Rapid Diagnostic Tool for β-Lactamase Detection and Antibiotic Susceptibility Determination

Currently, antibiotics are routinely prescribed before antibiotic susceptibility testing (AST) is available. The empiric antibiotic regimens can be associated with treatment failures and may also promote resistant strains. Essentially, a misuse of antibiotics can create a selection pressure, enabling drug-resistant populations to increase in number. Furthermore, standard procedures test low bacterial inoculums and are not time efficient. The increasing prevalence of antibiotic-resistant infections thus dictates the need for rapid detection of bacteria and determining respective antibiotic susceptibility profiles, including resistance mechanisms, if any. For severe infections, especially, rapid identification and AST are crucial factors that affect the treatment outcome [73, 74]. Strategies to simplify the prescription procedure based on recommendations from a rapid assessment tool are much needed [75]. β-LEAF is sensitive to β-lactamase, and can hence be used to detect this resistance biomarker. As described, β-LEAF mimics the structure of β-lactam antibiotics, and contains a cephalosporin core, including the cleavable lactam ring, conjugated to two identical EtNBS moieties [47]. By virtue of this structural similarity with β-lactam antibiotics, it can also be utilized to ascertain antibiotic susceptibility. The function of the chromophore as a fluorophore, rather than as a PS, is utilized for diagnostics and a rapid ($\sim$1 h) assay for detection of β-lactamases and determination of antibiotic susceptibility simultaneously has been developed. Timely information of this nature can aid clinicians in making an educated prescription choice about treatment options, rather than relying on empiric or 'best-guess' regimens.

Studies have demonstrated the β-LEAF substrate to be useful for rapid functional definition of extended-spectrum β-lactamases (ESBLS) [72]. β-LEAF can serve as a fluorescent probe for the detection of β-lactamase activity and also identify the effectiveness of antibiotics by a competitive inhibition kinetic analysis (Fig. 11.3). When two substrates compete for the active site of an enzyme, their relative binding affinities can be ascertained. Increasing the concentration of the competitive inhibitor increases the observed Km, as the competitor occupies the enzyme active site with respectively greater frequency. The concentration dependent increase in the observed Km can be used to determine the Ki for the competitor substrate [76]. This concept was applied to test different β-lactam antibiotics with penicillinase enzyme (a β-lactamase enzyme). β-LEAF was considered as the substrate and the β-lactam antibiotic as its competitive inhibitor. By calculating the kinetics of the reaction for β-LEAF (Vmax and Km) in the absence and presence of a competitor antibiotic, the affinity of the respective antibiotic for the β-lactamase was calculated (Fig. 11.3).The reaction velocity of β-LEAF cleavage was observed as the rate of fluorescent product formation (V). The dependence of V on β-LEAF concentration ([S]) was determined using multiple [S]'s and used to determine the Michaelis–Menten constant (Km). The ability of a competitor β-lactam antibiotic to increase the observed Km (Km, obs)

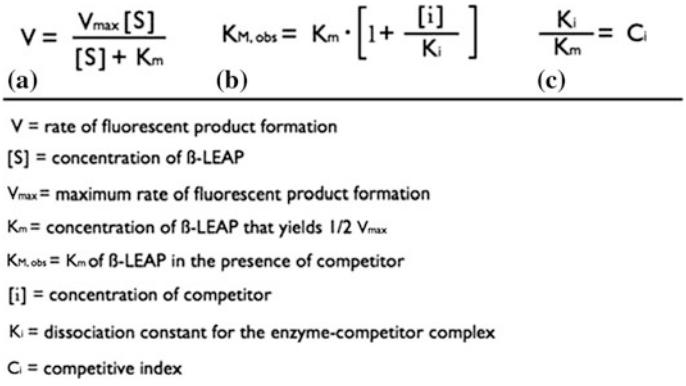

Fig. 11.3 Equations and definitions used to determine competitive index. Figure reproduced from Sallum et al., Photochemistry and Photobiology [72]. Copyright 2010 The Authors. Photochemistry and Photobiology. The American Society of Photobiology

of β-LEAF was probed for a range of concentrations and used to determine the dissociation constant of the enzyme competitor complex (Ki). Further, the Ki of the β-lactam antibiotic competitor was divided by the Km of β-LEAF to derive the competitive index (Ci) (Fig. 11.3).

The susceptibility of *B. cereus* 5/β to a panel of β-lactam antibiotics was tabulated, and Ci value established within 20 min (Fig. 11.4a). The competitive indices, thus determined, were shown to be related to minimum inhibitory concentrations (MIC) determined by conventional AST methods [72], for the different antibiotics respectively, thus validating the approach (Figs. 11.4a, c). (MIC = lowest concentration of antibiotic that inhibits the bacterial growth). These findings demonstrate that the β-LEAF assay is not only more rapid than the MIC assay, but also has a greater sensitive range. Furthermore, a panel of known extended spectrum β-lactamase (ESBL) producing *E. coli* strains from ATCC was assayed with β-LEAF and the antibiotic ceftazidime. These results also showed a good co-relation between the calculated Ci and conventional MICs (Figs. 11.4b, d). *The incubation time for the β-LEAF assay was 20 min while that of the MIC assay was 20 h*. Thus, competitive assays with β-LEAF can provide a rapid insight into antibiotic susceptibility.

Though several rapid test methods are available for predicting a resistance biomarker or antibiotic susceptibility, the β-LEAF assay is the only one to date that can provide information about both aspects in a single test. We propose that the β-LEAF assay is a reliable and rapid dual predictor of β-lactamase and antibiotic susceptibility, being at least 20-fold faster than conventional methods. An important aspect is that these studies serve as a platform technology and pave the way for the development of assays utilizing a broader variety of bacteria, targets and antibiotics.

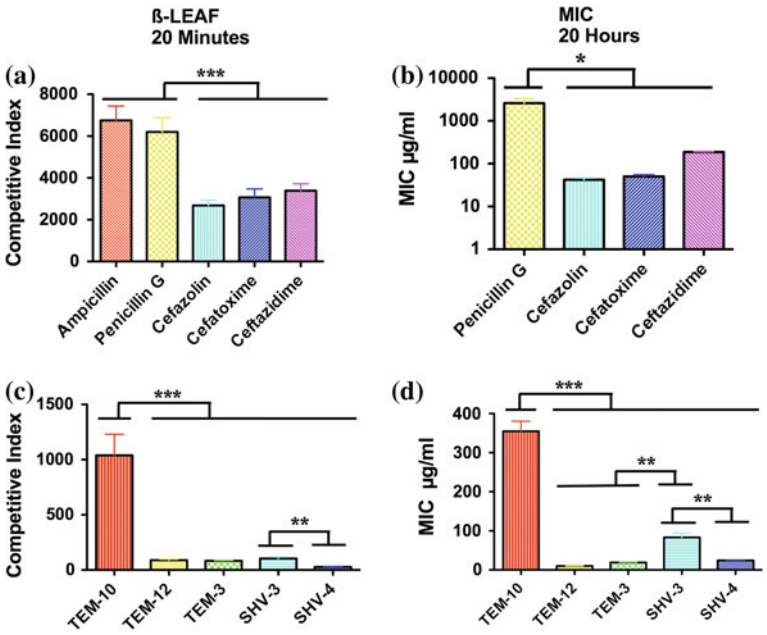

Fig. 11.4 Readouts of β-LEAF assay (20 min, **a** and **c**) and MIC assay (20 h, **b** and **d**). **a** Relative Ci values of β-lactam antibiotics for *B. cereus* 5/ß, **b** relative MIC values for *B. cereus* 5/ß, A Pearson correlation coefficient of 0.899 was determined for these two data sets (**a** and **b**) indicating that β-LEAF can accurately profile the susceptibility of *B. cereus* to a panel of β-lactam antibiotics, **c** the Ci values of ceftazidime for the panel of ESBLs, **d** the MIC values of ceftazidime for the panel of ESBLs were determined. The Pearson correlation coefficient of for these two data sets (**c** and **d**) was 0.984, indicating that β-LEAF accurately profiles the susceptibility of multiple ESBL producers to ceftazidime. All data was analyzed by one-way ANOVA with Tukey's post test (* $p < 0.05$, ** $p < 0.01$, *** $p < 0.001$). Data reproduced from Sallum et al., Photochemistry and Photobiology [72]. Copyright 2010 The Authors. Photochemistry and Photobiology. The American Society of Photobiology

The full significance of being able to test both these parameters—resistance biomarker β-lactamase and antibiotic susceptibility, in 1 h, can be appreciated better upon understanding the state of AST currently. We discuss below some salient points to put these issues in perspective.

11.7 Available Methods for AST and Resistance Detection

11.7.1 Current State of AST

Existing methodologies for determining antibiotic susceptibility include conventional broth/agar dilution and disk-diffusion methods, which involve culturing bacteria in presence of antimicrobials and observing their resultant growth pattern

[77–79]. Thereafter, based on results, the bacterial isolate is designated as susceptible, intermediate or resistant to the antibiotic tested, by comparing with the Clinical and Laboratory Standards Institute (CLSI) Interpretive Charts [80–83]. These methods take at least 24 h to get the results. Automated instruments that serve to detect bacterial growth optically work on the same principles, while reducing the time, manual labor and errors compared to the conventional AST tests. These instruments can aid in both identification and AST of bacteria.

These methods are essentially growth-based and useful only in cases of rapidly growing bacteria. Besides taking a large window of time (24–72 h), these methods may fail to predict antibiotic susceptibilities accurately. Perhaps the greatest pitfall of conventional test methodologies is the use of relatively low bacterial numbers for testing ($5 * 10^5$ CFU/ml). In this context, it becomes important to consider phenomenon such as the 'Inoculum effect'. Essentially, Inoculum effect is defined as a significant increase in Minimum Inhibitory Concentration (MIC; defined as lowest concentration of antibiotic that inhibits bacterial growth) of an antibiotic, when number of organisms inoculated is increased. This effect is observed most commonly with β-lactam antibiotics with β-lactamase producing bacteria, and can be a cause for treatment failures [84–90]. Thus, standard methods of AST utilizing ($5 * 10^5$ CFU/ml) [80–83] may fail to report antibiotic susceptibility accurately in high burden or heteroresistant infections (as genetic heterogeneity may go undetected due to the low numbers tested). The β-LEAF method of detection allows for testing of even 1,000-fold higher concentrations, and hence may provide a more realistic idea of antibiotic susceptibilities in clinical infections.

11.7.2 Detection of β-Lactamase-Based Resistance

In this era of varied antibiotic resistance mechanisms, diagnostics to detect resistance are gaining importance, and increasingly being performed in addition to simple antibiotic susceptibility determination. β-lactamase enzymes are produced by several clinically relevant bacteria. Several growth-based microbiological methods, most of which are variations of the disk-diffusion methods can be employed to determine β-lactamase activity [91], but are rarely used now. Examples include the three-dimensional disk tests and double-disk tests.

Other more simple and rapid techniques have become more popular over the years. β-lactamase cleaves the β-lactam ring of β-lactams to form penicilloic acid. Three main methodologies rely upon detection of the penicilloic acid as an indicator of β-lactamase production. These include the acidimetric method which works on the principle of pH change due to formation of penicilloic acid, resulting in phenol red changing color from red to yellow; iodometric detection wherein iodine reacts with penicilloic acid rather than penicillin and color of starch-iodine complex disappears and chromogenic tests which utilize chromogenic cephalosporins such as nitrocefin, CENTA, PADAC and S1. In this case, following the cleavage of the β-lactam ring, the molecule undergoes a color change [92].

These tests can be performed using commercially available strips or disks, and may also be performed by preparing strips, slides, or in tubes and microtiter plates 'in-house' [92]. These chromogenic methods of β-lactamase detection have emerged as the most popular and widely used in recent times.

PCR-based methods involving detection of the β-lactamase gene (e.g. *blaZ* in *S. aureus*) can be used to determine β-lactamase production indirectly [93, 94]. Patho-Proof Mastitis PCR Kit from Finnzymes is a commercially available kit that can be used for detection of the *blaZ* gene, among others, in milk. Multiplex PCR-based methods are useful to identify bacterial species as well as determine a wide array of antibiotic resistance genes [95–97]. These PCR-based methods have been suggested as diagnostic tools to complement existing methodologies. However, they are capable of predicting only the presence of a gene, which may or may not lead to resistant phenotype. Assaying for gene expression, i.e., the functional resistance enzyme is of paramount importance, and likely to be of greater significance than genotype alone.

11.7.3 Fluorescent β-Lactamase Substrates

β-lactamase has been employed as a reporter system for gene expression studies [98–100] and β-lactamase substrates are utilized to aid these analyses. Some fluorescent β-lactamase substrates, mainly to be employed for reporter gene assays, are available commercially from Invitrogen. These are fluorescence resonance energy transfer (FRET) -based substrates, designed to become fluorescent following cleavage by β-lactamase, and have potential for application in microscopy, FACS and microtiter plate assays. One of these, CCF2/AM substrate has been shown to be useful for protein interaction studies and distinguishing between β-lactamase positive and negative *E. coli* cells [101]. A fairly recent study reports novel near-infrared fluorogenic substrates to detect *Mycobacterium tuberculosis* β-lactamase BlaC, thus allowing for imaging tuberculosis [102]. All of these are detection modalities only.

The β-LEAF fluorescent substrate has shown encouraging results as a diagnostic modality for both AST and detection of β-lactamase-based resistance ([72], unpublished results). Thus far, it is the only methodology reported which can provide information about both parameters rapidly ($\sim$1 h). This approach needs to be validated and developed further toward being incorporated in clinical use, and we are currently extending this work in these directions.

11.8 Summary and Perspectives

It is apparent that the rapid emergence of drug-resistant strains necessitates treating each infection with appropriate modality, rather than using a generalized approach. Rapid diagnostics as well as new treatment strategies are being

developed to cope with these challenges. PDT has shown great potential for generalized as well as targeted therapeutic application, as described here as well as in other chapters of this book. β-LEAP provides an extra level of sensitivity and an option for the killing of drug-resistant bacteria, while minimizing damage to host cells. This opens the potential of using antimicrobial PDT systemically and regionally. Much development remains, including improved constructs, a clearer understanding of the pharmacokinetics, illumination intervals and light delivery for translation of the approach as a therapeutic modality.

In recent years, there has been an increase in development of diagnostics for pathogen infections. Different culture-based and PCR-based methods are available for pathogens like MRSA, for example [103–105]. The newer diagnostic methods seek to dissect resistance mechanisms, and also look at mixed pathogens to enable distinguishing them. Some methods like fluorescence in situ hybridization (FISH)-based pathogen ID kits from AdvanDx and Miacom Diagnostics are available, that can help identify different pathogens in a biospecimen. A diagnostic method to distinguish between bacterial and viral infections has also been developed [106]. Methods such as these, and others summarized in this chapter can be used to rapidly identify pathogens and resistance mechanisms, allowing for a more informed treatment choice. In this context, a multimodal method such as the β-LEAF approach, which can be used for rapid diagnostics to predict both resistance factor β-lactamase and antibiotic susceptibility, simultaneously, has shown great promise [72]. Further optimization of probes and assay conditions and more rigorous testing is, however, needed to develop and enable direct biospecimen testing for rapid determination of antibiotic susceptibility profiles for a given bacterial infection. Such a method can enable customized antibiotic therapy, improving treatment outcomes, lowering costs and reducing emergence of resistance. The β-LEAF technology, based on unique chemical probes that mimic antibiotic structure and target specific resistance enzymes, may be integrated with existing devices, funneled as a probe-array or probe kit that may be used in tandem with available automated instruments, and/or may be independently packaged with a small device as a portable system. Determination of treatment regimen very early on, as per severity of an infection and resistance of bacteria involved, along with prediction of effective antibiotics would be useful in primary healthcare settings, hospitals, as well as military settings. It should be noted, however, that much validation is needed to make this a routine procedure in order to negate the false positives and establish unequivocally the antibiotic drug resistance, susceptibility, virulence, etc. [105].

Finally, this technology should be viewed as a platform where constructs customized to different molecular targets (including targets other than lactamases) maybe developed for different pathogens. The lactamase targeted construct has shown effectiveness in killing of *Brugia malayi*, a parasite responsible for filariasis [107]. These and other applications merit further exploration to establish the impact of this rather simple technology.

Acknowledgments The authors acknowledge research funding from Department of Defense/Air Force Office of Research (DOD/AFOSR) (Grant number FA9550-11-1-0331), and NIH/NIBIB (National Institute of Biomedical Imaging and Bioengineering) (Point of Care Technology in Primary Care) through CIMIT (Center for Integration of Medicine and Innovation Technology) (Grant no.U54 EB015408).

References

1. DeBellis RJ, Zdanawicz M (2000) *Bacteria battle back: addressing antibiotic resistance.* Massachusetts College of Pharmacy and Health Sciences, Boston. http://www.tufts.edu/med/apua/Educ/CME/BBB.pdf. Accessed 5 Feb 2009
2. de Lencastre H et al (1991) Multiple mechanisms of methicillin resistance and improved methods for detection in clinical isolates of *Staphylococcus aureus*. Antimicrob Agents Chemother 35(4):632–639
3. Le Thomas I et al (2001) In vivo selection of a target/efflux double mutant of *Pseudomonas aeruginosa* by ciprofloxacin therapy. J Antimicrob Chemother 48(4):553–555
4. Pollack A (2010) Rising threat of infections unfazed by antibiotics. New York Times, 27 Feb 2010
5. New antibiotics: what's in the pipeline? The conversation 7 Dec 2012. http://theconversation.edu.au/new-antibiotics-whats-in-the-pipeline-10724
6. Radovic-Moreno AF et al (2012) Surface charge-switching polymeric nanoparticles for bacterial cell wall-targeted delivery of antibiotics. ACS Nano 6(5):4279–4287
7. Njoroge J, Sperandio V (2009) Jamming bacterial communication: new approaches for the treatment of infectious diseases. EMBO Mol Med 1(4):201–210
8. Fothergill JL, Winstanley C, James CE (2012) Novel therapeutic strategies to counter *Pseudomonas aeruginosa* infections. Expert Rev Anti Infect Ther 10(2):219–235
9. Romero M, Acuna L, Otero A (2012) Patents on quorum quenching: interfering with bacterial communication as a strategy to fight infections. Recent Pat Biotechnol 6(1):2–12
10. Borysowski J, Weber-Dabrowska B, Gorski A (2006) Bacteriophage endolysins as a novel class of antibacterial agents. Exp Biol Med (Maywood) 231(4):366–377
11. Fischetti VA (2010) Bacteriophage endolysins: a novel anti-infective to control Gram-positive pathogens. Int J Med Microbiol 300(6):357–362
12. Rodriguez-Rubio L et al (2012) Bacteriophage virion-associated peptidoglycan hydrolases: potential new enzybiotics. Crit Rev Microbiol: 1–8
13. Wolska KI, Grzes K, Kurek A (2012) Synergy between novel antimicrobials and conventional antibiotics or bacteriocins. Pol J Microbiol 61(2):95–104
14. Hamblin MR, Hasan T (2004) Photodynamic therapy: a new antimicrobial approach to infectious disease? Photochem Photobiol Sci 3(5):436–450
15. Raab O (1900) Uber die wirkung fluoriziender stoffe auf infusorien. Zeit Biol 39:524–546
16. von Tappeiner H (1904) Zur kenntis der lichtwirkenden (fluoreszierenden) stoffe 1:579–580
17. Friedberg JS et al (2004) Phase II trial of pleural photodynamic therapy and surgery for patients with non-small-cell lung cancer with pleural spread. J Clin Oncol 22(11):2192–2201
18. Baas P et al (1997) Photodynamic therapy as adjuvant therapy in surgically treated pleural malignancies. Br J Cancer 76(6):819–826
19. Hahn NM et al (2006) Hoosier oncology group randomized phase II study of docetaxel, vinorelbine, and estramustine in combination in hormone-refractory prostate cancer with pharmacogenetic survival analysis. Clin Cancer Res 12(20 Pt 1):6094–6099
20. Maisch T (2009) A new strategy to destroy antibiotic resistant microorganisms: antimicrobial photodynamic treatment. Mini Rev Med Chem 9(8):974–983

21. Kashef N et al (2011) Photodynamic inactivation of drug-resistant bacteria isolated from diabetic foot ulcers. Iran J Microbiol 3(1):36–41
22. Topaloglu N, Gulsoy M, Yuksel S (2013) Antimicrobial photodynamic therapy of resistant bacterial strains by indocyanine green and 809-nm diode laser. Photomed Laser Surg 31(4):155–162
23. Giuliani F et al (2010) In vitro resistance selection studies of RLP068/Cl, a new Zn(II) phthalocyanine suitable for antimicrobial photodynamic therapy. Antimicrob Agents Chemother 54(2):637–642
24. Pedigo LA, Gibbs AJ, Scott RJ, Street CN (2009) Absence of bacterial resistance following repeat exposure to photodynamic therapy. In: Proceedings of SPIE, vol 7380. Photodynamic therapy: back to the future, 73803H
25. Wainwright M (1998) Photodynamic antimicrobial chemotherapy (PACT). J Antimicrob Chemother 42(1):13–28
26. Jori G et al (2006) Photodynamic therapy in the treatment of microbial infections: basic principles and perspective applications. Lasers Surg Med 38(5):468–481
27. Akilov OE et al (2007) Photodynamic therapy for cutaneous leishmaniasis: the effectiveness of topical phenothiaziniums in parasite eradication and Th1 immune response stimulation. Photochem Photobiol Sci 6(10):1067–1075
28. Akilov OE et al (2007) Parasiticidal effect of delta-aminolevulinic acid-based photodynamic therapy for cutaneous leishmaniasis is indirect and mediated through the killing of the host cells. Exp Dermatol 16(8):651–660
29. Asilian A, Davami M (2006) Comparison between the efficacy of photodynamic therapy and topical paromomycin in the treatment of old world cutaneous leishmaniasis: a placebo-controlled, randomized clinical trial. Clin Exp Dermatol 31(5):634–637
30. Wainwright M, Baptista MS (2011) The application of photosensitisers to tropical pathogens in the blood supply. Photodiagnosis Photodyn Ther 8(3):240–248
31. Baptista MS, Wainwright M (2011) Photodynamic antimicrobial chemotherapy (PACT) for the treatment of malaria, leishmaniasis and trypanosomiasis. Braz J Med Biol Res 44(1):1–10
32. Lyon JP et al (2011) Photodynamic therapy for pathogenic fungi. Mycoses 54(5):e265–e271
33. Lyon JP et al (2011) Photodynamic antifungal therapy against chromoblastomycosis. Mycopathologia 172(4):293–297
34. Scwingel AR et al (2012) Antimicrobial photodynamic therapy in the treatment of oral candidiasis in HIV-infected patients. Photomed Laser Surg 30(8):429–432
35. Calzavara-Pinton PG et al (2004) Photodynamic therapy of interdigital mycoses of the feet with topical application of 5-aminolevulinic acid. Photodermatol Photoimmunol Photomed 20(3):144–147
36. Marotti J et al (2009) Photodynamic therapy can be effective as a treatment for herpes simplex labialis. Photomed Laser Surg 27(2):357–363
37. Rossi R et al (2009) Photodynamic treatment for viral infections of the skin. G Ital Dermatol Venereol 144(1):79–83
38. Kaufman RH et al (1978) Treatment of genital herpes simplex virus infection with photodynamic inactivation. Am J Obstet Gynecol 132(8):861–869
39. Kelley JP, Rashid RM (2011) Phototherapy in the treatment of cutaneous herpesvirus manifestations. Cutis 88(3):140–148
40. Costa L et al (2012) Photodynamic inactivation of mammalian viruses and bacteriophages. Viruses 4(7):1034–1074
41. Giomi B et al (2012) Off label treatments of genital warts: the role of photodynamic therapy. G Ital Dermatol Venereol 147(5):467–474
42. O'Riordan K et al (2007) Real-time fluorescence monitoring of phenothiazinium photosensitizers and their anti-mycobacterial photodynamic activity against *Mycobacterium bovis* BCG in in vitro and in vivo models of localized infection. Photochem Photobiol Sci 6(10):1117–1123

43. O'Riordan K et al (2006) Photoinactivation of Mycobacteria in vitro and in a new murine model of localized *Mycobacterium bovis* BCG-induced granulomatous infection. Antimicrob Agents Chemother 50(5):1828–1834
44. Lambrechts SA et al (2005) Photodynamic therapy for *Staphylococcus aureus* infected burn wounds in mice. Photochem Photobiol Sci 4(7):503–509
45. Gad F et al (2004) Targeted photodynamic therapy of established soft-tissue infections in mice. Photochem Photobiol Sci 3(5):451–458
46. Gad F et al (2004) Effects of growth phase and extracellular slime on photodynamic inactivation of gram-positive pathogenic bacteria. Antimicrob Agents Chemother 48(6):2173–2178
47. Zheng X et al (2009) Exploiting a bacterial drug-resistance mechanism: a light-activated construct for the destruction of MRSA. Angew Chem 121(12):2182–2185
48. Hamblin MR et al (2002) Rapid control of wound infections by targeted photodynamic therapy monitored by in vivo bioluminescence imaging. Photochem Photobiol 75(1):51–57
49. Mihu MR, Martinez LR (2011) Novel therapies for treatment of multi-drug resistant *Acinetobacter baumannii* skin infections. Virulence 2(2):97–102
50. Bedwell J et al (1990) In vitro killing of *Helicobacter pylori* with photodynamic therapy. Lancet 335(8700):1287
51. Brown S (2012) Clinical antimicrobial photodynamic therapy: phase II studies in chronic wounds. J Natl Compr Canc Netw 10(Suppl 2):S80–S83
52. Wilson M (2004) Lethal photosensitisation of oral bacteria and its potential application in the photodynamic therapy of oral infections. Photochem Photobiol Sci 3(5):412–418
53. Kharkwal GB et al (2011) Photodynamic therapy for infections: clinical applications. Lasers Surg Med 43(7):755–767
54. Raghavendra M, Koregol A, Bhola S (2009) Photodynamic therapy: a targeted therapy in periodontics. Aust Dent J 54(Suppl 1):S102–S109
55. Tang HM, Hamblin MR, Yow CM (2007) A comparative in vitro photoinactivation study of clinical isolates of multidrug-resistant pathogens. J Infect Chemother 13(2):87–91
56. Chen B et al (2006) Vascular and cellular targeting for photodynamic therapy. Crit Rev Eukaryot Gene Expr 16(4):279–305
57. Verma S et al (2007) Strategies for enhanced photodynamic therapy effects. Photochem Photobiol 83(5):996–1005
58. Demidova TN, Hamblin MR (2004) Photodynamic therapy targeted to pathogens. Int J Immunopathol Pharmacol 17(3):245–254
59. Rai P et al (2010) Development and applications of photo-triggered theranostic agents. Adv Drug Deliv Rev 62(11):1094–1124
60. Friedberg JS et al (1991) Antibody-targeted photolysis. Bacteriocidal effects of Sn (IV) chlorin e6-dextran-monoclonal antibody conjugates. Ann N Y Acad Sci 618:383–393
61. Strong L, Yarmush DM, Yarmush ML (1994) Antibody-targeted photolysis. Photophysical, biochemical, and pharmacokinetic properties of antibacterial conjugates. Ann N Y Acad Sci 745:297–320
62. Ferro S et al (2007) Efficient photoinactivation of methicillin-resistant *Staphylococcus aureus* by a novel porphyrin incorporated into a poly-cationic liposome. Int J Biochem Cell Biol 39(5):1026–1034
63. George S, Hamblin MR, Kishen A (2009) Uptake pathways of anionic and cationic photosensitizers into bacteria. Photochem Photobiol Sci 8(6):788–795
64. Pagonis TC et al (2010) Nanoparticle-based endodontic antimicrobial photodynamic therapy. J Endod 36(2):322–328
65. Lee YE, Kopelman R (2011) Polymeric nanoparticles for photodynamic therapy. Methods Mol Biol 726:151–178
66. Longo JPF, Muehlmann LA, de Azevedo RB (2011) Nanostructured carriers for photodynamic therapy applications in microbiology science against microbial pathogens: communicating current research and technological advances In: Méndez-Vilas A (ed), pp 189–196

67. Poole K (2002) Mechanisms of bacterial biocide and antibiotic resistance. J Appl Microbiol 92(Suppl):55S–64S
68. Bush K, Jacoby GA, Medeiros AA (1995) A functional classification scheme for beta-lactamases and its correlation with molecular structure. Antimicrob Agents Chemother 39(6):1211–1233
69. Livermore DM (1995) Beta-Lactamases in laboratory and clinical resistance. Clin Microbiol Rev 8(4):557–584
70. Rice LB (2012) Mechanisms of resistance and clinical relevance of resistance to beta-lactams, glycopeptides, and fluoroquinolones. Mayo Clin Proc 87(2):198–208
71. Verma S et al (2009) Antimicrobial photodynamic efficacy of side-chain functionalized benzo[a]phenothiazinium dyes. Photochem Photobiol 85(1):111–118
72. Sallum UW et al (2010) Rapid functional definition of extended spectrum beta-lactamase activity in bacterial cultures via competitive inhibition of fluorescent substrate cleavage. Photochem Photobiol 86(6):1267–1271
73. Bergeron MG, Ouellette M (1998) Preventing antibiotic resistance through rapid genotypic identification of bacteria and of their antibiotic resistance genes in the clinical microbiology laboratory. J Clin Microbiol 36(8):2169–2172
74. Byl B et al (1999) Impact of infectious diseases specialists and microbiological data on the appropriateness of antimicrobial therapy for bacteremia. Clin Infect Dis 29(1):60–66
75. Rice LB (2011) Rapid diagnostics and appropriate antibiotic use. Clin Infect Dis 52(Suppl 4):S357–S360
76. Motulsky HC, Christopoulos A (2004) A fitting models to biological data using linear and nonlinear regression. Oxford University Press, New York
77. Ericsson HM, Sherris JC (1971) Antibiotic sensitivity testing. Report of an international collaborative study. Acta Pathol Microbiol Scand B Microbiol Immunol 217: Suppl 217:1+
78. Bauer AW et al (1966) Antibiotic susceptibility testing by a standardized single disk method. Am J Clin Pathol 45(4):493–496
79. Bauer AW et al (1966) Antibiotic susceptibility testing by a standardized single disk method. Tech Bull Regist Med Technol 36(3):49–52
80. CLSI (2009) Performance standards for antimicrobial disk susceptibility tests; approved standard—10th edition. CLSI document M2-A10. Clinical and Laboratory Standards Institute, Wayne, 29(1)
81. CLSI (2011) Performance standards for antimicrobial susceptibility testing: Twenty-first informational supplement; M100-S21. Clinical and Laboratory Standards Institute, Wayne
82. CLSI (2012) Performance standards for antimicrobial susceptibility testing: twenty-second informational supplement; M100-S22. Clinical and Laboratory Standards Institute, Wayne
83. CLSI (2012) Performance standards for antimicrobial disk susceptibility tests; approved standard—11th edition. CLSI document M02-A11, vol 32(1). Clinical and Laboratory Standards Institute, Wayne
84. Brook I (1989) Inoculum effect. Rev Infect Dis 11(3):361–368
85. Nannini EC et al (2009) Inoculum effect with cefazolin among clinical isolates of methicillin-susceptible *Staphylococcus aureus*: frequency and possible cause of cefazolin treatment failure. Antimicrob Agents Chemother 53(8):3437–3441
86. Nannini EC et al (2010) Determination of an inoculum effect with various cephalosporins among clinical isolates of methicillin-susceptible *Staphylococcus aureus*. Antimicrob Agents Chemother 54(5):2206–2208
87. Bryant RE, Alford RH (1977) Unsuccessful treatment of Staphylococcal endocarditis with cefazolin. JAMA 237(6):569–570
88. Fernandez-Guerrero ML, de Gorgolas M (2005) Cefazolin therapy for *Staphylococcus aureus* bacteremia. Clin Infect Dis 41(1):127
89. Nannini EC, Singh KV, Murray BE (2003) Relapse of type A beta-lactamase-producing *Staphylococcus aureus* native valve endocarditis during cefazolin therapy: revisiting the issue. Clin Infect Dis 37(9):1194–1198

90. Quinn EL et al (1973) Clinical experiences with cefazolin and other cephalosporins in bacterial endocarditis. J Infect Dis 128: Suppl:S386–389
91. Livermore DM, Brown DF (2001) Detection of beta-lactamase-mediated resistance. J Antimicrob Chemother 48(Suppl 1):59–64
92. Kilic E, Yalinay Cirak M (2006) Comparison of staphylococcal beta-lactamase detection methods. FABAD J Pharm Sci 31:79–84)
93. Haveri M et al (2005) Comparison of phenotypic and genotypic detection of penicillin G resistance of *Staphylococcus aureus* isolated from bovine intramammary infection. Vet Microbiol 106(1–2):97–102
94. Vesterholm-Nielsen M et al (1999) Occurrence of the blaZ gene in penicillin resistant *Staphylococcus aureus* isolated from bovine mastitis in Denmark. Acta Vet Scand 40(3):279–286
95. Martineau F et al (2000) Multiplex PCR assays for the detection of clinically relevant antibiotic resistance genes in staphylococci isolated from patients infected after cardiac surgery. The ESPRIT trial. J Antimicrob Chemother 46(4):527–534
96. Strommenger B et al (2003) Multiplex PCR assay for simultaneous detection of nine clinically relevant antibiotic resistance genes in *Staphylococcus aureus*. J Clin Microbiol 41(9):4089–4094
97. Malhotra-Kumar S et al (2005) Multiplex PCR for simultaneous detection of macrolide and tetracycline resistance determinants in streptococci. Antimicrob Agents Chemother 49(11):4798–4800
98. Zlokarnik G et al (1998) Quantitation of transcription and clonal selection of single living cells with beta-lactamase as reporter. Science 279(5347):84–88
99. Gao W et al (2003) Novel fluorogenic substrates for imaging beta-lactamase gene expression. J Am Chem Soc 125(37):11146–11147
100. Xing B, Khanamiryan A, Rao J (2005) Cell-permeable near-infrared fluorogenic substrates for imaging beta-lactamase activity. J Am Chem Soc 127(12):4158–4159
101. Nord O, Gustrin A, Nygren PA (2005) Fluorescent detection of beta-lactamase activity in living *Escherichia coli* cells via esterase supplementation. FEMS Microbiol Lett 242(1):73–79
102. Kong Y et al (2010) Imaging tuberculosis with endogenous beta-lactamase reporter enzyme fluorescence in live mice. Proc Natl Acad Sci U S A 107(27):12239–12244
103. Marlowe EM et al (2011) Evaluation of the Cepheid Xpert MTB/RIF assay for direct detection of *Mycobacterium tuberculosis* complex in respiratory specimens. J Clin Microbiol 49(4):1621–1623
104. Malhotra-Kumar S et al (2008) Current trends in rapid diagnostics for methicillin-resistant *Staphylococcus aureus* and glycopeptide-resistant enterococcus species. J Clin Microbiol 46(5):1577–1587
105. Sturenburg E (2009) Rapid detection of methicillin-resistant *Staphylococcus aureus* directly from clinical samples: methods, effectiveness and cost considerations. Ger Med Sci 7:Doc06
106. Prilutsky D et al (2011) Differentiation between viral and bacterial acute infections using chemiluminescent signatures of circulating phagocytes. Anal Chem 83(11):4258–4265
107. Foster JS, Sallum UW, Slatko B, Hasan T (2012) Development of photodynamic therapy for parasitic filarial nematodes. In: Proceedings of 36th meeting of the American society for photobiology, Montreal (abstract no. MN8-1)

Chapter 12
Photodynamic Therapy: A Novel Promising Approach for the Treatment of Spontaneous Microbial Infections in Pet Animals

Clara Fabris, Marina Soncin, Monica Camerin, Furio Corsi, Ilaria Cattin, Fabrizio Cardin, Laura Guidolin, Giulio Jori and Olimpia Coppellotti

Abstract Photodynamic therapy with full spectrum visible light and porphyrin-type photosensitisers appears to efficiently induce the inactivation of a broad spectrum of microbial pathogens, including antibiotic-resistant strains, without in turn promoting the selection of PDT-resistant species. Application of this therapeutic modality to the treatment of spontaneously developed infections in dogs resulted in a very efficient healing of wounds with an extensive drop in the population of pathogens. The treatment appeared to be applicable for both mycotic and bacterial infections and was devoid of detectable undesired side effects. No significant differences in efficacy was observed whether a porphyrin, chlorin, or phthalocyanine photosensitising agent was used in spite of strong differences in the light absorption spectrum among the three tetrapyrrole derivatives.

12.1 Introduction

Porphyrins and their tetrapyrrole analogues, such as porphycenes, chlorins, phthalocyanines, and naphthalocyanines, are currently used as photosensitising agents in the photodynamic therapy (PDT) of tumors and other nononcological

C. Fabris · M. Soncin · M. Camerin · L. Guidolin · G. Jori (✉) · O. Coppellotti
Department of Biology, University of Padova, Padova, Italy
e-mail: giulio.jori@unipd.it

F. Corsi · I. Cattin
Veterinary Clinic "Prato della Valle", Padova, Italy

F. Cardin
Dipartimento dell'Anziano, Clinica Chirurgica Geriatrica,
Azienda Ospedaliera Padova, Padova, Italy

M. H. Abdel-Kader (ed.), *Photodynamic Therapy*,
DOI: 10.1007/978-3-642-39629-8_12,

diseases [1]. The photodynamic process is promoted by the combined effect of a photosensitiser and visible light wavelengths, and acts via the formation of either free radical species (type I mechanism) or most frequently via energy transfer to ground-state dioxygen which is converted to the highly reactive [1] Δg singlet oxygen derivative (type II mechanism [2]. As a consequence, several constituents of cells and tissues, including nucleotides, proteins, unsaturated lipids, and steroids [3] are irreversibly damaged leading to cell death. In the case of porphyrins, the subcellular binding sites are generally represented by membranous districts, such as the plasma membrane, the mitochondrial and lysosomal membranes, the Golgi apparatus, and the rough endoplasmic reticulum; therefore, cell death is usually caused by the alteration of a number of compartments in a multitarget process [4].

Most recently, the PDT approach has been shown to act very efficiently also for the inactivation of a variety of microbial pathogens, including the Gram-positive and Gram-negative bacteria, yeasts and fungi, mycoplasmas, and parasitic protozoa [5–7].This technique is characterized by a high degree of specificity for the target microorganisms, provided the chemical structure of the photosensitiser is suitably engineered to induce the selective association of the photodynamic agent with structural elements which are typical of microbial cells. In particular, cationic photosensitisers have been demonstrated to rapidly and tightly bind with the array of negatively charged functional groups that are known to be at the surface of the outer wall surrounding several types of microbial cells [8]. The photochemically induced modification of the outer wall significantly increases its permeability allowing the penetration of the photosensitiser to inner cellular areas whose integrity is critical for cell survival.

The application of PDT for the treatment of infections of microbial origins is thus finding an increasing interest in an attempt to overcome the rampant onset of multiresistance to antibiotics exhibited by bacterial and fungal pathogens [9].

12.2 Rationale for Antimicrobial Photodynamic Therapy

Microbial cells display a large variety of subcellular organizations, which has obvious effects in controlling the interaction of photosensitising agents with cell constituents, thereby affecting the efficiency of photosensitised cell death. However, the available evidences point out that a general frame can be adopted to describe the pathway of photosensitiser binding and the pattern of photobiological events leading to cell death. Thus, the predominantly hydrophobic nature of photodynamic sensitisers usually determines their preferential or selective binding to the plasma membrane of microbial cells; hence, the photoprocess is completed within the photosensitiser microenvironment with no appreciable involvement of the genetic material [5, 9]. This feature is extremely important since porphyrin-photosensitised inactivation of microbial cells does not lead to the onset of mutagenic processes or the selection of PDT-resistant strains [10]. At the same time, the multitarget nature of the photodynamic action typical of porphyrin

derivatives allows the efficient inactivation of both antibiotic-susceptible and antibiotic-resistant bacterial and fungal species with essentially identical efficacy [11].

Typically, membrane-marker enzymes, such as NADH-, succinic-, and LDH-dehydrogenase, are extensively inhibited after very short light exposure times. The consequent alteration of the plasma membrane three-dimensional organization is accompanied by severe functional and morphological changes promoting the diffusion of the photosensitiser from its original binding sites into the cytoplasm, thus leading to the additional modification of several cytoplasmic proteins, inhibition of cell-wall synthesis, and loss of potassium ions [12].

The photodynamic action of porphyrin-type photosensitisers causes both a bacteriostatic and a bactericidal effect. The interplay between these two effects is modulated by a combination of experimental variables, including the nature of the photosensitiser, the incubation time of microbial cells with the photosensitiser, the physical and chemical properties of the medium, the total delivered light dose, and the irradiation fluence rate [9, 12]. A proper selection of the individual parameters allows one to achieve an extensive (up to 5–6 log) decrease in the population of the pathogenic agents, as well as a high selectivity of microbial cell killing under conditions in which the cells of the host tissue (e.g., fibroblasts or keratinocytes) are spared [13].

The use of photodynamic processes for the treatment of microbial infections is thus gaining an increasing attention and initial clinical trials are under way in a number of European and North American and Brazilian centers [14]. The most suitable candidates for antimicrobial PDT are represented by localized lesions, which are susceptible to topical treatment: these include periodontitis, oral candidosis, chronic ulcers, nasal decolonization, as well as specific diseases such as ventilator-associated pneumonia. The broad spectrum of action shown by photodynamic sensitisers, such as cationic porphyrins and their analogues, is of utmost importance in the case of infectious diseases which are originated by a heterogeneous microbial flora.

On these bases, we performed a thorough investigation to define the potential and scope of PDT for the treatment of skin infections which are of spontaneous origin in dogs and are no longer responsive to the currently accepted antibiotic therapies. *Staphylococcus* pyoderma is the most common skin disease in dogs. Approximately 80 % of allergic dogs will have a secondary bacterial infection at the time of diagnosis of predisposing factors, such as atopic dermatitis, flea allergy dermatitis, demodicosis, or hypothyroidism. *Staphylococcus intermedius* has traditionally been identified as the primary pathogen isolated from canine superficial and deep pyoderma. The results of such investigations could provide useful information about the advantages and limitations of antimicrobial PDT for human patients, as well as open novel perspectives for the extension of this modality to the veterinary field. All the dogs treated by PDT were referred to veterinary treatment and controlled by a veterinarian before, during and for an at least 2-week follow up after the end of each PDT session.

12.3 Treatment of Spontaneous Infections in Dogs by Photodynamic Therapy

A total number of 21 dogs were treated by PDT after topical deposition of (a) a tetracationic Zn(II)-phthalocyanine, named RLP068, in a gel formulation, supplied by Molteni Farmaceutici (Italy), 6 dogs; (b) a chlorin derivative, m-THPC, in a liposome formulation, supplied by Biolitec (Germany), 7 dogs; (c) a tetracationic meso-substituted porphyrin, named C12, in a gel formulation, supplied by Frontier Scientific (USA), 8 dogs. A synthetic description of the pathologies affecting various dogs treated by PDT with the three photosensitising agents and the identified infective agents is given in Tables 12.1, 12.2, and 12.3.

In all cases, the deposition of the phthalocyanine, chlorin, or porphyrin on the infected lesions had no effect *per se* on the characteristics of the pyoderma and the same conclusion was obtained by performing the irradiation of the lesions in the absence of topically administered photosensitiser. Typically, the irradiations were carried out by using full spectrum visible light (400–800 nm) delivered by means of a bundle of optical fibers (total diameter of 8 mm) which was interconnected with the emission from a quartz/halogen lamp (Teclas, Lugano, Switzerland).

On the other hand, the combined effect of the topically deposited photosensitising agent and visible light wavelengths resulted in a significant decrease in the overall bacterial population, as determined by counting of the colonies after plating samples taken from the phototreated lesions. The drop in the number of surviving pathogens was parallel to the gradual healing of the lesions. The rate of

Table 12.1 Dogs treated with visible light after topical deposition of the phthalocyanine derivative in a gel formulation

Animals	Disease	Bacterial or mycotic infection	No.of lesions	Site of lesions	Number of phototreatments
Danko dog	Superficial pyoderma	Coagulase-positive *Staphylococcus* spp. *Streptococcus canis*	1	Muzzle	2
Aky dog	Superficial pyoderma	Coagulase-positive *Staphylococcus* spp. *Streptococcus canis*	1	Paw	3
Tekila dog	Deep pyoderma	Coagulase-negative *Staphylococcus* spp. *Escherichia coli*	2	Paw	1st lesion 3 2nd lesion 5
Amber dog	Superficial pyoderma	Coagulase-negative *Staphylococcus* spp. *Pseudomonas aeruginosa*	1	Back	3
Buffy dog	Deep pyoderma	Coagulase-positive *Staphylococcus* spp.	1	Muzzle	3
Lola dog	Deep pyoderma	Coagulase-negative *Staphylococcus* spp. *Pseudomonas aeruginosa*	2	Paw	3

Table 12.2 Dogs treated with visible light after topical deposition of the chlorin derivative in a liposomal formulation

Animals	Disease	Bacterial infection	Number of lesions	Site of lesions	Number of phototreatments
Vicky dog	Superficial pyoderma	Coagulase-positive *Staphylococcus* spp.	1	Muzzle	2
Pongo dog	Deep pyoderma	Coagulase-positive *Staphylococcus* spp.	1	Paw	3
Peggy dog	Deep pyoderma	Coagulase-positive *Staphylococcus* spp.	1	Abdomen	3
Freud dog	Superficial pyoderma	Coagulase-negative *Staphylococcus* spp. *Enterococcus* spp. *Pseudomonas aeruginosa*	3	Paw	1st lesion 3 2nd lesion 2 3rd lesion 2
Tito dog	Superficial pyoderma	Coagulase-positive *Staphylococcus* spp.	3	Muzzle leg	1st lesion 3 2nd lesion 2 3rd lesion 2
Linda dog	Superficial pyoderma	Coagulase-positive *Staphylococcus* spp.	1	Paw	3
Heidi dog	Superficial pyoderma	Coagulase-negative *Staphylococcus* spp	1	Paw	3

Table 12.3 Dogs treated with visible light after topical deposition of the porphyrin derivative in a gel formulation

Animals	Disease	Bacterial infection	Number of lesions	Site of lesions	Number of phototreatments
Caligola dog	Superficial pyoderma	Coagulase-positive *Staphylococcus* spp. *Pantea* spp.	5	Paws, head	3
Sophie dog	Superficial mycosis	*Microsporum canis*	1	Head	3
Andromeda cat	Superficial pyoderma	Coagulase-positive *Staphylococcus* spp.	1	Paw	2
Jenny dog	Superficial pyoderma	Coagulase-negative *Staphylococcus* spp.	1	Neck	2
Joy dog	Superficial pyoderma	Coagulase-positive *Staphylococcus* spp.	1	Back	1
Brando dog	Deep pyoderma	Coagulase-positive *Staphylococcus* spp.	1	Paw	5
Taboo dog	Superficial pyoderma	Coagulase-negative *Staphylococcus* spp.	1	Paw	1
Sissy dog	Superficial pyoderma	Coagulase-positive *Staphylococcus* spp.	1	Paw	1

the process was mainly depending on the depth of the lesion: for superficial lesions one PDT treatment was sufficient to induce a complete cure, while in most situations the treatment had to be repeated at intervals of about 1 week (see Tables 12.1, 12.2, 12.3).

The nature of the anatomical site of the lesion, or the number of repetitions of the PDT treatment had no apparent effect on the positive response of the infection and the extent or rate of healing. Analogously, for those dogs which were affected by multiple lesions, there was no difference in the rate and extent of wound healing for the different lesions. The three porphyrin derivatives tested by us showed no appreciable difference in the phototherapeutic efficacy, in spite of the significant differences existing between porphyrins, chlorins, and phthalocyanines in the spectral properties. It is also important to emphasize that all the three photosensitisers are characterized by a quantum yield of singlet oxygen generation (i.e., the most active intermediate phototoxic species produced through their electronic excitation) which is larger than 0.5 [15].

Finally, the dogs gave no sign of suffering or pain during the irradiation, which marks an important difference in comparison with PDT treatments using topically administered 5-aminolevulinic acid (ALA), where the exposure of the wounds to light often had to be interrupted owing to heavy sensation of pain [16]. This would indicate that the porphyrin derivatives deposited on the lesion by means of the formulations developed by us do not localize in significant amounts at the level of the nerve endings.

The behavior of the animals during and after the treatment was absolutely normal and no weight loss was observed. To adequately monitor the mode of action of the PDT treatment and the risk of possible undesired side effects, for all dogs the following analyses were performed and the following parameters were recorded:

- identification of the pathogens responsible for the pyoderma;
- sensitivity of the isolated pathogens to different antibiotics (antibiogram);
- complete blood count;
- measurement of selected enzymic activities, potassium ions, bilirubin, total protein and albumin, cholesterol, triglycerides, urea, and creatinine;
- electrophoresis of serum proteins;
- colony counting after plating on a solid growth medium (BHA) of wads collected from the lesion before and after treatment.

In all cases, no significant modification of the above-listed parameters was observed as a consequence of the photodynamic treatment.

Specific detailed examples of protocols used for the therapeutic approach with selected dogs are given in the following paragraph.

12.4 Specific Examples of Dogs Treated by Photodynamic Therapy for Mycotic and Bacterial Infections

The detailed protocol used is exemplified for two dogs.

Table 12.4 Typical antibiogram obtained for a PDT-treated dog

Antibiogram	
Amoxicillin + Clavulanic acid	Sensitive
Ampicillin–Sulbactam	Sensitive
Ampicillin–Amoxicillin	Intermediate
1st generation Cephalosporin	Sensitive
4th generation Cephalosporin	Resistant
2nd generation Quinolone	Sensitive
Erythromycin	Resistant
Lincosamides	Intermediate
Oxacillin	Resistant
Penicillin	Resistant
Spiramycin	Sensitive
Sulfamid-Trimethoprim	Sensitive
Tiamulin	Sensitive
Tilmicosin	Sensitive
Tylosin	Sensitive
Tetracycline	Sensitive

12.4.1 Sophie dog

English cocker spaniel dog 7 year-old having a lesion on the head. The medical diagnosis was: superficial mycosis.

The body weight was about 17.7 kg.

The dog was maintained on a mixed diet.

The prophylaxis against ectoparasites, the vaccinatio,n and the heartworm prevention have been regularly performed.

Bacteriological examination: bacterial infection characterized by *Bacillus* spp.

The sensitivity of the isolated microbial strain to different antibiotics is summarized in the table below (Table 12.4).

Fig. 12.1 Typical example of dermatophyte growth in a suitable culture medium

To ascertain the cause of a dermatophytosis, proper specimen collection and isolation and correct identification of dermatophytes are necessary. BioMed Diagnostics' InTray^{TM} DM in vitro diagnostic test provides a simple color test for the detection of dermatophytes. Generally, the colony needs to grow for 2–10 days before macroconidia are produced.

As one can see in Fig. 12.1 below a white cotton-to woolly appearing colony has grown and the pigment on the undersurface of the colony is yellow-orange, becoming dull orange-brown. This colony morphology is typical of *Microsporum canis.*

The following results for complete blood count, biochemical analysis, and electrophoresis of serum proteins were obtained before the treatments.

Complete blood count			
Parameter	Unit	Result	Reference range
RBC red blood cells	10^{12}/L	**8.71**	5.5–8.5
RDW red blood cell distribution width	%	**13.8**	14.0–18.1
MCV mean corpuscular volume	FL	**63**	43.4–52.8
HCT hematocrit	%	**55.2**	37–55
HGB hemoglobin	gr/dl	**17.7**	12–18
MCH mean corpuscular hemoglobin	pg	**20.4**	14.1–18.6
MCHC mean corpuscular hemoglobin concentration	gr\dl	**32.2**	30.6–35.8
PLT platelets	10^3 microL	**487**	300–631
MPV mean platelets volume	f/L	**11.6**	8.5–13.2
WBC white blood cells	10^9\L	**13.6**	6.0–16.9
Neutrophils	10^9\L	**15.7**	4–10
Neutrophil bands	10^9\L	**0**	0–1
Lymphocytes	10^9\L	**1**	1–3.5
Monocytes	10^9\L	**0.2**	0–0.3
Eosinophils	10^9\L	**1.7**	0.09–1.7
Basophils		**0**	rare
Neutrophils	%	**82**	60–77
Neutrophil bands	%	**0**	0–3
Lymphocytes	%	**5**	12–30
Monocytes	%	**4**	3–10
Eosinophils	%	**9**	2–10
Basophils		**0**	rare

Biochemical analysis		
Parameter	Result	Reference range
AST aspartate aminotransferase	**27**	U/L < 40
ALT alanine aminotransferase	**37**	U/L < 40
GGT gamma glutamyltransferase	**13**	U/L < 12
ALP alkaline phosphatase	**76**	U/L < 100
CK creatinine kinase	**91**	U/L 20–150
Total bilirubin	**0.39**	mg/dl 0.2–1.2
Direct bilirubin	**<0.1**	mg/dl
Lipase	**49**	U/L < 40
Glucose	**103**	mg/dl 70–110
Total Protein	**6.5**	mg/dl 6–8
Albumin	**3.3**	mg/dl 3–5
Urea	**48**	mg/dl 10–40
Creatinine	**0.87**	mg/dl 0.6–1.2
Sodium	**148**	mEq/L 140–152
Potassium	**5.5**	mEq/L 3.6–5.8
Chloride	**109**	mEq/L 105–115
Calcium	**9.7**	mg/dl 8–11
Phosphorus	**4.8**	mg/dl 4–7
Triglyceride	**85**	mg/dl 40–150
Cholesterol	**241**	mg/dl 140–200
CRP C-reactive protein	**1.24**	mg/dl < 1

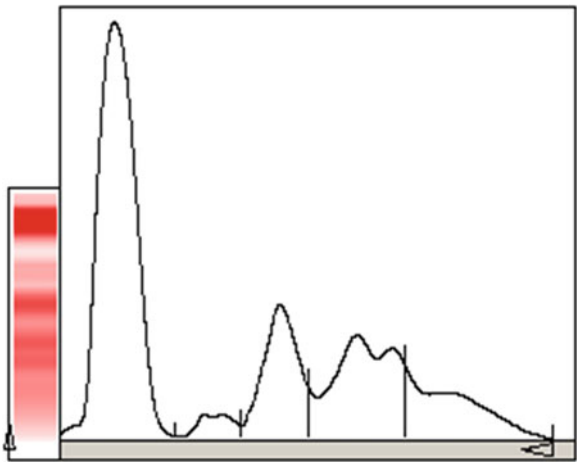

ELECTROPHORESIS OF SERUM PROTEINS

Fractions	%	Reference (%)
Albumin	**49.8**	53–65
Alpha 1	**2.9**	2–5
Alpha 2	**14.9**	8–14
Beta	**20.2**	10–15
Gamma	**12.2**	11–21

The wads collected from the lesion before and post-treatment were plated on a solid growth medium (BHA) and the number of colonies found after 18–24 h incubation at 37 °C were counted.

1 mM C12 gel	Before irradiation	After irradiation
1st treatment	>600	250
2nd treatment	378	121
3rd treatment	100	9

The lesion was subjected to 3 phototreatments after which it appeared to be completely healed. The images (Fig. 12.2) represent the lesion before and after each phototreatment.

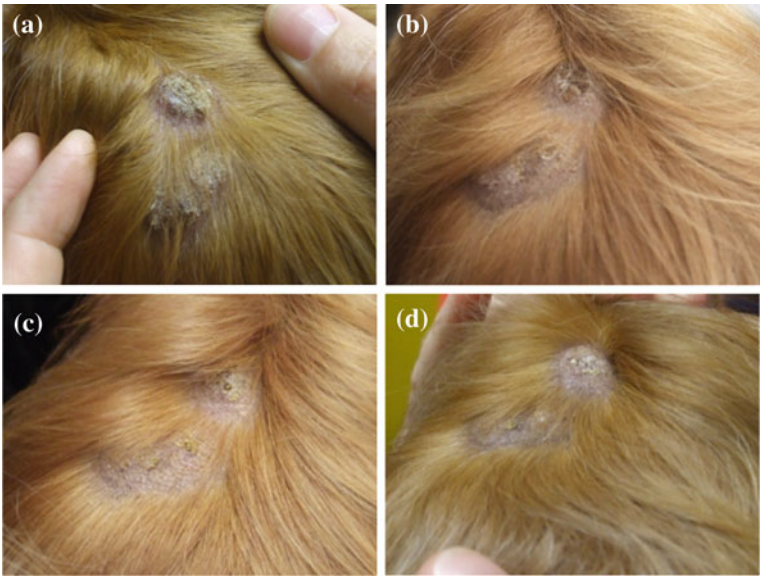

Fig. 12.2 Lesions of Sophie dog before (**a**) and 3 days after the first (**b**) or the second (**c**) or the third (**d**) phototreatment

12.4.2 Peggy Dog

Golden Retriever 14-year-old dog having an extensive deep lesion in the lower abdomen characterized by pus exudation and odor. The body weight was about 42 kg.

No antibiotic treatments were carried out before PDT.

Bacteriological examination: bacterial infection characterized by extensive growth of coagulase-positive *Staphylococcus* spp.

The sensitivity of the isolated bacterial strains to different antibiotics, tested in an authorized laboratory, is summarized in the table below:

Antibiogram	
Sens	Penicillin
Sens	Ampicillin
Sens	Amoxicillin + Acide Clavulanic
Sens	Oxacillin
Sens	1 degrees generation Cephalosporin
Sens	2 degrees generation Cephalosporin
Res/Sens	Spiramycin
Sens	Rifampicin
Sens	Tilmicosin
Sens	Tylosin
Sens	Tetracycline
Sens	Streptomycin
Sens	Gentamicin
Sens	Enrofloxacin
Sens	Trimethoprim-Sulfamethoxazole
Sens	Tiamulin

The animal was subjected to four phototreatments with the chlorin derivative.

The lesion, after the fourth treatment, showed a complete remission, a result which appeared to be especially noticeable given the initial large lesion (ca. 20 cm diameter).

During the phototreatments, the animal showed no signs of disturbance or intolerance.

The body weight of the dog was found to be unchanged after the fourth session of photodynamic therapy.

The images below (Fig. 12.3) represent the lesion before and after each phototreatment.

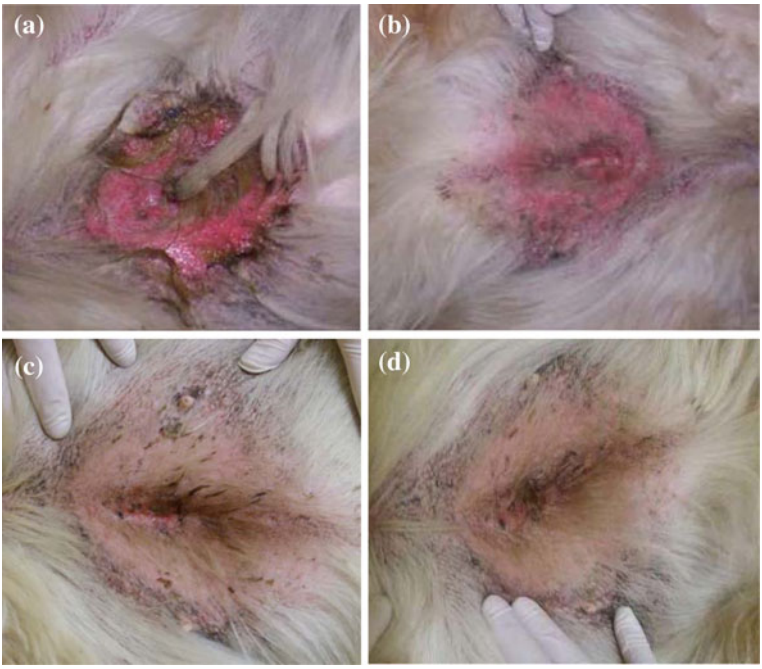

Fig. 12.3 Lesion of Peggy dog before (**a**) and 3 days after the second (**b**) or the third (**c**) or the fourth (**d**) phototreatment

12.5 Conclusive Remarks

The results reported in this chapter clearly demonstrate the high potential of PDT treatment for promoting the healing of skin lesions infected by bacterial and mycotic pathogens. Three photosensitisers having the tetrapyrrole macrocycle as the basic molecular skeleton were tested and showed no appreciable differences in the antimicrobial inactivation efficacy. Therefore, this approach appears to be very promising as regards both the extrapolation of the findings to human patients and the opening of a novel therapeutic modality for curing wounds in pet animals.

The approach appears to be devoid of undesired side effects and can be repeated a number of times without any detectable decrease in the efficiency. This observation is probably related with the well-known property of photodynamic processes to avoid the selection of PDT-resistant microbial strains. Thus, photodynamic therapy for infections originated by microbial pathogens will become more and more important in the near future as antibiotic resistance is only expected to continue to increase.

References

1. Brown SB, Brown EA, Walker I (2004) The present and future role of photodynamic therapy in cancer treatment. Lancet Oncol 5:497–508
2. Ochsner M (1997) Photophysical and photobiological processes in the photodynamic therapy of tumours. J Photochem Photobiol B: Biol 39:1–18
3. Moan J, Peng Q (2003) An outline of the hundred-year history of PDT. Anticancer Res 23:3591–3600
4. Jori G, Spikes JD (1994) Photobiochemistry of porphyrins. In: Smith KC (ed) Topics in photomedicine. Plenum Press, New York, pp 183–319
5. Jori G, Fabris C, Soncin M et al (2006) Photodynamic therapy in the treatment of microbial infections: basic principles and perspective applications. Lasers Surg Med 38:468–481
6. Maisch T (2007) Anti-microbial photodynamic therapy: useful in the future? Lasers Med Sci 22:83–91
7. Huang L, Dai T, Hamblin MR (2010) Antimicrobial photodynamic inactivation and photodynamic therapy for infections. Methods Mol Biol 635:155–173
8. Jori G, Brown SB (2004) Photosensitised inactivation of micro-organisms. Photochem Photobiol Sci 3:403–407
9. Wainwright M (2004) Photoantimicrobials—a PACT against resistance and infection. Drug Future 29:85–93
10. Hamblin MR, Hasan T (2004) Photodynamic therapy: a new antimicrobial approach to infectious disease. Photochem Photobiol Sci 3:436–450
11. Soncin M, Fabris C, Busetti A et al (2002) Approaches to selectivity in the Zn(II)-phthalocyanine-photosensitised inactivation of wild-type and antibiotic-resistant *Staphylococcus aureus*. Photochem Photobiol Sci 1:815–819
12. Jori G, Coppellotti O (2007) Inactivation of pathogenic microorganisms by photodynamic techniques: mechanistic aspects and perspective applications. Anti-infective Agents Med Chem 6:119–131
13. Maisch T (2009) A new strategy to destroy antibiotic-resistant micro-organisms: antimicrobial photodynamic therapy. Mini-review Med Chem 9:947–983
14. Dai T, Huang YY, Hamblin MR (2009) Photodynamic therapy for localized infections—state of the art. Photodiagn Photodyn Ther 6:170–188
15. Redmond RW, Gamlin JN (1999) A compilation of singlet oxygen yields from biologically relevant molecules. Photochem Photobiol 70:391–475
16. Conway C, Brown SB (2012) Photodynamic therapy. In: Griesbeck A, Oelgemoeller M, Ghetti F (eds) CRC handbook of organic photochemistry and photobiology, vol 2, 3rd edn. CRC Press, Boca Raton, pp 1511–1528

Chapter 13
Photodynamic Control of Malaria Vector, Noxious Insects and Parasites

Mahmoud H. Abdel-Kader and Tarek A. Eltayeb

13.1 Introduction

It is well documented that PDT has become a major approach for diagnosis and treatment of cancer. However, PDT was discovered early as a photodynamic antimicrobial chemotherapy and it has recently received considerable attention from researchers due to the fact that it has shown promise in the treatment of various tropical pathogens. In addition, PDT has been utilized successfully in recent years as a novel modality for noxious insects and parasite control, which is the subject of this chapter. The different classes of noxious insects, namely the activity of medical insects of vector borne- diseases such as Malaria, Filaria, and Dengue fever as well as agro-insects and pests which cause considerable damage to agro-economics, will be discussed in this chapter.

Focus will be done on the control of Malaria, Filaria, and Schistosomiasis vectors in infested epidemic swamps, which we have achieved through the use of chlorophyll derivatives extracted from plants as a photosensitizer. With sunlight it works as a novel photolarvicide to control the larvae of different species of mosquito. This technique was registered as a PCT patent (WIPO) titled: "Field Application for Malaria Vector Control Using Sunlight Active Formulated Extract (SAFE)" [1]. SAFE is sprayed onto the breeding site (such as a swamp) where its active ingredients accumulate in the larval body and induce photo-oxidative stress upon exposure to sunlight, producing cytotoxic singlet oxygen that results in larval death. It is a target selective formula that has shown no effect on the other beneficial organisms in the same breeding site. The advantages of chlorophyll

M. H. Abdel-Kader (✉)
Department of Pharmaceutical Technology, German university of Cairo, New Cairo, Egypt
e-mail: mahmoud.abdelkader@guc.edu.eg

M. H. Abdel-Kader · T. A. Eltayeb
Department of Laser application in Photochemistry and Photobiology, The National Institute of Laser Enhanced Sciences (NILES), Cairo University, Cairo, Egypt
e-mail: tarek.eltayeb@inradcorp.org

M. H. Abdel-Kader (ed.), *Photodynamic Therapy*,
DOI: 10.1007/978-3-642-39629-8_13,

derivatives are that they are used in very low concentrations (ppm), are inexpensive, easy to apply in the field by dusting in an aquatic environment and highly effective as they ensure a high mortality rate of the mosquito larvae. Most importantly, they are FDA approved for use as food additives.

13.1.1 Development of Photopesticides

The photosensitizer used in the control of noxious insects and parasites is called a photopesticide. Their development came along through many stages and over many years. From 1928 to mid-1982, there have been approximately 30 publications describing studies specifically designed to investigate the insecticidal activity of various dyes in the presence of visible light. Graham (1963) was one of the first to draw attention to the possibility of using "photosensitizing agents" as insecticides [2].

In 1979, Pimprikar et al. studied fluorescent light, and rose bengal at treatment levels of 1–20 ppm on mosquito larvae. He reported that *Culex* larvae were more susceptible than *Aedes* larvae and early instars were more susceptible than later instars. After treatment of the larval stage, physiological and morphological abnormalities were observed in the pupa and adult stages. These abnormalities made him suggest that there was improper chitin formation in the insect after treatment [3].

Similarly, Carpenter and Heitz showed that when mosquitoes larvae were exposed to rose bengal and visible light, significant acute mortality was observed [4]. Furthermore, if the treated mosquitoes were illuminated with visible light and then put into darkness, a latent mortality was observed. Light treatment was necessary to obtain latent mortality, since the control groups that were exposed to the same dye concentrations, but in the dark, exhibited no latent mortality. When latent mortality was added to acute mortality, it was observed that the total toxicity as a result of the rose bengal was 10 times greater than that due to the dark toxicity [4].

The relative toxicities of 6 xanthene dyes to *Culex* and *Aedes* mosquito larvae were reported by Pimprikar et al. Their results showed that rose bengal was the most toxic, followed by phloxin B and erythrosin B. They also showed that the same dyes exhibited a low toxicity to the fish present in the mosquito breeding site [5].

Lately, compounds of plant origin have been isolated, identified and studied as phototoxins against a wide range of pests such as insects, fungi and weeds [6]. Until now, the main classes of photosensitizers studied are the furanocoumarins, thiophenes, acetylenes, extended quinones, hypericin, cercosporin, miscellaneous materials, and porphyrins [6].

13.1.2 Porphyric Insecticides

Porphyrins are a large class of deeply colored red or purple fluorescent crystalline pigments. They are of natural or synthetic origin, and they all share a common a substituted aromatic macrocyclic ring that consists of four pyrrole-type residues linked together by four methine groups. So, what makes porphyrins special? Porphyrins are the basis of certain compounds that are essential to life. When porphyrin is coupled with iron, heme is formed. Heme is intimately associated with blood and many of the redox enzymes involved in the metabolic processes. Also, chlorophyll is a reduced magnesium porphyrin that orchestrates photosynthesis; without it, life as we know it would be impossible [7]. Most cited studies have used porphyrins as photoinsecticides. One of the reasons they are promising photopesticides is that they absorb most of the wavelengths of the solar spectrum. Hence, they can undergo very efficient photoexcitation through sunlight and produce a high quantum yield of reactive oxygen species [8]. In addition, they have several advantages such as low environmental impact and the absence of mutagenic action toward biological targets as reported by Jori and Ben Amor [9, 10].

Photodynamic damage can be induced by treating the insect with exogenous porphyric compounds. This is considered a new approach in the design of insecticides, commonly known as porphyric insecticides. It is assumed that the appeal of porphyric insecticides may reside in the potential to design a large number of very biodegradable formulations that can act as selective photodynamic insecticides and herbicides. However, there lies the problem of the insects developing resistance to such insecticides [11].

Recently, Abdel-Kader et al. have reported the use of hematoporphyrin and chlorophyll derivatives (natural derivatives of porphyric compounds) as efficient photosensitizing agents for the potential control of medical and agriculture pests and parasites [12–16]. They developed a novel method using these porphyric derivatives as sunlight-activated insecticides for outdoor control of noxious insects and parasites [1].

13.2 Photodynamic Control of Noxious Insects

13.2.1 Photodynamic Control of Mosquitos: The Vectors of Malaria, Filaria and Dengue Fever

Mosquitoes are estimated to transmit diseases to more than 700 million people annually in Africa, South America, Central America, Mexico and much of Asia, with one million of these cases resulting in death every year. In Europe, Russia, Greenland, Canada, USA, Australia, New Zealand, Japan, and other temperate and developed countries, mosquito bites are now mostly an irritating nuisance [17]. Historically, before mosquito-transmitted diseases were

brought under control, mosquitoes caused tens of thousands of deaths in these countries and hundreds of thousands of infections [18]. Walter Reed, William C. Gorgas, and associates in the U.S. Army Medical Corps showed that mosquitoes were the method by which yellow fever and malaria were transmitted from person to person in Cuba and then around the Panama Canal in the early 1900s [19]. Since then, other diseases have been shown to be transmitted the same way.

Mosquitoes are a perfect example of one of the many organisms that can host diseases. Of the known 14,000 infectious microorganisms, 600 are shared between animals and humans. Mosquitoes are known to carry many infectious diseases from several different classes of microorganisms, including viruses, and parasites. Mosquito-borne illnesses include Malaria, West Nile Virus, Elephantiasis, Dengue Fever, Yellow Fever, etc. These infections are normally rare to certain geographic areas. For instance, Dengue Hemorrhagic Fever is a viral, mosquito-borne illness usually regarded only as a risk in the tropics. However, cases of Dengue Fever have been reported in the U.S. along the Texas-Mexican border where it has never been seen before [17].

One of the greatest dilemmas that faces mosquito-borne diseases in epidemic countries is the use of DDT for Indoor Residual Spraying (IRS), which is considered an essential method for disease control [20]. The use of DDT with its acute toxicity and chemical stability poses a significant risk. It has been proven that DDT accumulates on the long run, which leads to a risk of toxicity for humans and wildlife. Consequently, it is one of the 12 chemicals that are identified as persistent organic pollutants and its production and use were strictly prohibited in 1972 by the Stockholm Convention, an international agreement on Persistent Organic Pollutants [21]. The use of DDT is already entirely banned in many industrialized countries and the United Nations Environmental Program is now negotiating its global ban [22].

Until it is well proven that the risks of DDT outweigh its benefits, the WHO declared a cautious stand toward its use, stating that the continued use of DDT in Malaria control is expected until equally cost effective alternatives are developed [21]. In its report, the WHO confirmed that there is an urgent need to develop alternative products and methods to both eradicate malaria and filaria, and to eliminate the use of DDT. Consequently, the WHO urged governments to provide the financial resources and technical support to help accelerate the development of these alternatives [23].

In the present work, we introduce the successful implementation of the photodynamic process as a tool to control the different species of mosquito. Previously, it was reported by Awad et al. that a novel hematoporphyrin formula was effective in controlling *culex pipens* larvae in a semi-field investigation [24]. A recent study by Lucantoni et al. demonstrated that C14-porphyrin exhibits a strong photosensitizing activity against *Aedes aegypti* [25]. Moreover, Fabris et al. reported on the potential of C12-porphyrin as a photolarvicide for the control of *Anopheles gambiae* and *An. Arabienesis* [26]. This new technique is designed for the outdoor control of Malaria, Filaria, and Dengue fever vectors using environmentally friendly photolarvicides

(chlorophyll derivatives) to control the larvae stage of *Anopheles, Culex,* and *Aedes* mosquitoes.

The plant derived chlorophyll derivatives, which proved their photosensitization efficiency in laboratory and semi-field studies, were implemented in field trials. These derivatives exhibit several advantages: they are low in cost, are natural products extracted from green plants, and are endorsed by the Food and Drug Administration (FDA) as food additives [27]. In addition, they are used in very low concentrations (μM), can be easily applied in the field by being dissolved in an aquatic environment, and most importantly, they are highly effective, ensuring 85–100 % mortality of the mosquito larvae for a long period of residual effect.

13.2.1.1 Laboratory and Semi-field Studies

The effects of the chlorophyll derivatives concentration, total light dose, and irradiation time were monitored on the mosquito larvae by measuring the survival percentage at selected time intervals after the insects were fed in a specific medium and then exposed to a solar simulator and/or sunlight. The results were compared to a control group subjected to the same treatment protocol, except that the feeding medium did not contain chlorophyll derivatives.

Results revealed that there are four interacting factors that affect the photodynamic activity of chlorophyll derivatives in the production of reactive oxygen species (ROS). These factors are the concentration and accumulation of chlorophyll derivatives, the light exposure dose, and the exposure time. For field applications, other factors have to be taken into consideration, such as the weather and its effect on solar irradiance, according to both location and season, and the economic level, in relation to the cost of chlorophyll derivatives and the extent of infestation by the studied vectors.

Two complementary methods were used in this study to investigate the efficiency of chlorophyll derivatives as photolarvicides of *Anopheles gambiae* and *Culex pipiens*. The first method examined the effect of external factors (chlorophyll derivative concentration, light dose, and exposure time) and the results were shown as percent survival of the larvae as a function of the magnitude of the external factor. The second method investigated the internal factors, which represent the accumulation inside the organs and tissues of the larvae.

Figure 13.1 shows the effect of different concentrations of chlorophyll derivatives (from 10 to 70 μM) on the survival percentage of the *Culex pipiens* larvae after 30 min of exposure to sunlight (for each concentration a group of 100 larvae per replicate was used). Not more than 15 % survival was observed during this exposure time when a concentration of 70 μM was used. On the other hand, the other concentrations caused less than 20 % survival 30 h after irradiation. The control group, which was fed in a chlorophyll-free feeding medium, showed 95–100 % survival even after three days.

The second experiment focused on light dose, which plays an important role in controlling the process of chlorophyll derivative photosensitization. Figure 13.2

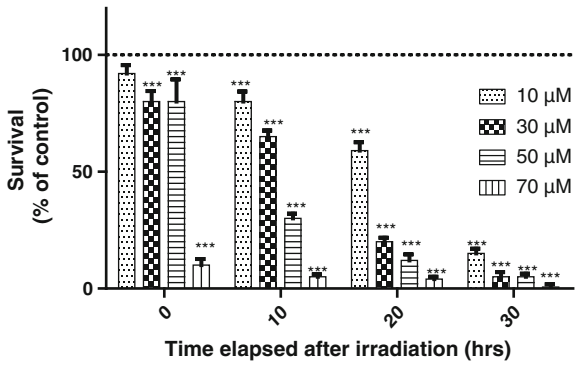

Fig. 13.1 Effect of different concentrations of the chlorophyll derivative on the survival percentage of the *Culex pipiens* larvae

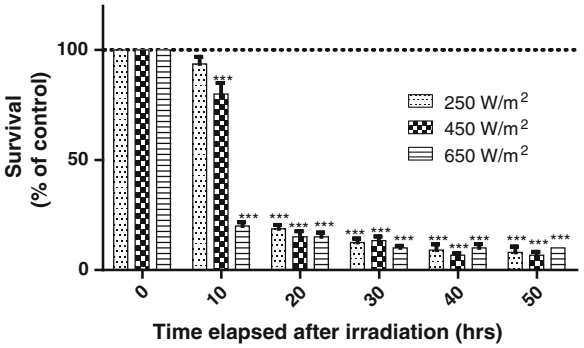

Fig. 13.2 Effect of different light irradiances on the percentage of survival of *Culex pipiens* larvae at different elapsed time

illustrates the effect of different irradiances from the solar simulator on the survival of *Culex pipiens* larvae in the presence of a 50 µM chlorophyll derivatives concentration. ORIEL CORPORATION Solar Simulator (USA) was used as source of incoherent artificial light, simulating sunlight. The difference in survival between the highest and lowest irradiance was less than 20 % after 48 h.

It is worth mentioning that *Anopheles* and *Culex* larvae integuments, which are partially transparent to light, play an important role by enabling higher sensitivity to lower light doses as shown in the obtained results. In addition, exposure time can compensate for the lower chlorophyll derivative concentrations. Therefore, during field implementation, it is possible on long sunny days to use chlorophyll derivative concentrations lower than those used on cloudy days.

Confocal laser scanning microscopy (CLSM) results provide the best information source for investigating the chlorophyll derivative distribution inside the body organs of *Anopheles gambiae* and *Culex pipiens* larvae. It also supplies three information rich functions: fluorescence images, fluorescence spectra and lifetime measurements.

Fluorescence images provide a qualitative view of chlorophyll derivative distribution inside the larvae bodies, monitoring its dynamics as a function of time.

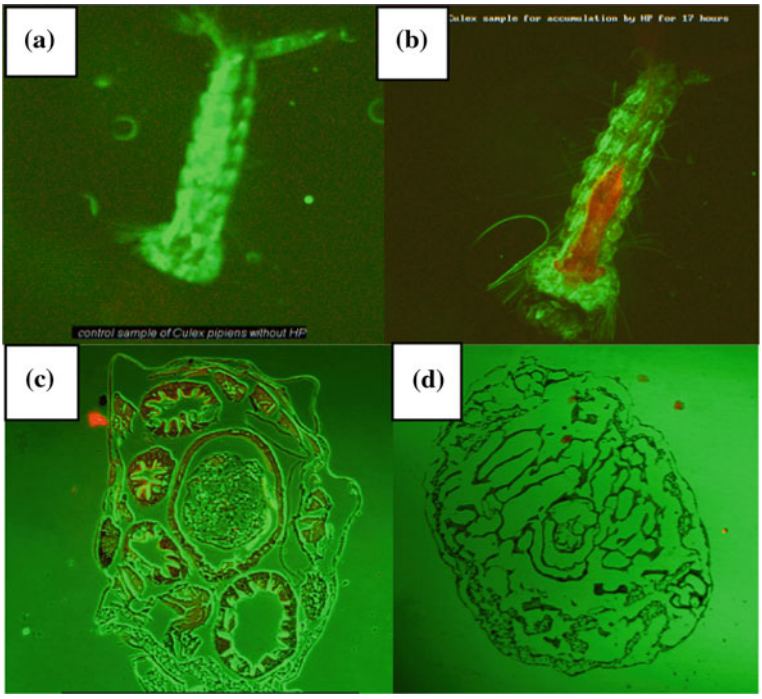

Fig. 13.3 Confocal laser scanning microscopy (CLSM) images of *Culex pipiens* larva incubated with porphyrin derivatives before light exposure (**a**, **c**) and after light exposure (**b**, **d**)

Figure 13.3a, b illustrate the difference between a mosquito larva without and with chlorophyll derivatives inside it, respectively. The fluorescence images investigate the extent of the effect of the photo-oxidation process that damages the organs and tissues of the mosquito larvae, as can be seen in Fig. 13.3c, d by comparing the mosquito larva transverse section (T.S) before and after treatment.

Fluorescence spectra measurements inside the tissues of *Anopheles* larvae provide a quantitative method for estimating the accumulated chlorophyll derivatives at any incubation time and after light exposure. These are very essential measurements for field applications to optimize the parameters of the photochemical processes for the target species and to save nontarget species that are living in the same infected swamp (target selectivity) (Fig 13.4).

Fluorescence lifetime measurements at definite spots inside the tissues of *Culex pipiens* and *Anopheles gambiae* larvae provided a good estimation of the distribution ratio of aggregated and nonaggregated forms of the photosensitizer. Lifetime measurements of spots inside the *Culex* larvae were determined to be 1.5 ± 1.04 ns for the 5 h incubation period and 11.9 ± 3.3 ns for the 15 h incubation period. The data was obtained by monoexponential fitting. The differences may be attributed to the different ratios of aggregated and nonaggregated forms of chlorophyll derivatives, which affect the efficacy of the photosensitization process [15].

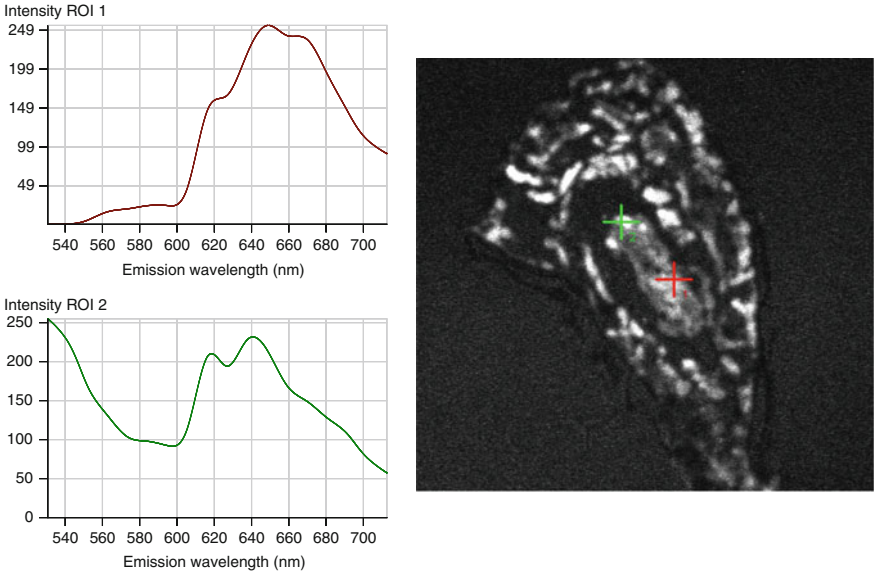

Fig. 13.4 CLSM spectral image for transverse section of *Anopheles gambiae* larva showing the extent of porphyrin derivatives accumulation in different sites of alimentary canal (ROI 1 = *red* and ROI 2 = *green*)

13.2.1.2 Field Application

Field investigations were carried out based on laboratory and semi-field results. In these trials, chlorophyll derivatives were added to the infested swamps to be taken up by the mosquito larvae. The accumulated photoactive compound inside the larvae body induces, upon sunlight exposure, an oxidation stress that results in the organism's death.

As an example, in Kasangati and Namanve cities of Wakiso, a district in Uganda, chlorophyll derivatives (as sunlight active photosensitizers) were applied to cover 250,000 square meter of infected swamps and sand pits (4 gm/m^2). The infected cities were mapped for this field study using Geographical Positioning System (GPS). All the biotic and abiotic factors were measured before and after treatment. Confocal laser scanning microscopy (CLSM) measurements were used to monitor the concentration and the dynamic distribution of chlorophyll derivatives inside the larvae of *Anopheles gambiae* mosquito.

The results were collected 2 h after onset of exposure to sunlight. They revealed that 85–100 % mortality of larvae population was obtained at different concentrations of chlorophyll derivatives (ranging from 0.1 to 100 μM). Other biological beneficiary organisms, such as the dragonfly larvae and mosquito predator larvae, which were present in the same treated swamps, were not affected (target selectivity). Both light control group (larvae without chlorophyll derivative treatment) and dark control group (larvae treated with chlorophyll derivatives and were

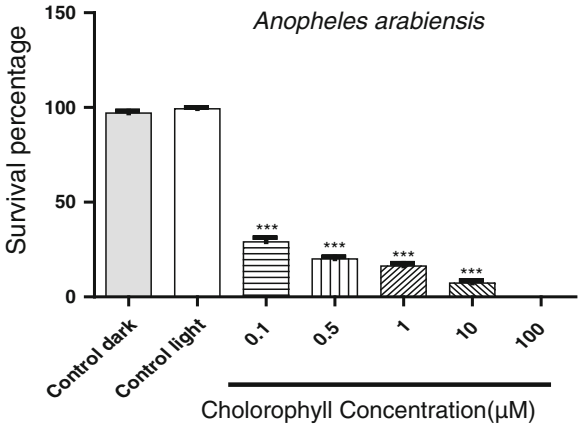

Fig. 13.5 Effect of different chlorophyll derivative concentrations on survival percentage of *Anopheles arabiensis* larvae

protected from light in a small area covered with a thin layer of black metal sheet) showed maximum mortality of only 2 %. Figure 13.5 shows the effect of chlorophyll derivatives on the mosquito larvae (*Anopheles arabiensis*) exposed to sunlight in the mosquito infected swamp area.

The resistance of insects to chlorophyll derivatives during treatment of different generations needs further assessment. The results of this work and the concepts of insect resistance may provide primary observation for the ability of the insects to counteract the effect of chlorophyll derivatives.

These field trials are the result of three years of continuous and persistent work, which have allowed the identification of different forms of mosquito infected swamps as well as their access roads through the villages. The results of the field trials have shown promising success in eliminating vectors over a short period of time by cutting the mosquito's lifecycle without formation of new generation or reinfestation. Cooperation with the local inhabitants, among whom awareness to this project was raised by instructing them on the official fieldwork procedures, will pave the road to future large-scale countrywide projects.

13.2.2 Photodynamic Control of Housefly (Musca domestica)

It has been proved that houseflies carry, both externally and internally, certain disease producing germs. For example, several observers have shown that bacilli pass through the alimentary canals of flies. The bacilli of cholera were found in great numbers on the bodies of flies within 17 h after the insects had been fed on cholera-infected material. It was found that the bacilli persisted in the specks for several days and there were enough colonies to transmit disease [28].

Around 1920, the common methods of housefly control were screening, fly traps, fans, sprays and fly-poisons. There are some natural enemies capable of killing the house fly at its different stages such as *Bacterium delendae*, Rickestiae, viruses, spirochetes, fungi and mites [29].

The number of different types of fly-poisons has grown over the past decades. Many of these chemical poisons have been tested and applied on houseflies such as the chitin synthesis inhibitor, triflumuron, propetamphos, pyrethroid, azamethiphos, chlorpyrifos plus permethrin and malathion [30, 31].

Biocontrol has played an important role in the process of housefly (*Musca domestica)* control through the use of different biological systems such as *Spalangia endius*, *Spalangia nigroaenea*, *Bacillus thuringiensis*, *Bacillus bassiana*, Muscovy ducks (*Cairina moschata*), *S. cameroni* and *M. raptor* [32–36].

Yoho et al. [37] investigated the efficacy of photodynamic action against the adult housefly using primarily the halogenated series of fluorescein dyes. The toxicological data was compared with the parameters of light source and its intensity, duration of light exposure, dye structure and concentration in the diet [38]. Later on, Yoho et al. studied a series of 14 food, drug and cosmetic dyes for their usefulness in being photodynamically toxic to housefly adults [6]. Pimprikar et al. [5] attempted to control houseflies in a commercial caged layer house using weekly applications of aqueous solutions of erythrosin B directly on the manure. In a 5-week duplication treatment period, they reported a decrease of up to 90 % of adult and larva houseflies with respect to pretreatment levels and no changes in the beneficial soldier fly larval population. In the manure that was illuminated by indirect sunlight, the dye was reported to be rapidly degraded, such that only about 20 % was extractable one week after spraying. As a result of these tests, Primprikar et al. [39] studied the effects of several fluorescein derivatives on each developmental stage of the housefly. Treated adults exhibited lower fecundity, the eggs exhibited a reduced viability and mortality was observed in each life stage of the housefly.

Respicio and Heitz [40] began a study of the development of resistance to erythrosin B in the housefly. A laboratory strain developed only 6-fold resistance after 40 generations of challenge by erythrosin B. Later, the cross-resistance of erythrosin B-resistant houseflies was studied against strains resistant to propoxur, DDT, permethrin and dichlorvos.

Recently, El-Tayeb used the hematoporphyrin dihydrochloride (HP) to control *Musca domestica*. He reported in his study the high efficiency of HP in controlling houseflies in their breeding sites [41].

Two complementary methods have been used to investigate the efficiency of HP as a photopesticide against *Musca domestica* flies. One method investigated the effect of external factors (HP concentration, light dose and exposure time) in which the results were revealed by Robinson and Beatson [42] as percent of survival of flies as a function of the magnitude of the external factors. The second method, investigated the internal factors. The most important of these are the dynamic behavior and accumulation distribution of HP inside the organs and tissues of *Musca domestica* flies. These characteristics may describe and explain the strange effects of some external factors, such as the differences in time of mortality after light exposure, and the best time of HP application before light exposure (incubation period).

Confocal laser scanning microscopy (CLSM) supports the investigation of the behavior of HP in the organs of *Musca domestica* flies and explains the results of the final effects of the photosensitization process on their mortality rates. Fluorescence images provide a qualitative view of HP dynamics inside the flies; this makes it easy to differentiate between the treated flies and control ones and to differentiate among the flies treated with different concentrations of HP. By comparing the images of the alimentary canals (a.c.) of control and treated flies (Fig. 13.6a, b), it is easy to find the stress caused by HP accumulation on the a.c. walls. This may have caused the diffusion of HP from inside the a.c. to the outside. This is seen in the images of other organs outside the a.c. such as the fat bodies and the muscles of treated flies. This may solve the debate around the reason for the presence of photosensitizers in the tissues outside the a.c. [6].

The veins of the housefly wings showed some extent of HP (Fig. 13.6d) compared to the control housefly wing (Fig. 13.6c). This may give an indication of the cause of the damage of the fly's external organs such as the wings and the eyes (Fig. 13.7). The optical slices of the housefly's alimentary canal give an indication of HP distribution in the lumen of the a.c. (Fig. 13.8).

Fluorescence spectra of CLSM of the houseflies provided quantitative estimation of the accumulated HP inside their organs. By comparing the results obtained by the spectrometer of CLSM, it was found that the treated fly had some HP in the organs outside the alimentary canal, even those that did not appear in the fluorescence images. This may explain the reason for the flies' mortality during light

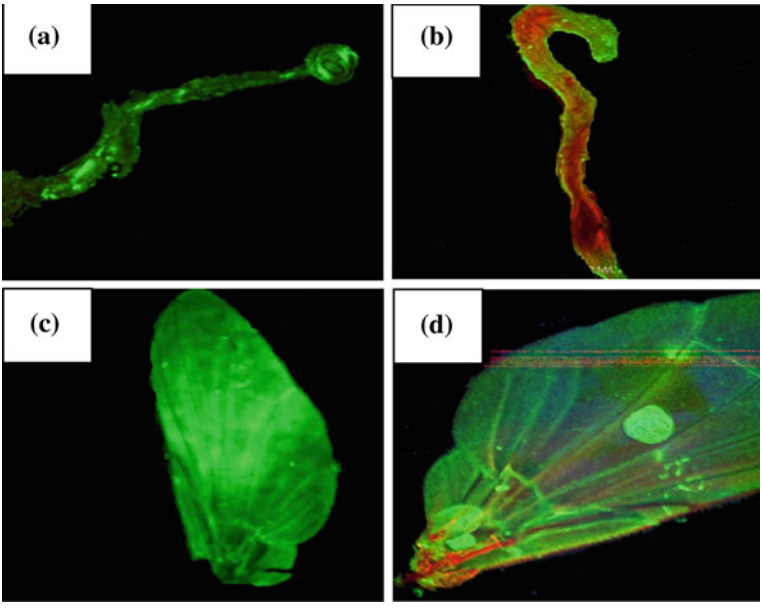

Fig. 13.6 CLSM images for housefly alimentary canal and wings incubated in HP free medium (**a** and **c**) and HP medium (**b** and **d**)

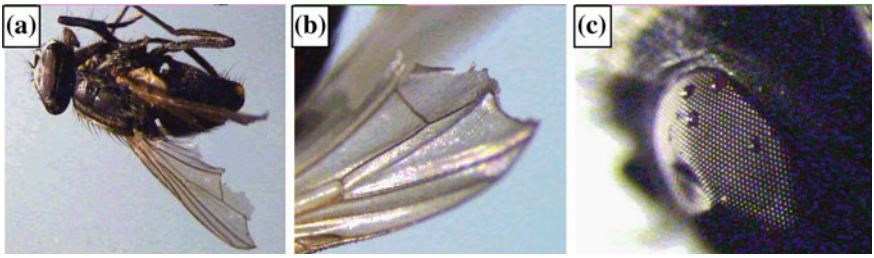

Fig. 13.7 Stereo microscope images for HP-treated housefly whole body (**a**), wing (**b**), and eye (**c**)

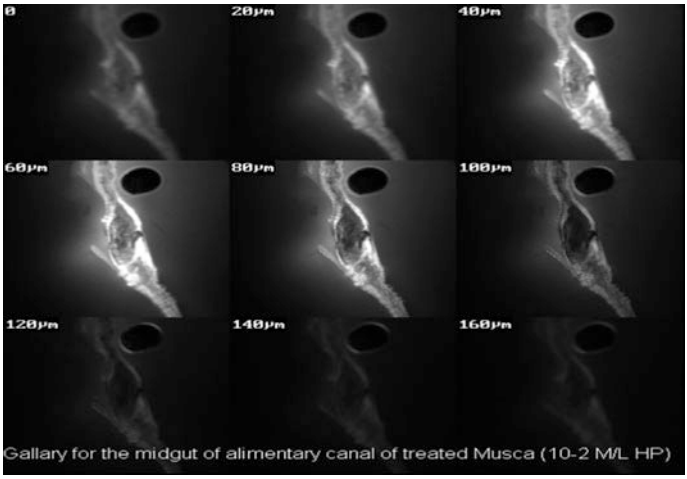

Fig. 13.8 CLSM optical slices images for housefly alimentary canal in different optical depths (0–160 μm)

exposure. It may be related to the presence of HP around the cells of the nervous system and the respiratory system outside the alimentary canal. The observed slow mortality of the flies (which requires a long time after light exposure), may be related to the effect of the photooxidation stress of HP inside the alimentary canal which causes damage to the a.c.'s cell layer lining. Therefore, the main reason of death will be indirectly due to starvation. Since epithelial cells that are responsible for food absorption line the alimentary canal, the damaged alimentary canal stops the absorption of digested food and no longer supplies the other body organs.

It is worth mentioning that the distribution ratio of monomeric and oligomeric forms of HP inside the tissues plays an important role in the efficiency of the photosensitization process. This information is well-demonstrated by measuring the lifetime of HP fluorescence in different positions inside and outside the

alimentary canal. The lifetime of the monomeric HP & oligomeric sites was 11 ± 2.3 and 4 ± 1.1 respectively.

The results obtained reveal that HP is an efficient photopesticide for the control of houseflies. This instigates us to start to pursue field studies to control *Musca domestica* in their open breeding sites.

13.2.3 Photodynamic Control of WhiteFly

The whitefly *(Bemisia tabaci)* is a hazardous pest of cotton and vegetable crops. It's primary damage on cotton results from honeydew deposits on cotton lint, which reduces its quality and value. Some trials were done to produce plants such as soybean that resist the whitefly infection [43]. The widespread use of insecticides has disturbed the parasite and predator populations, and enhanced whitefly fertility. This has also led to an increase in the development of resistance to most of the insecticides used in conventional programs [44, 45]. That is why we are interested in investigating the effect of the photodynamic process on whitefly control.

In this investigation, natural and artificial light sources were used in combination with two types of photosensitizers, Hematoporphyrin IX (HP) and Aluminum Phthalocyanine (PC), for the control of whitefly (*Bemisia tabaci*) adult, nymph and eggs stages (Fig. 13.9). HP and PC have high photosensitizing activity toward biological systems. They lack significant toxicity in the dark and they are environmentally friendly [14]. The efficiency of using these photosensitizers depends on their concentration, the light irradiance, and the light exposure time.

The effect of different concentrations of HP (1×10^{-2}, 1×10^{-4} and 1×10^{-6} mol/l) on the whitefly's eggs exposed to sunlight irradiance (390–490 W/m^2) for 1 h were investigated. Results reveal that at a concentration of 1×10^{-2} mol/l the survival percentage of the eggs is 8 % after 5 days from irradiation. At the same time, the concentration of 1×10^{-4} mol/l resulted in 55 % eggs survival percentage. The lowest concentration of 1×10^{-6} mol/l resulted in the highest survival percentage ($\sim$70 %) after 5 days from irradiation. Data showed the effect of different concentrations of PC (1×10^{-2}, 1×10^{-4} and 1×10^{-6} mol/l) on whitefly's eggs when exposed to the same conditions as in the case of HP. The concentration of 1×10^{-2} mol/l resulted in 16 % of the eggs' survival after 5 days from irradiation. In comparison, the concentration of 1×10^{-4} mol/l resulted in 70 % of the eggs' survival after the same time interval. The lowest concentration of 1×10^{-6} mol/l resulted in the highest survival percentage ($\sim$90 %) after 5 days from irradiation [46].

The range of irradiance which was chosen in this study matches the range of sunlight irradiance between winter (average 250 W/m^2), and summer (average 600 W/m^2) in Egypt. In this experiment, three different irradiance (200, 400 and 600 W/m^2) were applied. Data of HP and PC eggs treatment indicates the effect of different irradiance from the solar simulator light and show the significant changes

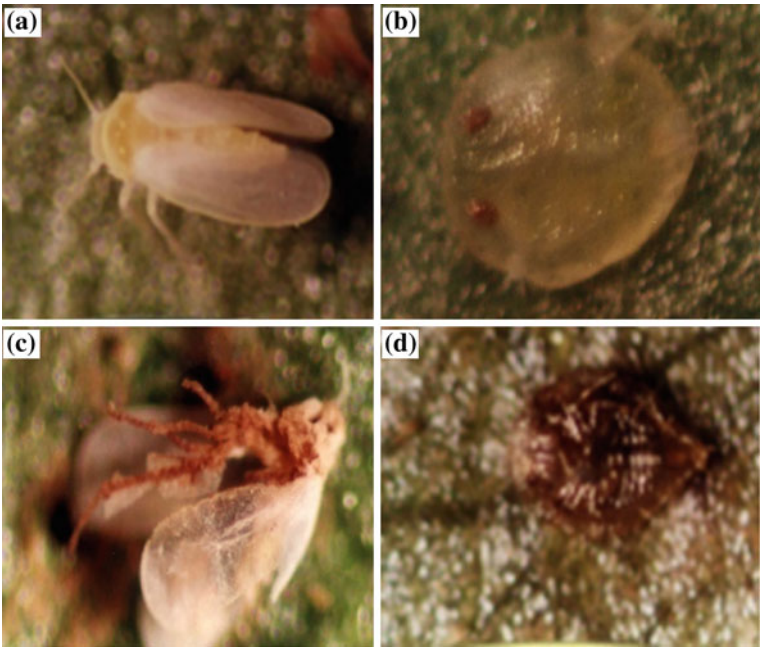

Fig. 13.9 Stereo-microscope images for whitefly adult and nymph stages before treatment (**a** and **b**) and after treatment (**c** and **d**)

($P < 0.05$) in percentages of survival rates with the change of the irradiance. It shows that higher irradiance (600 W/m^2) results in a lower percentage of survival of eggs (25 % for HP treatment and 47 % for PC treatment) while the lower irradiance, (200 W/m^2), results in higher percentage of survival of eggs (88 % for HP treatment and 92 % for PC treatment) after 5 days from irradiation.

It was found that the mortality percentage of eggs increases significantly with the increase of the exposure time for both treatments of HP and PC ($P < 0.05$). It should be noted that the exposure times used were 30, 60, and 90 min, respectively. The exposure time of 90 min resulted in 50 and 68 % of eggs survival for eggs treated with HP and PC, respectively, after 5 days from irradiation by the sunlight. The exposure time of 60 min resulted in a survival rate of 70 and 83 % of the eggs treated with HP and PC, respectively, after the same time interval. The exposure time of 30 min led to a survival rate of 85 and 90 % of the eggs treated with HP and PC, respectively, on the 5th day after irradiation.

In conclusion, results of this work revealed that a few micromoles of the dye are sufficient to induce lethal effects after one-hour exposure to sunlight irradiance, which is typical of a mid-autumn day at Mediterranean latitudes. Results also indicate that the hematoporphyrin IX efficiency is better than aluminum phthalocyanine efficiency in the control of whiteflies. However, both HP and PC represent promising environmentally friendly photoinsecticidal agents [46].

13.3 Photodynamic Control of Parasites

13.3.1 Photodynamic Control of Schistosomiasis

Schistomiasis, also known as bilharzias, is a chronic worm infection caused by several species of blood flukes of genus Schistosoma. It's the most prevailing endemic disease in the world, mainly in tropical and subtropical regions. Schistosomiasis is estimated to affect 200 million people around the world, causing high levels of morbidity and mortality in 74 countries in tropical and subtropical areas [47]. Three main Schistosoma species infect humans: *Schistosoma masoni,* present mainly in Africa and South America, *Schistosoma haematobium,* found in Africa and the Middle East, and *Schistosoma japonicum,* which is endemic in Asia. Eighty percent of the transmission of this disease occurs in sub-Saharan Africa. The construction of many dams providing hydroelectric power and water for irrigation has given rise to the spread of this disease despite transmission control programs [48].

In Egypt, in 1851, Theodor Bilharz discovered, in autopsy material, that the causative agent of hematuria is *Schistosoma*. It was again in Egypt, around 1914, that Leiper discovered the two genera of *Bulinus* and *Biomphilaria* snails that transmitted the two species *Schistosoma haematobium* and *Schistosoma mansoni,* respectively [49].

During the past four decades, numerous efforts have been made to overcome schistosomiasis throughout the world. In 1985, the World Health Organization (WHO) reported that reducing or limiting the transmission of the parasite by snail control strategies could be a rapid and efficient method. Thus, priority was given to the extensive use of molluscicides in the field. Five years later, as a result of advances in parasitological diagnostic techniques and chemotherapy, the WHO modified the strategy, giving priority to the control of morbidity rather than the control of transmission, and preferentially developed chemotherapy [50]. In 1993, the WHO raised the alarm with a necessary return to snail control strategies in association with chemotherapy [51]. Over the past 20 years, the treatment of Schistosomiasis has been considerably improved by the use of praziquantel, a drug that is effective generally in a single dose against all Schistosoma species. However, its extensive use in endemic populations seems to be the origin of the possible development of parasite tolerance to praziquantel. Reduced efficiency of praziquantel treatment was recorded in Senegal and Egypt, and different field and laboratory studies indicated the appearance of praziquantel-resistant isolates of schistosomes. Existing control methods are aimed principally at the management of snail populations that inhabit endemic areas [52].

Control of schistosomiasis is concentrated mainly on the treatment of patients against schistosomes and the elimination of the intermediate hosts mentioned previously (snail vectors). For the past 15 years, our research group has used the photodynamic process as a tool to control schistosomiasis. Focus has been done on the investigation of Hematoporphyrin IX (HP) on the different life cycle stages of

the schistosome, mainly the eggs, cercariae, and snails of the *haematobium* and *mansoni* species.

In this work, hematoporphyrin IX (HP) concentration was considered to be the main variable when studying the photosensitization process compared to other factors (light intensity, rate of up-take and time of irradiation), and the effective limits of the other factors were measured according to the amount of HP used. This was done to get a cost effective control method for a field application. In the prospective field application, under sunlight exposure, the effective HP concentration will be related to the other uncontrollable parameters such as sunlight intensity and exposure times.

The most sensitive stage to PDT treatment in the life cycle of the schistosome were the cercaria and the eggs. In this context, cercaria results demonstrate clearly the successful control of schistosomes parasites. This will be summarized by investigating the effect of HP concentration on the survival of cercaria.

At a concentration of 10^{-2} mol dm^{-3}, 100 % mortality of *Schistosoma haematobium* cercaria was observed after 10 min from exposure to sunlight. 10^{-3} mol dm^{-3} caused 22.4 % cercariae survival after 10 min of irradiation, while the concentration 10^{-4} mol dm^{-3} caused 35.2 % survival for the same exposure time. When the concentration of HP was decreased to 10^{-7} mol dm^{-3}, the percentage of survival was 72 %.

The extent of cercaria damage by PDT in whole body and surface texture caused by the photosensitization process is shown in the electron microscope images (Figs. 13.10 and 13.11). It is obvious that the photosensitization process caused head and tail to be cut from the whole body as well as causing permanent change in the surface texture such as damage to the body surface protrusions.

According to the results of this experiment, lethal and sublethal HP concentrations are enough to induce cercarial reduction. These results represent conclusive proof of the high potential and efficiency of the PDT technique in cutting the life cycle of the schistosomes and controlling their parasites [52] (Fig. 13.11).

13.3.2 Photodynamic Control of Fascioliasis Intermediate Host (Lymnaea Natalensis)

Fascioliasis is an important food-and water-borne parasitic disease caused by liver flukes of the genus *Fasciola (*e.g., *Fasciola gigantica)*. Human fascioliasis has been reported in numerous countries. It is estimated that millions of people are infected worldwide and the number of people at risk exceeds 180 million. Also, fascioliasis is one of the most important parasitic diseases in grazing animals, with over 700 million production animals being at risk of infection. Therefore, these parasites cause significant public health problems and substantial economic losses to the livestock industry.

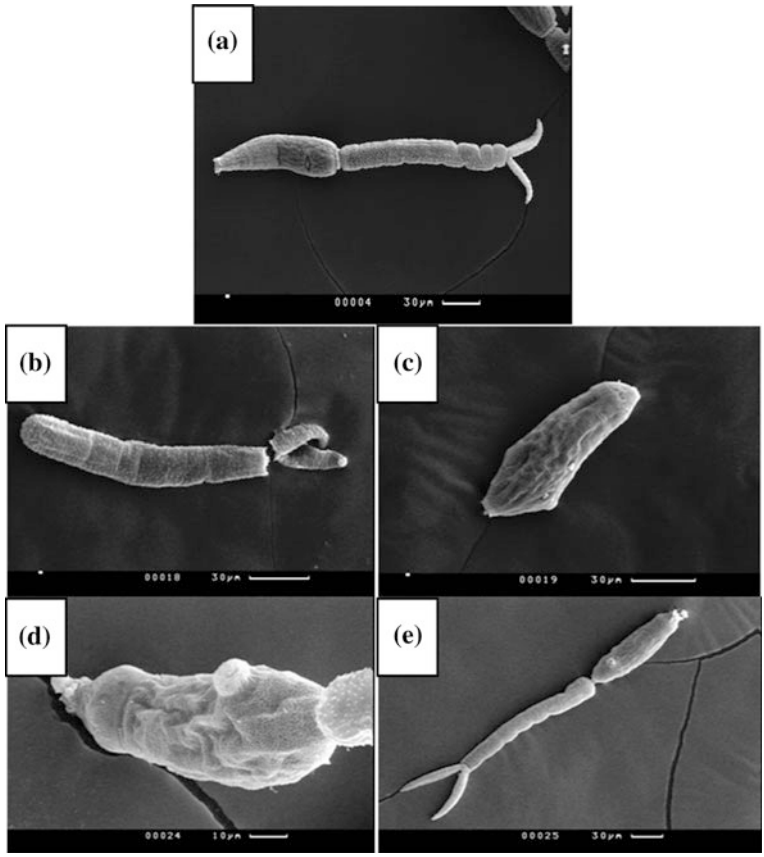

Fig. 13.10 Electron microscope images for control (**a**) and treated (**b**–**e**) showing head and tail damage of *S. haematobium* cercaria body

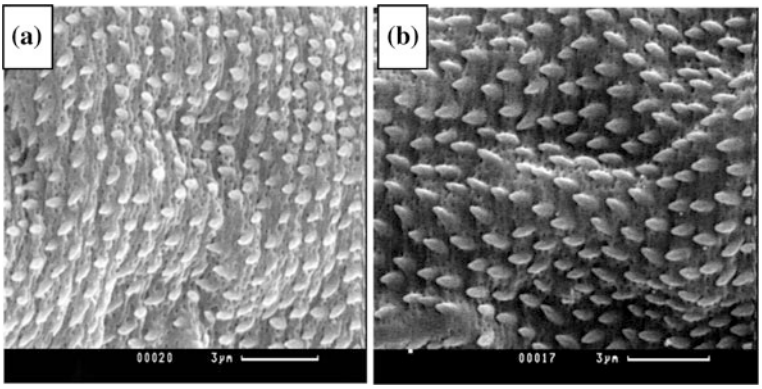

Fig. 13.11 Electron microscope images for surface texture of control (**b**) and treated (**a**) showing spike damage on the surface of *S. haematobium* cercaria

Lymnaeid snails are the first intermediate hosts for several *Fasciola* spp. The main snail host for the liver fluke, *Fasciola gigantica*, is *Lymnaea natalensis,* which is widely distributed in Africa [53, 54].

In this study, an experimental investigation was performed to monitor the efficiency of HP to control *L. natalensis* snails as well as a number of environmental factors that affect this efficiency [55]. This protocol was designed to estimate the rate of photosensitization reactions under such environmental conditions e.g., pH, minerals, water depth, and temperature.

One of the most important environmental factors is the salt content of the Nile River (Ca^{+2}, Na^{+1} and Mg^{+2}). Although the concentration of these salts are very low, they have a significant effect on the rate of the photosensitization process [56]. The efficiency of the photosensitization process in the Nile river water was found to be higher than in distilled water (d.w.). This difference in efficiency is not related to the effect of the media on the accumulation rate, which shows no significant difference in the two media. Therefore, the HP efficiency difference may be related to high density of electrons due to the presence of salts in the medium of the photosensitization process. Grosso et al. claimed that high polar media are usually preferred in the synthetic application of photoinduced electron transfer reactions because in these media most photoinduced electron transfer reactions afford free radical ions well. However, it is known that some free radical ions may react quickly with polar solvent molecules [57].

HP concentrations induced different effects on the rate of survival of *Lymnaea natalensis* eggs. This is significant at HP concentrations of 10^{-5} and 10^{-4} mol dm^{-3} in case of saline water and distilled water, respectively. This means that the presence of Nile river salts may improve the economic value of the photosensitization process in the case of *Lymnaea natalensis* egg control.

The acidity of Nile River water can be changed as a result of pollution, acidic rains, and human–water interaction. So it is important to examine the efficiency of the photosensitization process in case of changes in water pH (within the tolerance range of living organisms). The present results indicate that the photosensitization process is more efficient in an alkaline medium than in an acidic medium. However, *Lymnaea* eggs in the acidic medium had a significantly higher HP accumulation rate than in the alkaline medium. It was reported that [58] at higher pH, the quantum yield increased due to increased OH^{-} availability for electron donation. This interprets the significant higher efficiency of the photosensitization process in the alkaline medium in this work.

In this work, the effect of HP sublethal concentrations on *Lymnaea natalensis* eggs and hatched snails was studied. The effect of HP sublethal concentrations on egg hatching ability was investigated. In addition, the growth, survival and longevity of the hatched snails was studied. The hatching ability was significantly decreased with an increase in HP concentrations from 10^{-7} to 5×10^{-5} mol dm^{-3}. The hatching percent of *Lymnaea* eggs that were treated with HP concentration of 5×10^{-5} mol dm^{-3} was 51.1 %. This concentration appeared to be the lowest limit of sublethal HP concentrations, which can affect *Lymnaea* eggs.

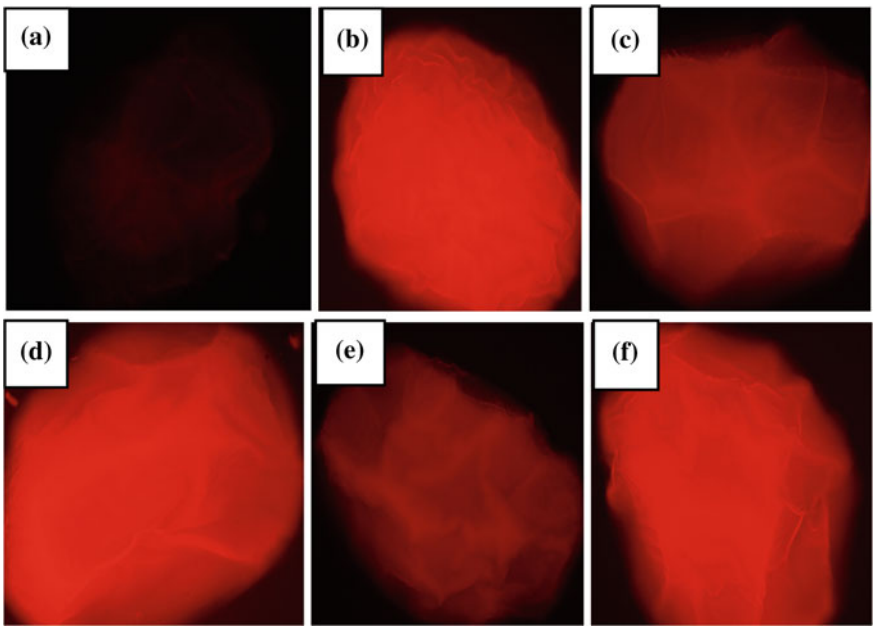

Fig. 13.12 Fluorescence image captured using Fluorescence Microscope for *Lymnaea natalensis* eggs incubated with HP for (**a**) 0 h, (**b**) 4 h, (**c**) 6 h, (**d**) 9 h, (**e**) 14 h, and (**f**) 23 h

The survival rate of snails in the control group 9 weeks after hatching was 60 %. Meanwhile, for HP concentrations of 10^{-7} and 5×10^{-5} mol dm^{-3}, the survival rates were 30 and 25 %, respectively. This may result from the effect on the HP-treated embryos during their developmental stage and, this can be monitored at the adult stage of the snails.

The survival of eggs treated with a lethal concentration of HP at different temperatures and pH was followed up in this work. The aim of this experiment was to investigate the fate of surviving eggs treated with lethal HP concentration. Higher temperature (30 °C) and higher pH (pH 8) caused significant decrease in the hatching percent of eggs (26.3 and 29.7 %, respectively) versus 100 % hatching of the control group (26 ± 1 °C and pH 7).

Figure 13.12 shows fluorescence microscope images of *Lymnaea natalensis* eggs incubated with HP for different periods (0, 4, 6, 9, 14, and 23 h). It is obvious that there is a changeable relation (alternative increase and decrease in the amount of HP) between HP accumulation and HP release. At zero incubation time the egg samples had no HP. After 4 h they had a high amount of HP, and after 9 h they also had a high amount of HP. At the accumulation period of six hours, HP amounts were less than the 4 and 9 h accumulation periods. Still, it is easy to detect some constant amounts of HP throughout the period of HP release.

13.4 Conclusion

The use of photochemical processes as a tool to control the population of several types of insects and parasites has been repeatedly examined in both laboratory experiments and field studies. These photoactivatable insecticides, which act through photodynamic pathways, clearly appear to possess several favorable features and a broad scope of applications.

The greatest challenge for our team has been in our efforts in using porphyrins against noxious insects and parasites, such as agricultural pests, and to control different diseases, like malaria, filaria, and schistosomiasis. The field trials that we have performed in the African swamps to control malaria were very successful. They were designed for outdoor treatment using a target selective formula against mosquito larva that has no effect on the other beneficial organisms in the same breeding sites. These efforts will pave the road to future large-scale countrywide projects. In conclusion, results of this work introduce a promising and innovative modality for noxious insects and parasites control. Future aims include the incorporation of nanoparticles in this photodynamic process in order to produce a photoinsecticide that combines efficiency, low cost, and highest levels of human safety and environmental friendliness.

Acknowledgments We hereby acknowledge the following colleagues and postgraduate students for their contributions to this chapter:

Prof. Dr. El-Sayed El-Sherbini, Dr. Souad El-Feky, Dr. Abdel-Hakim El-Tarky, and Omima Mandour.

References

1. Abdel-Kader MH, El-Tayeb TA (2009) Field application for malaria vector control using sunlight active formulated extract. Patent No. WO 2009/149720 A1, Patent Cooperation Treaty (PCT), Austria
2. Graham K (1963) Concepts of forest entomology. Reinhold Publishing Corp., New York. p 256
3. Pimprikar GD, Georghiou GP (1979) Mechanisms of resistance to diflubenzuron in the housefly *Musca domestica* (L.). Pestic Biochem Physiol 12:10–22
4. Carpenter TL, Heitz, JR (1980) Light-dependent latent toxicity of rose bengal to *Culex pipiens quinquefasciatus*. Environmental Entomology 9:533–537
5. Pimprikar GD, Fondern JE, Heitz JR (1980) Small-and large-scale field tests of erythrosin B for housefly control in caged layer chicken houses. Environ Entomol 9:53–58
6. Yoho TP, Butler L, Weaver JE (1976) Photodynamic killing of house flies fed food, drug, and cosmetic dye additives. Environ Entomol 5:203–204
7. Lionel RM (1997) The Color of Life. Oxford University Press Inc, Oxford, pp 3–5
8. Bensasson RV, Jori G, Land EJ, Truscott TG (eds) (1985) Primary Photoprocesses in Biology and Medicine. Plenum Press, New York, pp 349–355
9. Jori G (1996) Tumor photosensitizers: approaches to enhance the selectivity and efficiency of photodynamic therapy. J Photochem Photobiol B: Biol 36:87–93

10. Ben Amor T, Tronchin M, Bortolotto L , Verdiglione R, Jori G (1998) Porphyrin and related compounds as photoactivatable insecticides. I. Phototoxic activity of hematoporphyrin toward *Ceratitis capitata* and *Bactrocera oleae*. Photochem Photobio 67:206–211
11. Rebeiz CA, Juvik JA, Rebeiz CC (1988) Porphyric insecticides: concept and phenomenology. Pestic Biochem Physiol 30:11–27
12. Abdel-Kader MH, El-Sherbini SA, El-Tayeb TA, Jori G, Ben-Amor T (2006) Using environmentally friendly and solar activated compounds for control of Musca domestica. Patent No. 23571. Egyptian Patent office (EPO), Academy of Scientific Research and Technology, Ministry of High Education & Research, Egypt
13. Abdel-Kader MH, El-Sherbini SA, El-Tayeb TA, Mandour OS (2005) Photosenstizers for control of *Schistosoma hematobium* and *Schistosoma Mansoni* Cercaria and eggs. Patent No. 23397 (2005). Egyptian Patent office (EPO), Egypt
14. Abdel-kader MH, El-Sherbini SA, Balal MH, El-Tayeb TA, Ayoub S, El-Feky SA (2005) Using sunlight and the derivatives of porphyrine and phthalocyanine to control the stages of whitefly (Bemisia tabaci). Patent No. 23385, Egyptian Patent office (EPO), Egypt
15. Abdel-Kader MH, Giulio J, El-Sherbini SA, El-Tayeb TA (2008) Using Environmentally friendly and solar activated compounds for control of Culex pipiens larvae (Mosquito). Patent No. 34113 (2008), Egyptian Patent office (EPO), Egypt
16. Abdel-kader MH, El Sherbini SA, El-Tayeb TA, Hassan E, El-Emam M, El-Taraky A (2008) Using Photo-oxidation reactions by photosensitizer for control of Schistosomes snail vector. Patent No. 23969, Egyptian Patent office (EPO), Egypt
17. Fradin MS (1998) Mosquitoes and mosquito repellents. Ann Internal Med 128:931–940
18. Crosby MC (2007) The American Plague: the untold story of yellow fever, the epidemic that shaped our history. Berkley Books, New York
19. McCullough DG (1978) The path between the seas: the creation of the Panama Canal 1870–1914. Simon and Schuster, New York, p 289
20. World Health Organization (2006) Indoor residual spraying: Use of indoor residual spraying for scaling up global malaria control and elimination. Geneva, Switzerland
21. Weber R, Watson A, Forter M, Oliaei F (2011) Review article: persistent organic pollutants and landfills-a review of past experiences and future challenges. Waste Manage Res 29:107–121
22. Beard J (2006) DDT and human health. Sci Total Environ 355:78–89
23. World Health Organization (2011) WHO position statement. The use of DDT in malaria vector control
24. Awad HH, El-Tayeb TA, Abd El-Aziz NM and Abde-Kader MH. (2008) A semi-field Study on the effect of novel hematoporphyrin formula on the control of *Culex Pipens* Larvea. J. Agri. Soc. Sci., 4:85–88
25. Lucantoni L, Magaraggia M, Lupidi G, Ouedraogo R, Coppellotti O, Esposito F, Fabris C, Jori G, Habluetzel A (2011) Novel, Meso-substituted cationic porphyrin molecule for photo-mediated larval control of the dengue vector *Aedes aegypti*. PLoS Negl Trop 5(12)
26. Fabris C, Ouédraogo RK, Coppellotti O, Dabiré RK, Diabaté A, Di Martino P, Guidolin L, Jori G, Lucantoni L, Lupidi G, Martena V, Sawadogo SP, Soncin M, Habluetzel A (2012) Efficacy of sunlight-activatable porphyrin formulates on larvae of *Anopheles gambiae* M and S molecular forms and *An. arabiensis*: A potential novel biolarvicide for integrated malaria vector control. Acta tropica 123:239–243
27. U.S. Food and Drug Administration (2002) Federal Register. Listing of Color Additives Exempt From Certification; Sodium Copper Chlorophyllin 67(97):35429–35431
28. West LS (1951) The housefly: its natural history, medical importance, and control, 1st edn. Comstock Publishing Company
29. Dent D (2000) Insect pest management, 2nd edn. CABI
30. Deken de R, van Loon M (1989) The presence of knock down resistance in houseflies on Belgian farms following the use of long-acting pyrethroids and its implication on housefly control. Vlaams-Diergeneeskundig-Tijdschrift 58:200–203

31. Hafez JA (1992) Evaluation of insecticidal efficiency of certain new selective formulations against *Musca domestica*. J Egypt Soc Parasitol 22:839–849
32. Hodgman TC, Ziniu Y, Ming S, Sawyer T, Nicholls CM, Ellar DJ (1993) Characterization of a *Bacillus thuringiensis* strain which is toxic to the housefly *Musca domestica*. FEMS Microbiol Lett 114:17–22
33. Glofcheskie BD, Surgeoner GA (1993) Efficacy of Muscovy ducks as an adjunct for housefly (Diptera Muscidae) control in swine and dairy operations. J Econ Entomol 86:1686–1692
34. Watson DW, Geden CJ, Long SJ, Rutz DA (1995) Efficacy of Beauveria bassiana for controlling the housefly and stable fly (Diptera Muscidae). Biol Control 5:405–411
35. Kuramoto H, Shimazu M (1997) Control of house fly populations by Entomophthora muscae (Zygomycotina Entomophthorales) in a poultry house. Appl Entomol Zool 32:325–331
36. King BH (1997) Effects of age and burial of housefly (Diptera Muscidae) pupae on parasitism by Spalangia cameroni and Muscidifurax raptor (Hymenoptera Pteromalidae). Environ Entomol 26:410–415
37. Yoho TP, Butler L, Weaver JE (1971) Photodynamic effects of light on dye-fed house flies: preliminary observations of mortality. J Econ Entomol 64:972–973
38. Yoho TP, Butler L, Weaver JE (1971) Photodynamic action in insects: levels of mortality in dye-fed light-exposed house flies. Environ Entomol 2:1092–1096
39. Pimprikar GD, Noe BL, Norment BR, Hetiz JR (1980) Ovicidal, larvicidal and biotic effects of xanthene derivatives in the house fly *Musca domestica*. Environ Entomol 9:785–788
40. Respicio NC, Heitz JR (1986) Cross resistance of erythrosine B-resistant house flies to different pesticides. Econ Entomol 79:315–317
41. Eltayeb TA (1999) The use of photo-activated pesticide for control of *Culex pipiens* (*Diptera: Culicidae*) and *Musca domestica* (*Diptera: Muscidae*). MSc Thesis, Cairo University, Egypt
42. Robinson JR, Beatson EP (1985) Effect of selected antioxidants on the phototoxicity of erythrosin B toward house fly larvae. Pestic Biochem Physio 24:375–383
43. Akbar W, Abdul Khaliq AM (2000) Rating of some early maturing soybean varieties for whitefly responses and its population trends in autumn and spring seasons. Int J Agric Biol 2:99–103
44. Ishaaya I, Kontsedalov S (2005) Biorational insecticides: mechanism and cross-resistance. Arch Insect Biochem Physiol 58:192–199
45. Ghosh S, Laskar N, Basak S, Senapati S (2004) Seasonal fluctuation of *Bemisia tabaci* Genn. on brinjal and field evaluation of some pesticides against *Bemisia tabaci* under terai region of West Bengal. Environ Ecol 22:758–762
46. Abdel-Kader M., El-Tayeb T, El-Sherbini E, El-Feky S (2008) Environmentally-friendly Photosensitizers to control Bemisia tabaci, Gennadius (Homoptera: Aleyrodidae). Eg Bull Ent Soc Egypt 34:49–60
47. Lardans V, Dissous C (1998) Snail control strategies for reduction of schistosomiasis transmission. Parasitology Today 14:413–417
48. World Health Organization (1997) Schistosomiasis. Aide Memoire 115:1–4
49. Wu GY, Halim MH (2000) Schistosomiasis: progress and problems. World J Gastroenterol 6:12–19
50. World Health Organization (1980) Epidemiology and control of schistosomiasis. WHO Tech Rep Seri 843:3–63
51. World Health Organization (1993) The control of schistosomiasis. WHO Tech Rep Seri 830:1–85
52. Hasan TI (2003) Photosensitization processes induced by Laser and incoherent light to control Shistosoma worms. MS Thesis. (N.I.L.E.S), Cairo University, Cairo, Egypt. Print
53. Moema EB, King PH, Baker C (2008) Cercariae developing in *Lymnaea natalensis* Krauss, 1848 collected in the vicinity of Pretoria, Gauteng Province, South Africa. Onderstepoort J Vet Res 75:215–223

54. Ai L, Chen M, Alasaad S, Elsheikha HM, Li J, Li H, Lin R, Zou F, Zhu X, Chen J (2011) Genetic characterization, species differentiation and detection of Fasciola spp. by molecular approaches. Parasites and vectors 4:101
55. El-Tayeb T (2003) Laser scanning microscopy for determination of the efficiency of hematoporphyrin in control of *Culex Pipiens* larvae and the snail vector of *Fasciola Gigantica*. PhD thesis, National Institute of Laser Enhanced Sciences (NILES), Cairo University
56. Soltan ME, Awadallah RM (1994) Chemical survey on the river Nile water from Aswan into the outlet. National conference on river Nile, Assiut University, Center for Environmental Studies (AUCES), 157–168
57. Grosso VN, Previtali CM, Chesta CA (1998) Salt-induced charge separation in photoinduced electron transfer reactions. The effect of ion size. Photochem Photobiol 68:481–486
58. Suslick KS, Watson RA (1992) The photochemistry of chromium, manganese, and iron porphyrin complexes. New J Chem 16:633–642

About the Authors

Prof. Dr. Mahmoud Abdel Kader is the editor of this book. For more information, please see the editor's biography.

Prof. Dr. Ulrich E. Steiner
Department of Chemistry
University of Konstanz, Germany

Dr. Ulrich Steiner received his Ph.D. and habilitation from the Faculty of Chemistry, University of Stuttgart in 1973 and 1979, respectively. In 1981, he became a Professor of Spectrochemistry at the University of Konstanz. His research interests include mechanisms of elementary photoinduced reactions such as electron transfer, proton transfer, isomerizations, solvatochromy, electronic energy transfer and magnetic field effects in chemical kinetics.

M. H. Abdel-Kader (ed.), *Photodynamic Therapy*,
DOI: 10.1007/978-3-642-39629-8,

Prof. Dr. Barbara Krammer
Department of Molecular Biology
University of Salzburg, Austria

Dr. Krammer holds a Ph.D. in Biology and Biophysics from the university of Salzburg, where she is also currently Associate Professor. Her current research interests include photodynamic laser therapy and diagnosis of tumors, photodynamic processes, apoptosis, gene expression, signaling pathways, fluorescence detection methods, cell culture tests, antimicrobial therapeutics, anticancer therapeutics, visible light effects on health, the role of the immune system in PDT and low-level radiobiological effects and skin-related questions, in cooperation with the EB center Salzburg.

Dr. Thomas Verwanger
Department of Molecular Biology
University of Salzburg
Salzburg, Austria

Dr. Verwanger completed his Ph.D. at the Institute of Physics and Biophysics at the University of Salzburg where he is currently employed as a post-doctoral researcher. His research focuses on molecular biological effects of PDT and the mechanisms of cell damage and endogenous protection in the course of radon therapy.

Prof. Dr. Rudolf W. Steiner
Institute for Laser Technologies in Medicine
Ulm, Germany

Dr. Steiner completed his Ph.D. at the CNRS in Montpellier, France and worked as the head of the Laser Laboratory for Diagnosic Applications in Medicine and Biology at the University of Düsseldorf for over 10 years. Currently, Dr. Steiner is a member of the medical faculty at the University of Ulm. His research focuses on diagnostic and therapeutic applications of lasers in medicine and biology, microscopic techniques and imaging of cells and tissue, fluorescence spectroscopy, laser Doppler technology, perfusion of tissue, laser-tissue interactions and photodynamic diagnostics and therapy.

Prof. Dr. Hans-Peter Berlien
Elizabeth-Klinik
Berlin, Germany

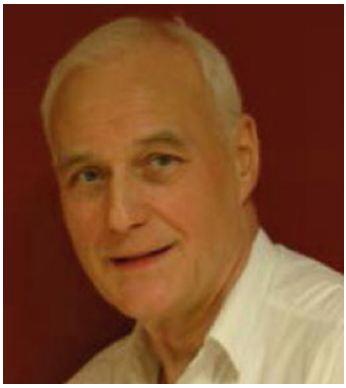

After graduating from the faculty of medicine at the Free University Berlin in 1976, Dr. Berlein became a medical assistant at the university clinic Berlin Steglitz where he certified as a physician, started his surgical education, and received his doctorate specializing in pediatric surgery in 1981. Since 1985, he is Medical Director of the Centre for Laser and Medical Technology Berlin (LMTB). After his post-doctoral lecturing qualification, he became professor for laser medicine at the Free University Berlin in 1989. From 1996 to 2005, he was head physician of the newly found department for laser medicine at the Städtische Krankenhaus

Neukölln (now Vivantes), Berlin. In 2005, he transferred the whole department for laser medicine to the Elisabeth Hospital, Berlin where he still works. Dr. Berlien is president of the International Society for the Study of Vascular Anomalies (ISSVA) and of the Berliner Wissenschaftliche Gesellschaft as well a member of the National Academy of Science and Engineering (acatech).

Dr. Kristian Berg
Department of Radiation Biology
Norwegian Radium
Hospital
Oslo University Hospital
Montebello, Oslo, Norway

Dr. Berg completed his Ph.D. in experimental photodynamic therapy at the University of Oslo in 1990. Currently, he is Head of Department at the School of Pharmacy and Department at the University of Oslo. His research interests include photodynamic therapy (PDT), mechanisms involved in the treatment effects of PDT in vitro and in vivo, and photochemical internalization (PCI).

Dr. Anette Weyergang
Department of Radiation Biology
Norwegian
Radium Hospital
Oslo University Hospital
Oslo, Norway

Dr. Weyergang completed her Ph.D. in photochemical internalization (PCI) at the University of Oslo in 2009. Since then, she has been working as a post-doctoral researcher in the PCI group at Oslo University Hospital. Her areas of research include intracellular drug delivery induced by photochemical internalization, PCI of tumor- and vascular-targeted toxins in vivo and in vitro, as well as cellular signaling and pharmacology induced by multimodal therapy of PDT and EGFR-targeted therapeutics.

Dr. Marie Vikdal
Department of Radiation Biology
Norwegian
Radium Hospital
Oslo University Hospital
Oslo, Norway

Dr. Vikdal is a qualified medical doctor who is currently completing a Ph.D. in the PCI group with Kristian Berg. Dr. Vikdal focuses on laboratory and animal research on the impact of photochemical internalization on vasculature and endothelial cells.

Dr. Ole-Jacob Norum
Department of Orthopedic Oncology
Oslo University Hospital, Oslo, Norway

Dr. Norum is a qualified medical doctor and Senior Consultant in the Department of Orthopedic Oncology at Oslo University Hospital. His research interests include orthopedic oncology, bone and soft tissue sarcomas and clinical orthopedic-oncological trials.

Dr. Pål Kristian Selbo
Department of Radiation Biology
Norwegian Radium Hospital
Oslo University Hospital
Oslo, Norway

Dr. Selbo is a Senior Scientist at the Department of Radiation Biology, Norwegian Radium Hospital and PCI Biotech. His research interests include photobiology, photomedicine and photodynamic therapy and drug resistance. Drug delivery systems and experimental cancer therapy, as well as the use of photochemical internalization (PCI) as a method for drug delivery are also part of his interests. Currently, Dr. Selbo works on using PCI as a method for the delivery of cancer stem cell-targeting therapeutics. Dr. Selbo has been head of the Norwegian Society for Photobiology and Photomedicine since 2010.

Dr. Carsten M. Philipp
Elisabeth Klinik
Berlin, Germany

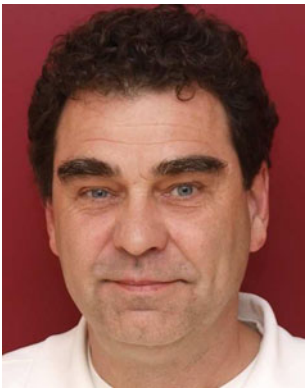

Dr. Philipp is Assistant Medical Director of Germany's largest hospital-based department of laser medicine. Since 1987, he has been working in laser applications in medicine including vascular lesions, surgery, endoscopy, PDT, and diagnostics. He is Co-Editor-in-Chief of the journal Photonics and Lasers in Medicine and current president of Deutsch Gesellschaft für Lasermedizin (DGLM).

Dr. Herwig Kostron
Department of Neurosurgery
University of Innsbruck
Austria

Dr. Kostron is Associate Professor and Senior Neurosurgeon at the Department of Neurosurgery at the Medical University of Innsbruck. His research interests include neuro-oncology, clinical neuro-oncological trials, photodynamic applications for neurosurgery, intraoperative fluorescence/tumordelineation, and transvection-enhanced drug delivery.

Prof. Dr. Keyvan Moghissi
The Yorkshire Laser Centre
Goole, UK

Dr. Moghissi studied medicine at the University of Geneva where he obtained his BSc and MD. His post-graduate study was in Geneva and various hospitals in the UK following which he obtained the Diploma of Specialist in Surgery (MSChir) in Geneva and the Fellowship of the Royal College of Surgeons (FRCS) Edinburgh. In 1982, he was honored by receiving Membre Associe de Academie de Chirurgie (Paris) and was awarded FRCS (England). In 1989, he was awarded Fellow of the European Board of Thoracic and Cardiovascular Surgeons (FETCS). His current appointments consist of Clinical Director and Consultant Cardiothoracic Surgeon at the Yorkshire Laser Centre, UK and Honorary Consultant in Laser Surgery and Photodynamic Medicine in Hull and East Yorkshire NHS Trust and North East Lincolnshire and Goole Hospitals NHS Trust. Dr. Moghissi is also the Editor-in-Chief of the journal Photodiagnosis and Photodynamic Therapy. He has been involved in research in a wide variety of subjects in cardiothoracic surgery and, more recently, in laser surgery and photodynamic therapy (PDT). He is currently one of the experts for the National Institute of Clinical Excellence (NICE) on PDT in lung and esophageal cancer and also advises the National Institute for Health Research. Dr. Moghissi is the Chairman of the Moghissi Laser Trust charity and Chairman of the UK Photodiagnosis and Photodynamic Therapy Charity.

Dr. Ron R. Allison
20th Century Oncology
Greenville, NC, USA

Dr. Allison graduated with a BS degree from Brooklyn College in 1983 and in 1987, and he received his MD from State University of New York (SUNY) Downstate Medical School. Dr. Allison completed his internship at Kings County Hospital Center in 1988 and completed residency in 1991 at SUNY Health Science Center, where he was named as chief resident. He then joined SUNY-Buffalo and the NCI-designated Roswell Park Cancer Institute as an attending physician and Associate Professor. In 2000, Dr. Allison joined the ECU Brody School of Medicine as Professor and Chair of Radiation Oncology and also served as director of the Leo W. Jenkins Cancer Center. In 2010, he joined 21st Century Oncology as Medical Director. He is a board certified-radiation oncologist by the American Board of Radiology and a Diplomate of the National Board of Medical Examiners.

Prof. Dr. Hubert van den Bergh
Swiss Federal Institute of Technology (EPFL)
Lausanne, Switzerland

Dr. van den Bergh obtained his Ph.D. in physical chemistry from the University of Cambridge, UK in 1971. Among his many achievements, Dr. van den Bergh has contributed to the development of FDA-approved drugs (Visudyne together with Novartis Ophthalmics for treating wet age-related macular degeneration and Hexvix together with Photocure and GE Healthcare for early detection of bladder cancer). He is the author of over 250 peer-reviewed scientific publications, and he is an inventor on 20 patents. In addition, he is member of the Scientific Advisory Board of a number of companies.

Dr. Michel Sickenberg
Lausanne, Switzerland

Dr. Sickenberg received his MD title in 1995 in the Jules Gonin hospital in Lausanne, Switzerland, where he was a resident and chief resident as ophthalmologist and ophthalmic surgeon. He was a principal investigator for the development of the Visudyne phototherapy treatment for various forms of wet macular degeneration between 1995 and 2000. In 2006, he introduced Avastin in Switzerland as the first anti-VEGF substance for intravitreal injections in various forms of macula edema. In 2011, he introduced a new method to Switzerland to regenerate diverse forms of atrophic macula diseases using bioregulator peptides. As of 2000, he runs a private ophthalmic practice in Lausanne.

Dr. Patrycja Nowak-Sliwinska, Ph.D.

Dr. Nowak-Sliwinska got her Ph.D. in biological chemistry from the Jagiellonian University in Cracow, Poland, in 2006. She did her post-doctoral research in the Medical Photonics Group at the Swiss Federal Institute of Technology (EPFL) in Lausanne, Switzerland, and in the Angiogenesis Laboratory at the VU University Medical Center in Amsterdam, The Netherlands, working on specific targets overexpressed in tumor endothelium for use in targeted PDT. Her major research interests are (1) the vascular effects of PDT in ophthalmology and cancer, (2) non-VEGF angiogenesis pathways, (3) targeted PDT, (4) combination strategies. Dr. Nowak-Sliwinska has authored 20 peer-reviewed scientific publications and she is an inventor on two patents.

Prof. Dr. Giulio Jori
Department of Biology, University of Padova

Dr. Jori is Professor of Bio-organic Chemistry at the University of Padova, Italy. He is a founding member of the European Society for Photobiology where he also served as president. Dr. Jori has a wide range of writing and editing experience, and currently, he is a co-editor of the book series Comprehensive Series in Photochemical and Photobiological Sciences (Springer). Dr. Jori's research is focused on the mechanisms of photosensitised processes in biological systems with specific interest in medical applications (photodynamic therapy of tumors, skin diseases and microbial infections), as well as in the development of environmentally friendly photobiological approaches (decontamination of microbially polluted water and sunlight-activated agents for the control of noxious insects in the larval and adult stage).

Shazia Khan, Ph.D.

Dr. Shazia Khan is a PostDoctoral Research Fellow at the Wellman Center for Photomedicine, Massachusetts General Hospital and Harvard Medical School. In this capacity, she works on the developing a rapid diagnostic modality for simultaneous detection of bacterial resistance and determination of antibiotic susceptibility. She also works on 3-D models of cancer and cancer biology. She

completed her PhD from the National Institute of Immunology, New Delhi, India. Towards this, she worked in the field of signal transduction, focusing on kinase enzymes of Mycobacterium tuberculosis. The broad aspects included characterization of the kinases and identification of their substrates, including elucidation of the phosphorylation events.

Prof. Tayyaba Hasan, Ph.D.

Tayyaba Hasan, Ph.D., is a Professor of Dermatology at Harvard Medical School (HMS) and a Professor of Health Sciences and Technology (Harvard-MIT). She is based at the Wellman Center for Photomedicine. Dr. Hasan received her Ph.D. in Organic Chemistry from the University of Arkansas followed by postdoctoral training in Biochemistry at the University of Pennsylvania after which she joined the Harvard Medical School, Massachusetts General Hospital in 1982 as a Research Scientist. Dr. Hasan's research is directed to basic and translational studies in photochemistry, photobiology, and photodynamic therapy. The major research theme of the group is Mechanisms and Image Guided Optimization of Photodynamic Therapy. More broadly, the research program includes investigations in cancer, microbiology, infectious diseases, arthritis, and cardiovascular pathologies.

Dr. Fabris Clara

Dr. Fabris graduated in biological sciences at the University of Padova in 1992 and she obtained her Ph.D. in photobiological techniques at the University ''La Sapienza'' of Rome in 1999. She now works at the Biology Department of the University of Padova. Her research activities were first focused on the characterization of the mechanisms of photosensitized processes and their potential applications in biology and medicine, particularly on experimental photodynamic therapy of tumors. More recently, her research has been extended to the environmental field with the application of photodynamic therapy in the treatment of microbial infections and prevention and treatment of water- and vector-borne diseases. Dr. Fabris also investigates the application of topical photodynamic therapy to experimental and spontaneous skin infections.

Dr. Soncin Marina

Dr. Soncin graduated in biological sciences at the University of Padova in 1991, and she obtained the Ph.D. in photobiological techniques at the University ''La Sapienza'' of Rome in 2000. She worked until 2012 at the Biology Department of the University of Padova. At the present, she works at the Department of Biomedical Sciences of University of Bologna. Her research interests are focused on the study of basic mechanisms of photodynamic action at a cellular and tissue level, as well as on the application of photodynamic therapy for the treatment of tumors and microbial infections. Moreover, her research is also devoted to the application of photodynamic treatment of waters contaminated by pathogenic agents of parasitic diseases.

Dr. Camerin Monica

Dr. Camerin graduated in Biological Sciences at the University of Padova in 2000 and she now works at the Biology Department of the University of Padova. Her research interest is focused on the study of basic mechanisms of photodynamic

action at a cellular and tissue level; the application of the photosensitized processes to experimental photodynamic therapy of tumors is the main subject of her study. In particular, she investigates the in vivo efficacy of nanoparticles for the photodynamic therapy of experimental tumors. At present, her research is also focused on decontamination of waters polluted by microbial pathogens.

Dr. Furio Corsi

Dr. Corsi graduated in veterinary medicine at the University of Bologna in 1986 and now works in Padova in the ''Prato della Valle'' and ''Clinica Veterinaria Montecchia' veterinary clinic. He has over 20 years experience in orthopedic and general surgery.

Dr. Ilaria Cattin

Dr. Cattin graduated in veterinary medicine at the University of Padova in 2000, she now works in the ''Prato della Valle'' veterinary clinic in Padova where she deals mainly with internal medicine dermatology and cytology. She has attended specialized courses in these subjects. She also worked in the laboratory of the Department of Veterinary Medicine of Bologna and has had training in Dr. Fabia Scarampella's clinic in Milan.

Dr. Fabrizio Cardin

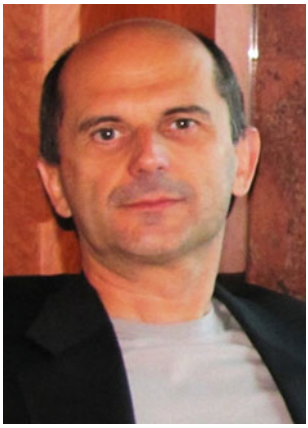

Dr. Cardin graduated in medicine and surgery in 1982 in the Faculty of Medicine and Surgery of the University of Padova. He now works in the Department of the Elderly, Unity of Geriatric Surgical Clinic. Dr. Cardin has worked in the following research topics: gastrointestinal physiopathology, with particular attention to peptic ulcer and precancerous gastrointestinal lesions, portal hypertension, studying particularly the treatment of the gastrointestinal hemorrhages; organization and technique of the digestive endoscopy, appraising in particular the way the effectiveness of laser and PDT therapy in the palliative treatment of intestinal neoplasies.

Dr. Guidolin Laura

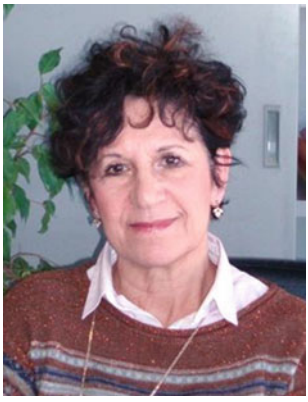

Dr. Guidolin graduated in biology in 1977 from the University of Padova. She now works in the Department of Biology and her scientific activities includes biogeographical investigations on the monitoring of the wild fauna and studies on the distribution of small mammals and their role in the ecosystem, characterization

of metallothioneins in the study of heavy metal detoxification, phenol oxidase purification from Botryllus schlosseri and studies on cell differentiation and repulsion reaction between genetically incompatible colonies. At present, her research is also devoted to porphyrin photosensitized processes for the control and inactivation of Protozoa causative agents of water- and vector-borne diseases; development of photoactivatable formulates of low environmental impact in the larval control of the malaria vectors; and photobiological techniques for water disinfection.

Prof. Dr. Olimpia Coppellotti

Olimpia Coppellotti is Associate Professor of Zoology at the University of Padova, Italy. During her 40 year research career, Dr. Coppellotti has mainly focussed on protozoology, including the movement and the energetic reservoirs for the movement in flagellates and ciliates; heavy metal detoxification and metallothioneins; morphological and taxonomic studies of ciliates from various environmental sites; role of Ciliates as biological indicators of the quality of different milieus; physiological adaptation of protozoa to extreme conditions; identification; and classification of fossil microorganisms in the Triassic amber from the Dolomites. In the last 10 years, her research is mainly devoted to the photosensitization of protozoa by means of porphyrinic compounds to inactivate pathogenic agents of water- and vector-borne diseases, development of photoactivatable formulates of low environmental impact in the larval control of the malaria vectors and photobiological techniques for disinfection of waters contaminated by pathogenic microorganisms.

Prof. Dr. Tarek A. El-Tayeb
National Institute of Laser Enhanced Sciences (NILES),
Cairo University
Egypt

Dr. El-Tayeb is an Associate Professor in Photobiology at the National Institute of Laser Enhanced Science, Cairo University. The research topics he is most interested in are related to photobiology, especially photodynamic and photothermal mechanisms in cancer therapy, as well as pest and parasite control. He is currently acting as a scientific consultant in a project in Africa for technology transfer and is planning a strategy for applying novel photo-larvicides on mosquito-infected swamps. Dr. Tarek has been awarded many prizes for his patents in the field of photobiology.

Index

M. H. Abdel-Kader (ed.), *Photodynamic Therapy*,
DOI: 10.1007/978-3-642-39629-8,